Master thesis

A techno-economic analysis of the implementation of grid-connected battery energy storage systems into shore power installations in the port of Rotterdam

Sustainable Energy Technology

S.F.J. van Kleef

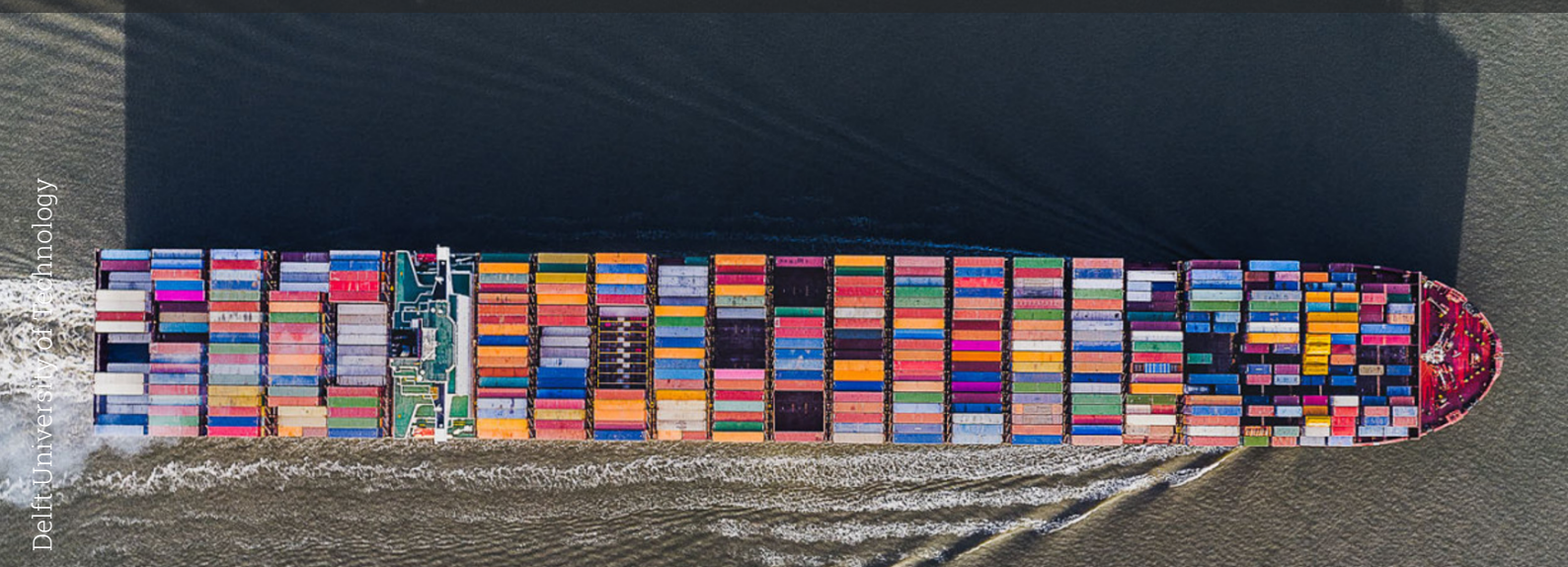

Delft University of Technology

TU Delft

Port of Rotterdam

Master thesis

A techno-economic analysis of the implementation of grid-connected battery energy storage systems into shore power installations in the port of Rotterdam

by

S.F.J. van Kleef

A thesis submitted to the Delft University of Technology in partial fulfillment of the requirements for the degree of Master of Science in Sustainable Energy Technology

Student Number:	4753739	
Project Duration:	April, 2023 - November, 2023	
Thesis Committee:	Dr. E.M. Kelder	TU Delft
	Prof. Dr. Z. Lukszo	TU Delft
	Dr. R.A.C.M.M. van Swaaij	
Company Supervisors:	T. Arkesteijn	Port of Rotterdam
	R. Cornelisse	Port of Rotterdam

TU Delft

Preface

Six years ago, my academic career at the Technical University of Delft started with the BSc program in Chemical Engineering. Over the years I slowly discovered my passion for sustainability. The ever emerging problem of climate change has ignited my interest. I decided to combine my knowledge of chemical engineering and passion for sustainability by enrolling in the MSc program in Sustainable Energy Technology. During the past two years I focused on energy storage with batteries and hydrogen as well as on energy production with photovoltaic panels and wind turbines. These topics include a financial aspect which is as important as the technical side. The bridge between those two areas is where I have focused on in this research and on which I will hopefully focus for the coming years.

During the past six years, and especially in the last eight months, I have developed among other skills, complex problem-solving capabilities which I am going to use throughout my future career. In addition to the substantive skills, I have developed myself in terms of social interactions by working with people of many different nationalities. Furthermore, I have also built lifelong relationships with people I met during this period. I would like to thank my family and friends for their support and time to listen to and read through my thesis.

I am also thankful for my colleagues at the Port of Rotterdam for the interesting conversations and the insights about the biggest port of Europe. Especially I would like to thank Tiemo and Ryan for the supervision and guidance through the research and the port. Besides them, I want to express my deepest gratitude to Dr. E.M. Kelder for being a friendly and helping supervisor during the past eight months. With this thesis I would like to encourage people and the Port of Rotterdam in accelerating the energy transition by seeking to opportunities instead of being deterred by potential setbacks.

S.F.J. van Kleef
Delft, November 2023

Abstract

A climate change mitigation strategy seen in the maritime sector is the electrification of berths through implementing shore power installations. The incorporation of grid-connected battery energy storage systems (BESS) into shore power installations, thereby creating hybrid installations, potentially accelerates the implementation of shore power. According to a gap in literature, this research evaluates the potential of various BESS to enhance the economic viability of shore power projects in the portal area in Rotterdam by prioritising consumer energy arbitrage and also trading on the day-ahead market, which is referred to as wholesale energy arbitrage.

This research consists of a techno-economic approach of assessing hybrid installations' economic viability. First, a literature analysis provided insights in the most suitable BESS types for hybrid installations. Then, evaluation of various shore power projects in the port of Rotterdam resulted in the decision to focus on two impacting berths, namely on the Stena Line (SL) and the Cruise Port (CP) terminal. To assess the economic viability of hybrid installations, two models were designed, namely a BESS costs model and an energy management strategy algorithm. Eventually, the economic viability is evaluated by the net present value, the energy efficiency and effectiveness of the various hybrid installations.

This study reveals that none of the hybrid installations are economically feasible in the way they are examined. Nevertheless, it is indicated that lithium iron phosphate batteries are most suitable to enhance the economic viability of hybrid installations due to a high round-trip efficiency and low system costs. The energy demand of the SL terminal is smaller and more frequent compared to the CP terminal, thereby enhancing the potential of the BESS to cycle more often and to create more revenue. The research includes certain assumptions and uncertainties of which the individual impact on the outcome of the research is analysed. Also, potential scenarios ensuring economic viability are presented.

Keywords
Battery energy storage system(s) (BESS), shore power, hybrid installation(s), techno-economic analysis (TEA), consumer energy arbitrage, wholesale energy arbitrage

Contents

Nomenclature

Abbreviations

Abbreviation	Definition
aFRR	Automated frequency restoration reserve
AGM	Adsorbent glass mat
Ah	Ampere-hours
amap	As much as possible
BESS	Battery energy storage system(s)
BTM	Behind-the-meter
CAGR	Compound annual growth rate
CAPEX	Capital expenditure
CO_2	Carbon dioxide
CP	Cruise Port
DAM	Day-ahead market
DoD	Depth-of-discharge
DoF	Degrees-of-freedom
DP	Dynamic programming
DSO	Distribution system operator
EC	European Commission
EMS	Energy management strategy
EPC	Engineering, procurement and construction
EPD	Engineering, procurement and deconstruction
ESS	Energy storage system(s)
EU	European Union
FB	Flow batteries
FCR	Frequency containment reserve
FTM	Front-of-the meter
GHG	Greenhouse gas(es)
HBB	Hydrogen bromine hybrid flow battery
HFB	Hybrid flow batteries
H_2-Br_2	Hydrogen bromine
H_2O	Water
HMC	Heerema Marine Contractors
HV	High-voltage
ICB	Iron chromium redox flow battery
IDM	Intra-day market
IRENA	International Renewable Energy
KOH	Potassium hydroxide solution
KPI's	Key performance indicators
LCO/$LiCoO_2$	Lithium cobalt oxide
LCOS	Levelised costs of storage
LFP/$LiFePO_2$	Lithium iron phosphate
Li	Lithium
Li-S	Lithium sulfur
LMO/$LiMn_2O_4$	Lithium manganese oxide
LP	Linear programming
LTO/Li_2TiO_3	Lithium titanate oxide
LV	Low-voltage
MDP	Markov decision process

Abbreviation	Definition
mFRR	Manually activated frequency replacement reserve
MGO	Marine gasoil
MILP	Mixed Integer Linear Programming
MS	Microsoft
Na	Sodium
$NaAlCl_4$	Sodium chloroaluminate
Na_2S_2	Sodium polysulfide
$NaNiCl_2$	Sodium nickel chloride
NaOH	Sodium hydroxide solution
Na-S	Sodium sulfur
$NCA/LiNicoAlO_2$	Lithium nickel cobalt aluminum oxide
Ni	Nickel
Ni-Cd	Nickel cadmium
Ni-Fe	Nickel iron
$Ni-H_2$	Nickel hydrogen
Ni-MH	Nickel metalhydride
NiOOH	Nickel oxide hydroxide
Ni-Zn	Nickel zinc
$NMC/LiNiMnCoO_2$	Lithium nickel cobalt manganese oxide
NO_x	Nitrogen oxide
NPV	Net present value
O&M	Operational & maintenance
O_2	Oxygen
OPEX	Operational expenditure
PCA	Paris Climate Agreement
PCR	Primary control reserve
PM	Particulate matter
PoR	Port of Rotterdam
PRP	Program responsible party
PSB	Polysulfide bromine redox flow battery
PV	Photovoltaic
Redox	Reduction-oxidation
RES	Renewable energy sources
RFB	Redox flow batteries
ROI	Return on investment
RoPax	Roll-on/roll-off passenger
RoRo	Roll-on/roll-off
RSP	Rotterdam shore power
RT	Room temperature
RTE	Round-trip-efficiency
SB	Storage block
SBOS	Storage balance of system
SEI	Solid electrolyte interphase
SL	Stena Line
SoC	State-of-charge
SoE	State-of-energy
SO_2	Sulfur dioxide
TEA	Techno-economic analysis
TSO	Transmission system operator
USD	US Dollars
V	Volt
VBB	Vanadium bromine redox flow battery
VRB	Vanadium vanadium redox flow battery
VRLA	Valve regulated lead-acid

Abbreviation	Definition
V2G	Vehicle-to-grid
ZBB	Zinc bromine hybrid flow battery
ZCB	Zinc cerium hybrid flow battery
ZEBRA	ZEolite Battery Research Africa
Zn-Cl_2	Zinc chloride
ZnO	Zinc oxide

Symbols

Symbol	Definition	Unit
α_{SB}	Annual learning rate of the SB	[%]
C_{bat}	Yearly costs of charging a battery	[€/MWh]
C_{CAPEX}	Capital expenditure	[€/kWh]
$C_{CAPEX,IN}$	Initial capital expenditure	[€/kWh]
$C_{CAPEX,REP}$	Replacement capital expenditure	[€/kWh]
C_{Decom}	Decommissioning costs	[€/kWh]
C_{EPD}	Engineering, procurement and deconstruction costs	[€/kWh]
C_{OPEX}	Operational expenditure	[€/kWh]
$C_{OPEX,FIXED}$	Fixed OPEX costs	[€/kWh]
$C_{OPEX,VARIABLE}$	Variable OPEX costs	[€/kW-year]
$C-rate$	The amount of energy discharged in one hour	[h^{-1}]
$C_{recycling}$	Recycling costs	[€/kWh]
C_{SB}	Storage block costs	[€/kWh]
C_{system}	Total system costs	[€/kWh]
Dev_i	Deviation of the average (DAM)	[€/MWh]
$E_{B,0}$	Initial amount of energy stored in the battery	[MWh]
$E_{B,L}$	Energy provided by the battery to vessel at berth	[MWh]
$E_{capacity}$	Energy capacity	[MWh]
$E_{G,c}$	Energy provided by the grid to charge the battery	[MWh]
$E_{G,L}$	Energy provided by the grid to vessel at berth	[MWh]
$E_{G,s}$	Energy provided by the battery to sell to the grid	[MWh]
E_L	Energy demand of vessel at berth	[MWh]
E_{sold}	Amount of electricity sold	[MWh]
E^0	Standard electrode potential	[V]
η	Electrode overpotential	[V]
η_{Charge}	Efficiency of charging a battery	[%]
$\eta_{Discharge}$	Efficiency of discharging a battery	[%]
h	The time period considered in the day-ahead market	[h]
k	Number of replacements during system lifetime	[-]
L_{cycle}	Cycle lifetime	[years]
L_f	Location factor	[-]
μ	Average of a data set (DAM)	[€/MWh]
N	Lifetime of hybrid installations	[y]
N_{cycle}	Total cycles during system lifetime	[-]
P_{bat}	Price of the electricity in the battery	[€/MWh]
$P_{bat,t0}$	Price of the electricity in the battery at t=0	[€/MWh]
$P_{capacity}$	Power capacity	[MW]
P_{grid}	Price of the electricity of the grid	[€/MWh]
q	The time period considered in the algorithm	[h]
r	Discount rate	[%]
R_{con}	Yearly revenue stream of consumer energy arbitrage	[€/MWh]
RTE	Round-trip efficiency of a battery	[%]

Symbol	Definition	Unit
R_{who}	Yearly revenue stream of wholesale energy arbitrage	[€/MWh]
SoE	State-of-energy of a battery	[MWh]
$SoE_{initial}$	Initial state-of-energy of a battery	[MWh]
SoE_{max}	Maximum state of energy of a battery	[MWh]
SoE_{min}	Minimum state of energy of a battery	[MWh]
$Storageduration$	The number of hours it takes to completely (dis)charge a battery	[h]
σ	Standard deviation of the data set (DAM)	[€/MWh]
σ^2	Variance of the data set (DAM)	[€/MWh]
T	Threshold for charging a battery	[€/MWh]
T	Full period of time of a year, per 15-min period	[-]
t	Moment in time, per 15-min period	[-]
V_{EoL}	End of life value	[€/kWh]
V^0	Standard cell voltage	[V]
$XXDemand$	Demand of shore power installation	[MWh]
Y_{cycle}	Yearly cycles	[years^{-1}]

List of Figures

List of Tables

1. Introduction

1.1. Background

The world is experiencing global climate change (Gillis, 2017). Climate change refers to changes in temperature and weather patterns over extended periods (Bhuvanesh et al., 2018). Causes of climate change can be either through natural factors or driven by human activities. Since the 1800s, it has been discovered that human activities are the primary catalyst of global climate change, primarily due to the emissions of greenhouse gases (GHG) caused by burning fossil fuels (Action, 2023). The emissions, released through fossil fuel combustion, have led, in among other effects, to a global temperature increase of 1.1°C compared to pre-industrial levels (around 1800s) (IPCC, 2021).

To mitigate the effects of global warming, the Paris Climate Agreement (PCA) has aimed to limit global warming well below 2°C above pre-industrial levels, ideally even at 1.5°C (Commission, 2023b). Therefore, GHG emissions must peak before 2025 at the latest and decline 43 percent by 2030, since 2019 (Change, 2023b). The PCA, adopted by over 190 countries since 2015, has encouraged global action on climate change in numerous ways (Change, 2023a).

The impact of the PCA is evident in the transformation of energy systems. Before its adoption, electricity distribution was centralised and followed a unidirectional pattern while relying on GHG-emitting grey power plants. With the PCA's influence, investments in renewable energy production have become a globally recognised action to limit the negative effects of climate change. The integration of renewable energy sources (RES) caused a shift towards decentralised and bidirectional electricity distribution, enhancing the overall network efficiency and reducing GHG emmissions (Bhuvanesh et al., 2018). Solar and wind energy are most present and rapidly growing among renewable energy production methods (IEA, 2022).

However, the intermittent nature of solar and wind energy production is a big challenge. The fluctuations, caused by the varying presence of sun or wind, disrupt the stability and reliability of the grid, which must ensure a consistent balance between supply and demand at all times (Isabella, 2022a; Stram, 2016). Large-scale energy storage systems (ESS) can potentially offer a solution by storing surplus energy during peak production and supplying energy during absence of production (Administration, 2023). Consequently, ESS integration into the electricity network leverages renewable energy production. Therefore, power generation in a sustainable future will as such necessitate use of grid-integrated ESS.

A consequence of the global development and implementation of RES is the increasing amount of applications which are able to use electricity instead of fossil based energy as a power source. With the increasing share of renewable energy to the electricity grid, the emissions caused by these applications are therefore decreasing. The maritime sector is an example of where electricity usage is increasing to reduce GHG emissions, particularly in portal areas. The European Commission's (EC) proposal for alternative fuel deployment resulted in among other developments in the adaption of shore power for vessels at berth (Mirza, 2022).

By using shore power, vessels are not longer burning fossil fuels when berthing but are connected to the electricity grid instead. The aim of shore power is to improve air quality in portal areas (and cities nearby) and to reduce GHG emissions and noise (Environment & Inspectorate, 2012). Eventually, shore power can remove up to 90 percent of the emissions of ships at berth (Qi et al., 2020). The remaining 10 percent arises from arrival and departure, when the vessel is close to the berth.

The focus of this thesis is on whether or how the development of shore power combined with certain functionalities of an ESS is or can be economically attractive. The research is conducted in the portal

area of Rotterdam. The following Subsection explains more about the port of Rotterdam (PoR) whereafter the concept of shore power is explained more thoroughly in Subsection 1.1.2. Then, Subsection 1.1.3 elaborates on the focus of this thesis in regards to different ESS. Lastly, Subsection 1.1.4 explains about the topic of hybrid installations, which are composed of an ESS combined with shore power.

1.1.1. Port of Rotterdam

The PoR is a global hub for international trade since it is the biggest port and petrochemical complex in Europe. Consequently, the PoR is responsible for 20 percent of the Dutch GHG emissions (PoR, 2019). Therefore, the PoR is committed to be one of the leaders in the energy transition. The goals set by the PoR in 2007 are proof of their sustainability ambitions, namely reducing emissions of the port and its industrial complex by 50 percent by 2025 and consequently by 60 percent by 2030, compared to 1990 levels (Samadi et al., 2016). The PoR strives to be a zero emission port by 2050 (PoR, 2021).

The sustainability strategy of the PoR is based on four pillars. Their approach consists of (i) increasing efficiency of existing industry, (ii) renewing energy, (iii) renewing raw materials and fuel system and (iv) making logistic chains sustainable (PoR, 2023). Within the fourth pillar, the shore power strategy has been developed. Depending on the availability of subsidies, the target of the PoR is to use shore power for 90 percent of the visits of roll-on/roll-off (RoRo), ferry, cruise and off-shore vessels and for at least 50 percent of the visits of the largest container vessels by 2030 (A. Bonte, 2021).

1.1.2. Shore power

Shore power, also referred to as cold ironing, shifts the supply of electricity necessary for onboard activities while berthing from the auxiliary engine of the vessel towards the local grid, via a cable connection. Hereby, exhaust emissions in portal areas caused by the auxiliary engines are decreased. Ship generators emit nitrogen oxides (NO_x), sulfur dioxide (SO_2), carbon dioxide (CO_2), and particulate matter (PM). Here, CO_2 is most polluting in terms of the environment whereas the other three are worse in terms of human health (Bakar et al., 2023).

The exact benefits in terms of global emissions can be calculated if the electricity mix from the local grid is known. However, since the electricity mix is becoming more green over time, shore power is becoming more beneficial for the environment compared to using auxiliary engines while berthing. Currently, the environmental benefits of using shore power instead of auxiliary engines are proven, irrespective of the exact location and thus mix of the electricity grid (Ballini & Bozzo, 2015; Prousalidis et al., 2014; Zis, 2019).

Shore power utilisation is differentiated between berths designated for inland shipping vessels and those intended for sea-going vessels. The most significant distinction relevant to this thesis is the amount of electricity which is demanded by the different vessel types. Inland shipping vessels are smaller and therefore require less electricity than sea-going vessels. Usage of an ESS combined with a shore power installation is more impactful in the situation of a larger electricity demand. Therefore, this thesis focuses on integration of ESS in shore power installations at berths occupied by sea-going vessels.

1.1.3. Grid-integrated storage systems

As mentioned, energy storage is inevitable in a renewable energy based future. Multiple storage systems have been analysed in literature as enablers to the power grid, including electrical, chemical, electrochemical, mechanical and thermal storage systems (H. Chen et al., 2009; Dunn et al., 2011; X. Luo et al., 2015). Figure 1.1 provides an overview of different types of storage technologies.

The focus of this study is on electrochemical rechargeable (secondary) batteries, referred to as battery energy storage systems (BESS). This choice is motivated by the fact that BESS can be flexible in design and therefore in their operational location as well which is desired for connection to various shore power installations (Rouholamini et al., 2022).

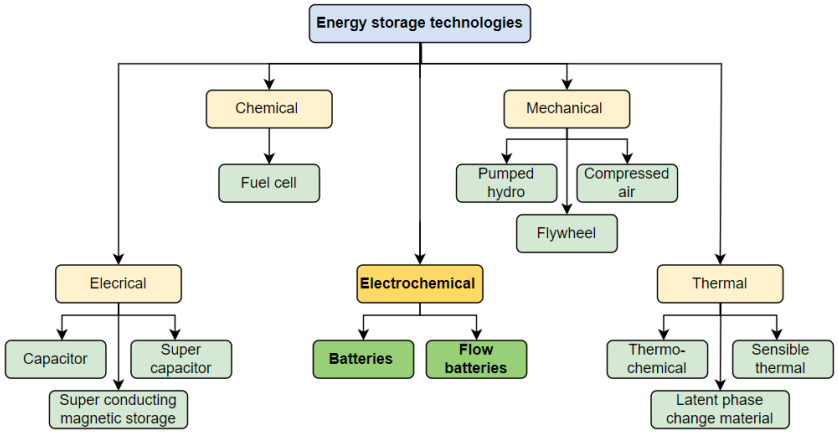

Figure 1.1: Overview of energy storage technologies

In general, electrochemical storage devices are either classified as (i) primary batteries which are discarded after their first discharge and (ii) secondary batteries which are rechargeable. When secondary batteries are being discharged, the battery is restored to the original conditions by charging (Winter & Brodd, 2004). Within the system of electrochemical storage, two different categories of batteries are explored, conventional batteries and flow batteries.

Typical characteristics of BESS such as flexibility, fast response times and short construction cycles make them appropriate for large-scale grid-connected applications (Fan et al., 2020). By assessing the potential of different BESS, performance parameters such as specific energy and power, energy efficiency, costs, lifetime and safety are of importance (T. Chen et al., 2020).

The global stationary BESS market is forecasted to follow an exponential growth, from 9 GW/ 17 GWh of installed power/ energy capacity in 2018, towards 1095 GW/ 2850 GWh of installed power/ energy capacity in 2040. As the market is growing, the cost per kWh is forecasted to decrease over time (Rouholamini et al., 2022).

Batteries used for applications connected to the grid can be classified into three different categories based on the function they serve towards the network: (i) generation, (ii) transmission and distribution and (iii) customer service (Butler, 1994). Within each category, there are various roles to be fulfilled, each with their own characteristics. The roles can be either energy or power related, which is affecting the discharging time of the BESS (Soloveichik, 2011). The roles, as well as their characteristic position on the power to energy and discharging time range are explained in Appendix A.1. The roles which are potentially fulfilled by a BESS in combination with a shore power installation are discussed next.

1.1.4. Hybrid installations

Possible topologies of battery systems integrated in the electricity network are explained in Appendix A.2. The focus of this study is on the configuration where a battery is connected to the grid as well as to a shore power installation. In this thesis, this type of installation is referred to as a hybrid installation.

BESS have multiple possible functionalities to generate revenue, of which some are considered as suitable for enhancing economic viability of hybrid installations. An overview of the possible functionalities is provided in Appendix A.1. This study prioritises the BESS function of electricity provision to vessels, also referred to as consumer energy arbitrage, and considers trading through wholesale energy arbitrage as well. The decision is based on the literature review which is conducted and explained in Chapter 2. The reason for considering multiple revenue streams is based on various conclusions drawn in papers from the literature review, suggesting that a single revenue stream, such as from customer energy arbitrage, is currently insufficient (Braeuer et al., 2019; C. Jongsma, 2021).

The activity of energy arbitrage in general requires a BESS with a high energy capacity and a storage duration in the range of one to multiple hours. This is visualised in Figure A.1 in Appendix A.1 (Argyrou et al., 2018). These requirements determine the first boundaries of the size of the BESS in hybrid installations. Both the general concept of energy arbitrage and the distinction between the two methods considered in this thesis are explained next.

Energy arbitrage

Integration of RES into the electricity network has led to increased price volatility. Figure 1.2 presents the electricity prices of the day-ahead market (DAM) of three consecutive years. The increasing volatility is recognised by the increasing deviations from the average value of the data sets over the years. Surpluses of renewable energy are driving electricity prices down, while shortages drive prices up. In 2022, the shortages are caused by the war in Ukraine. Energy arbitrage is known as buying electricity at one moment for a certain price and selling it later for a higher price, determined by market conditions (Kadri & Raahemifar, 2019). Energy arbitrage enhances the match between electricity supply and demand, thereby counteracting the volatility.

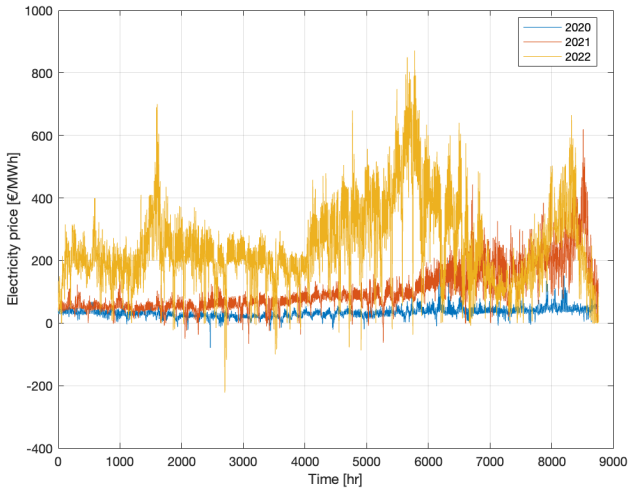

Figure 1.2: Day-ahead market prices in 2020, 2021 and 2022, data retrieved from (Entsoenergy, 2023; Pool, 2023)

Consumer energy arbitrage

Consumer energy arbitrage aims to reduce the overall electricity price for the consumer by storing electricity during price valleys (also referred to as off-peak) to subsequently provide it during price spikes (also referred to as peak). In the case of this study, the decline in overall price is captured by the terminal owner as a stream of revenue, while the vessel owner still pays the same price for the shore power electricity as in the original situation, when no BESS was present.

The consumer energy arbitrage revenue stream is therefore determined by the amount of electricity demanded by the vessel and supplied by the BESS multiplied with the difference between the price of the grid at the moment of storage and the moment of demand. By generating the revenue stream, consumer energy arbitrage potentially enhances the economic viability of a hybrid installation compared to a shore power installation on its own, from the terminal owner's point of view.

Simultaneously, the power consumption of the shore power installation is optimised since less peak electricity from the grid is used by the vessels, which is desirable for counteracting the grid volatility. When less peak electricity is used, a system's energy efficiency is enhanced. By improving the energy efficiency, the capacity of the connection of the original shore power installation to the grid can potentially be reduced in the case of a hybrid installation, leading to corresponding cost reductions.

Consumer energy arbitrage essentially accomplishes the same as peak shaving or load leveling does. Peak shaving only removes the peaks and valleys whereas load leveling totally flattens the load curve (Fan et al., 2020). Both principles are visualised in Figure 1.3 where the load profile is correlated with price. During off-peak hours when the demand is low, the load profile shows a valley, the price is low and the battery charges. Opposite, during times of peak hours when there is high demand, there are peaks in the load profile resulting in high prices and a discharging battery. Hereby, price and demand spikes are either shaved or totally prevented.

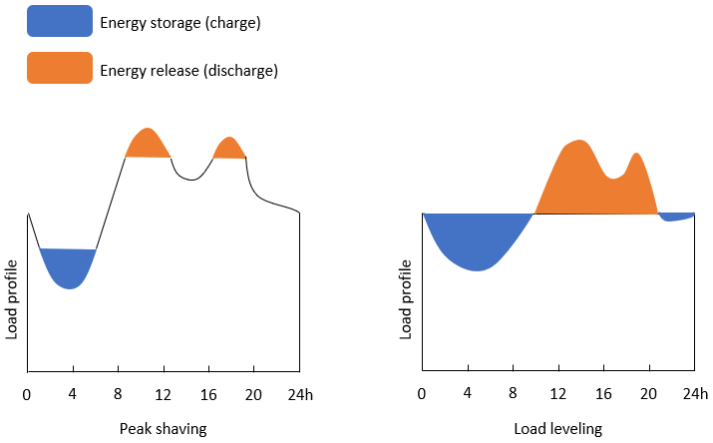

Figure 1.3: Principles of peak shaving and load leveling

In general, the capacity of peak shaving batteries falls within the range of 0.1 - 10 MW whereas load leveling requires a power capacity of 1 - 100 MW (Butler, 1994; Soloveichik, 2011). Since load leveling achieves a flat curve and therefore decreases costs most, this is most desirable for the revenue of the hybrid installation. However, the BESS as considered in this thesis are in the lower range of load leveling/ in the higher range of peak shaving (1 - 10 MW) due to physical space limitations.

Wholesale energy arbitrage

The second way of enhancing the economic viability of a hybrid installation is the ability of a BESS to trade on the electricity markets. The electricity markets system is discussed in greater detail in Appendix A.3. In this thesis, the focus is solely on energy arbitrage within the DAM, which involves energy trading in time periods of one hour. This activity is referred to as wholesale energy arbitrage. Besides acitivity on the DAM, trading on the the intra-day market (IDM) and on the frequency containment reserve (FCR) market is possible for a stationary BESS as well.

The reason why trading on the IDM and/or the FCR is not considered is based on specific factors. Firstly, the volume which is traded on the IDM is smaller compared to the volume traded on the DAM (epexspot.com, 2023). For example in June 2023, according to EPEX SPOT data, the volume traded on the IDM was 13624 GWh (25 percent of total) whereas the volume traded on the DAM was 44078 GWh (75 percent of total), for a similar average price of around 93 €/MWh (Epexspot, 2023). In addition, due to the absence of clear IDM data, this study focuses on the DAM and excludes the IDM. In Chapter 5, the impact of excluding the IDM is discussed in greater detail.

Secondly, in addition to the fact that participation in the FCR market requires a pre-qualification test which is more complicated for a hybrid installation compared to a stand alone BESS, an FCR participating BESS must be in the range of higher power (Zwang, 2022). Since consumer energy arbitrage is prioritised in hybrid installations, which requires BESS in the range of higher energy, the functionality of FCR is less suitable for the type of BESS as considered.

With wholesale energy arbitrage, the BESS operator capitalises the time-dependent price differences of the electricity market (Braeuer et al., 2019). Thereby, a wholesale energy arbitrage revenue stream is created. The battery can only be active with trading when there is no electricity demand from

vessels since the load from the shore power installation is prioritised.

To conclude, the profit generated by a hybrid installation is examined in this study, taking into account the boundaries of the capacity of the BESS (1 - 10 MW) and the necessity of high energy capacity and storage duration of (an) hour(s).

1.2. Research questions

The aim of the research is established according to the research gap as is described in Section 2.4. The research objective is summarised in the research question and sub-questions which are provided in this Section. The answers on the questions can be found in Chapter 6.

The objective of this study is to provide an overview of whether different types of BESS can potentially improve the economic viability of shore power installations in portal areas, by consumer- and wholesale energy arbitrage. The PoR is being utilised as a case study for this research. As the PoR is the largest port in Europe, the impact of sustainability is most noticeable here. Additionally, the PoR is a pioneer in the transition towards a sustainable future, making it easier for other, smaller ports to learn from their practices. The results of the study can be applied more broadly, for instance, to other ports such as the Port of Antwerp. The objective of the study is summarised according to the following research question.

Which battery energy storage 04systems are most suitable to enhance the economic viability of shore power projects in the portal area of Rotterdam by using consumer- and wholesale energy arbitrage?

To answer the question throughout the research, the following sub-questions have been formulated.

1. *Which battery energy storage systems are considered and how are they different from each other?*

2. *Which shore power projects are evaluated and what are their specifications?*

3. *How do the revenue streams generated by consumer- and wholesale energy arbitrage of battery energy storage systems contribute to the economic viability of the hybrid installations?*

4. *How does consumer energy arbitrage contribute to the economic viability of the hybrid installations by enhancing the energy efficiency*[1] *and effectiveness*[2] *?*

1.3. Research approach

The course of the research is presented in a flow diagram, based on the questions as mentioned previously. The process flow diagram is presented in Figure 1.4.

The first step of the research is the design of the model, which starts with the design of the process. The process design consists of two parts answering research sub-questions 1 and 2, where an analysis of different battery types and shore power projects are conducted respectively. The output of the process design is a selection of batteries and shore power projects including their specific parameters.

For the selected batteries the safety, costs and technical performance are of importance and for the shore power installations the electricity usage of vessels, geography and physical space are essential. These specific parameters are the input of the second part of the model design, namely the process modeling. Within this model the different configurations are tested. The model is constructed with Matlab and is referred to as the algorithm. The algorithm has been created to simulate diverse types of batteries, with size (energy and power capacity) as a variable, in various shore power installations.

[1] The energy efficiency of a hybrid installation refers to the percentage of the total annual energy demand of the vessels that is supplied by electricity from the battery.

[2] The effectiveness of a hybrid installation refers to the percentage of the yearly total operational revenue generated by consumer energy arbitrage.

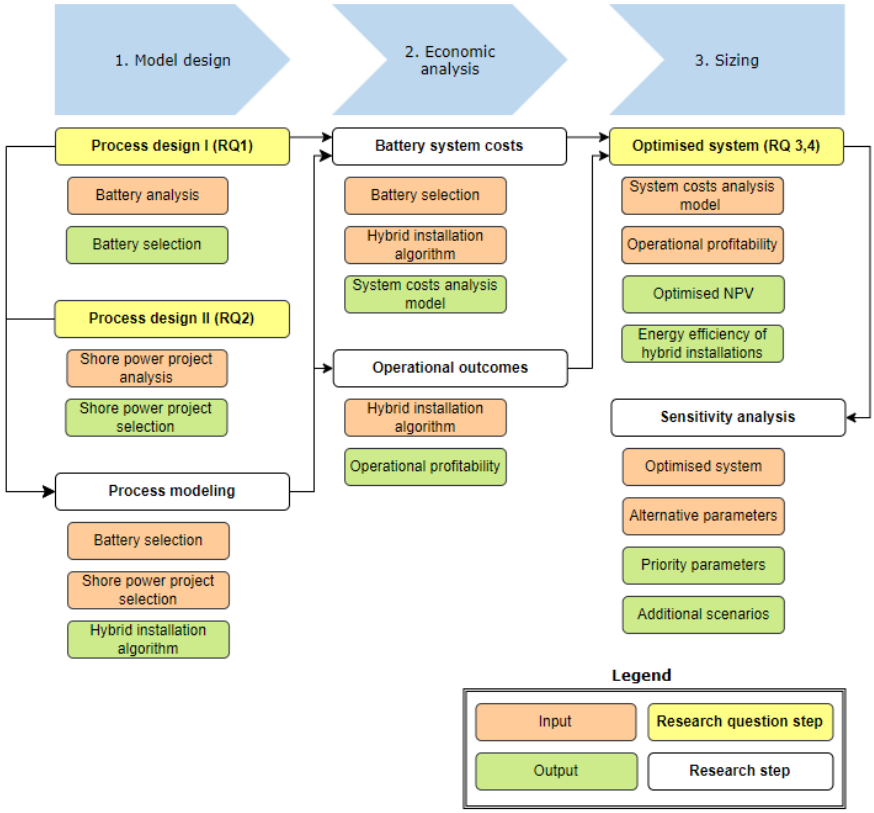

Figure 1.4: Research process flow diagram

Furthermore, it allows for the adjustment of electricity prices based on a specified year.

The second step involves an economic analysis of the system. First, an economic evaluation model is built in Microsoft (MS) Excel, where the total system costs of various BESS types and sizes can be determined. Besides general- and BESS specific input parameters and cost data, results of the hybrid installation algorithm are used as input of the cost model as well, namely the yearly number of cycles of a certain BESS type and size. Then, the operational profitability, which is a result of the algorithm, is combined with the system costs to determine the economic viability for a certain BESS type and size in a hybrid installation.

The final process step is sizing the BESS in hybrid installations. Based on the optimal net present value (NPV) for a certain hybrid installation, which is calculated with the operational profitability and the system costs, the optimal size of a BESS in the hybrid installation can be determined. The NPV seeks to provide insights into the economic viability of the hybrid installation by subtracting the present value of cash in and outflows over a period of time (Fernando, 2023). The second step of the sizing is to determine the energy efficiency enhancement and the effectiveness which is potentially created by the hybrid installations compared to individual shore power installations.

After succeeding the sizing of BESS in various hybrid installations, the results are evaluated by sensitivity analyses. In the sensitivity analyses various parameters are varied one by one in order to determine the effect on the result, namely the most optimal NPV of the hybrid installation. The goal of the sensitivity analyses is to determine which input parameters are affecting the outcome the most and therefore these parameters must be prioritised when designing hybrid installations. In addition to the sensitivity analyses, potential economically attractive scenarios of hybrid installations are mentioned. Eventually, the various process steps provide answers on the research sub-questions, which leads to the answer on the research question.

1.4. Document outline

This Chapter mainly focused on introducing the topics which are addressed in this thesis. Also, the research questions and the approach to answer the questions were mentioned. Chapter 2 elaborates on the state-of-the-art in scientific literature of these topics. The state-of-the-art review provides insights in the research gap which is addressed with this study, aiming to contribute to scientific literature. The literature review is followed by an explanation about the methodology in Chapter 3, explaining the approach to answer the research question in more detail. Then, Chapter 4 elaborates on the case study which is conducted in the portal area of Rotterdam and explains which shore power installations are the focus of this study. After the case study, Chapter 5 delves into the results and the discussion of the research which is conducted and provides insights in various additional potential scenarios for enhancing economic viability of hybrid installations. To prevent repetition, the results and their discussion are interwoven in the same Chapter. Lastly, Chapter 6 provides the conclusion, including the answer on the research questions as well as recommendations for future research.

In addition to the research presented in the Chapters as previously mentioned, a substantial portion of the background knowledge and information is documented in the Appendices. The first Appendix, Appendix A, elaborates on BESS whereas Appendix B focuses on shore power. Appendix C provides additional results supporting Chapter 5. For further details, one is kindly referred to the Appendices.

2. Literature review

This Chapter comprises a literature review of the state-of-the-art of essential topics for this study. First, Section 2.1 elaborates on the selection process of different types of suitable BESS for hybrid installations as considered in this study. The theory and details behind the different types of batteries which are analysed can be found in Appendix A.4. This part of the literature study comprises the first step of the process design, according to the research process flow diagram presented in Figure 1.4. Then, Section 2.2 provides information on the most recent developments in the field of shore power in portal areas. Third, Section 2.3 elaborates on the latest knowledge found in literature about the combination of shore power and BESS. The goal of the theoretical framework at the end is to provide an overview of present knowledge as well as to define the current knowledge gap. The relevance of this study arises from the research gap.

2.1. Battery energy storage systems

This Section elaborates on the process of searching, selecting and evaluating different categories, sub-categories and types of BESS by assessing literature, with the aim to determine whether they have the potential to operate in grid-connected mode. The process follows a pyramidal shape, existing of four consecutive steps. When the first step is concluded, the second and third step are conducted consecutively for each battery type. Eventually, after the selection process, the growth over the past period of time of every selected battery type is analysed to narrow down the final selection to the most suitable and promising batteries for hybrid installations. The process is visualised in Figure 2.1.

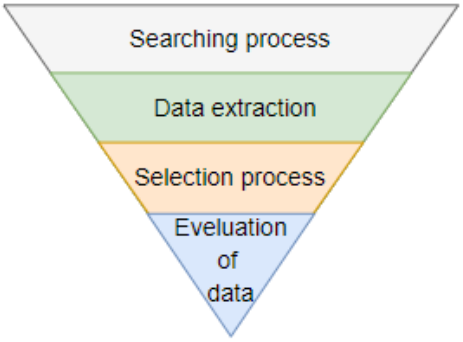

Figure 2.1: Literature review of battery energy storage systems process steps

As mentioned in Chapter 1, among various storage systems, BESS are selected for analysis in this research. To be suitable for integration into the electricity network and specifically into hybrid installations, BESS have to fulfill certain general requirements. For example, the technology needs to be proven prior to integration taking place, the costs need to be as low as possible, the design needs to have a degree of flexibility and the performance should be sufficient for the specific needs of the application. Additionally, an important characteristic which is considered is safety, to which a lot of attention has been devoted in recent literature.

Solyali et al. examine the relationship between battery storage and the grid (Solyali et al., 2022). The BESS explored in the review are conventional secondary batteries based on lithium (Li), sodium (Na), nickel (Ni), lead-acid and flow batteries (FB). Besides this review, there exist numerous reviews that investigate a similar set of batteries related to grid-connected systems (Argyrou et al., 2018; Dunn et al., 2011; Fan et al., 2020; Hussain et al., 2020; Kebede et al., 2022; X. Luo et al., 2015).

There are also more specific reviews that focus on each of the different sub-categories or even on only one battery type, some examples are (Benato et al., 2015; Chakkaravarthy et al., 1991; T. Chen

et al., 2020; Kurzweil, 2015; Leung et al., 2012) Also, some reviews tend to compare different sub-categories of BESS to each other, for example in (Albright et al., 2012; Fetcenko et al., 2015; Spanos et al., 2015; Tran et al., 2021; Zeng et al., 2015).

The literature review provided knowledge about which battery sub-categories are currently suitable for commercialisation for stationary grid-connected applications within the categories of conventional secondary batteries and FB. Within conventional secondary batteries, four different sub-categories are analysed: Li-, Ni-, Na-based and lead-acid batteries. Within each sub-category of secondary batteries different types of batteries are assessed as well. Additionally, two different sub-categories of FB are assessed, redox flow batteries (RFB) and hybrid flow batteries (HFB) as well as the various types accompanied.

Figure 2.2 provides an overview of the battery sub-categories and types which are assessed within the two main categories of BESS. The first step of the process was thus successful and the batteries for further analysis were defined.

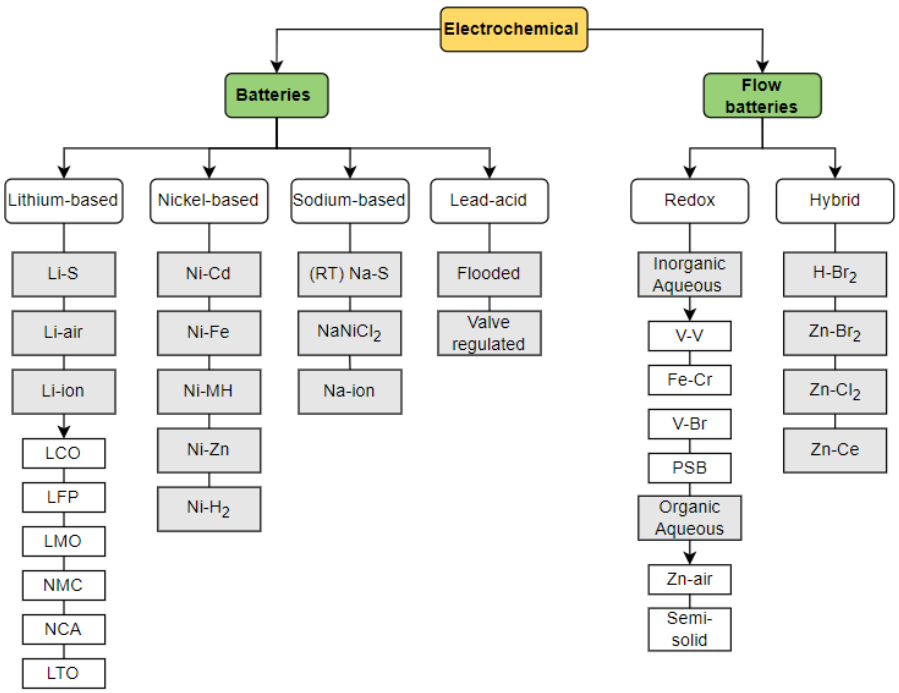

Figure 2.2: Overview of batteries assessed

The searching process is followed by data extraction from literature. With this data, the most suitable batteries for the hybrid installations are selected for further research. Besides taking into account the pre-defined boundary conditions and key performance indicators (KPI's), both presented in Appendix A.4, technologies are chosen which are either commercialised already, or which are not possessing too many challenges preventing the development. The following Subsections elaborate on the data and information extracted from literature for each BESS type which is assessed.

Lithium-based batteries

As mentioned by T. Chen et al., Li-ion batteries have seen a significant potential in grid-integrated storage systems (T. Chen et al., 2020). Reasons are based on the fact that Li-ion batteries have high specific energies and power, high efficiencies and also a long lifetime. The high specific energy is valuable in the situation of a high penetration of renewable electricity in the grid, as shown in Figure A.1 (Argyrou et al., 2018). These characteristics are validated by various reviews found in literature (Abu et al., 2023; Hesse et al., 2017; Kebede et al., 2022; Kurzweil, 2015; Mongird et al., 2019; Nemeth et al., 2020; Petrov et al., 2021; Rouholamini et al., 2022).

Deng et al. (Deng et al., 2018) state that despite the fact that Li-ion batteries are a mature technology, the scarcity of Li, and thus the high costs, and safety concerns limits Li-ion to be even more widely deployed in large-scale, stationary applications. However, the review of Eftekhari has provided more realistic insights on this topic (Eftekhari, 2019). Eftekhari acknowledges that Li is less abundantly available than Na or Ni. However, it is believed that there should be a sufficient supply of Li available in nature to support the growing market for Li-based batteries in the longer term.

T. Narins explains that the problem with Li is based on the disparity between Li consumption and production, rather than the availability of Li as a raw material (Narins, 2017). Consumption exceeds production, leading to higher prices. The 2015 deficit, which caused price spikes, raised concerns about Li scarcity. According to Eftekhari, the motivation to explore alternatives to Li-based batteries is not driven by Li scarcity but rather the pursuit of new technological opportunities (Eftekhari, 2019). The review also provides some insights about the currently low Li recyclability. The recycling costs are exceeding the value of Li, making regulations essential to incentivise Li recycling.

Within the sub-category of Li-based batteries, research has explored new candidates that offer similar performance and increased energy density compared to Li-ion batteries. Among the candidates, Li-sulfur (Li-S) and Li-air are considered as most promising, as indicated by Skundin et al. (Skundin et al., 2018). However, a comprehensive review of Solyali et al. raises concerns about the suitability of Li-S batteries for large-scale storage applications due to their low reliability (Solyali et al., 2022). Additionally, as noted by E. Kelder and by L. Su et al., Li-air batteries show potential for enhancing the energy density of Li-based batteries compared to Li-ion (Kelder, 2019; L. Su et al., 2015). Nonetheless, due to the numerous challenges they face, their commercialisation has been discontinued.

In 2015, P. Kurzweil conducted a state-of-the-art study on Li-based BESS (Kurzweil, 2015). Kurzweil's work marks the initial step from research to selection by explaining the distinction between metal-based and ion-based Li batteries. Given the secondary nature of Li-ion batteries, Kurzweil's study primarly focuses on them. Five different cathode materials were analysed, which are lithium cobalt oxide (LCO), lithium iron phosphate (LFP), lithium manganese oxide (LMO), lithium nickel cobalt manganese oxide (NMC) and lithium nickel cobalt aluminum oxide (NCA).

Several reviews have examined the same cathode materials (Hesse et al., 2017; Kurzweil, 2015; Nemeth et al., 2020; Rouholamini et al., 2022). Therefore, the five Li-ion cathode materials are selected in this thesis as well. It became clear from the reviews that the cathode materials LFP and NMC are most suitable for the hybrid installations, since their capabilities in peak shaving/ load leveling applications are proven.

Additionally, Hesse et al. provided insights into lithium titane oxide (LTO), which is a possible alternative anode material to graphite in Li-ion batteries (Hesse et al., 2017). Batteries equipped with an LTO anode have the capability of fast-charging, according to Nemeth et al. (Nemeth et al., 2020). Hesse et al. and Nemeth et al. share the conclusion about LTO batteries being most suitable for high power applications (Hesse et al., 2017; Nemeth et al., 2020). Therefore, Li-ion batteries with graphite anodes are most interesting since the alternative anode material LTO is more costly and used for high power applications.

Among the various Li-ion cathode materials, LFP is most interesting because of the high stability for moderate costs, accompanied by a high power capacity. 80 percent of the energy stored in LFP battery is provided at a stable voltage, recognised as a plateau in the voltage curve. This constant voltage makes the design more easy and stable. Also, the absence of cobalt is beneficial. This combination of characteristics makes LFP more interesting among other Li-ion batteries for stationary applications, according to Hesse et al. (Hesse et al., 2017).

NMC batteries are safe, have a high lifetime and energy density and are cost competitive. Among others, Hesse et al. explain however that using Co is never ideal because of the scarcity and thus a high raw material price as well as because the supply chain risks (Hesse et al., 2017). This conclusion is reinforced by Abu et al. and Rouholamini et al. (Abu et al., 2023; Rouholamini et al., 2022). Since

safety and costs are considered as more important than the energy density, this study considers LFP as more suitable than NMC. Therefore, only LFP is selected for further analysis into the implementation in hybrid installations. This conclusion is substantiated by the results of a study into the projected market share of different Li-ion BESS over the period from 2015 to 2030. The market share of LFP batteries is steadily increasing while NMC's is diminishing. The result of the study is visualised in Figure 2.3 (Mackenzie, 2020).

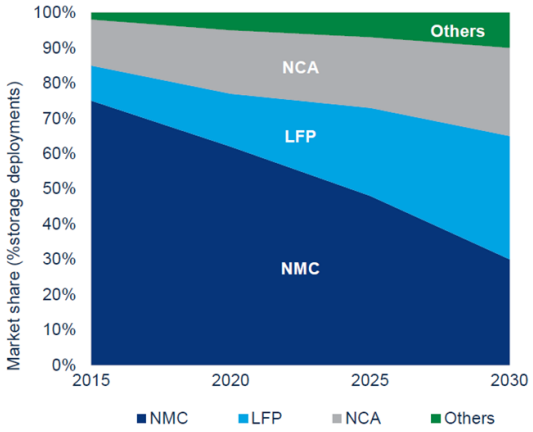

Figure 2.3: Lithium ion battery market share forecast over the period 2015 - 2030 (Mackenzie, 2020)

Nickel-based batteries

According to Wang et al., Ni-based batteries are used in stationary applications because of their high energy density at low costs, caused by the abundant availability of Ni (L. Wang et al., 2022). Various anode materials exist for Ni-based batteries. The five Ni-based sub-categories which are mostly reviewed in literature are Ni-cadmium (Ni-Cd), Ni-iron (Ni-Fe), Ni-zinc (Ni-Zn) Ni-hydrogen (Ni-H_2) and Ni-metal hydride (Ni-MH) (Chakkaravarthy et al., 1991; Hussain et al., 2020; Kebede et al., 2022; Salkuti, 2021; Solyali et al., 2022). Hence, this thesis also focuses on this selection of Ni-based batteries.

The review of Hussain et al. contains information on multiple different BESS (Hussain et al., 2020). Also, a similar selection of Ni-based batteries as is considered in this thesis is being discussed. The review highlights the fact that Ni-Cd batteries possess high performance parameters, making them suitable for the application of this research. This conclusion is substantiated by Kebede et al. and Salkuti (Kebede et al., 2022; Salkuti, 2021). However, Ni-Cd batteries contain toxic Cd of which recycling processes are not widely developed yet. Fortunately, progression is being recognised as is mentioned by Salkuti (Salkuti, 2021). In addition, Argyrou et al. explain the memory effect of Ni-Cd batteries (Argyrou et al., 2018). When the battery is recharged multiple times after being partly discharged, the capacity and lifetime decrease fast. In the case of peak shaving or load leveling applications the memory effect is likely to happen.

The review of Hussain et al. provides information about the price of environmentally friendly Ni-Fe batteries, being four times as high as compared to lead-acid or Li-ion batteries (Hussain et al., 2020). Chakkaravarthy et al. and Solyali et al. mention the usability of Ni-Fe batteries in vibrating applications (Chakkaravarthy et al., 1991; Solyali et al., 2022). However, Chakkaravarthy et al. mention the drawback of the low round-trip efficiency (RTE) of Ni-Fe batteries which is below the boundary condition of 75 percent which is employed in this thesis (Chakkaravarthy et al., 1991). More information on the boundary conditions on which the various BESS types are assessed can be found in Appendix A.4.

The review of Hussain et al. proceeds with the characteristics of Ni-Zn batteries, which are environmentally friendly and non-toxic (Hussain et al., 2020). However, the main disadvantage is the cycle life which is lower than the boundary condition of this study, which is one cycle a day for five years at least. Other problems associated with Ni-Zn batteries are assessed by Chakkaravarthy et al. and Spanos et al. (Chakkaravarthy et al., 1991; Spanos et al., 2015).

Ni-H_2 batteries are mainly used for aerospace applications, which is among others mentioned by Chen et al. (W. Chen et al., 2018). Eventually, Ni-MH seems to be the most promising Ni-based battery, according the reviews of Hussain et al. and Salkuti (Hussain et al., 2020; Salkuti, 2021).

Ni-MH batteries are environmentally friendly and possess suitable characteristics for hybrid installations. A major drawback is the use of rare earth materials in Ni-MH batteries, which are mainly sourced from China. China has stopped the export of rare earth materials, therefore imposing supply chain risks for Ni-MH batteries (Mancheri, 2015). According to Argyrou et al., Ni-MH batteries do not get affected so much by the memory effect as Ni-Cd batteries do (Argyrou et al., 2018). Therefore, among the Ni-based batteries Ni-MH seems most promising for grid-connected BESS. However, due to the current supply chain risks, Ni-MH batteries are not taken into account for the remainder of this thesis.

Sodium-based batteries

Butler elaborates on the potential of Na-based batteries in implementation of large-scale grid-connected BESS, which is caused by the abundance of Na on earth (Butler, 1994). Butler also explains about the biggest drawback of Na-based batteries, which is their high operational temperature. However, the drawback is not considered as disastrous for applications which are used routinely, which is the case for hybrid installations. However, it should be kept in mind that the necessary encapsulation for thermal regulation is unfavourable for operational maintenance and system costs.

References (Solyali et al., 2022; Y.-X. Wang et al., 2017; Yan et al., 2022) explain about the characteristics of Na-sulfur (Na-S) batteries. After development of high temperature Na-S batteries, room temperature Na-S batteries were developed as well. However, the latter is still facing too many challenges to be considered as suitable for hybrid installations.

References (Benato et al., 2015; Mongird et al., 2019; Solyali et al., 2022; Sudworth, 2001) elaborate on the potential of sodium nickel chloride ($NaNiCl_2$ or ZEBRA) batteries in grid-connected systems. Compared to Na-S batteries, $NaNiCl_2$ batteries are more safe. Argyrou et al. elaborate on the disadvantages which are experienced by $NaNiCl_2$ batteries, namely their lower energy and power density compared to Na-S batteries (Argyrou et al., 2018). However, safety is considered as more important. Since both batteries are suitable for load-leveling applications, $NaNiCl_2$ is selected for further analysis.

Skundin et al. mention the potential of Na-ion batteries to replace Li-ion batteries (Skundin et al., 2018). The progress report of Deng et al. agrees with the statements as mentioned in the review (Deng et al., 2018). However, Deng et al. have provided insights on the challenges of commercialisation of Na-ion batteries, which are currently preventing them from further development. Therefore, Na-ion batteries are not selected for further research.

Lead-acid batteries

Fan et al. and Zhang et al. provide reviews about the performance, advantages and challenges of lead-acid batteries (Fan et al., 2020; Y. Zhang et al., 2022) . The review of Spanos et al. highlights the fact that lead-acid batteries have the lowest environmental footprint due to their developed recycle infrastructure since lead-acid batteries are among the most mature of all battery types (Spanos et al., 2015). Another important factor causing lead-acid batteries to be suitable for grid-connected applications is their high safety.

However, their low cycle life and lower energy density are considered as drawbacks. According to Soloveichik, the valve regulated lead-acid (VRLA) battery type is more often used for stationary applications compared to flooded lead-acid batteries (Soloveichik, 2011). This is due to the fact that VRLA batteries are maintenance-free, increasing the lifetime of the BESS, whereas the flooded lead-acid battery needs addition of distilled water.

Butler assesses three different BESS sub-categories (lead-acid, Na-S and zinc bromine HFB (ZBB)) as well as all various applications of grid-connections (Butler, 1994). This review reveals insights on the fact that every specific application has their own best choice of battery type. According to the analysis

provided by Butler, Na-S and ZBB batteries are both excellent for customer demand peak reduction whereas VRLA batteries are considered adequate.

Based on the findings, VRLA batteries are decided to be taken into account as potential for the hybrid installations mainly due to their high safety and commercial maturity. The short cycle life is taken into serious consideration, however, this does not outweigh the other characteristics.

Redox flow batteries

A report of the International Renewable Energy Agency (IRENA) elaborates on the distinct performance and characteristics of FB compared to conventional secondary electrochemical batteries (Renewable, IRENA, et al., 2017). The facts that FB can scale energy and power independently, have a high cycle life and a high safety in terms of thermal runaway are explained here. However, the review also explains the negative aspects of FB which are the high amount of moving elements in the system, which could potentially lead to increased repair costs and a lower energy efficiency compared to conventional secondary BESS. The advantages and potential as well as the disadvantages of using FB for large-scale BESS are also highlighted in other references, for example by Argyrou et al. and Fan et al. (Argyrou et al., 2018; Fan et al., 2020). Additionally, the report of the IRENA provides information on the two possible sub-categories within FB, namely RFB and HFB (Renewable, IRENA, et al., 2017). In a review of Yao et al., the trade-off between a HFB with a higher energy density or a RFB with a more simple design and which is more easy to scale is highlighted (Yao et al., 2021).

Tang et al. explain the different sub-categories within RFB (Tang et al., 2022). First, the distinction between aqueous and non-aqueous systems is made, namely whether the electrolytes are water based or not, respectively. Tang et al., as well as the review of Cao et al., provide insights on why non-aqueous systems are lacking performance (Cao et al., 2020; Tang et al., 2022). Namely, the viable active materials are not easily found. Therefore, non-aqeous RFB are not considered for the remainder of this thesis.

Tang et al. also elaborate on the two possible types of aqueous RFB, namely inorganic and organic active species can be solved in the water-based electrolyte. Inorganic RFB are most often based on metal ions and potentially suffer from corrosion and high costs, whereas organic RFB strive to solve these problems. The IRENA's report explains similar characteristics (Renewable, IRENA, et al., 2017). Based on literature reviews, the selected aqueous (in)organic RFB and HBF for further research are discussed below.

The review of Zeng et al. compares two inorganic aqueous RFB, vanadium RFB (VRB) and iron chromium RFB (ICB) (Zeng et al., 2015). Other reviews focusing on VRB and ICB are found in literature as well (Alotto et al., 2014; Argyrou et al., 2018; Blanc & Rufer, 2010; Ciotola et al., 2021; Leung et al., 2012; Lim et al., 2015; Petrov et al., 2021; Revankar, 2019; Rodby et al., 2023; Soloveichik, 2011; Zeng et al., 2015). Zeng et al. aim to answer the question which of both systems is most suitable for large-scale ESS, taking into account the energy efficiency, cycle life and capital costs. It is highlighted that VRB possess high capital costs because of the use of vanadium, which is costly. However, VRB have the benefit of the similarity of the active species which are used on both sides of the cell, making the system simple. Also, the kinetics are excellent. On the other hand, the ICB uses cheaper materials but has a high degree of system complexity due to mitigation of capacity degradation. Eventually, VRB is selected for the remainder of this thesis. ICB's high maintenance is considered as less favourable compared to the high costs of VRB, which could potentially be lowered by economies of scale in the future.

The vanadium bromine RFB (VBB) was developed with the aim to replace the costly VRB by changing vanadium to bromine. Cunha et al. and Soloveichik explain the benefits and disadvantages of this type of RFB compared to VRB (Cunha et al., 2015; Soloveichik, 2011). VBB has an increased energy density, thereby reducing costs. However, the potential environmental hazards which are associated with the bromine gas rejection upon failure of the battery are considered as important, therefore this thesis is not considering VBB as potential for the hybrid installation.

The potential negative effect on the environment is also recognised by polysulfide bromine RFB (PSB). Argyrou et al. and Fan et al. provide information on PSB, which are most suitable for power related storage applications (Argyrou et al., 2018; Fan et al., 2020). Additionally, the challenges which are limiting the roll-out of PSB towards commercialisation are significant and therefore PSB is not considered as suitable for the remainder of this study as well.

The reviews presented in references (Y. Kumar et al., 2023; Leung et al., 2012; W.-F. Wu et al., 2023) mention the promising aspects of a type of organic aqueous RFB, namely Zn-air. The safety, low costs and abundance of materials are considered as advantageous. However, the development of the technology is limited by the performance. Additionally, E. Kelder et al. and Kiriinya et al. provide insights on another organic aqueous RFB which is very immature, namely the semi-solid RFB (Kelder et al., 2022; Kiriinya et al., 2023). Since there are no hurdles to be overcome yet, this battery technology is taken into consideration as suitable for this thesis. The low costs and abundantly available and safe materials are driving the potential.

Hybrid flow batteries

The report of Arenas et al. provides a list of different HFB, based on negative Zn electrodes (Arenas et al., 2018). From the list, the three most mentioned in literature, which have the highest voltages among all, were further analysed since high voltages correspond to lower losses. Two of them, ZBB and Zn-chloride (Zn-Cl_2) HFB, are based on potentially dangerous materials (Br_2 and Cl_2). Leakage of those materials in the gaseous state towards the environment is harmful.

Despite these concerns, ZBB is suitable for peak shaving/ load leveling applications, which is highlighted by among others Soloveichik (Soloveichik, 2011). Therefore, ZBB is selected for further research, taking the safety concerns as well as the size of the system in mind.

The third Zn-based HFB, Zn-cerium HFB (ZCB), assessed is explained by references (Arenas et al., 2018; Soloveichik, 2011; Xie et al., 2013) and does not suffer from potential environmental hazards but lacks development towards commercialisation because of high costs and capacity decay by cross-mixing of the electrolyte. Therefore, ZCB are not selected for further analysis.

Additionally, a HFB based on hydrogen bromine (H_2-B_2 or HBB) is analysed as well since its potential for large scale BESS is sufficient according to Cho et al. and Petrov et al. (Cho et al., 2012; Petrov et al., 2021). However, due to the doubled chance of environmental problems since both $H_{2(g)}$ and $Br_{2(g)}$ are formed within the battery, HBB is not further analysed within the scope of this thesis.

2.1.1. Selection of batteries

The literature review of which the most important aspects are described previously and the (technical) details are provided in Appendix A.4, has led to a selection of different battery types within the two categories assessed, which are considered as suitable for further analysis. Since each hybrid installation has its own specifications as well as every BESS, multiple (six) BESS types are selected. The selected conventional secondary electrochemical batteries are LFP, $NaNiCl_2$ and VRLA whereas the selected FB are VRB, semi-solid RFB and ZBB.

To ensure that the selection is not solely based on literature but also on practicality, the selection process is expanded by evaluating data on market growth of the various BESS types over the past years. As mentioned in Chapter 1, the size of the global stationary BESS market was 9 GW/ 17 GWh in 2018 and is expected to reach 1095 GW/ 2850 GWh of installed power/ energy capacity by 2040.

According to Killer et al., the implementation of Li-ion BESS in the region of Europe, Middle East and Africa experiences an exponential growth with an annual growth rate of 50 percent (Killer et al., 2020). According to a report of Schmidt and Staffell, the annual demand for Li-ion batteries is projected to grow from 500 GWh in 2020 to > 3000 GWh by 2030 (Schmidt & Staffell, 2023). An example of an Li-ion manufacturer is CSI Energy Storage. CSI Energy Storage is an LFP manufacturing company in China (Kennedy, 2022). Their projected annual battery manufacturing output capacity is projected to reach 10 GWh by the end of 2023, which is more than half of the global BESS energy capacity which

was present in 2018.

Another recent publication of Maisch elaborates on a large-scale grid-integrated LFP project as well (Maisch, 2023). There are multiple other proven LFP practical implementations (Colthorpe, 2021, 2022). This implies an increasing market growth and demand for LFP batteries, supporting the conclusion to take LFP batteries into account as suitable for hybrid installations.

A report of Shamim et al. provides insights on grid connected battery projects around the world (Shamim et al., 2019). The report mostly focuses on projects using Li-ion batteries, but also on projects using $NaNiCl_2$, VRLA, VRB and ZBB batteries. However, besides this report, limited practical examples of the use of $NaNiCl_2$ batteries were found, except from $NaNiCl_2$ batteries used in electromobile applications (O'sullivan et al., 2006). Therefore, the use of $NaNiCl_2$ batteries in hybrid installations is not further analysed.

The global lead-acid battery market is expected to exhibit a compound annual growth rate (CAGR) of 5.2 percent during the period of 2019 to 2030. According to a report of the Storage Future Study series of NREL, lead-acid batteries already have a large market share, existing of lead-acid batteries used for mobile and stationary applications (NREL, 2022). According to a report which can be found here (insights, 2023), the use of lead-acid batteries in stationary applications is growing. Therefore, VRLA batteries are taken into consideration for the remainder of this study.

The global VRB market is expect to experience a CAGR of almost 20 percent during the period 2023 to 2030 (Forecast, 2023a; market research, 2023). The reason for the growth is mainly due to the immaturity of the market of VRB in combination with the potential of VRB to be implemented in grid-connected systems. As stated by Schmidt and Staffell, the VRB market was around 100 MW in 2020 (Schmidt & Staffell, 2023). A practical example of the implementation of VRB in connection to the grid is located in Dalian, northeast China. The power station has an operational power of 100 MW and energy of 400 MWh (Todorovic, 2022).

Also, the global ZBB market has an expected CAGR of around 18 percent during the period of 2023 to 2028 (Forecast, 2023b; market forecast, 2023). A real-life example is the 20 MWh ZBB project in California, provided by Redflow (Redflow, 2023). Therefore, the two FB are taken into account as suitable for hybrid installations.

Since the semi-solid RFB is still immature, the expected CAGR for practical implementation cannot be mentioned here. However, since there are no drawbacks known yet, this type of battery is taken into further consideration because of the promising features.

To conclude, from the secondary electrochemical batteries category, LFP and VRLA batteries are taken into consideration whereas from the FB category VRB, semi-solid RFB and ZBB are considered in the remainder of this thesis. In terms of size, the first category is mainly implemented into smaller applications, where less physical space is available whereas the FB category is mostly recognised in more substantial industrial applications where space not the limiting factor and an extended energy capacity is desired. The selection, which is based on literature and practical data, is visualised in Figure 2.4. Since the literature review has provided insights into the highest potential BESS for hybrid installations, the upcoming Section focuses on the development of the other component of a hybrid installation, namely on shore power.

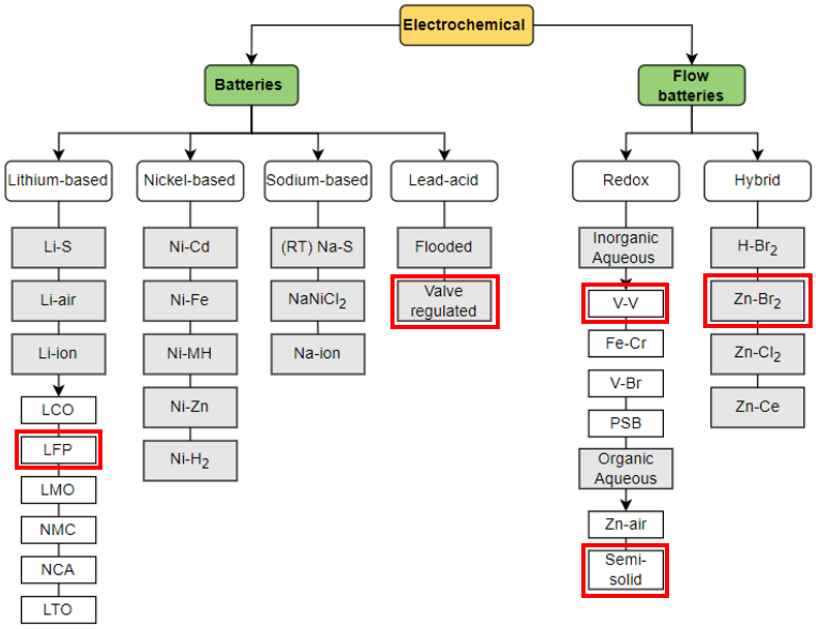

Figure 2.4: Overview of batteries selected

2.2. Shore power

This Section focuses on the state-of-the-art literature about shore power installations in portal areas and the challenges associated with the development. Most literature focuses on one or more of the following aspects: economics, environment and regulations. Table 2.1 presents the literature assessed, categorised by the specific topics.

Table 2.1: Comparison of studies related to shore power

Reference	Economics	Environment	Regulations
(Feng & Li, 2017)	✓		✓
(Winkel et al., 2016)	✓	✓	✓
(Coppola & Quaranta, 2014)	✓		
(Ketterer, 2014)	✓		
(Stolz et al., 2021)		✓	✓
(Bakar et al., 2023)	✓		✓
(Sciberras et al., 2015)			✓
(Williamsson et al., 2022)			✓

Feng and Li have studied the safety and economics of utilising shore power for seagoing vessels (Feng & Li, 2017). This study highlights the importance of following safety procedures during the full process of developing, placing and utilising shore power. The economic analysis highlights the dependence of the willingness of vessel owners to use shore power on the auxiliary engines' fuel price. The study concludes with the statement that policies from the government are necessary incentives in the roll-out of shore power.

R. Winkel et al. assess the potential for the application of shore power installations in European ports, from both an environmental and economic point of view (Winkel et al., 2016). The report concludes that cruise ships and ferries are most interesting for using shore power installations since they use the most electricity while berthing. Locations where the impact is mostly recognised should implement shore power first, near residential areas for example. Furthermore, the potential for deployment of shore power in Europe is high, based on the associated health benefits and the goals in emission reduction. As in multiple other reports, the necessary incentive which should be provided by governmental regulations is highlighted.

Coppola and Quaranta explain how the economic viability of shore power installations varies per case since this is determined by the total costs of onboard electricity usage as well as the total costs of the shore power which is potentially used (Coppola & Quaranta, 2014). The total costs of onboard electricity usage depend on the type of vessel whereas the costs of shore power depend on the contract between the vessel owner and the terminal operator as well as on the local electricity price.

Economic viability of the utilisation of shore power is assessed from two points of view, namely from the terminal owners and the vessel owners. Besides the up-front investment costs, the operational costs of the vessel owner associated with using shore power are challenging the development. When berthing, the vessel owners' operational costs are made up of the price of the electricity which is necessary for the on-board activities. The electricity prices are strongly fluctuating (which is also referred to as volatile) because of the increasing penetration of RES in the electricity network, which is validated by Ketterer (Ketterer, 2014).

The report of Acemoglu et al. explains how prices are determined in the electricity markets, namely by balancing supply and demand (Acemoglu et al., 2017). The cheapest electricity produced is used first whereafter the more expensive produced electricity follows, until the demand is satisfied. Since RES have low to zero marginal costs, their electricity is used first in the merit order, pushing back the more expensive (grey) electricity producers. Hereby, RES eventually decreases the electricity equilibrium price. Increasing RES penetration is accompanied by a lower average electricity price as well as by higher price volatility. The economic viability of using shore power from the vessel owner's point of view is therefore dependent on the penetration of RES into the electricity grid.

The report of Stolz et al. elaborates on the potential environmental benefits of shore power utilisation in Europe and on the European regulations in 2021 (Stolz et al., 2021). First, the environmental benefits are defined by calculating the emissions at 714 berth locations through Europe when auxiliary engines are used. Eventually, the specific environmental benefits are calculated by their own developed model to estimate auxiliary power demand. Similar as mentioned before in this literature review, the report highlights the unfavourable market conditions with little to no incentives for installing shore power installations or receivers. Details on European regulations can be found in the report.

Shore power's success has been proven, however implementation of shore power installations is progressing slowly across different ports around the world. The upfront investment costs for the port operator as well as the high amount of vessels which are not ready yet, result in a low demand for shore power. Without direct (economic) incentives, ports do not establish shore power installations until enough ships are retrofitted to accept shore power. On the other hand, vessel owners resist retrofitting unless enough ports provide shore power at berths.

Fortunately, regulations for using and implementing shore power are upcoming (Bakar et al., 2023). The PCA has had an effect on the emergence of complementary policies regarding the environmental issue of today. For example in the European Union (EU), the Sulfur Directive limits the sulphur content of fuels consumed by vessels in EU ports to less than 0.1 percent by mass in the case the scheduled stay is longer than 2 hours (Sciberras et al., 2015). Also, the regulation for deployment of alternative fuels are motivating the use of renewable energy sources and electrification. Therefore, pressure from authorities is driving the development of more shore power installations (Bakar et al., 2023; Williamsson et al., 2022).

The EC has proposed a set of legislation and policies with the aim to accelerate the energy transition and to achieve the climate targets set by the EU. The set of policies is referred to as the ”Fit for 55” package. The effect of the package on the development of shore power is expected to be significant. The package proposes several measures to incentivise the adoption of shore power infrastructure and its use by vessels. This includes financial support, regulatory requirements, and the establishment of standards and guidelines for the implementation of shore power facilities in ports.

To be specific, the alternative fuel and infrastructure regulation obliges major seaports such as the PoR to be able to provide at least 90 percent of the vessels bigger than 5000 Gigatonnes and of the vessel types cruise, container or passenger (ferries) with shore power in 2030. In addition, the vessels are obliged to be able to receive and use shore power from 2030 and onwards.

Besides incentives provided by regulations, there are ways how ports could enhance the adoption rate of shore power installations by themselves such as by the additional implementation of BESS instead of developing a shore power installation on its own. The current state-of-art in literature on the topic of shore power combined with BESS is explained in the upcoming Section.

2.3. Shore power and battery energy storage

This part of the literature study aims to define the state-of-the-art of research into shore power installations in combination with BESS, in different configurations. The first part of the Section focuses on the physical configuration whereas Subsection 2.3.1 focuses on the various energy management strategies (EMS) which are implemented. The EMS determines the functionalities and the operation of the BESS. The reviews assessed are classified based on the configurations explained in their report, which is presented in Table 2.2.

Table 2.2: Comparison of studies related to the combination of shore power and battery energy storage systems

Reference	Shore power	Smart grid	Grid-connected	On-board (fixed) mobile battery		On-board (interchangeable) mobile battery	Stationary battery
				Electric vehicle integrated	Vessel integrated		
(Pintér et al., 2021)		✓			✓		
(Meliani et al., 2021)		✓		✓			✓
(Prousalidis et al., 2014)	✓	✓					✓
(J. Kumar et al., 2021)	✓	✓				✓	
(Caprara et al., 2022)	✓	✓					✓
(W. Wang et al., 2019)	✓	✓					✓
(Mutarraf et al., 2021)	✓	✓					✓
(Kanellos, 2017)	✓		✓	✓			
(J. Kumar et al., 2017)	✓	✓			✓		
This thesis	✓		✓				✓

The first distinction between the reviews is based on the flow of electricity, which is either through a local (portal area) smart grid or through the local electricity grid, of which the first was found more frequently in literature when combined with a shore power installation.

Smart grids are local energy networks where energy suppliers and consumers as well as controlling, monitoring and optimising tools are connected to each other (Pintér et al., 2021). Meliani et al. emphasise the importance of the presence of an EMS, to maintain a controlled smart grid (Meliani et al., 2021). The aim of smart grids is to increase the energy efficiency of transactions between energy supply and demand (Prousalidis et al., 2014). References (Caprara et al., 2022; D. Kumar et al., 2017; J. Kumar et al., 2021) contain information about smart grids as well.

Wang et al. propose a framework for the optimal design of a smart grid in portal areas, here consisting of RES, shore power, energy storage and conventional power (W. Wang et al., 2019). Prousalidis et al. explain in their review that combining the concept of smart grids with shore power installations reduces the necessary electricity infrastructure and therefore enhances the economic viability of the shore power installation as well as of the smart grid (Prousalidis et al., 2014).

The report of Kumar et al. highlights the added value of the integration of BESS in shore power installations in portal area smart grids (J. Kumar et al., 2017). According to Kumar et al., BESS enhance reliability and stability of the smart grid since the intermittency is increasing by implementing RES. The report explains the economic benefit of charging the battery during periods of cheap electricity, either caused by a low demand or a high penetration of RES, and discharging during periods of peak load. Also, the reduction of infrastructure by the integration of BESS in smart grids in portal areas is highlighted. Eventually, the design of a shore power installation is presented which is focusing on charging interchangeable batteries from electric vessels on the shore side.

The reports of Capara et al. and Mutarraf et al. elaborate on the design of a smart grid where photovoltaic (PV) energy and other RES are connected to among others shore power installations in portal areas (Caprara et al., 2022; Mutarraf et al., 2021). To prevent the infrastructure of the port to be reconstructed, a stationary BESS is necessary, accompanied by the corresponding EMS.

The report of Kanellos, which is found here (Kanellos, 2017), highlights the potential of the usage of the batteries of mobile electric vehicles (cars, forks, etc.) combined with grid-connected shore power installations in reducing GHG emissions in portal areas.

Additionally, vehicle-to-grid (V2G) integration is assessed by Pintér et al. (Pintér et al., 2021). Here, the potential of a V2G infrastructure to maintain grid stability is explained, where bidirectional power flow is possible, as is the case with stationary BESS. Specifically, this report focuses on boat-to-grid bidirectional power streams. Since electrical boats are increasingly developed, using them for stabilising the grid is beneficial without many extra costs and/ or efforts. However, the cycle lifetime of the relatively small mobile batteries limits their usability.

Kumar et al. explain the process of designing and sizing a stationary BESS which is connected to a shore power installation, which is referred to as hybrid installation in this study (J. Kumar et al., 2021). The proposition is different from this thesis since the aim is solely to provide extra energy capacity to the shore power installation in case the capacity of the grid is insufficient, during peak demand. The economic aspect which is taken into account is the avoidance of expanding the port's electricity infrastructure by optimising the size of a BESS. The economic aspect of providing off-peak electricity during peak hours as well as trading with electricity is not taken into account here. Additionally, the BESS is a charging station for vessel batteries as well. Also, the review takes into account smart grid connection instead of electricity grid connection.

As mentioned, optimal operation of BESS requires an EMS. An EMS can be designed in various ways, depending on the configuration of the BESS (stand-alone or (smart)-grid connected, for example). An explanation of different kinds of EMS which were found in literature is provided in the next Subsection.

2.3.1. Energy management strategy

An EMS is required when a BESS is used in a system where the goal is to optimise the system performance. The operation of a grid-connected BESS in combination with shore power requires an EMS to control the flow of energy based on pre-defined restrictions, thereby determining the optimal behaviour of the system to maximise profits. The EMS therefore determines the specific functionality of the BESS and which revenue streams are generated. As can be obtained from the references in Table 2.3, various EMS exist, all based on mathematical models. This Section aims to identify which EMS are used in literature for partly similar optimising systems containing BESS, with the purpose to explore the gap in knowledge of scientific literature in regards to EMS.

The system of interest is classified as behind-the-meter (BTM) since the BESS operates on site of the terminal owner and self-consumption is present. This is explained more thoroughly in Appendix A.3. The goal of the BTM, hybrid system is to provide a stable and safe system where continuity of power supply is ensured when a vessel is berthing, while simultaneously the profits are continuously being maximised. To be specific, systems are considered as (partly) similar when it contains at least an optimisation strategy focused on maximising profits and a BTM BESS. Table 2.3 provides an overview of the literature which is classified as (partly) similar and analysed in this Section. The literature does not necessarily include shore power installations in the systems which are analysed.

Kadri and Raahemifar elaborate on the sizing and scheduling of a BTM BESS which is integrated into a home-based microgrid with PV (Kadri & Raahemifar, 2019). The goal of the system is to maximise profits obtained by energy arbitrage which is generated by the volatility of spot market prices. The model takes into account uncertainty of PV electricity production by using a mixed integer linear programming method (MILP).

Table 2.3: Comparison of studies related to energy management strategies for behind-the-meter battery energy storage systems

Reference	Peak shaving	Energy arbitrage	Self-consumption	Primary control reserve	Frequency regulation	EMS method
(Kadri & Raahemifar, 2019)		✓				MILP
(Braeuer et al., 2019)	✓	✓		✓		LP
(H. Su et al., 2022)	✓	✓			✓	DP and MILP
(Cheng & Powell, 2016)		✓			✓	MDP
This thesis	✓	✓	✓			Algorithm + grid search

Braeuer et al. explain how the economic viability of fifty different industrial enterprises is influenced by installing a BTM BESS which is connected to a power plant (Braeuer et al., 2019). The BESS provides flexibility in the energy flow of the system, with the aim of minimising overall system costs. The report concludes that, in order to be potentially economically viable, a grid-connected BESS should deploy multiple functionalities. The analysis considers therefore three different streams of revenue generated by the BESS, namely through peak shaving, provision of primary control reserve (PCR) and by energy arbitrage on the DAM and IDM. The system is being modelled with linear programming (LP), whereby uncertainty of RES electricity generation is not taken into account since the BESS is connected to a grey power plant with a stable production. The overarching goal of the analysis is to identify the optimal battery capacity while simultaneously minimising the costs and also minimising the size of the grey production plant.

In addition to the report of Braeuer et al., H. Su et al. (H. Su et al., 2022) explain about a model which includes multiple revenue streams of BTM BESS as well. A similar conclusion is drawn about the necessity of two or more functionalities of the BESS. The revenue streams considered here are peak shaving, energy arbitrage and frequency regulation. The difference between the two reports is that Braeuer et al.'s paper takes the uncertainty of electricity generation into account by using dynamic programming (DP) and MILP.

Cheng and Powell elaborate on optimising the utilisation of a BTM BESS, taking into account the revenue streams of energy arbitrage and frequency regulation (Cheng & Powell, 2016). The model is stochastic (taking uncertainty into account) and a Markov decision process (MDP) is being used.

The literature review has provided two key insights, about the functionality of the BESS and the EMS method to optimally operate the BESS in hybrid installations. Firstly, several reports conclude that multiple revenue streams are necessary for a grid-connected battery to be economically viable. In addition, some of the reports analysed use both energy and power related BESS functionalities (namely energy arbitrage, peak shaving and PCR, frequency regulation). Since this study has chosen to prioritise the vessel demand which is connected to the functionality of consumer energy arbitrage/ peak shaving, only energy related functionalities are considered. Therefore, to maximise the prioritised consumer energy arbitrage revenue stream, only wholesale energy arbitrage is considered as well.

Secondly, the EMS method which is used in the report of Kadri and Raahemifar, which only considers energy related functionalities, cannot be implemented in this study since this thesis solely focuses on sizing a BESS instead of sizing multiple components (PV and BESS) (Kadri & Raahemifar, 2019). Therefore, an EMS algorithm is going to be specifically designed for the hybrid installations and the methodology of this design as well as of the sizing is explained more thoroughly in Chapter 3.

2.4. Research gap

This thesis contributes to scientific literature by defining and subsequently addressing a research gap which is based on information provided in this Chapter. This Section explains the research gap as well as other important aspects which became clear from the literature research.

The first part of the literature research has provided insights into which types of BESS exist and which are most suitable for hybrid installations, taking into account the necessary ability of consumer-

and wholesale energy arbitrage. Also, safety and costs have had an important role in the selection, as well as some pre-defined KPI's which are explained in Appendix A.4. The research has combined various reports found in literature about the different types of BESS since no report was found describing the full selection which is assessed in this study. By combining the literature reports to create the full selection of existing battery types, a sub-selection of battery types which have the potential to be suitable for hybrid installations was made. Since each specific shore power installation has unique requirements, various BESS with different characteristics are considered with the aim to be able to successfully connect each type of shore power installations with one of the selected BESS. The literature research has thus provided a comprehensive selection of suitable battery types for hybrid installations.

The literature review also has provided insights into a solution to the economic barriers experienced by shore power development. To enhance the economic viability and create incentives for both perspectives to implement and use shore power, shore power installations can be combined with BESS. Most reviews found in literature are analysing the benefits of implementing a portal area micro-grid containing BESS, instead of conventional grid-connected BESS. This thesis focuses on shore power installations combined with grid-connected stationary BESS, referred to as hybrid installations since there was not found any literature on this specific topic. The profit of implementing a BESS can be maximised by optimally dispatching the battery among various revenue streams, such as flattening the curve towards the shore power installation by consumer- and wholesale energy arbitrage.

In order to optimally design, size and operate a hybrid installation, an EMS is required. Literature has provided insights in the knowledge gap of scientific literature since no analyses were found to consider a similar hybrid installation as in this study. Therefore, the EMS is chosen to be a self-designed algorithm taking into account the necessary boundary conditions applicable for the specific installations.

To summarise, this thesis contributes to scientific literature by exploring the economic synergy of various shore power installations and different BTM grid-connected BESS, considering the revenue streams of consumer- and wholesale energy arbitrage. The following Chapter elaborates on the methodology which is used in order to successfully answer the research questions as proposed in Chapter 1.

3. Methodology

This Chapter describes the methodology that is used to formulate an answer on the research questions. First, Section 3.1 explains the overarching research methodology approach. Section 3.2 elaborates on the system design from a physical and virtual point of view. Here, the design of the EMS is introduced. With the EMS, operational profits of the BESS can be calculated. Then, the methodology of how to determine the BESS costs is explained in Section 3.3. Subsequently, Section 3.4 explains how the BESS is sized in order to achieve the most optimal design for the hybrid installations. Also, the approach to evaluate the output values accompanied by the sized system is explained. Lastly, Section 3.5 mentions the reason for and the approach to perform sensitivity analyses on the obtained results of the sizing and the financial analysis.

3.1. Techno-economic approach

To formulate an answer on the research question, this thesis is based on the approach of a techno-economic analysis (TEA). TEA is a type of method which combines technology and economics by assessing technological quality and economic feasibility (Lauer, 2008). Within the scope of this research, TEA is essential to evaluate the feasibility, both in terms of technology and economics, of different hybrid installation combinations. TEA consists of multiple sub-analyses which must be completed consecutively (S. Yew Wang Chai, 2022). Multiple TEA have been analysed in order to create a TEA approach specified for this thesis (Minke & Turek, 2018; Murthy, 2022; Zimmermann et al., 2020).

The first steps of a TEA are to identify the different technologies of interest as well as the different processes in which the technologies need to be implemented. These steps can be recognised as the first two research steps in Figure 1.4. The technologies of interest have been already defined in Chapter 2, based on a literature review. The specific processes are identified based on a case study, which is presented in Chapter 4.

The various BESS and shore power installations are the building blocks of the hybrid installations assessed with the TEA. Once these fundamental components are established, the algorithm for the EMS of the hybrid installations is written in Matlab. The resultant algorithm produces the operational profitability achievable by the system as well as the accompanied number of cycles per year. Furthermore, the algorithm's outcome can be influenced by adjusting various parameters to explore their effects.

Subsequently, a model is created in MS Excel to evaluate the financial aspects of the various BESS. The evaluation focuses on key financial parameters, including the system costs and the NPV. An input parameter of the financial model is the annual number of cycles performed by a BESS in a specific hybrid installation. Consequently, the outcomes of the financial model are depending on the algorithm's output and therefore on the input parameters of the algorithm as well.

The NPV of the hybrid installations is evaluated to determine whether or not the system is economically viable. The NPV combines the operational profit with the system costs. Then, the NPV is used for sizing of the hybrid installations. The sizing is based on striving to arrive at an optimal system where the economic viability is maximised while certain constraints are met.

Eventually, sensitivity analyses are done by varying parameters of the hybrid installation systems (one at a time) and observe their effect on the outcome. With the sensitivity analyses, the parameters having the most impact on the outcome can be identified. These parameters should be prioritised in the system design.

3.2. System description

This Section aims to describe the design of the hybrid installation which is analysed in this thesis. The system can be analysed in its physical and virtual state, of which the latter is referring to the EMS algorithm. Regarding the physical state of the system, the topology has already been defined earlier in Chapter 1 and is generally explained in Appendix A.2. The topology of interest consist of a grid-connected BTM BESS which is also connected to a load, which is a shore power installation.

3.2.1. System design

The three components, as well as the three possible energy flows through the hybrid installation are visualised in Figure 3.1, which strives to explain the physical design of the hybrid installation in more detail.

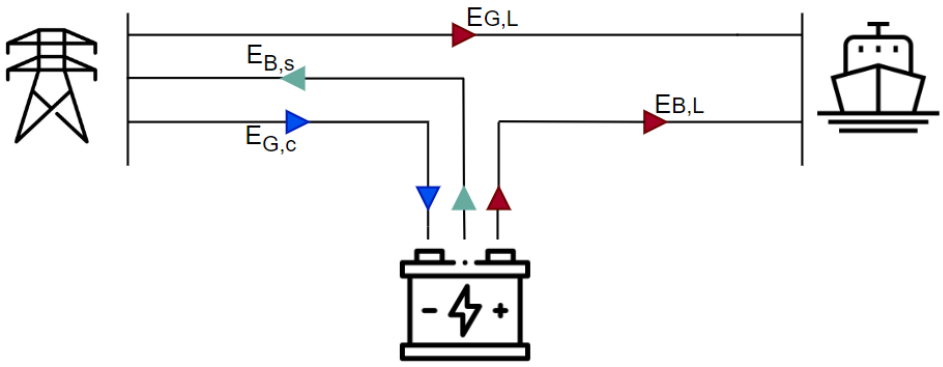

Figure 3.1: Schematic view of the system analysed, including the various possible energy flows from and to the grid, battery and shore power installation

In the schematic view of the system, the red arrows represent the possible energy flows at the moments when a vessel is present at the berth. The blue arrows represent the possible flow of energy which charges the BESS whereas the green arrows show the possible energy flow of selling electricity back to the grid, both when no vessel is present. At each moment in time (t represents the moment and *T* the full period of time which is considered) only one flow of energy can be active. Equation 3.1 presents existing relations of the energy flow parameters.

$$\begin{aligned} E_{\mathrm{L,t}} &= (1-\alpha) * E_{\mathrm{G,L,t}} + \alpha * E_{\mathrm{B,L,t}} \quad \forall t \in T \\ \alpha &\in 0,1 \quad \forall t \in T \\ E_{\mathrm{B,t}} &= E_{\mathrm{B,0}} + \sum E_{\mathrm{G,c,t\text{-}1}} - \sum E_{\mathrm{B,L,t\text{-}1}} - \sum E_{\mathrm{B,s,t\text{-}1}} \quad \forall t \in T \end{aligned} \tag{3.1}$$

The energy demand of the load (E_L) is an exogenous parameter which must be satisfied at all times. The demand at a moment t can be covered either by electricity drawn from the grid ($E_{G,L}$) or by electricity provided by the BESS ($E_{B,L}$), depending on the electricity price of the grid and the amount of energy in the BESS. This is presented in the first line of the equation and α is a binary variable with values one and zero, thereby indicating which of the energy providers is active. When the vessel demand is met by the BESS, $\alpha = 1$ and consumer energy arbitrage takes place.

To be able to provide electricity to the load, the BESS charges electricity from the grid ($E_{G,c}$) when the price of the grid is below a certain threshold value, which is clarified later. Besides charging and discharging to a vessel, the BESS is able to sell electricity back to the grid ($E_{B,s}$). This refers to wholesale energy arbitrage, which is in this case trading on the DAM.

The third line of the equation represents the amount of energy which is stored in the BESS at a certain moment in time ($E_{B,t}$). This amount is determined by the initial amount of energy which was stored in the BESS ($E_{B,0}$), the total amount of energy which is charged from the grid between the first moment of time and the considered moment in time ($\sum E_{G,c,t-1}$), the total amount of energy which is provided to a vessel between the first moment of time and the considered moment in time ($\sum E_{B,L,t-1}$)

and by the amount of energy which is sold back to the grid between the first moment of time and the considered moment in time ($\sum E_{B,s,t-1}$). Here, the subscript 't-1' refers to the energy transfers which have happened before the certain moment in time which is considered.

The upcoming Section elaborates on the virtual point of view of the hybrid installation system by explaining the design of the algorithm which is used for optimised operation of hybrid installations.

3.2.2. Energy management strategy design

The flowchart in Figure 3.2 visualises the system virtually by showing the algorithm of the EMS for every time step t in period *T* (which are respectively 15 minutes and a year in the case of this study). The algorithm is used to optimally operate hybrid installations, by maximising the operational profitability while keeping track of the accompanied number of yearly cycles. This Section starts with an elaboration on the various input parameters of the algorithm, followed by a Section focusing on the various steps of the algorithm and concludes with a Subsection about the algorithm's output.

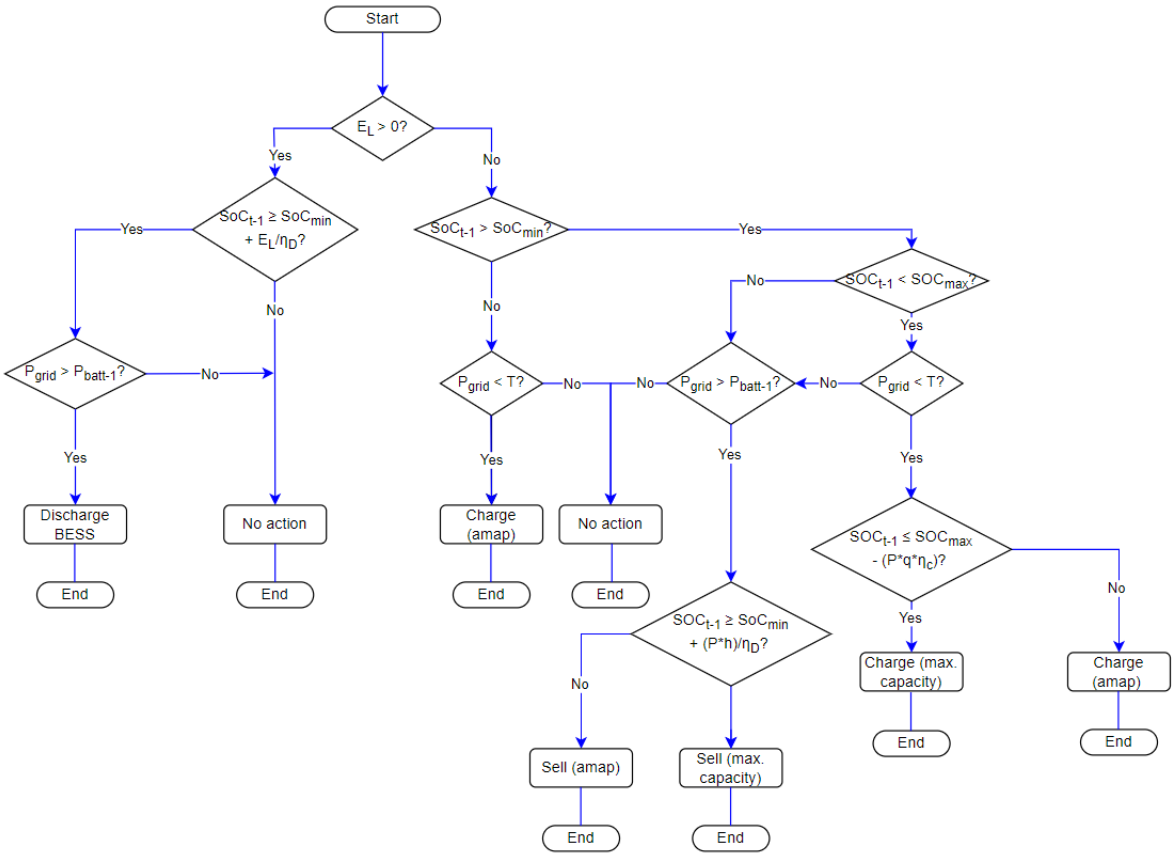

Figure 3.2: Flowchart representing the algorithm of the energy management strategy used for operating the hybrid installation at every time step t in period *T* (the abbreviation 'amap' means 'as much as possible')

Input parameters

Before focusing on the various steps of the algorithm, the input parameters are discussed first. As mentioned, the step size of the algorithm is 15 minutes for the period of a full year. The reason behind the step size is based on the goal of maintaining the balance between capturing the dynamics of supply and demand as well as minimising computational time. Also, the shore power data is provided in steps of 15 minutes. However, a part of the algorithm is based on selling electricity at the DAM and is therefore based on step sizes of 1 hour. In those specific pieces, the algorithm skips the following three time steps in order to capture 1 hour. As presented in equation 3.2, in the algorithm the parameter 'q' refers to 1/4th of an hour, or 15 minutes or 0.25 and 'h' refers to an hour or 1.

$$\begin{aligned} q &= 0.25 \\ h &= 1 \end{aligned} \tag{3.2}$$

Battery specifications
The BESS characteristic input parameters are partly fixed and partly variable, of which the latter are also referred to as the decision variables. The fixed BESS characteristic input parameters of the algorithm are the RTE, the (dis)charging limits (also referred to as the depth-of-discharge (DoD)), the initial amount of energy which is present, also referred to as the initial state-of-energy ($SoE_{initial}$) [MWh] and the price of the energy which is initially present in the BESS ($P_{bat,t0}$) [€/MWh].

The RTE represents the efficiency of a full cycle of the BESS. Since the algorithm uses half cycles, specifically charging and discharging, it is essential to separate the RTE into the discharging and charging efficiency ($\eta_{Discharge}$ and η_{Charge}, respectively). An even distribution is assumed and the separate efficiencies are therefore both determined by taking the root square of the RTE. This is presented in equation 3.3.

$$\begin{aligned} \eta_{Discharge} &= RTE^{0.5} \\ \eta_{Charge} &= RTE^{0.5} \end{aligned} \tag{3.3}$$

The BESS characteristic decision variables are the BESS energy and power capacity and storage duration (or C-rate). The three parameters are related as presented in equation 3.4.

$$\begin{aligned} P_{\text{capacity}} &= \frac{E_{\text{capacity}}}{\text{Storage duration}} \\ P_{\text{capacity}} &= E_{\text{capacity}} * \text{C-rate} \\ \text{C-rate} &= \frac{1}{\text{Storage duration}} \end{aligned} \tag{3.4}$$

Hence, by determining any of two parameters, the third parameter automatically becomes defined. The algorithm employs power capacity and storage duration as the decision variables, effectively establishing the energy capacity.

Grid specifications
The electricity and the accompanied prices of the DAM are used for providing shore power, for charging the BESS and for selling electricity of the BESS. Therefore, data of the electricity prices of the DAM for a full year is used as input. The hourly data must be converted to 15-minute data, resulting in a table containing 96 rows and 365 columns. In the algorithm, the DAM prices data table is referred to as P_{grid}.

Shore power specifications
The shore power installation electricity demand is used as input as well. The demand data has a step size of 15 minutes and has the same dimensions as the DAM input data table. In the algorithm, the shore power demand data table is referred to as ”XXDemand” where XX is the abbreviation of the specific shore power installation.

Other specifications
Besides the fixed and variable input parameters as mentioned above, the algorithm uses various initially empty arrays to store updated variables after each time step t. The SoE, the price of the electricity in the battery (P_{bat}), the revenue generated by consumer energy arbitrage (R_{con}), the revenue generated by wholesale energy arbitrage (R_{who}), the costs associated with charging the BESS (C_{bat}) and the number of cycles are updated after every time step t and the value is stored in the accompanied array. The SoE and P_{bat} are updated based on their previous value at t-1 since these variables are continuous, as is presented in equation 3.5. On the other hand, R_{con}, R_{who}, C_{bat} and the number of cycles are handled separately for each time step. Eventually, all individual values are added to obtain the result at the end of the simulation.

$$\text{If charging occurs:} \quad SoE_{\text{t}} = SoE_{\text{t-1}} + P_{capacity} * q * \eta_{Charge} \tag{3.5}$$

The price of the battery P_{bat} is averaged between the prices which were paid for the electricity during charging for each time step t. Therefore, when the battery is charged at time step t, the price is recalculated by either adding the initial stored electricity price or the current stored electricity price to the price which is paid for the electricity at time step t and then divide it by the SoE of the battery.

Lastly, another variable is used as fixed input parameter, namely threshold value T. T defines the benchmark for the system to determine whether or not to charge the BESS. If P_{grid} is lower than T, the electricity is considered as cheap enough for charging. T is defined as the average electricity price during the corresponding year of the DAM input data.

Steps of the algorithm

As mentioned above and in Chapter 1, the hybrid installation generates two revenue streams, namely by consumer- and wholesale energy arbitrage. The consumer energy arbitrage revenue stream is generated when the load of a vessel at berth is satisfied by the BESS. At every time step t the system starts with identifying whether there is a vessel at berth ($E_L > 0$) or not. If there is a vessel present, the demand of the vessel must be met at all times since this is an exogenous value.

To determine whether the demand is going to be fulfilled by the BESS or by the grid, and thus whether consumer energy arbitrage occurs, the SoE of the battery is determined first. Then, in the case that the BESS contains enough electricity at t-1 to provide the load at t, P_{grid} is compared to P_{bat}. The load is always satisfied with the cheapest electricity. Therefore, if P_{bat} is lower than P_{grid}, the BESS provides enough and the cheapest electricity and consumer energy arbitrage occurs. If not, the grid satisfies the load and the SoE of the BESS remains the same.

If there is no vessel at berth, either wholesale energy arbitrage revenue is generated by selling, or costs are generated by charging or nothing occurs. In this case, the first step of the algorithm is to determine the SoE of the BESS. Here, three possible SoE are considered.

- The BESS can be empty (SoE = SoE_{min}) and the battery can either be charged or no action occurs. Charging occurs when P_{grid} is lower than threshold value T.

- The BESS can be fully charged (SoE = SoE_{max}) and subsequently considers to sell electricity on the DAM or nothing happens. This decision is based on whether the price which could be earned by selling the electricity (P_{grid}) is more than the price of the electricity which is stored in the BESS (P_{bat}). If not, no action happens.

- The BESS is charged partly (SoE_{min} < SoE < SoE_{max}) and the price of the electricity of the grid determines whether the BESS charges, namely when this price is below T. When this is not the case, it is examined whether selling the electricity is attractive, namely when the price for which it could be sold to the grid is higher than the price of the electricity which was stored. If both are not true, no action occurs.

Output parameters

When the algorithm has iterated through every time step t, the initially empty arrays are filled and the revenue and costs streams as well as the amount of battery cycles which have passed can be calculated.

The yearly number of cycles is determined by the total amount of electricity [MWh] which flows in and out the BESS during the year, taking the (dis)charging efficiencies into account. The sum of all the in- and outflows is divided by two times the range of the SoE of the BESS, since a full cycle is defined as is presented in Figure 3.3. Equation 3.6 presents the calculation of the total number of cycles per year.

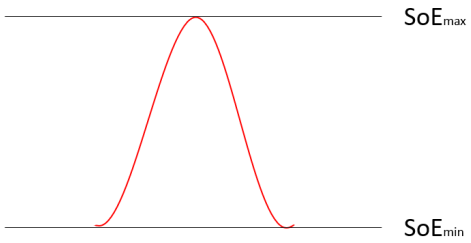

Figure 3.3: Representation of one full cycle in terms of the state of energy of a battery

$$\begin{aligned} \text{Total electricity in/out flow} &= \sum_{t=1}^{T}(cycle) \\ \text{Yearly cycles} &= \frac{\sum_{t=1}^{T}(cycle)}{2 * (SoE_{\text{max}} - SoE_{\text{min}})} \end{aligned} \tag{3.6}$$

To determine the yearly profit generated by operating the hybrid installation, the revenue streams generated through consumer- and wholesale energy arbitrage for each time step t are added and the costs of charging are subtracted. Equation 3.7 presents the mathematical relations.

$$\begin{aligned} R_{con} &= \sum_{t=1}^{T}(P_{grid,t} * E_{L,t}) \\ R_{who} &= \sum_{t=1}^{T}((P_{grid,t} * P_{capacity} * h) + (P_{grid,t} * (SoE_{t-1} - SoE_{min})) \\ C_{bat} &= \sum_{t=1}^{T}((P_{grid,t} * P_{capacity} * q) + (P_{grid,t} * (SoE_{max} - SoE_{t-1})) \\ \text{Operational profit} &= R_{con} + R_{who} - C_{bat} \end{aligned} \tag{3.7}$$

The revenue generated through consumer energy arbitrage is defined by the price of the grid times the amount of energy which is demanded by the vessel, during moments when consumer energy arbitrage occurs. The revenue generated through wholesale energy arbitrage is determined by the price of the grid multiplied by the amount of electricity which is sold, during moments when selling occurs (always as much as possible (amap), sometimes this means the full energy capacity which could be transferred in an hour or it is less due to the limited SoE of the BESS). Subsequently, the sum of the costs associated with charging the BESS are subtracted to obtain the yearly operational profit. The costs of charging is calculated by the price of the grid multiplied by the amount of energy which is transferred to the BESS, during moments when charging occurs (always amap, sometimes this means the full energy capacity which could be transferred in 15 minutes or it is less due to the limited SoE of the BESS).

As can be seen from the relations in equation 3.7, the operational profit depends on the energy and power capacity. Therefore, by optimally sizing the decision variables, operational profit and subsequently the economic viability, determined by the NPV, can be optimised. In order to determine the optimal size, the total system costs for various BESS sizes and types need to be determined first, whereafter the NPV can be calculated. The following Section elaborates on the methodology to determine the battery system costs.

3.3. Battery energy storage system costs

The methodology of determining the costs of BESS is discussed in this Section. The total BESS costs for the full lifetime of the hybrid installation is determined for each type of BESS considered. The total

costs are eventually used to determine whether the investment makes sense, namely when the NPV is positive (when NPV ≥ 0). The NPV is explained more thoroughly in Section 3.4.

The system costs comprise the total costs of investing in a BESS, including all the costs incurred during the lifetime of the hybrid installation. The BESS system costs (C_{System}) are composed of the capital expenditure (CAPEX) (C_{CAPEX}), operating expenditure (OPEX) (C_{OPEX}), decommissioning costs (C_{Decom}) and the end of life value (V_{EoL}). The V_{EoL} is considered as a cost-decreasing value and therefore it is subtracted from the cost components in the total system costs.

During the lifetime of the hybrid installation, the time value of money changes. Therefore, the costs which are incurred during the lifetime (everything excluding the investment costs) must be discounted in order to get the present time value of the future cash flows. r is used as the discount rate which represents the required return on investment (ROI) of the PoR in this research.

Equation 3.8 represents the system costs over the period of the lifetime of the hybrid installation N, which is 15 years. The individual cost components and the methodology on how these are determined are explained in the remainder of this Section.

$$C_{System} = C_{CAPEX} + \sum_{n=1}^{N} \frac{C_{OPEX}}{(1+r)^{n}} + \frac{C_{Decom}}{(1+r)^{N+1}} - \frac{V_{EoL}}{(1+r)^{N+1}} \tag{3.8}$$

Figure 3.4, which is inspired by a figure retrieved from a report of Mongird et al., represents the BESS subsystems which are considered separately to systematically define the total costs of various BESS (Mongird, Viswanathan, Alam, et al., 2020). Despite the fact that the end of life value is included in the total system costs, it is not included in the Figure since this is not a real cost component but actually a revenue component.

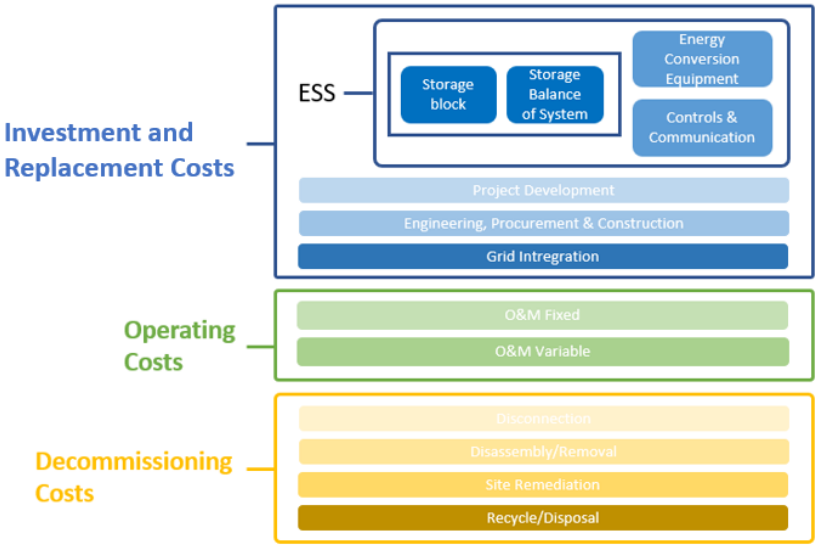

Figure 3.4: Energy storage subsystems nomenclature, inspired by (Mongird, Viswanathan, Alam, et al., 2020)

3.3.1. Capital expenditure

The CAPEX of a BESS consists of the initial CAPEX ($C_{CAPEX,IN}$) (also referred to as investment costs) and the replacement costs ($C_{CAPEX,REP}$) which are possibly incurred during the lifetime of the installation. Equation 3.9 represents the relation.

$$C_{CAPEX} = C_{CAPEX,IN} + C_{CAPEX,REP} \tag{3.9}$$

Initial capital expenditure

$C_{CAPEX,IN}$ depends on the technology of the BESS as well as on the specifications. Regarding the technology of the BESS, the raw materials used in the battery as well as the technique of storing electricity are important here. Considering the specifications, the energy and power capacity have an effect on the size and storage duration, which influences the price.

$C_{CAPEX,IN}$ can be broken down by a bottom-up approach, based on references (Mongird, Viswanathan, Alam, et al., 2020; Ramasamy et al., 2021). The cost components considered in $C_{CAPEX,IN}$ are from bottom to top:

- **Storage block (SB)** [€/kWh]: includes the costs for the electrochemical storage elements and the encapsulation used in the BESS
- **Storage balance of system (SBOS)** [€/kWh]: includes costs of SB supporting components such as the container, cabling, switchgear, pumps in case of a RFB and heating, ventilation and air conditioning if necessary
- **Energy conversion equipment** (also referred to as power equipment) [€/kW]: includes a bidirectional inverter, isolation protection, software
- **Controls and communication** [€/kW]: includes the BESS EMS software costs as well as associated hardware costs for computers
- **Project development** [€/kW]: includes costs associated with permitting, power purchase agreements, site control, and financing
- **Engineering, procurement and construction (EPC)** [€/kWh]: includes costs associated with equipment necessary for engineering and construction as well as the shipping of the equipment, installation and commissioning of the BESS
- **Grid integration** [€/kW]: includes costs incurred for connecting the BESS to the grid, both labor and equipment, including metering costs

As can be seen from the list above, some cost components are expressed in terms of energy [€/kWh] whereas others are expressed in terms of power [€/kW]. The $C_{CAPEX,IN}$ can be decomposed in the sum of the expression in power capacity ($C_{CAPEX,IN,P}$) [€/kW] and in energy capacity ($C_{CAPEX,IN,E}$) [€/kWh], as presented in equation 3.10. $C_{CAPEX,IN}$ can also be expressed in €/kW or in €.

$$C_{\text{CAPEX,IN}}[€/kWh] = C_{\text{CAPEX,IN,E}}[€/kWh] + \frac{C_{\text{CAPEX,IN,P}}[€/kW]}{\text{Storage duration}[h]} \tag{3.10}$$

The energy capacity part of the equation, $C_{CAPEX,IN,E}$ contains the cost of the technology which is necessary to store energy. This part contributes more to the total $C_{CAPEX,IN}$ compared to $C_{CAPEX,IN,P}$. Therefore, $C_{CAPEX,IN,E}$ decreases with increasing storage duration. The power capacity part of the expression, $C_{CAPEX,IN,P}$, is built up of costs of equipment that converts energy into electricity, and the other way around. Therefore, $C_{CAPEX,IN,P}$ increases with increasing storage duration. The inverse relationship of power and energy with increasing storage duration highlights the importance of sizing the system at optimal power/ energy values in order to minimise costs and maximise performance.

Replacement capital expenditure

In case that the lifetime of the BESS is shorter than the lifetime of the hybrid installation, the replacement costs, $C_{CAPEX,REP}$, need to be considered. $C_{CAPEX,REP}$ contain costs associated with replacing the battery electrochemical components (i.e. the SB) during the lifetime of the hybrid system. It is assumed that the shore power installation and the BESS are installed simultaneously and therefore the total hybrid installation's lifetime is determined by the lifetime of a shore power installation, which is 15 years.

The moment and frequency of replacement of the BESS is determined by the cycle life of the battery, since batteries with a longer life have to be replaced less often. The replacement costs are calculated according to equation 3.11, which is based on an equation retrieved from a report of Xu et al. (Xu et al., 2022).

$$
\begin{aligned}
C_{CAPEX,REP} &= \sum_{\beta=1}^{k} \left(\frac{C_{\mathsf{SB}}(1-\alpha)^{L_{cycle}\beta}}{(1+r)^{L_{cycle}\beta}}\right) \\
L_{cycle} &= \frac{\mathsf{N_{cycle}}}{Y_{\mathsf{cycle}}} \\
k &= \frac{\mathsf{N}}{L_{cycle}} \\
\alpha_{SB} &= -\left(\left(\frac{C_{SB}@2030}{C_{SB}@2020}\right)^{1/nr.years} - 1\right) * 100
\end{aligned}
\tag{3.11}
$$

Here, k is the number of replacements which is necessary during the lifetime of the system (N), considering the cycle lifetime (L_{cycle}) of the BESS in years. The cycle lifetime is calculated with the total number of cycles ($\mathsf{N_{cycle}}$) divided by the number of cycles per year ($\mathsf{Y_{cycle}}$). The number of cycles per year can be determined after sizing the system.

β is the β^{th} replacement during the system lifetime. The $\mathsf{C_{SB}}$ represents the SB costs as determined for $\mathsf{C_{CAPEX,IN}}$, in the base year of the battery. r corresponds to the discount rate to account for the value change of money over time and α represents the annual learning rate of the costs of the SB over time. α can be calculated according to the fourth line of equation 3.11.

Eventually, the $\mathsf{C_{CAPEX}}$ can be calculated by adding $\mathsf{C_{CAPEX,IN}}$ and $\mathsf{C_{CAPEX,REP}}$, according to equation 3.9.

3.3.2. Operational expenditure

As presented in Figure 3.4, the OPEX incurred during the lifetime of a BESS can be broken down by a bottom-up approach. The approach is based on the approach presented in references (Mongird, Viswanathan, Alam, et al., 2020; Ramasamy et al., 2021) and is presented in equation 3.12. The OPEX cost components considered from bottom to top are:

- **Fixed operation and maintenance (O&M)** [€/kW-year]: includes costs associated with fixed maintenance, which is necessary to keep the BESS in operation, independent of the energy conversion and usage during the lifetime
- **Variable O&M** [€/kWh]: includes costs associated with maintenance, dependent on the energy conversion and usage during the lifetime

$$
\sum_{n=1}^{N} \frac{C_{\mathsf{OPEX}}}{(1+r)^{\mathsf{n}}} = \sum_{n=1}^{N} \frac{C_{\mathsf{OPEX,FIXED}} + C_{\mathsf{OPEX,VARIABLE}}}{(1+r)^{\mathsf{n}}} \tag{3.12}
$$

For the OPEX costs to be added correctly, either the fixed or variable O&M costs have to be translated to €/kWh or €/kW-year, respectively. Furthermore, since the OPEX costs are incurred each year during the lifetime of the hybrid installation, the yearly OPEX costs need to be discounted and eventually added to each other to obtain the total discounted OPEX costs.

3.3.3. Decommissioning costs

Decommissioning costs are incurred at the end of the last year of operation of the BESS. Therefore, the decommissioning costs are discounted to the moment of decommissioning, which is the year after the last year of operation (N+1). As presented in Figure 3.4, the decommissioning costs are broken down by the same bottom-up approach as is used for CAPEX and OPEX. The cost components considered for the decommissioning of a BESS from bottom to top are:

- **Disconnection** [€/kW]: costs incurred by disconnecting the BESS from the grid
- **Disassembly/removal** [€/kW]: costs to deconstruct the BESS
- **Site remediation** [€/kW]: costs associated with returning the site back to initial state
- **Recycle/disposal** [€/kW]: recycling costs, including shipping to recycling plant

The costs associated with disconnecting and recycling the BESS are assumed to be equal for each location, whereas disassembly and site remediation costs are dependent on the specific location. Since disassembly and remediation is more complex in urban areas, these two cost components are more significant in the total decommissioning costs in urban areas compared to at industrial locations.

Due to the lack of specific information on decommissioning costs, the EPC costs which were incurred by installing the BESS, are incurred for decommissioning as well, referred to as engineering, procurement and decommissioning (EPD). The EPD costs are assumed to include the disconnection, disassembly and site remediation cost components. As mentioned, the EPD costs are influenced by the location of the BESS. Also, recycling costs are varying per BESS type and therefore this should be taken into account separately. The decommissioning costs at the end of the lifetime of the installation are calculated according to equation 3.13.

$$\frac{C_{\text{Decom}}}{(1+r)^{N+1}} = \frac{C_{\text{EPD}} * L_F + C_{\text{Recycling}}}{(1+r)^{N+1}} \tag{3.13}$$

L_F represents the factor which accounts for the increased labor costs associated with an increased complexity of deconstructing the BESS at a specific location. The decommissioning of BESS in urban areas requires a higher level of precision and therefore the decommissioning costs per unit of energy are higher, compared to industrial locations. One third of the total EPD costs are determined by the deconstruction of BESS systems. Furthermore, within deconstruction, materials and labor costs are included. It is assumed that two third and one third respectively is covered by these two cost components. Therefore, labor costs are around 10 percent of the total EPD costs. To account for the increased labor costs at more complex locations, the 10 percent of labor costs increases to 20 percent. Table 3.1 contains the location factors which are relevant for this thesis.

Table 3.1: The decommissioning location factor per type of location

	Urban area	**Industrial area**
L_F	1.1	1

3.3.4. End of life value

The end of life value of the SB is obtained at the moment of decommissioning and is determined based on the age of the SB at the moment of decommissioning, which is dependent on the cycle life of the BESS. The end of life value is calculated according to equation 3.14 and is therefore discounted to the year after the last year of operation (N+1). Since the value is the opposite of a cost component, namely a revenue component, V_{EoL} is eventually subtracted from instead of added to C_{CAPEX}.

$$\frac{V_{EoL}}{(1+r)^{N+1}} = \frac{(1 - \frac{\text{years since last replacement}}{L_{cycle}}) * C_{\text{SB}}}{(1+r)^{N+1}} \tag{3.14}$$

3.4. Sizing

This Section elaborates on the approach which is used for sizing the BESS in the hybrid installations. The goal of the sizing is to determine the most optimal size of the BESS based on evaluating the NPV while taking the fixed input of the algorithm, the BESS costs model, and additional constraints into account. Subsequently, the energy efficiency[1] as well as the effectiveness[2] of the sized hybrid installations are assessed. These elements are explained throughout this Section.

Figure 3.5 provides a detailed visualisation of the sizing approach based on the NPV, where the output of the algorithm and the costs model are optimised. The first step is the start of the optimisation, where the pre-defined fixed input and decision variables are iterated through the algorithm, resulting

[1]The energy efficiency of a hybrid installation refers to the percentage of the total annual energy demand of the vessels that is supplied by electricity from the battery.

[2]The effectiveness of a hybrid installation refers to the percentage of the yearly total operational revenue generated by consumer energy arbitrage.

in intermediate algorithm output. The intermediate yearly cycles are then put in the cost model and the second step refers to calculating the intermediate BESS costs. Combining the intermediate BESS costs and hybrid installation operational profit results in an intermediate NPV. The third step refers to repeating the process until the optimal NPV is found. Eventually, the optimal NPV is accompanied by knowledge of the optimal values for the decision variables, the power capacity and the C-rate (and therefore also the storage duration and the energy capacity), thereby completing the system sizing, based on evaluating the NPV.

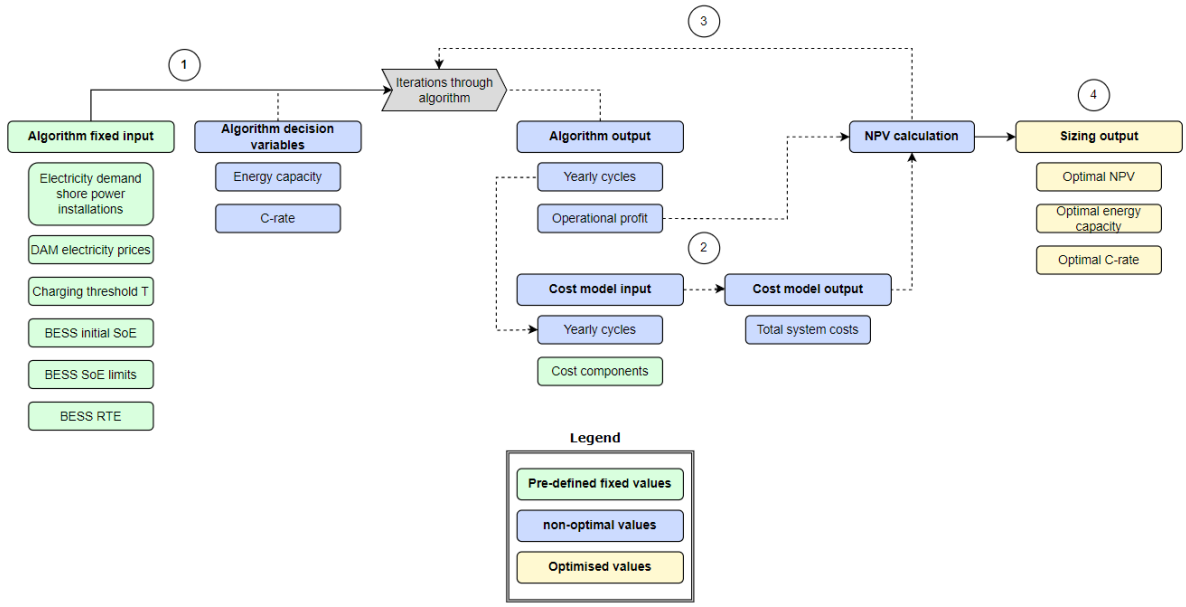

Figure 3.5: Detailed visualisation of the system sizing process steps, including all variables

3.4.1. Objective function

An objective function is used as a benchmark to assess the output accompanied by a set of decision variables, established by iterating through the algorithm. The objective of this study is presented in equation 3.15. Section 3.4.3 elaborates on how to determine the NPV.

$$\textbf{Objective function}: \text{Max(NPV)} \tag{3.15}$$

The operational profit is directly dependent on the decision variables. Subsequently, the optimal decision variables determine the yearly number of cycles of the BESS which in turn influences the system costs. Therefore, the yearly number of cycles should be assessed as well in order to eventually determine the maximised NPV of the hybrid installation.

3.4.2. Degrees of freedom

The decision variables in optimisation problems determine the number of degrees-of-freedom (DoF) in the system. The DoF represent the number of independent variables that can be adjusted without violating any constraints and they determine the complexity of the optimisation process. Since the decision variables in this problem are continuous (which means that there are infinite possible values within a defined range), their DoF are infinite.

The decision variables are discretised in order to be suitable input for the algorithm. Therefore, the DoF become finite. However, depending on the step size and the range of the variables, the number of DoF still remains high. A sizing approach is chosen which is able to handle a high number of DoF, which is grid search. The upcoming Subsection elaborates on the reasoning why it is used in this study and what it means.

Grid search sizing approach

The grid search method was chosen for the sizing in this study because it exhaustively evaluates all possible parameter combinations within predefined ranges. Two advantages of the grid search method are first that it is guaranteed that no combination of decision variables is missed and second the ease of implementation. A disadvantage is the computational time grid search can take (Liashchynskyi & Liashchynskyi, 2019). However, since the sizing problem only contains two decision variables, this is considered as acceptable.

Within the grid search optimisation, the algorithm iterates through each possible decision variable combination by using a loop. For each iteration, the input and output is stored and eventually the optimal NPV value determines the optimal decision variable values. The following Subsection elaborates on the methodology of how to determine the NPV.

3.4.3. Net present value

The NPV calculates the difference between the cash in- and outflows during the lifetime of the project. If the NPV is equal to zero or positive after 15 years, the investment in the BESS for the hybrid installation makes sense from a financial point of view. The NPV makes use of discounted cash flows, the future value is discounted to the present value with the discount rate r. The NPV of the investment in a BESS for a hybrid installation is calculated according to equation 3.16.

$$NPV = \sum_{n=1}^{N} \frac{\text{Operational profit}}{(1+r)^{\text{n}}} - C_{\text{system}} \tag{3.16}$$

The discounted value of the operational profit during the period of the lifetime of the hybrid installation determines the present value of cash inflows, whereas the system costs represents the discounted cash outflows (the cost components are already discounted individually before they were added).

3.4.4. Levelised costs of storage

The NPV can be forced towards a neutral NPV (NPV = 0) by applying the levelised costs of storage (LCOS). The LCOS determines the minimal price which must be paid for the electricity which is sold by the hybrid installation with consumer- and wholesale energy arbitrage in order to be economically viable (Schmidt & Staffell, 2023). The LCOS is the present value of all cost components of the storage system, divided by the present value of the energy output of the system. The conversion from equation 3.16 towards the LCOS is presented by equation 3.17. The equation is composed based on various equations retrieved from literature to calculate LCOS, combined to be specifically for hybrid installations (Augustine & Blair, 2021; Schmidt, 2018; Schmidt et al., 2019; Schmidt & Staffell, 2023).

$$\begin{aligned}
\sum_{n=1}^{N} \frac{\text{Operational profit}}{(1+r)^{\text{n}}} &= C_{\text{system}} \\
\sum_{n=1}^{N} \frac{E_{\text{sold}} * LCOS - C_{\text{bat}}}{(1+r)^{\text{n}}} &= C_{\text{system}} \\
\text{LCOS} &= \frac{C_{\text{system}} + \frac{\sum_{n=1}^{N} C_{\text{bat}}}{(1+r)^{\text{n}}}}{\frac{\sum_{n=1}^{N} E_{\text{sold}}}{(1+r)^{\text{n}}}} \\
E_{\text{sold}} &= 0.5 * Y_{cycle} * \eta_{Discharge}
\end{aligned} \tag{3.17}$$

The electricity which is discharged by the BESS during an operational year is half of the sum of each action of charging and discharging during an operational year, which is indicated by Y_{cycle}, as is presented in equation 3.6. The discharged electricity has to be corrected for the losses caused by the RTE of the BESS. The electricity which is sold by the hybrid installations (E_{sold}) is the result and LCOS is based on this. The difference between the discharged electricity and E_{sold} is lost.

By multiplying the hybrid installations' LCOS with E_{sold}, the minimal cash-inflows for a viable project can be calculated. The cash-inflow can be used to size the system according to this constraint.

If the price which is paid for the hybrid installation's electricity is lower than the LCOS, the project is not economically viable. After determining the optimal system size, the sizes are evaluated on whether they are violating any system constraints or not. If so, the most optimal size is chosen which does not violate any of the constraints, as explained in the next Section.

3.4.5. Sizing constraints

In addition to the optimal BESS size determined by the NPV and the LCOS, the size must be sufficient according to additional sizing constraints. The physical space as well as the vessel demand at the terminals are considered as sizing constraints.

The physical space of the sized BESS is estimated according to data of real life examples of the various BESS types. The data must contain information about the correlation between the physical size of the BESS and the size in terms of capacities and storage duration. Details of the real life examples are provided in Subsection 5.3.1.

In addition, the hybrid installations are designed with the aim to enhance the sustainability goals of the PoR by increasing the energy efficiency as well as the economic viability of shore power installations. The accompanied constraint is the minimal battery size in terms of the power capacity. The BESS must be able to potentially serve the demand of at least half of the vessels at berth. In other words, the power capacity must be equal to or higher than the power capacity demanded by fifty percent of the vessels. Section 4.2 further elaborates on this.

When sizing is successful, the economic viability of the sized hybrid installations is also evaluated by analysing the energy efficiency and effectiveness, which is explained in the following Subsections.

3.4.6. Energy efficiency

The energy efficiency of a hybrid installation refers to the percentage of the total annual energy demand of the vessels that is supplied by electricity from the battery. To determine how much of the yearly vessel demand is captured by the BESS, the energy efficiency of the various hybrid installations is calculated according to equation 3.18.

$$\text{Energy efficiency} = \frac{\text{Vessel energy demand provided by the BESS}}{\text{Total vessel energy demand}} * 100\% \tag{3.18}$$

The reduced amount of electricity which is drawn from the grid can potentially result in a decrease of the necessary capacity of the connection of the hybrid installation to the grid. A decreased capacity of the grid connection generates an additional revenue stream compared to conventional shore power installations, thereby contributing to the economic viability of hybrid installations. It must be noted that there is not a clear goal or information on whether and when this could be achieved. Therefore, only the potential of the resulting energy efficiency is discussed in Section 5.3.2.

3.4.7. Effectiveness

To completely assess the economic viability of a hybrid installation, the effectiveness is tested as well. The effectiveness of a hybrid installation refers to the percentage of the yearly total operational revenue that is generated by consumer energy arbitrage. The effectiveness is determined by evaluating the distribution of the two revenue streams of the hybrid installations. If the goal of prioritising consumer energy arbitrage is not successful because most of the revenue is generated by wholesale energy arbitrage, the hybrid installation can be considered as not effective, independent of the energy efficiency.

The reason why it is desired that at least half of the revenue is generated through consumer energy arbitrage is based on the certainty of both revenue streams. Consumer energy arbitrage is based on the vessel visits which is considered as certain. Wholesale energy arbitrage depends on the DAM volatility which is considered as more uncertain since the prices are fluctuating. Therefore, it would be

more risky to invest in a hybrid installation where more than half of the revenue is generated by the more uncertain wholesale energy arbitrage.

Then, the operational profit margin of the installations is analysed as well. The operational profit margin is the ratio of the hybrid installations' operating profit to the operational revenue. The higher the percentage, the more profitable the operations of the hybrid installation are. This metric is assessed solely based on the operational performances, excluding the costs of the BESS and is calculated according to equation 3.19.

$$\text{Operational profit margin} = \frac{\text{Operational profit}}{\text{Operational revenue}} * 100\% \tag{3.19}$$

The following Section elaborates on the methodology of the sensitivity analyses where the effects of varying certain input parameters on the hybrid installations' NPV are going to be assessed.

3.5. Sensitivity analyses

The addressed outcome in the sensitivity analyses is the NPV since this is the most impacting result of the research. The NPV consists of the operational profit, resulting from the EMS, and the BESS costs, resulting from the EMS and the costs model. The resulting NPV of the hybrid installations is affected by many input parameters.

The sensitivity of the resulting NPV to the decision variables and the type of BESS is going to be examined throughout the research already. Prior to the sensitivity analyses in Section 5.4, the resulting size is determined for each BESS type per hybrid installation. Therefore, the sensitivity analyses are conducted for each unique, sized hybrid installation.

Some of the other input parameters are pre-defined and are not likely to change, some of them are changing over time according to expected trends and some of them are determined by choice. In the portal area of Rotterdam, the EMS operates in a wide range of parameter variations and the system performance changes accordingly. By conducting sensitivity analyses, insights are gained on the influence of each of the variable parameters on the system performance.

The sensitivity analyses begin by categorising the input parameters into fixed, time-varying, or choice-dependent variables. The categorised list of input parameters of the hybrid installations can be found in Appendix Section C.4. This Appendix Section also elaborates on which parameters are expected to affect the NPV most. Henceforth, these parameters are the focus of the sensitivity analyses which is presented in Section 5.4. The categorised list of the parameters which are going to be focused on is provided in Table 3.2.

Table 3.2: Categorised list of the selected input parameters of hybrid installations for sensitivity analyses

Dependence	EMS parameters	Unit	Cost model parameters	Unit
Time	RTE	[%]	Cost data, RTE, cycle life	[€/kWh, %, -]
	DAM	[€/MWh]		
	Renewable energy connection	[%]		
Choice	BESS functionalities	[-]		
	T	[€/MWh]		

The sensitivity of the resulting NPV to the various input parameters is quantified and subsequently analysed by the percentage increases or decreases which are determined for each part of the analysis. The analyses start with assessing the sensitivity of the NPV to the time-dependent input parameters. This is based on the fact that these are dependent on time, which naturally passes. Without having to make any adjustments to the design of the system, these results provide information about the future level of economic viability of the hybrid installations. Subsequently, this knowledge can also be taken

into account when assessing the sensitivity of the NPV to choice-dependent parameters. For completeness, both base years 2020 and 2030 are assessed for the RES connection, BESS functionalities and T sensitivity analyses.

The upcoming Subsections tend to explain the methodology of how to conduct the various components of the sensitivity analyses. First, the RTE, cost data and cycle life are changed simultaneously upon varying the base year of the installations, and subsequently their effect on the NPV is examined. Then, the DAM electricity data is varied to analyse the sensitivity of the NPV to the volatility of the DAM. Next, the impact of a connection to a RES on the NPV is shown. Then, the impact of the various BESS functionalities are tested, by comparing their individual effect on the NPV to the result of the research, containing both functionalities. Next, the effect of various threshold values T to the NPV is analysed. Lastly, leveraging the insights gained from the sensitivity analyses, a specific potential scenario is recommended in Section 5.4.6, based on the electricity demanded by shore power at the hybrid installations, with the aim to ensure the economic viability of the hybrid installations through alternative avenues.

3.5.1. Base year

This Subsection explains the methodology of the sensitivity analyses of the NPV to certain time-dependent parameters by varying the installations' base year from 2020 to 2030. The base year has an effect on input parameters from the EMS and from the costs model, namely on the RTE, cycle life, the BESS costs and the DAM. For this section, the 2022 DAM data is used. The volatility of the DAM data is assessed separately in the following Subsection.

The RTE and cycle life for the two base years is presented in Table 3.3.

Table 3.3: The cycle life and round-trip efficiency (RTE) of the two battery types for base years 2020 and 2030

Parameter	Unit	LFP	VRB
2020 cycle life	[-]	3000	13000
2020 RTE	[percent]	91	75
2030 cycle life	[-]	5000	13000
2030 RTE	[percent]	94	78

The sensitivity of the NPV to varying the base year is analysed in consecutive steps. First, the sensitivity of the operational profit, which results from the EMS, to changing the RTE is analysed. Then, the sensitivity of the BESS system costs to varying the cycle life and the BESS input costs is examined. Then, the resulting NPV is calculated and the sensitivity to varying the base year is analysed by sensitivity percentages. Next, the approach of the sensitivity analysis of the resulting NPV to the DAM data is explained.

3.5.2. Day-ahead market

This Subsection elaborates on the approach of determining the sensitivity of the NPV of the hybrid installations to the DAM data. The effect of the DAM data on the NPV is captured by the volatility as well as in the average value of the data set. The volatility influences the price differences between the moments of charging and selling electricity. The hypothesis is that increasing the volatility enhances the operational profit of the BESS. It is expected that the volatility of electricity prices will inevitably be driven up in the future due to a growing penetration of electricity from RES, as is explained in Chapter 1 already. Simultaneously, due to an increasing share of storage systems, the volatility is partly counteracted. Therefore, the volatility of the DAM in the future is insecure and hard to predict.

The DAM data which is used throughout the research is of the year 2022. Since there is no knowledge of the future DAM data, assumptions have to be made. First, the volatility of the initial (2022) and two historical (2020 and 2021) DAM data sets is determined by analysing the data sets. Then, to test the hypothesis on the sensitivity of the NPV to the DAM data, three other scenarios are defined based on the analysis of the historical results. One of the three other scenarios includes the data set of 2021 whereas the other two are hypothetically determined based on analysing the historical data in Section

5.4. The approach to determine the volatility of a data set is explained next, which is mathematically presented by equation 3.20.

$$\begin{aligned} \mu &= \frac{(\sum x_i)}{n} \\ Dev_i &= x_i - \mu \quad \text{for i = 1 to n} \\ Dev_i^2 &= (x_i - \mu)^2 \\ \sigma^2 &= \frac{(\sum Dev_i^2)}{n} \\ \sigma &= \sqrt{\sigma^2} \end{aligned} \tag{3.20}$$

In order to determine the volatility of a (DAM) data set, the average (DAM electricity price) is determined first (μ). Then, for each value of the data set the deviation (Dev_i) from the average is determined whereafter this is squared to ensure each value is positive, since the deviation from the average can be either negative or positive. Then, the variance of the data set (σ^2) is determined by calculating the mean of the squared deviation, whereafter the square root of the variance results in the standard deviation (σ). The standard deviation is an indication about the dispersion of the data set. The volatility as considered in this thesis is similar to the standard deviation.

The approach to test the sensitivity to increasing the amount of RES which is connected to the hybrid installations is explained in the next Subsection.

3.5.3. Renewable energy connection

This Subsection explains more about the current connection of hybrid installations with RES and about the future goals set by the PoR. Then, the approach to determine the sensitivity of the NPV to the connection of hybrid installations with RES is explained.

The initial operational profit of the hybrid installations is composed of the time-dependent price difference of the DAM only. The PoR strives to provide shore power installations with renewable energy, thereby decreasing the price of the electricity which is used for charging the BESS and keeping the price of the electricity which is sold equal. This results in less charging costs and subsequently a higher operational profit of the hybrid installations. There are no exact goals set by the PoR for the moment of providing and the amount of the RES to hybrid installations.

In order to determine the sensitivity of the NPV to connecting the hybrid installations with RES, three scenarios are compared. The first scenario consists of the current situation, where no additional RES is considered to be connected to the hybrid installations (except from the percentage of RES which is penetrated in the grid). The second and third scenario consist of a connection with RES for 50 and 100 percent of the time. The low price of RES impacts the charging costs by 50 and 100 percent, and therefore the operational profit. The BESS costs remain constant through all three scenarios. Subsequently, the NPV is affected by the decreased charging costs.

The approaches of the sensitivity analyses of the resulting NPV to the two choice-dependent input parameters are explained next. First, the approach of determining the sensitivity to varying BESS functionalities is given whereafter the method to test the effect of varying the threshold T is explained.

3.5.4. BESS functionalities

This Subsection elaborates on the approach of determining the sensitivity of the NPV to the BESS functionalities. The BESS as considered in this research possess two different functionalities, namely consumer- and wholesale energy arbitrage. To test their effect on the NPV, both consumer- and wholesale energy arbitrage are implemented in the EMS separately as well as together. By varying the BESS functionalities, both EMS outcomes are changing. Therefore, since the yearly number of cycles affect the BESS costs, the resulting NPV is influenced by both. The analysis is provided for two base years, 2020 and 2030, both with DAM 2022 data.

3.5.5. Threshold T

This Subsection elaborates on the methodology of how to examine the sensitivity of the resulting NPV to varying the threshold value T. The analysis is conducted for two base years, 2020 and 2030. First, the meaning and potential effects of changing threshold value T are explained. Then, five scenarios for threshold value T are determined which are going to be implemented in the sensitivity analysis.

The EMS algorithm uses T as a benchmark to determine whether or not to charge the BESS. If P_{grid} is lower than T at a certain moment in time, the BESS charges. Otherwise, nothing occurs. When T increases, the likelihood of P_{grid} being lower than T increases and therefore the BESS potentially charges more often. Simultaneously, the price of the electricity which is stored in the BESS increases. Therefore, the amount of money which could be earned for each action of using the electricity for either consumer- or wholesale energy arbitrage decreases. On the other hand, when T decreases, the likelihood of charging decreases whereas the amount of money which could be earned by each action is increased.

Initially, T is defined as the average price of the corresponding DAM data set. In the sensitivity analysis, the effects of increasing and decreasing T are examined as well. In order to determine the scenarios of interest, the normal distribution of DAM data of 2022 is analysed to define the most frequently occurring electricity price and the 25th, 50th and 75th percentile prices. By varying T, the EMS output as well as the costs output are affecting the NPV.

Based on the results obtained with the sensitivity analyses, scenarios are presented which aim to ensure the economic viability of the hybrid installations. Since the scenarios depend on results, the methodology is explained simultaneously with the results in Subsection 5.4.6. The following Chapter elaborates on the results of the case study, which is conducted in the PoR.

4. Case study: port of Rotterdam

According to the TEA research steps and the process flow diagram presented in Figure 1.4, this Chapter describes the second part of the process design. This Chapter contains information about the case study which is conducted in the portal area of Rotterdam. The aim of the Chapter is to define the scope of the shore power projects interesting for this research. These projects are going to be analysed in the remainder of this thesis, in combination with a BESS. The complete case study, including background information on shore power and Rotterdam's strategy on this topic can be found in Appendix B. This Chapter only contains the relevant outcomes of the case study, namely the shore power projects on which this thesis focuses are explained more thoroughly. Thereby the scope of the case study is defined and Section 4.1 elaborates on this. Furthermore, an explanation on the collection of demand data of the shore power installations of the case study is given in Section 4.2.

4.1. Result of the case study

Based on the case study which is conducted in the portal area of Rotterdam, two berths are chosen to be the focus of this thesis for evaluation of viability of hybrid installations. The motivation behind the scope derives from the potential of shore power development at the locations, which is aligned with the impact. The selection is based on three criteria, namely current regulations, the emission savings which are achieved by shifting from auxiliary engines to electricity and thirdly the location of the berth. The selection criteria are motivated by literature, as mentioned in Chapter 2.

The selection process is visualised in Table 4.1.

Table 4.1: Comparison of terminals in regards to the potential of the development and the impact of shore power

Terminals	Regulations	Electricity demand	Urban area nearby	Overall score
Cruise Port	Focus	High	Yes	3
Stena Line	Focus	Moderate	Yes	2
P&O	Focus	Moderate	No	1
Maasvlakte	Focus	High	No	2
HMC	Less focus	Moderate	Yes	1
Lloydkade and Parkkade	Less focus	Moderate	Yes	1

Current regulations on shore power development are focusing on the roll-out of shore power for container vessels, RoRo passenger (RoPax) ferries and cruises. In terms of electricity usage while berthing, container vessels and cruise ships are among the most demanding vessels. Regarding the locations, the Cruise Port (CP) terminal, the Stena Line (SL) ferry terminal, the Heerema Marine Contractors (HMC) off-shore terminal and the Lloydkade and Parkkade are near urban areas.

Each terminal is assessed based on the criteria mentioned above. The weight of each criterion is equal and a score is assigned to the specific terminals for each criteria. The overall score shows the result of the selection process, namely the terminals with the highest score are selected, which are the CP and the SL terminal. The Maasvlakte has as similar score as the SL terminal but is excluded from the case study since the strategy for the roll-out of shore power at the Maasvlakte is less developed.

Two important considerations which hold for each terminal, are about the electricity off-take contract and the limited physical space in the portal area of Rotterdam. The off-take contract between the electricity grid and the shore power installation is based on the price of the DAM. The terminal operator pays the price of the DAM during moments of an active shore power installation. These prices have been directly passed on to the shipowners. This is incorporated in the algorithm as explained in Section 3.2.2. Therefore, P_{grid} is the price of the DAM. As mentioned in Section 3.4.4, depending on

the result of the research, a recommendation on a more specific pricing strategy for the terminal owner towards the vessel owner is provided. This recommendation is explained in Section 5.4.6 in the form of a scenario, taking the findings of the sensitivity analyses into account.

Furthermore, most terminals in the portal area in Rotterdam have a limiting factor in terms of physical space. Therefore, the physical space availability should be taken into account when sizing the BESS, as is explained in Subsection 3.4.5. The specifications and details of the terminals which are selected for the case study, are provided in the upcoming Subsections.

4.1.1. Stena Line terminal

SL is one of the world's largest ferry companies, operating RoRo and RoPax vessels. RoRo vessels are used to import or export cars or trucks between destinations whereas RoPax vessels are also transporting passengers (A. Bonte, 2021). SL owns a terminal in the Hook of Holland, which is visualised on the map in Figure B.8.

SL is committed to be actively involved in the energy transition and therefore already uses shore power at the berth of the ferry in Hook of Holland since 2012 (ABB, 2012). Since the berth is near an urban area, the impact is significant. The fact that SL both owns the vessels as well as the terminal, facilitated the rapid implementation of shore power. The economic risks of both the perspective of the ship owner and the terminal owner were mitigated by subsidies and simultaneous retrofitting of the vessels and terminal. Also, the economic viability of both perspectives is shared by SL, simplifying the business case. The connection from shore-to-ship is visualised in Figure 4.1.

Figure 4.1: Visualisation of the cable connection between shore and ship at the Stena Line ferry terminal in the Port of Rotterdam (AMP, 2012)

Since the owner of the installation has shown its interest in the research on whether it is economically attractive to install a BESS connected to the shore power installation, real data on electricity usage of vessels was shared and could be used for the calculations. Furthermore, despite the urban area nearby, the specific terminal is classified as an industrial area, influencing the decommissioning and subsequently the total system costs as explained in Chapter 3.

4.1.2. Cruise Port terminal

The Wilhelminakade connects the portal area to the city centre of Rotterdam since the cruise visitors play a significant role in the city's tourism and because of the location of the terminal which is near the urban area. Because of the location as well as because of the fact that cruises use a lot of electricity while berthing, the impact of using shore power is significant and therefore the shore power strategy has a focus here. A visualisation of the terminal is shown in Figure 4.2 and the location is shown on a map which is presented in Figure B.8.

The decision to implement shore power at the CP terminal has already been made and the design and subsequently the implementation is planned to start in the near future. The shore power installation is expected to be operational in the third quarter of 2024. The client has shown interest in the addition

Figure 4.2: The cruise terminal with the AIDA cruise at berth (PortofRotterdam, 2023)

of a BESS to the shore power installation to enhance economic viability. Furthermore, the CP terminal is located near an urban area and also the shore power installation is planned to be located inside an historical building. Therefore, the terminal is classified as an urban area. Consequently, safety is an extra important metric here which needs to be considered by the design of the hybrid installation.

4.2. Data of shore power installations

The electricity demand data of the terminals is necessary input data for the algorithm in order to determine the most optimal size of BESS in hybrid installations. Both data sets originate from the year 2022 but could be used for other years as well. The reason is based on the fact that for the SL terminal the energy demand is not expected to change over time. For the CP terminal the energy demand is calculated according to the hypothetical energy demand of cruise vessels since the vessels are not yet ready to receive shore power. When they are, their demand will remain constant over time. Both data sets are discussed next.

Stena Line terminal

The data which is obtained presents a table containing information for each vessel visit during the year 2022. The information for each visit consists of the total energy demand of the vessel [MWh] for the full period of the visit and for how many hours the vessel was present. The information is converted into a table of 96 rows (the number of 15-minute periods per day) and 365 columns (the number of days in a year). For each 15-minute period a vessel was present, the data is nonzero. Otherwise, in absence of a vessel, the demand data is zero.

First, the power demand [MW] for each vessel visit is calculated by dividing the total energy demand by the number of hours the visit lasts. Then, the power demand is used to determine the energy demand for each period of 15-minutes during the visit of the vessel, by multiplying the power demand by 1/4th. The maximal 15-minute energy demand was 1.52 MWh and the maximum power capacity demand of a vessel is 2.25 MW. The total electricity which was demanded in 2022, by the SL shore power installation, was 5.18 GWh during 669 visits. Figure 4.3 visualises the total energy demand [MWh] for each month in 2022 at the SL terminal.

Cruise Port terminal

The data which is obtained is similar as the data which is obtained from SL. Also, this data is converted into a table with the dimensions of 15-minute periods for a full year.

The number of visits at the CP terminal was 97 and the total energy demand was 10.6 GWh. This means that there is a higher electricity demand during less visits. This conclusion aligns with the fact that cruise vessels use more electricity than the ferries of SL. The maximal 15-minute energy demand

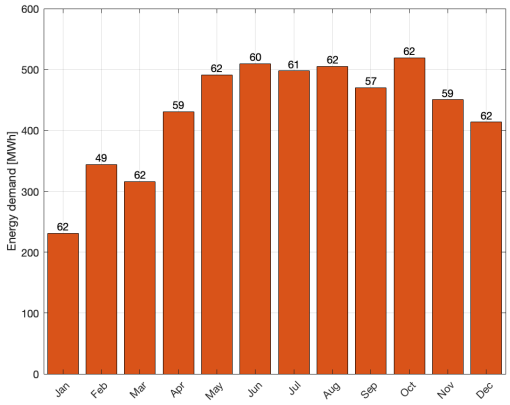

Figure 4.3: Monthly total energy demand [MWh] in 2022 of the Stena Line terminal presented by the bars, the number of vessel visits per month is presented by the number on top of the bars

was 2.5 MWh and the maximal power capacity demanded by a cruise vessel was 10 MW. Figure 4.4 shows the total energy demand [MWh] for each month in 2022 at the CP terminal.

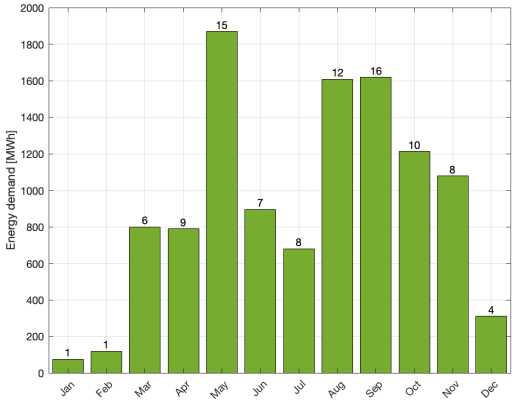

Figure 4.4: Monthly total energy demand [MWh] in 2022 of the Cruise Port terminal presented by the bars, the number of vessel visits per month is presented by the number on top of the bars

5. Results and discussion

This Chapter focuses on the results of the research conducted in this study according to the methodology as explained in Chapter 3. The discussion of the results is incorporated in this Chapter as well. An important note is that the results of the semi-solid FB are missing in this Chapter and are absent during the remainder of the research. This is due to the lack of knowledge of specific performance parameters and cost data. However, the costs model has been designed in such a way that when more cost insights become available, the model can be adjusted easily, enabling automated cost calculations. The algorithm is also designed in a general way that it can be used for any combination of shore power, battery type, and DAM data.

The Chapter commences with Section 5.1 which elaborates on the output of the algorithm, which is the yearly number of cycles and the operational profit for certain battery sizes, per battery type. Then, Section 5.2 dives into the results obtained by the economic analysis, based on calculations of the costs model. The resulting system costs for each BESS type and for various BESS sizes are explained here. Next, the sizing process calculates the NPV according to the grid search method and takes additional sizing constraints into account for the various BESS types, which is explained in Section 5.3. In this Section the economic viability of the sized hybrid installations is examined from the energy efficiency and effectiveness points of view as well. Lastly, the results of the sensitivity analyses are discussed in Section 5.4.

5.1. Energy management strategy algorithm

This Section provides the results of the EMS algorithm, categorised per BESS type, for each shore power installation of the case study. Subsection 5.1.1 discusses the results of the SL terminal whereas Subsection 5.1.2 explains the results of the CP terminal.

The results of the EMS are the yearly operational profit generated by a certain size, as well as the number of yearly cycles which is accompanied by the specific size. The yearly operational profit is directly used to calculate the NPV of the hybrid installation whereas the number of yearly cycles has an effect on the BESS costs, and therefore indirectly influences the NPV.

In order to generate the results, the EMS requires input. The necessary general and BESS specific input which is used in the algorithm is presented in Tables 5.1 and 5.2, respectively.

Table 5.1: General input parameters of the energy management strategy algorithm

Parameter	Unit	Value
2022 DAM electricity data	[€/MWh per hour]	Retrieved from Nord Pool (Pool, 2023)
2022 T	[€/MWh]	Average electricity price of 2022
Stena Line Terminal demand data	[MWh per 15-minutes]	Retrieved from Stena Line Terminal
Cruise Port Terminal demand data	[MWh per 15-minutes]	Retrieved from Cruise Port Terminal
SoE_{t0}	[MWh]	0.5 * SoE_{max}
$P_{bat,t0}$	[€/MWh]	T

As can be seen from Table 5.1, the electricity prices of the DAM which is used as input is from the year 2022. T, the average electricity price is based on the electricity data. When the DAM electricity prices of another year are used, T changes accordingly. Furthermore, the DAM electricity prices are constant for one hour. Since the algorithm's time steps are 15 minutes, the data is converted to electricity prices which are constant for four consecutive 15-minute periods. The initial values of the SoE and P_{bat} are set equal to half of the maximal capacity and T, respectively.

The BESS specific input data, presented in Table 5.2, is obtained from Tables A.5, A.8, A.9.

Table 5.2: Battery specific input parameters of the energy management strategy algorithm

Parameter	Unit	LFP	Lead-acid	VRB	ZBB
2020 RTE	[percent]	91	80	75	75
2020 η_{charge}	[percent]	95	89	87	87
2020 $\eta_{discharge}$	[percent]	95	89	87	87
SoE_{max}	[MWh]	1 * $E_{capacity}$	0.9 * $E_{capacity}$	1 * $E_{capacity}$	1 * $E_{capacity}$
SoE_{min}	[MWh]	0.2 * $E_{capacity}$	0.2 * $E_{capacity}$	0	0

5.1.1. Stena Line terminal

To analyse the results of the EMS algorithm for the SL terminal, the algorithm output accompanied by different BESS sizes is collected and shown on heat maps for each type of BESS. A heat map visually represents data in a table using a range of colors, transitioning from lighter shades for lower values to darker shades for higher values. The 40 different battery sizes which are considered are determined by four storage durations (4, 6, 8 and 10) and ten power capacities (1 to 10, with step size 1). By multiplying each power capacity with each storage duration, 40 energy capacities are assessed. The choice on the specific sizes is aligned with the sizes which are evaluated in Section 5.2, namely the sizes for which cost data is available.

For each type of BESS, the output consists of three components, the number of yearly cycles, the annual profit per unit of battery energy capacity [€/kWh] and the annual profit [€]. The first trend which is observed for all BESS types in general, is that the number of yearly cycles decreases with increasing energy capacity. This makes sense as a battery with greater energy capacity is able to store more energy, leading to fewer cycles.

The second trend which is observed in general is the increase in annual profit with greater energy capacity. The reason for this is based on the variation between the annual profit per unit of battery energy capacity values across different battery sizes. While batteries with lower energy capacities have the highest annual profit per unit of energy capacity, there is a difference of around 2 to 2.5 times between the smallest and largest profit per unit of energy capacity values considered. Consequently, when the annual profit per unit of battery energy capacity is multiplied by the energy capacity, the annual profit is significantly higher for higher battery energy capacities, given the substantial 25-fold difference in the battery energy capacities used for this calculation. The heat maps which are visualising the yearly number of cycles and the annual profit are shown in Appendix C.1.

In addition to the general trends observed, the operational profit which is generated varies per type of BESS. Therefore, the heat maps visualising the annual profit per unit of battery energy capacity are shown in Figures 5.1a, 5.1b, 5.2a and 5.2b for LFP, lead-acid, VRB and ZBB BESS, respectively.

What can be concluded from the four different heat maps presented, is that the annual profit per unit of battery energy capacity for a certain size is the highest in case of LFP batteries, followed by lead-acid batteries. This can be clarified by the higher RTE of LFP and lead-acid batteries, compared to VRB and ZBB, which influences the profitability. Also, the annual profit for a certain size is highest for LFP and lead-acid batteries.

On the other hand, as can be seen in Appendix C.1, for a certain size the number of cycles is lower for VRB and ZBB due to their extended SoE range compared to LFP and lead-acid. Furthermore, output is similar for VRB and ZBB. The reason for this are their similar input values in the EMS algorithm.

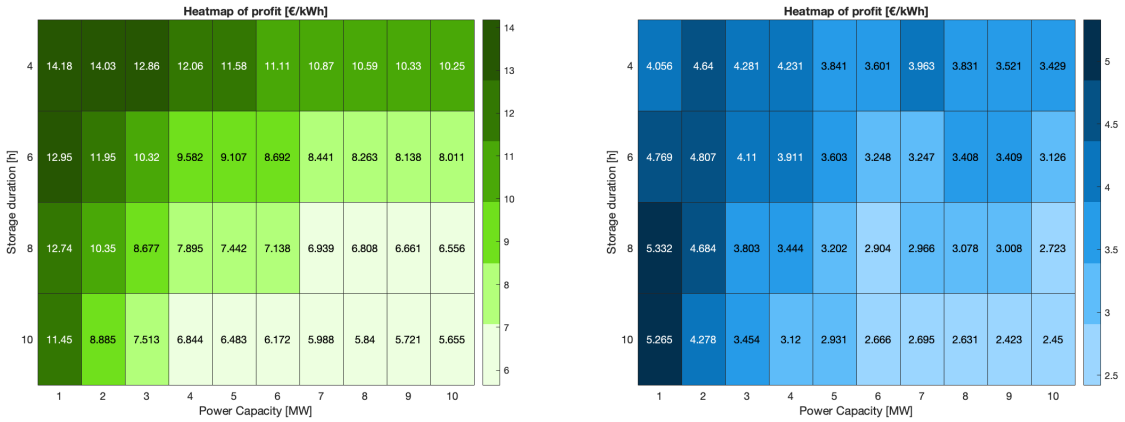

(a) Lithium iron phosphate (LFP) batteries

(b) Lead-acid batteries

Figure 5.1: Heat maps depicting the yearly profit per unit of battery energy capacity of LFP and lead-acid batteries with various energy capacities with colors for the Stena Line terminal in 2022

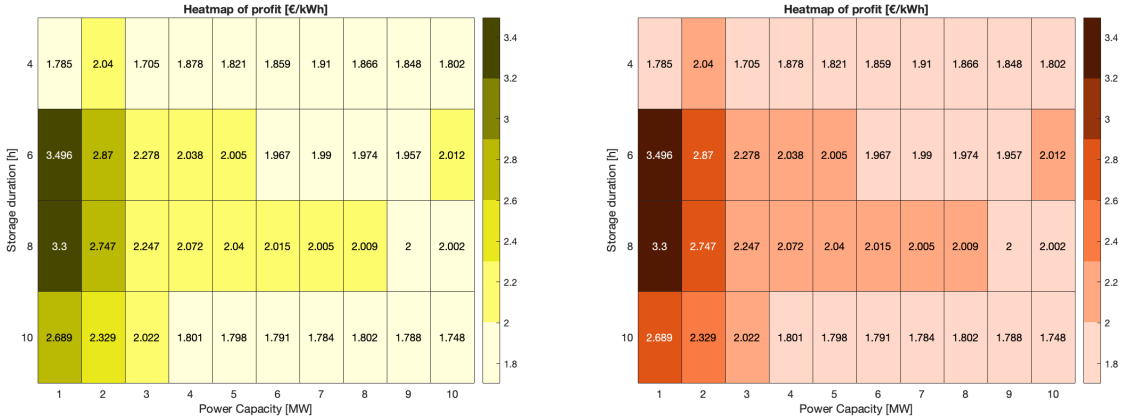

(a) Vanadium redox flow batteries (VRB)

(b) Zinc bromine hybrid flow batteries (ZBB)

Figure 5.2: Heat maps depicting the yearly profit per unit of battery energy capacity of VRB and ZBB with various energy capacities with colors for the Stena Line terminal in 2022

5.1.2. Cruise Port terminal

Similar as with the output of the EMS algorithm of the SL terminal, the output accompanied by different BESS sizes is collected for the four BESS types at the CP terminal and is shown on heat maps as well.

Again, the output of each type of BESS consists of three components, the number of yearly cycles, the annual profit per unit of battery energy capacity [€/kWh] and the annual profit [€], each for 40 different BESS sizes considered. As with the SL terminal, where the smallest batteries in terms of both duration and power capacity had the highest amount of cycles, the yearly number of cycles for all BESS types at the CP terminal is highest for the lowest storage duration, but not for the lowest power capacity. The number of cycles is highest at a power capacity of 5 MW and 3 MW for LFP and lead-acid and for ZBB and VRB, respectively.

Similar as was observed for the annual profit of the SL terminal, the bigger the BESS in size (storage duration and power capacity), the higher the annual operational profits are. Again, this is based on the variation between the annual profit per unit of battery energy capacity values across different battery sizes, which is smaller than the variation of the battery energy capacity across different battery sizes. At the CP terminal, for LFP batteries the highest profit per unit of battery energy capacity is observed for the second lowest storage duration (6-hours) and in the middle of the range of power capacity, namely

around 5 MW. For lead-acid batteries it is observed at the second highest storage duration (8-hours) and also around a 5 MW power capacity. For VRB and ZBB, the highest value is observed for the biggest size (10-hours, 10 MW).

The difference in both the trends of the yearly number of cycles and the profit per unit of battery energy capacity for the CP terminal compared to the SL terminal can be clarified based on the demand of the terminal, since this is the only variable which has changed. As became clear from the case study as presented in Chapter 4, the shore power demand at the CP terminal is less frequent but more intense. In the case of batteries with a size at the lower end of the battery energy capacity range which is assessed here, the batteries are too small compared to the demand of the vessels at berth. Therefore, BESS of small sizes are solely participating in wholesale energy arbitrage. Subsequently, the BESS cycles less and the revenue stream is based on the component of wholesale energy arbitrage only. Therefore, the battery sizes with the highest number of cycles and the profit per unit of battery energy capacity are the minimum size for batteries in hybrid installations at the CP terminal in order to be effective for both consumer- and wholesale energy arbitrage.

To compare the various BESS types with each other in case of the hybrid installation at the CP terminal, the yearly profit per unit of battery energy capacity for various BESS sizes is visualised here as well. Figures 5.3a, 5.3b, 5.4a and 5.4b represent the heat maps for LFP, lead-acid, VRB and ZBB, respectively.

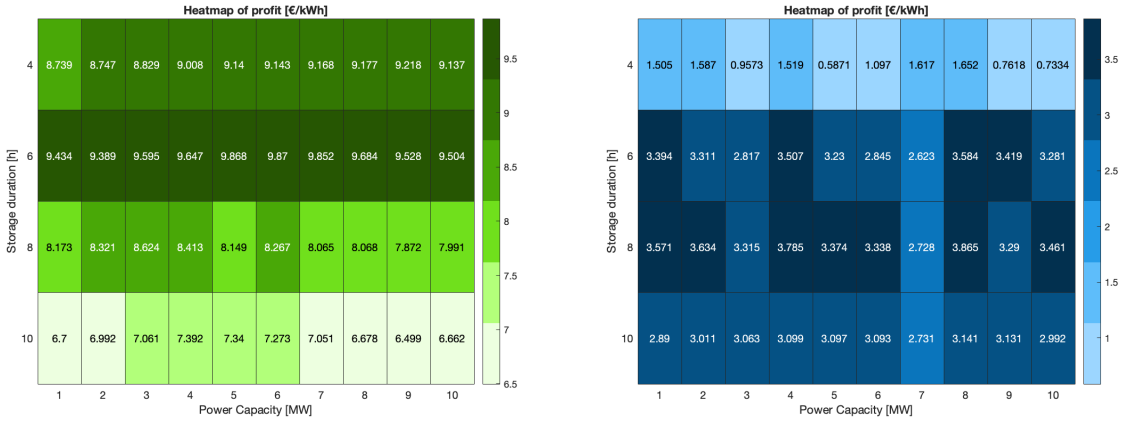

(a) Lithium iron phosphate (LFP) batteries

(b) Lead-acid batteries

Figure 5.3: Heat maps depicting the yearly profit per unit of battery energy capacity of LFP and lead-acid batteries for various energy capacities with colors for the Cruise Port Terminal in 2022

Similar conclusions can be drawn as with the results of the SL terminal, namely that the annual profit per unit of battery energy capacity for a certain size is highest for LFP batteries, followed by lead-acid batteries. This relationship is again clarified by their higher RTE compared to VRB and ZBB. Additionally, the annual profit for a certain size is highest for LFP and lead-acid batteries as well.

Furthermore, the number of cycles for a certain size are again the lowest for VRB and ZBB which is clarified by their increased SoE range in comparison with LFP and lead-acid batteries. This is visualised in Appendix C.1. Again, the results are similar for VRB and ZBB due to their similar input values.

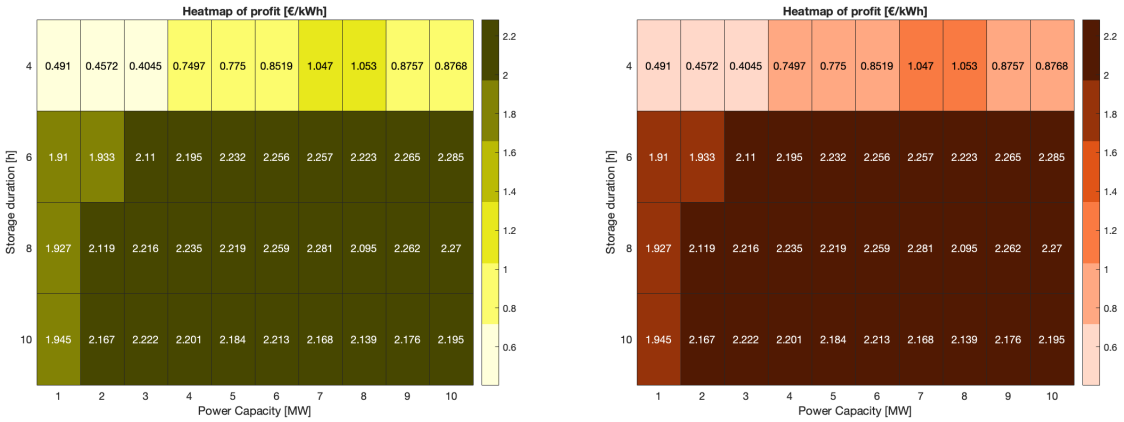

(a) Vanadium redox flow batteries (VRB)

(b) Zinc bromine hybrid flow batteries (ZBB)

Figure 5.4: Heat maps depicting the yearly profit per unit of battery energy capacity of VRB and ZBB batteries for various energy capacities with colors for the Cruise Port Terminal in 2022

5.1.3. Conclusion of results

The output of the EMS algorithm for both the SL terminal and for the CP terminal has provided insights in the trends of the yearly number of cycles, the profit per unit of battery energy capacity and the annual profit for various BESS types in hybrid installations and across the assessed size range. Based on the findings in this Section, it is observed that the CP terminal has a boundary in terms of minimal BESS energy and power capacity and storage duration in order to be able to participate in consumer energy arbitrage, whereas for the SL terminal this minimum is found outside of the size range which is assessed in this thesis. The reason why the ranges for storage duration and power capacity are not extended to smaller values is explained in Table A.1 and in Section 5.3, respectively.

Besides knowing the minimum BESS sizes, it became clear that the bigger the BESS, the higher the annual profits are. However, the same logic is expected to be observed with costs. Therefore, the NPV eventually provides insights into the optimal BESS size. The following Section focuses on the results of the battery system costs calculations.

5.2. Battery energy storage system costs

This Section elaborates on the results of the BESS costs analysis. The various cost components, as according to the methodology, are discussed here. The system costs [€/kWh] are solely based on the specifications of the different sorts of BESS and independent of the specific shore power installation.

The costs of the shore power installation including the costs of the connection to the grid are not considered in this research since it is assumed that the installations are already existing. This seems also logical given that in the future shore power installations will be mandatory for a ports license to operate.

The input data on CAPEX and OPEX for the four selected BESS types is extracted from references (Augustine & Blair, 2021; IRENA, 2017; Mongird, Viswanathan, Alam, et al., 2020; Viswanathan et al., 2022). The data set for LFP, lead-acid, VRB and ZBB was provided in two years (2020 and 2030), three battery sizes (1 MW, 10 MW and 100 MW), and four storage durations (4 hours, 6 hours, 8 hours, 10 hours). However, this does not hold for ZBB. For ZBB, data was only available until 10 MW. Within the costs analysis, no distinction is made between flooded lead-acid and VRLA batteries. Due to the fact that one of the sensitivity analyses, presented in Section 5.4, is about the variation of costs across various years, the cost analysis of this Section is done for two years.

The data of the reports is based on the year 2020 and forecasted for 2030, while the DAM and shore power installation use data of the year 2022. The reason for not extrapolating the 2020 BESS

cost input data to 2022 is based on the risk of miscalculations. This choice is not impacting the conclusion significantly.

Since this thesis solely focuses on the 1-10 MW range, the results in this Section are exclusively pertaining to this range. However, the model did consider 100 MW for the sake of completeness, except in the case of ZBB. Furthermore, regarding the range of storage durations, only two are displayed: specifically, 4 and 6 hours, the two smallest. This choice is motivated by the positive correlation between storage duration and physical space. Since physical space is scarce at the terminals, smaller batteries are desirable. All data is presented for both the years. Additionally, the unit of the results is in terms of costs per unit of battery energy capacity [€/kWh] (will be referred to as per unit of energy) but the model also includes each cost component terms of costs per unit of battery power capacity [€/kW].

5.2.1. Input parameters

The model uses general input parameters, which holds for each type of BESS, as well as BESS specific input. The general input is presented in Table 5.3. The BESS specific input is presented in Table 5.4.

Table 5.3: General input parameters of the battery energy storage system costs model

Parameter	Unit	Value
Conversion rate	[USD/EUR]	1
Discount rate, r	[percent]	8.5
Hybrid system lifetime, N	[years]	15
Location factor industrial area	[-]	1
Location factor urban area	[-]	1.1
Year 1 of data	[-]	2020
Year 2 of data	[-]	2030
Storage durations	[hours]	4, 6, 8, 10
Power capacity	[MW]	1, 10, 100

Table 5.4: Battery specific input parameters of the battery energy storage system costs model

Parameter	Unit	LFP	Lead-acid	VRB	ZBB
Cycles	[per year]	depends on algorithm	-	-	-
2020 cycle life	[-]	3000	1500	13000	10000
2020 RTE	[percent]	91	80	75	75
2030 cycle life	[-]	5000	3000	13000	10000
2030 RTE	[percent]	94	83	78	78
DoD	[percent]	80	70	100	100
Degradation	[percent per year]	2	2	0	0
Fixed OPEX	[percent]	0.43	0.43	0.43	2
Variable OPEX costs	[€/MWh]	0.5125	0.5125	0.5125	0.5125
2020 recycling costs	[€/kWh]	2.4	0	0	0
2030 recycling costs	[€/kWh]	0	0	0	0

Regarding the general input parameters, the data which is used for the model, extracted from literature, was converted from US Dollars (USD) to Euro. In reality, this conversion rate changes from time to time. To avoid having to change it constantly, the conversion is done according to a general conversion rate of 1. The discount factor which is used is the required ROI demanded by the PoR. The factor of inflation has not been considered for any hybrid installation for the same reason as for the conversion rate. For a more detailed analysis these two factors could be included.

Furthermore, the reasoning behind the choices of the location factor are explained in Section 5.2.6. The specific years, storage durations and power capacities which are used are aligned with the data set.

Regarding the specific input parameters, the yearly cycles depend on the size of the BESS and is an output parameter of the sized EMS algorithm. To be able to compare the results of the cost components of the various BESS correctly, in this Section the yearly number of cycles is set equal to 365 for all BESS types. Moreover, the 2020 cycle life, RTE and DoD are retrieved from Tables A.5, A.8 and A.9 for LFP, lead-acid, VRB and ZBB respectively.

Due to innovation, the 2030 RTE is increased compared to 2020 for all BESS types and in the case of LFP and lead-acid batteries, the 2030 number of cycles are increased compared to 2020 as well. These 2030 values are based on insights provided by the IRENA (IRENA, 2017). This thesis assumes that once the BESS is installed, the SB characteristics remain the same throughout the full lifetime, despite possible replacement. In reality however, a SB with the most favourable characteristics would be installed at the replacement during the lifetime. The impact of this assumption is considered as small and therefore acceptable.

The degradation of LFP and lead-acid batteries, which is 2 percent per year was retrieved from literature as well as the knowledge about the absence of degradation of VRB and ZBB. The reason why VRB and ZBB do not experience yearly degradation is due to the FB nature of these batteries. The degradation is not taken into account in the costs model and is therefore assumed to be negligible. To be more realistic, the degradation should be incorporated in the LCOS calculation as well as in the calculation of the total system costs. Furthermore, the O&M cost percentages are determined by literature and is elaborated on in Subsection 5.2.5.

The only recycling costs which are considered are for LFP batteries in 2020. According to Viswanathan et al., the recycling costs per unit of energy of LFP batteries in 2020 are based on the weight of the SB (Viswanathan et al., 2022). The weight of an LFP SB is around 2 kg/kWh and the recycling costs per kg are €1.2. Therefore, the recycling costs per unit of energy of an LFP battery are €2.4/kWh. The recycling costs are expected to be zero in 2030 due to innovation. The absence of recycling costs for lead-acid is attributed to the maturity of the BESS and the corresponding recycling procedures. No recycling costs are considered for VRB and ZBB either due to their high remaining cycle life at decommissioning. The SB's do not need recycling yet and can be used again. Therefore, no recycling costs are considered.

Besides the input parameters, cost data is used as input as well. The exact data which is inserted in the graphs which are presented throughout the Section, can either be found in the costs model and is also included in Appendix C.2. The costs model starts with defining the CAPEX per unit of energy, beginning with the initial CAPEX.

5.2.2. Initial capital expenditure

The initial CAPEX components *power equipment* and *controls and communication* both do not vary across increasing storage duration for a certain power capacity. Therefore, to minimise efforts, these components are combined. The various cost components which are originally expressed in terms of power are converted into terms of energy. Subsequently, the various cost components are added to $C_{CAPEX,IN}$ in terms of energy. Figures 5.5, 5.6, 5.7 and 5.8 represent $C_{CAPEX,IN}$ for the four different BESS types, for each two different storage durations, two different power capacities and two different years.

Analysis of results

In general, the costs per unit of energy decrease with increasing storage duration and power capacity and over time. This can be clarified by three concepts. Firstly, the decrease of the costs per unit of energy across increasing storage duration is caused by the components which are originally expressed in units per power. To translate these components into units of energy, these values are divided by the respective storage duration, resulting in a decrease by increasing storage duration. The second reason is based on scale effects. According to Schmidt and Staffell, it has been found that smaller projects have higher investment costs compared to bigger projects of the same storage duration (Schmidt & Staffell, 2023). Also, the costs per unit of energy decrease over time, between the two years of the data set. This is driven by innovation and it is reflected in the learning rate α (see Table 5.5). The more

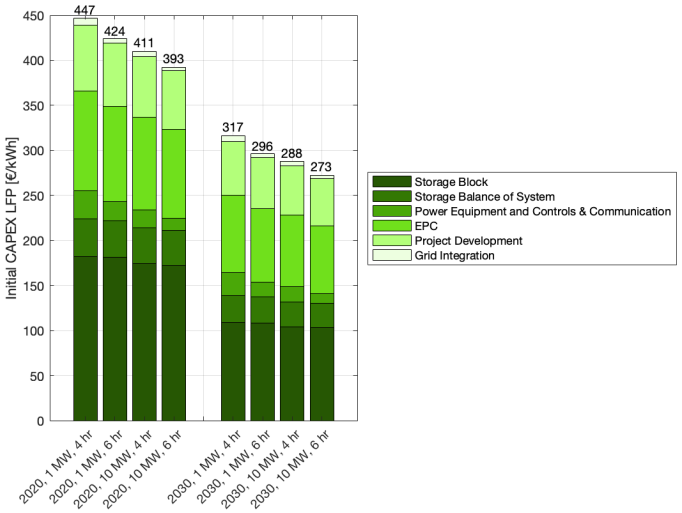

Figure 5.5: Initial capital expenditure breakdown in terms of energy [€/kWh] of LFP 4 and 6 hour batteries of power capacities 1 and 10 MW in 2020 and 2030, data retrieved from (Mongird, Viswanathan, Alam, et al., 2020; Viswanathan et al., 2022)

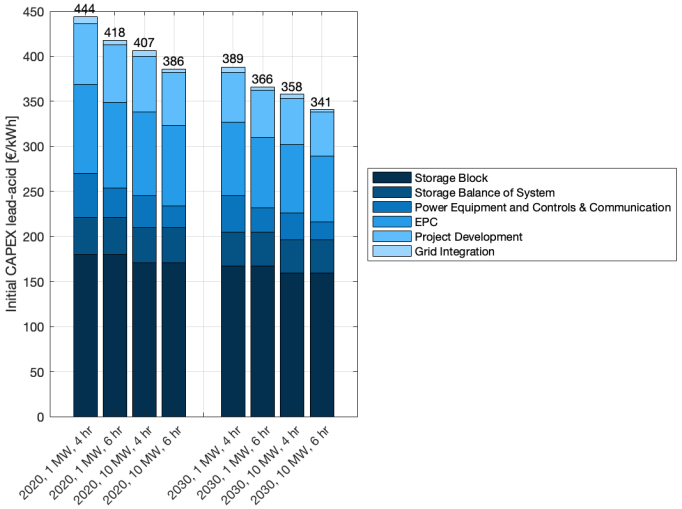

Figure 5.6: Initial capital expenditure breakdown in terms of energy [€/kWh] of lead-acid 4 and 6 hour batteries of power capacities 1 and 10 MW in 2020 and 2030, data retrieved from (Mongird, Viswanathan, Alam, et al., 2020; Viswanathan et al., 2022)

the BESS type is developed, the lower the learning rate is over time. Therefore, the learning rate of lead-acid batteries is the lowest.

Furthermore, the *SB* costs per unit of energy are the biggest cost components among all for the four BESS types. For LFP and lead-acid, the *SB* costs consist of around 40 percent of the total $C_{CAPEX,IN}$ and for VRB and ZBB of 48 and 54 percent, respectively. The reason why the SB of VRB and ZBB is more expensive, has to do with the increased complexity of the flow batteries. Also, the materials which are used are more expensive. In case of ZBB, the electrolyte contains costly and complex forming agents to prevent the toxic bromine to escape from the solution to the environment. The SB of LFP batteries experiences the highest learning rate, and thus decline in price, among all cost components considered. This is due to the rapidly evolving Li market and changing chemistries (Mongird, Viswanathan, Alam, et al., 2020).

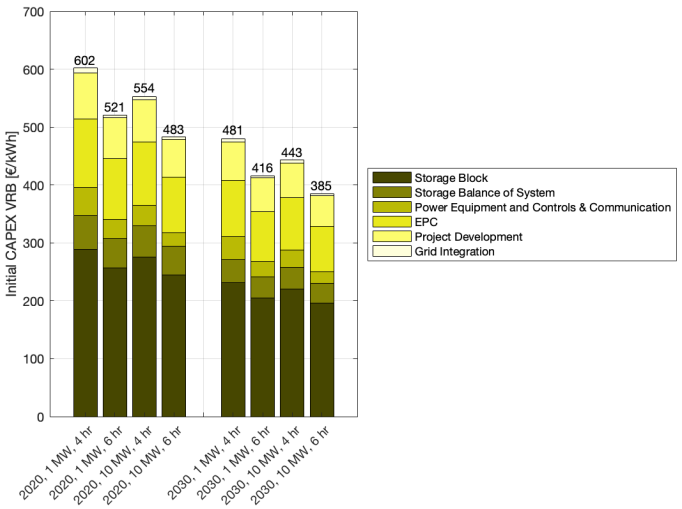

Figure 5.7: Initial capital expenditure breakdown in terms of energy [€/kWh] of VRB 4 and 6 hour batteries of power capacities 1 and 10 MW in 2020 and 2030, data retrieved from (Mongird, Viswanathan, Alam, et al., 2020; Viswanathan et al., 2022)

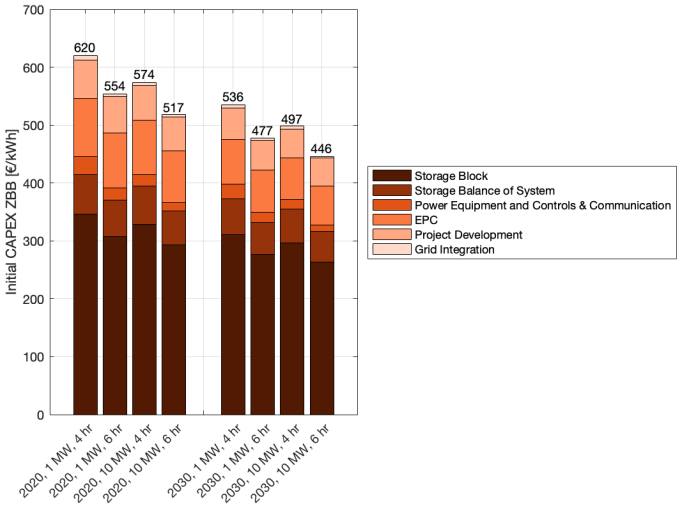

Figure 5.8: Initial capital expenditure breakdown in terms of energy [€/kWh] of ZBB 4 and 6 hour batteries of power capacities 1 and 10 MW in 2020 and 2030, data retrieved from (Mongird, Viswanathan, Alam, et al., 2020; Viswanathan et al., 2022)

The SBOS depends on the energy and power capacity of the system. Systems with higher power capacities are required to resist higher current and thus to have thicker cables. On the other hand, high energy capacity systems require more containers with battery racks in series, therefore more rack-to-rack cabling. Heating and cooling components are sized according to the power capacity but safety components are based on the energy content of the system (Mongird, Viswanathan, Alam, et al., 2020).

For LFP batteries, the *SBOS* costs per unit of energy is set at 23 percent of *SB* costs per unit energy. The *SBOS* costs per unit of energy for lead-acid batteries is set at the same percentage whereas for VRB and ZBB the percentage decreases to 20 percent. The percentages were extracted in literature (Mongird, Viswanathan, Alam, et al., 2020). In absolute terms, the SBOS for flow batteries is higher because of the presence of extra pumps.

The *communication and controls* part of the cost component *power equipment and communication and control* is similar for all battery types and decreases with increasing storage duration and also with increasing capacity. The learning rate over time is only 2 percent for the four BESS types since

solely the software is expected to increase in efficiency. The *power equipment* costs are similar for LFP and ZBB batteries and for lead-acid and VRB. The necessity for isolation protection causes the power equipment costs per unit of energy for lead-acid and VRB to be higher.

The *EPC* and *project development* costs per unit of energy are lower for lead-acid and ZBB compared for LFP and VRB because of the fewer safety-related issues associated with lead-acid and no need for thermal regulators for ZBB batteries. The *grid integration* costs per unit of energy are similar for all types of BESS since these costs are related to actions outside of the BESS and have nothing to do with the specific type of battery.

As a sanity check, the report of Mongird et al. has analysed various references to obtain knowledge of the capital costs of different types of BESS in 2020 (Mongird, Viswanathan, Balducci, et al., 2020). Also, the IRENA has shown results of capital costs (IRENA, 2017). The results show that for example the capital costs of an LFP battery of 1 MW and 4 hour storage duration ranges from 340 - 590 €/kWh. Since the resulting $C_{CAPEX,IN}$ for the same type of BESS is 447 €/kWh, which is almost in the middle of this range, the results are considered as accurate.

The following Subsection elaborates on the replacement CAPEX, which needs to be added to the initial CAPEX to eventually determine the total CAPEX.

5.2.3. Replacement capital expenditure

The input variables necessary for calculating $C_{CAPEX,REP}$ for the various BESS types are expressed in Table 5.5.

Table 5.5: Replacement capital expenditure input values per battery energy storage system type

Parameter	Unit	LFP	Lead-acid	VRB	ZBB
α_{SB}	[percent]	5	0.75	2.2	1.05
2020 L_{cycle}	[years]	8.2	4.1	35.6	27.4
2020 nr. of replacements during N (=15)	[-]	1	3	0	0
2030 L_{cycle}	[years]	13.7	8.2	35.6	27.4
2030 nr. of replacements during N (=15)	[-]	1	1	0	0

Among all components, the costs of the SB are observed to have the highest learning rate over time. This is due to the fact that the SB innovates most over time compared to other BESS components. The Table shows that the SB of LFP batteries experiences the highest learning rate whereas lead-acid batteries experience the lowest learning rate. This is explained by the maturity of lead-acid batteries and the currently ongoing innovations of LFP batteries. VRB and ZBB are less mature than lead-acid BESS but less innovations are occurring, therefore they experience a learning rate in between.

The total number of cycles of the SB increase over the period of ten years in the case of LFP and lead acid batteries, due to innovation. For VRB and ZBB the total number of cycles does not change over time since this number is fixed due to the nature of flow batteries. The replacement costs per unit of energy are mostly dependent on the number of necessary replacements of the SB during the lifetime of the hybrid installation, which is dependent on the total number of cycles and the yearly cycles. For lead-acid, the necessary number of replacements decreases over time whereas for LFP only L_{cycle} increases.

In the case of VRB and ZBB, the replacement costs per unit energy are zero since the number of cycles exceeds the lifetime of hybrid installations and no replacements are necessary. The replacement costs per unit of energy for LFP and lead-acid BESS are presented in Figure 5.9.

Analysis of results

The replacement costs per unit energy of lead-acid batteries in 2020 is high due to the high number of necessary replacements, whereas LFP batteries only require one replacement. The higher replacement costs per unit of energy for the single replacement of lead-acid in 2030 compared to the single

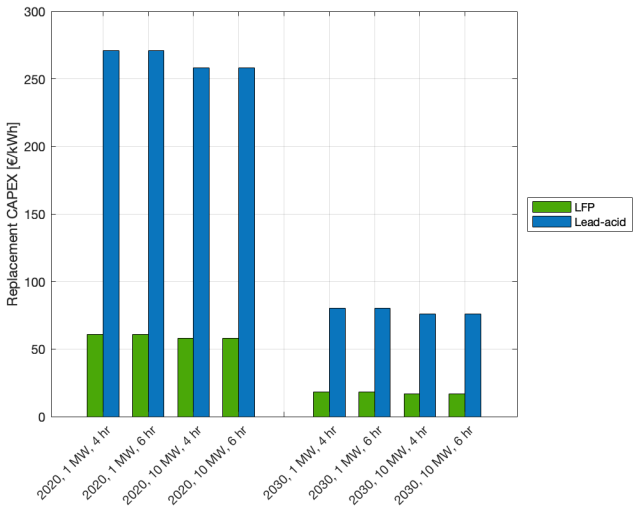

Figure 5.9: Replacement capital expenditure in terms of energy [€/kWh] of LFP and lead-acid 4 and 6 hour batteries of power capacities 1 and 10 MW in 2020 and 2030

replacement of LFP, can be declared by the fact that LFP batteries (and specifically here the SB) experience a higher learning rate over time. Therefore, LFP replacement costs per unit of energy of one replacement are lower in 2030 compared to one replacement of the SB of lead-acid batteries.

Only the SB costs are considered for replacement in this study. It is also likely that other components may fail before the entire lifetime of the BESS is reached. This study assumes that full replacement of components other than the SB will not be necessary; otherwise, such replacement costs will be covered by O&M expenses. To provide a more comprehensive analysis, it would be advisable to include other costs components as well or a factor to account for the likelihood of other components needing replacement.

5.2.4. Total capital expenditure

The total CAPEX per unit of energy for the four different types of BESS is visualised in Figure 5.10b. For comparison, the initial CAPEX of the four BESS are combined into a single Figure, which is presented in Figure 5.10a.

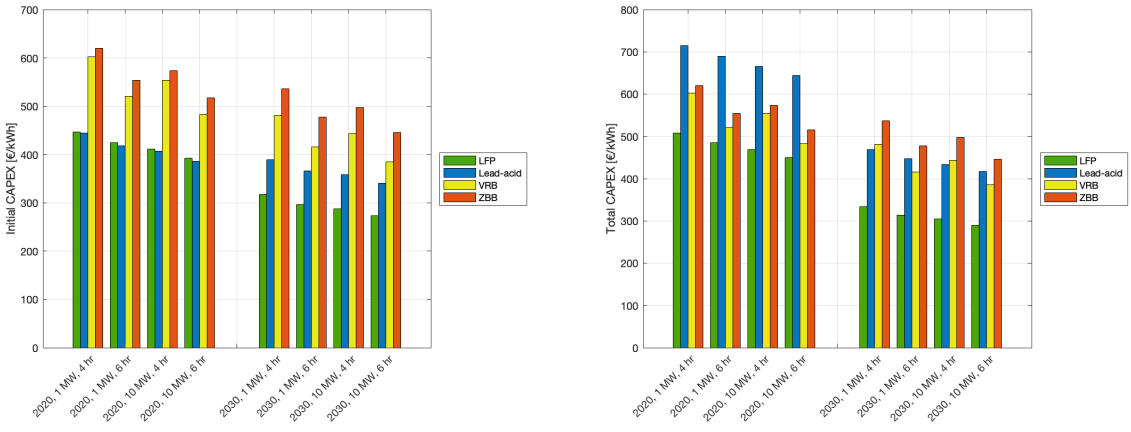

(a) Initial capital expenditure (CAPEX)

(b) Total CAPEX

Figure 5.10: CAPEX in terms of energy [€/kWh] of LFP, lead-acid, VRB and ZBB 4 and 6 hour batteries of power capacities 1 and 10 MW in 2020 and 2030

Analysis of results

The increases in total CAPEX costs per unit of energy compared to initial CAPEX costs per unit of energy for LFP and lead-acid are the result of the replacement costs. In 2020, the replacement costs per unit of energy of lead-acid batteries cause lead-acid batteries to be the most expensive among all BESS. Due to an innovation in number of cycles, the replacement costs per unit of energy for lead-acid are less significant in 2030, causing lead-acid to be the second and third most expensive battery in 2030.

Furthermore, despite the necessary replacement costs per unit of energy and due to the highest learning rate as well as the lowest SB costs, LFP batteries have the lowest total CAPEX costs per unit of energy in both years.

VRB and ZBB total CAPEX costs per unit of energy are least declining since the replacement costs are absent in both years and the only trend which is observed is due to the learning rate. Besides CAPEX, the OPEX of the various BESS types is determined by the model as well, of which the results are explained in the following Subsection.

5.2.5. Operational expenditure

The fixed OPEX component is calculated as a fixed percentage of the total initial CAPEX costs. Therefore, the same trends are recognised in fixed OPEX as in CAPEX initial. The variable OPEX component is pre-determined and independent of storage duration, power capacity or BESS type. The only trend which is observed for variable OPEX is the same learning rate as is observed for fixed OPEX (and thus originating from CAPEX initial). Innovations enhance efficiency and quality and therefore maintenance is reducing accordingly. The fixed OPEX percentage of CAPEX initial and pre-determined variable OPEX value can be found in Table 5.4. Figure 5.11 represents the OPEX per unit of energy for the four types of BESS. The learning rates experienced by the fixed and variable OPEX are presented in Appendix Subsection C.2.

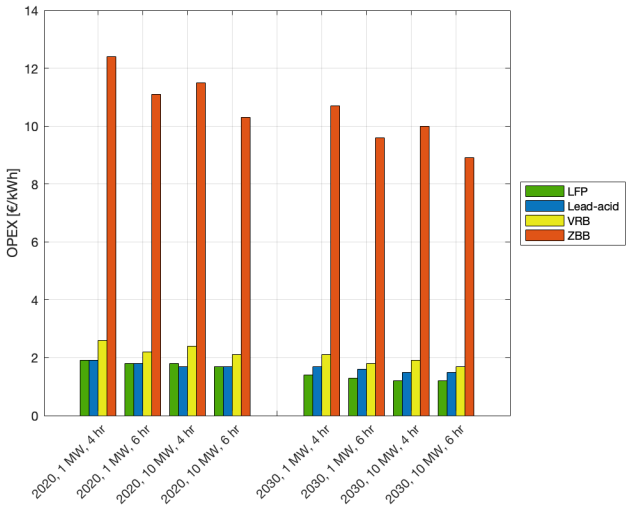

Figure 5.11: Operational expenditure in terms of energy [€/kWh-yr] of LFP, lead-acid, VRB and ZBB 4 and 6 hour batteries of power capacities 1 and 10 MW in 2020 and 2030

Analysis of results

Among all batteries, the OPEX of ZBB is the highest due to the fact that the fixed component is a more significant percentage of CAPEX initial compared to the other BESS types. The reason for this is that ZBB must be fully discharged once a week, which requires extra maintenance. The fixed OPEX percentages as well as the variable OPEX value is determined by literature.

Besides the high OPEX of ZBB, similar trends as for CAPEX initial are recognised, where LFP and lead-acid have the lowest OPEX costs in 2020 and where due to a higher learning rate, the OPEX of LFP declines most over time.

After analysis of the results of the CAPEX and OPEX calculations, the results of two remaining components of total system costs are considered, namely the results of decommissioning costs, which are discussed in the following Subsection, and the results of the end of life value which is discussed thereafter.

5.2.6. Decommissioning costs

The decommissioning costs per unit of energy of all BESS types and for two locations types are visualised in Figure 5.12.

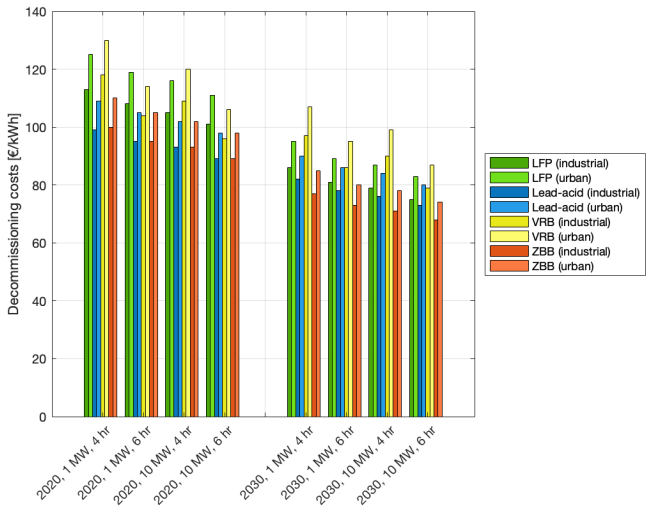

Figure 5.12: Decommissioning costs in terms of energy [€/kWh] of LFP, lead-acid, VRB and ZBB 4 and 6 hour batteries of power capacities 1 and 10 MW in 2020 and 2030 for industrial and urban locations

Analysis of results

The ten percent increased decommissioning costs per unit of energy for urban area decommissioning is recognised throughout the Figure. Furthermore, the only battery type which has to consider recycling costs is LFP in 2020. Therefore, LFP in 2020 does not have the lowest decommissioning costs per unit of energy among the BESS. Also, the trend which was recognised for the EPC costs component in CAPEX initial, is recognised in the decommissioning costs per unit of energy since EPD costs are essentially the EPC costs. The decommissioning costs per unit of energy for ZBB and lead-acid are lower due to the absence of extra safety measures which are present in VRB and LFP batteries.

Also, the decommissioning costs are simplified to the addition of EPD and recycling costs, accounting for the specific location of the BESS instead of considering the four decommissioning cost components as explained. For completeness, the four cost components should be considered separately. However, due to a lack of correct data, this is simplified as explained in Section 3.3.

5.2.7. End of life value

The end of life values per unit of energy for all BESS types are shown in Figure 5.13.

Analysis of results

Since the end of life value per unit of energy is actually not an expense but a revenue, a high end of life value per unit of energy is desired. The end of life value per unit of energy of LFP batteries in 2020 is the smallest, due to the age of the SB at the end of the lifetime of the hybrid installation. The SB has lost almost all of its value and is close to needing a replacement. On the other hand, the end of life

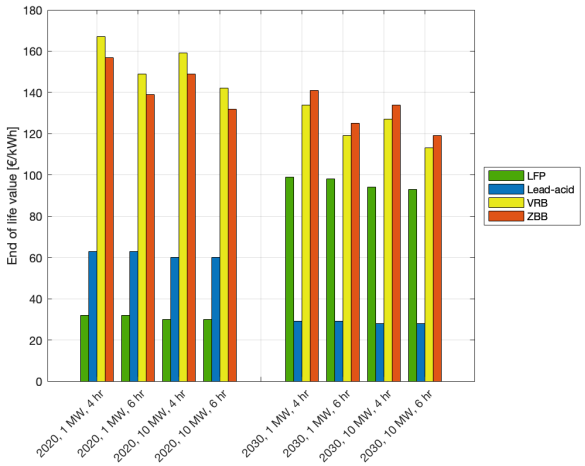

Figure 5.13: End of life value in terms of energy [€/kWh] of LFP, lead-acid, VRB and ZBB 4 and 6 hour batteries of power capacities 1 and 10 MW in 2020 and 2030

value per unit of energy of lead-acid is therefore higher, since replacement has occurred more recently.

The end of life values per unit of energy of VRB and ZBB are highest in both years since the high number of cycles of the flow batteries. The cycle life is almost twice as long as the hybrid installation lifetime, which explains the high end of life value per unit of energy.

Only the *SB* costs are considered for the end of life value in this study. It is also likely that other components might have a value at the end of the lifetime of the hybrid installation. However, to compensate for the assumption that only the SB needs to be replaced, as explained in Section 5.2.3, only the SB is considered to have an end of life value. To provide a more comprehensive analysis, it would be advisable to include other components as well or a factor to account for the likelihood of other components having an end of life value.

All the components together have led to the final total system costs per unit of energy. The replacement costs, OPEX, decommissioning costs and the end of life value per unit of energy have been discounted. The total system costs per unit of energy are discussed in the next Subsection.

5.2.8. Total system costs

The total system costs per unit of energy for all BESS types are shown in Figure 5.14, the distinction for industrial and urban areas is present.

Analysis of results

The total system costs per unit of energy in 2020 are ranging from 484 (LFP 10 MW 6 hr) - 744 (lead-acid 1 MW 4 hr) €/kWh whereas in 2030 the range is from 294 (LFP 10 MW 6 hr) - 611 (ZBB 1 MW 4 hr) €/kWh, mainly due to innovation. In absolute terms, the system costs [€] are lowest for LFP batteries (1 MW 4 hr) in both reference years, highest for lead-acid (10 MW 6 hr) in 2020 and for ZBB (10 MW 6 hr) in 2030.

The difference of total system costs per unit of energy for the two different location types are 3 €/kWh for each type of BESS, for each duration and power capacity combination. In the case of the cheapest system costs per unit of energy among all, LFP (10 MW 6 hr 2030), this is a difference of around 1 percent. Therefore, the difference is assumed as negligible for the remainder of this analysis.

In both reference years, the total system costs for LFP and VRB are the lowest. Comparing ZBB and VRB, VRB has lower system costs per unit of energy due to the slightly lower CAPEX and ZBB has higher system costs per unit of energy due to the high OPEX costs. The total system costs per unit of energy of lead-acid batteries mainly suffers from high replacement costs, relatively low end of

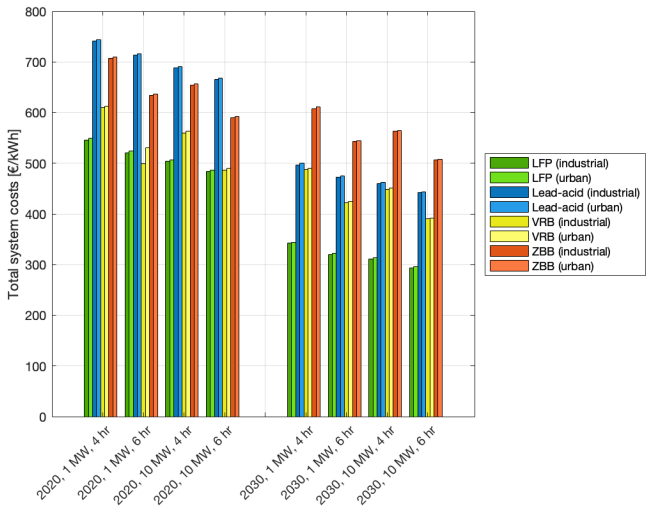

Figure 5.14: Total system costs in terms of energy [€/kWh] of LFP, lead-acid, VRB and ZBB 4 and 6 hour batteries of power capacities 1 and 10 MW in 2020 and 2030 for industrial and urban locations

life values and the absence of the learning rate over time.

In the period between 2020 and 2030, the total system costs reduction in percentages for the various BESS types are: 37 percent for LFP, 33 percent for lead-acid, 20 percent for VRB and 14 percent for ZBB.

The learning rates over time of ZBB and VRB are conservative. This is also highlighted by the reports which provide the learning rate. The learning rate of ZBB is considered here as similar as the learning rate of lead-acid batteries while ZBB are less mature. The reason for the conservative annual learning rate value is probably because the data used for the cost breakdown of ZBB is based on percentages of other BESS, explained by (IRENA, 2017; Mongird et al., 2019; Viswanathan et al., 2022). The expectation is that the learning rate of ZBB would be around the same as for VRB, so 2.2 - 2.3 percent. However, since there is a lack of data on ZBB cost components, no adjustments are made to the data found in literature. Also, in the case ZBB reaches at the cost level of VRB, VRB is safer and would still be the more interesting option.

Conclusion of results

Knowing the total system costs and the operational profit of the four BESS types at 40 size points, it can be concluded that LFP batteries are the most economically attractive in both reference years whereas ZBB are least attractive. Comparing the other two BESS types, lead-acid is more attractive in terms of profitability whereas VRB is more attractive regarding costs. Since the costs are much more significant than than the operational profit, VRB is considered as more attractive than lead-acid.

In addition to the economic point of view, safety is an important parameter for evaluating BESS, especially when they are located near urban areas. Consequently, the VRB, which is not only the second most economically attractive option but also one of the safest, takes precedence in terms of safety considerations. Given that both LFP and VRB perform best across the most critical assessment criteria, namely costs and safety, these two BESS types emerge as the most interesting choices for hybrid installations. Therefore the sizing process, as well as the remainder of this thesis, is exclusively focusing on LFP and VRB, with lead-acid and ZBB being excluded from further consideration throughout this study. The following Section provides an explanation of the sizing results of the 40 sizes considered for the four hybrid installations.

5.3. Sizing

The grid search approach, as explained in Section 3.4, has led to a set of NPV with the accompanied BESS sizes for each hybrid installation. Figures 5.15, 5.16, 5.17 and 5.18 present the NPV for hybrid installations with LFP and VRB at the SL and CP terminal, respectively. Figures presenting the NPV per unit of energy for the same hybrid installations can be found in Appendix Section C.3. The following two Subsections provide a conclusion and discussion of the resulting NPV.

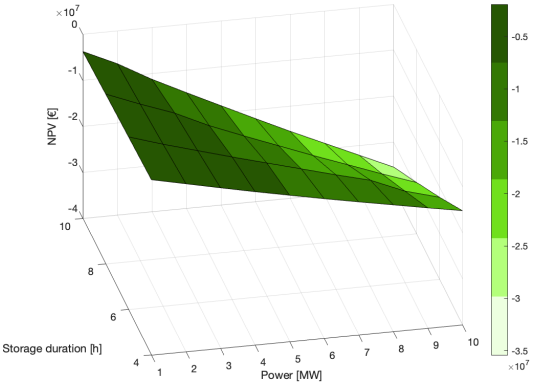

Figure 5.15: Net present value [€] of various sizes of LFP batteries at the Stena Line terminal in 2020

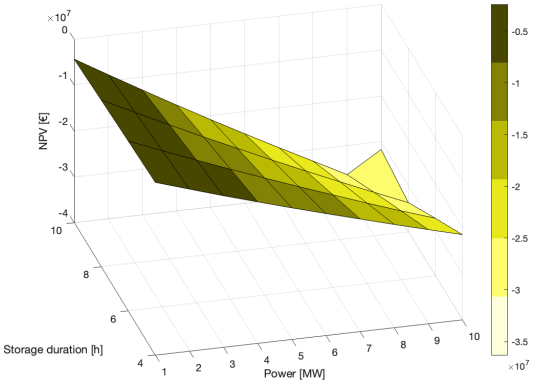

Figure 5.16: Net present value [€] of various sizes of VRB batteries at the Stena Line terminal in 2020

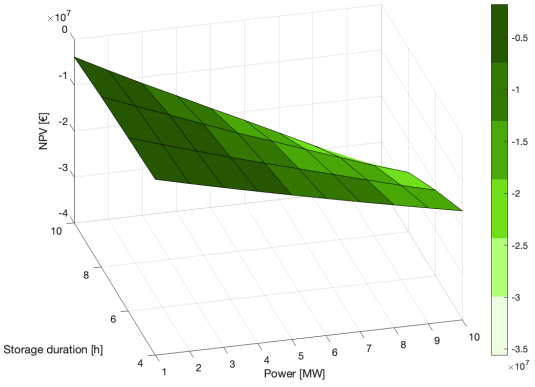

Figure 5.17: Net present value [€] of various sizes of LFP batteries at the Cruise Port terminal in 2020

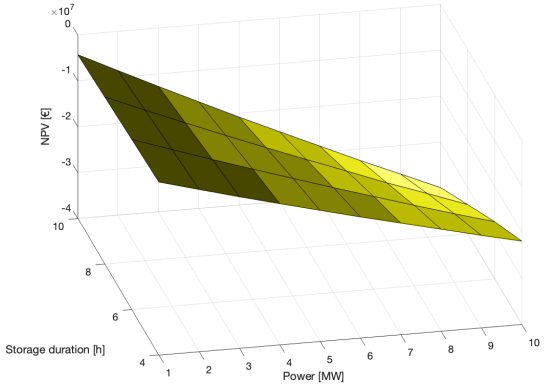

Figure 5.18: Net present value [€] of various sizes of VRB batteries at the Cruise Port terminal in 2020

Conclusion of results

The analysis demonstrates that by considering the operational profit obtained by consumer- and wholesale energy arbitrage only, the operational profit of each hybrid installation is too small to cover the total system costs within a timeline of 15 years. The NPV of each BESS type and size is negative, implicating that the hybrid installations as considered are not economically attractive. For each hybrid installation, the highest NPV is obtained for the smallest storage duration and power combination.

The findings indicate that due to the fact that the costs are much more significant than the operational profits, the costs are the decisive factor in determining the NPV. The trend which is observed for all four hybrid installations is that the NPV is highest per unit of energy [€/kWh] for the largest BESS whereas in absolute terms [€] the NPV is highest for the smallest BESS. This is due to the fact that the difference between the lowest and highest NPV per unit of battery energy capacity is smaller than the battery energy capacity factor difference with which it is multiplied to obtain the absolute NPV (1.4 versus 18).

Discussion of results

An important note is that the EMS only takes trading on the DAM into account despite the fact that trading on the IDM is possible as well. Trading on the IDM influences the performances of the hybrid installations, namely by possibly increasing the number of cycles and thereby the BESS costs, by creating an additional revenue stream and thereby increasing the operational profit and by potentially decreasing the already existing revenue streams and thereby decreasing the potential operational profit increase.

As explained in Chapter 1, the yearly volume of electricity traded on the IDM is three times as small as is traded on the DAM, for around the same price. By incorporating trading on the IDM the wholesale energy arbitrage revenue stream increases by 33 percent. For simplicity, the potential increased number of cycles and the potential decreased initial revenue stream are neglected. The results are that the NPV of the four hybrid installations remain negative. Therefore, when the potential increased number of cycles and decreased initial revenue stream are taken into account, the effect of adding trading on the IDM is considered as not significant.

Furthermore, an alternative system which could possibly be (more) economically attractive would be based on a different physical design. The current system as defined in Section 3.2, relies on an algorithm that either selects the battery or the electricity grid for electricity supply to a vessel at berth. For every time step t, the algorithm determines which option is selected for electricity provision. This results in a necessary minimal grid connection size for the shore power installation as well as the desire for the BESS to be as close as possible to the size of the highest power capacity demanded by a vessel.

In the case of considering the BESS solely as a peak demand electricity provider, the grid and the BESS can be used simultaneously as electricity providers. The advantage is the possibility of a decreased grid connection size resulting in lower grid connection costs as well as in smaller BESS and therefore lower costs. On the other hand, the accompanied disadvantage is the resulting decreased operational profit which is influenced by the BESS size as well. Therefore, this alternative is not further considered here but provided as a recommendation fur future research.

Two characteristics of the algorithm are discussed. The algorithm considers direct trading of electricity and is not anticipating future events. Direct trading is explained first whereafter the fact that the algorithm is non-predictive is discussed. In reality, trading on the DAM happens the day before production and delivery. The amount of electricity from the BESS which is traded on the DAM is then reserved for a day. Since the algorithm as designed in this research is non-predictive, the reality is simplified by considering the real-time DAM prices for every time step t, resulting in direct selling (or not). The disability of the algorithm to take into account future events results in the fact that the BESS is not operated as optimally as it would be when forecasts of price movements would have been incorporated.

Although the hybrid installations as considered are not viable, the BESS are sized nevertheless, based on other metrics than the NPV. It is necessary to complete the sizing in order to conduct and gain insights from the sensitivity analyses which are provided in Section 5.4. The results of the sizing approach based on the additional constraints are provided in the following Subsection.

5.3.1. Sizing constraints

Since sizing based on the NPV does not make sense, it is completely based on the additional sizing constraints. This Subsection elaborates on the results of the sizing process based on the trade-off between the constraints of physical size and vessel demand at the terminals of the hybrid installations. It is important to be aware of the positive correlation between an increased storage duration and/or power capacity and the physical size of the BESS.

Physical size constraint

First, the correlation between the physical size and the size in terms of capacity is estimated with real life examples of LFP and VRB, with a storage duration of 4-hours. The reason for the choice of systems with a 4-hour storage duration (instead of 6, 8 or 10) is based on the positive correlation with increasing storage duration and increasing size. In the case of LFP batteries, ZES-packs are used as an example

(Services, 2023). The LFP containers (20 ft, with a volume of 33 m^3) have a power capacity ranging from 500 to 1000 kW and an energy capacity of 2.6 MWh. For the container to have a storage duration of 4-hours, it is calculated that the average power capacity is around 650 kW.

For VRB, an example of a system with a storage duration of around 4-hours was found at the website of the Clean Energy Institute (Institute, 2023). The physical size of the system is equal to a shipping container (20 ft, with a volume of 33 m^3) and the energy and power capacity are 2.2 MWh and 0.6 MW, respectively. As expected, the energy and power capacity of an LFP 20 ft container is somewhat higher compared to the VRB 20 ft containers.

Vessel demand constraint

In case of the SL terminal, the maximum power capacity demanded by a vessel in 2022 is 2.25 MW. This results in the need of 3.5 and 3.75 20 ft containers for LFP and VRB, respectively. The size is considered as acceptable, considering the trade-off between the demand and physical space constraint. With this size, the BESS has the potential to provide 100 percent of the vessels with electricity from the BESS. Therefore, the SL terminal vessel's maximum power capacity determines the power capacity of the two types of BESS at the SL terminal. This results in both LFP and VRB to have a power capacity of 2.25 MW and an energy capacity of 9 MWh with a storage duration of 4-hour.

The maximum power capacity demanded by a vessel at the CP terminal in 2022 is 10 MW. This results in the need of 15.38 and 16.66 20 ft containers for LFP and VRB, respectively. In order to decrease the BESS size amap, the potential serviceable demand is accepted to be decreased to 50 percent. Therefore, for the CP terminal it is accepted if the BESS has a power capacity with the ability to serve 50 percent of the vessels at their maximum power demand. Figures 5.19a and 5.19b represent the normal distribution of the shore power demand for the SL and CP terminal, respectively.

In case of the CP terminal, the power capacity of the BESS is accepted to range from 6 - 10 MW, resulting in an energy capacity of 24 - 40 MWh due to the storage duration of 4-hours and the accompanied number of 20 ft containers are 9.2 - 15.38 and 10 - 16.66 for LFP and VRB, respectively. The final size of the BESS at the CP terminal hybrid installation is determined based on the results of the energy efficiency and effectiveness analyses.

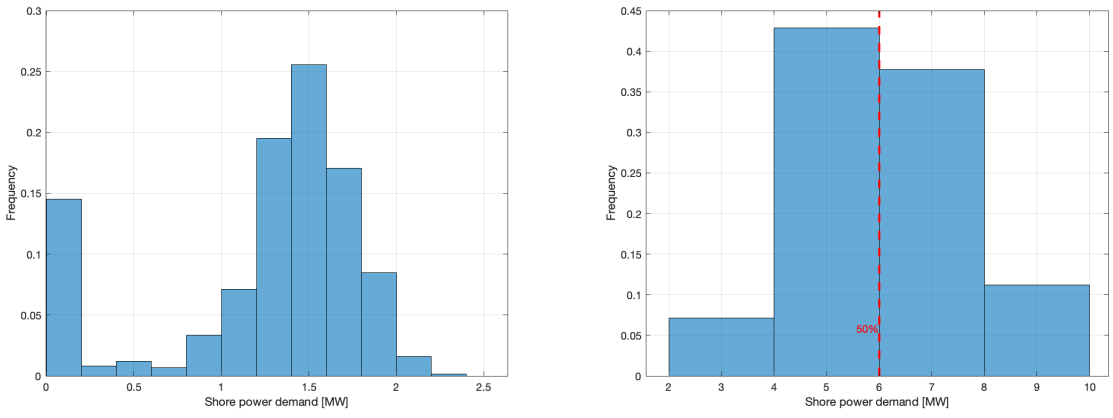

(a) Stena Line (SL) terminal

(b) Cruise Port (CP) terminal

Figure 5.19: Normal distributions of shore power demand [MW] of the SL and CP terminal in 2022

The operational profit, yearly number of cycles, total battery system costs, NPV and the LCOS of the four different sized hybrid installations considered are presented in Table 5.6. For both the LFP and VRB CP hybrid installations, the two BESS sizes of 6 MW and 10 MW are considered.

The Table shows similar results as before, the higher the power capacity of the BESS, the more negative the NPV of the hybrid installation. Taking this correlation into account as well as the desire to

Table 5.6: Results of the battery energy storage system sizing process

Parameter	Unit	LFP SL	VRB SL	LFP CP	VRB CP
Power capacity	[MW]	2.25	2.25	6 & 10	6 & 10
Storage duration	[h]	4	4	4	4
Energy capacity	[MWh]	9	9	24 & 40	24 &40
Nr. of containers (20 ft)	[-]	3.5	3.75	9.2 & 15.38	10 & 16.66
Volume	[m^3]	116	124	304 & 508	330 & 550
Yearly cycles	[-]	390	348	307 & 306	273 & 270
Operational profit per unit of energy	[€/kWh]	13.8	1.9	9.1 & 9.2	0.9 & 0.9
Operational profit	[k€]	120	17	220 & 365	20 & 35
System costs per unit of energy	[€/kWh]	554	604	500 & 482	577 & 554
System costs	[M€]	5	5.4	12 & 19.3	13.8 & 22.2
NPV per unit of energy	[€/kWh]	-440	-588	-424 & -406	-570 & -547
NPV	[M€]	-4	-5.3	-10.2 & -16.2	-13.7 & -21.8
LCOS	[€/MWh]	421	473	477 & 506	555 & 549

limit the physical space, the resulting energy efficiency and effectiveness are assessed critically. The following Sections elaborate on the energy efficiency and effectiveness of the six hybrid installations.

5.3.2. Energy efficiency

The energy efficiency of the hybrid installations are presented in Table 5.7.

Table 5.7: Energy efficiency of six hybrid installations

Parameter	Unit	LFP SL	VRB SL	LFP CP	VRB CP
Total vessel demand capacity	[GWh]	5.18	5.18	10.6	10.6
Consumer energy arbitrage capacity	[GWh]	1.55	1.66	0.72 & 1.18	0.82 & 1.28
Energy efficiency	[%]	29.9	32.0	6.8 & 11.2	7.8 & 12.0
Max. serviceable demand	[%]	100	100	50 & 100	50 & 100

In the case of the 10 MW BESS at the CP terminal, the energy efficiency is higher compared to the case of 6 MW CP BESS. However, the energy efficiencies of the SL hybrid installations are nevertheless more than two times higher. Therefore, it can be concluded that the potential decrease in the connection size and thus costs of the hybrid installation and the grid is more likely to happen at the SL terminal and unlikely to happen at the CP terminal, irrespective of the size of the BESS. Therefore, there are no incentives based on the results of the analysis of the energy efficiency of the hybrid installations to use 10 MW BESS at the CP terminal hybrid installations. In order to be complete, the effectiveness of the hybrid installations is discussed in the following Subsection.

5.3.3. Effectiveness

The results of the analysis on the effectiveness of the six hybrid installations are shown in Figure 5.20.

The blue bars in the Figure illustrate how the total operational revenue is distributed across the two functionalities, consumer- and wholesale energy arbitrage for each hybrid installation. The red and green bar represent the charging costs and the operational profit, which are equal to the total operational revenue. The total operational revenue is expressed on top of the blue bar and the installations' operational profit margin are presented on top of the red and green bar.

For the CP terminal hybrid installations with BESS size 6 MW, the consumer energy arbitrage revenue stream is only 12.2 and 13.5 percent of the total revenue for LFP and VRB, respectively. When the CP terminal BESS is 10 MW, these percentages are 12.1 and 12.6, respectively. At the SL terminal hybrid installations, the consumer energy arbitrage contributes 56.5 and 59.0 percent of the total revenue for LFP and VRB, respectively. This implies that the installations at the CP are not effective and not efficient. The opposite holds for the installations at the SL, which are efficient and effective.

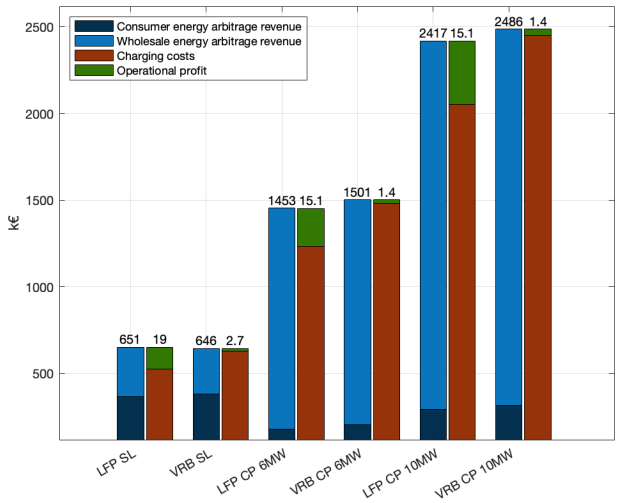

Figure 5.20: Revenue streams compared to the charging costs and the operational profitability of four hybrid installations, the total revenue is shown on top of the blue bar whereas the operational profit margin is expressed on top of the red and green bar

Besides the energy efficiency and the effectiveness, the operational profit margins do not differ when the BESS size is increased at the CP terminal.

Furthermore, the operational profit margin experienced by hybrid installations with LFP batteries is higher than with VRB. This is explained by the difference in RTE between the technologies. Therefore, it is concluded that for the hybrid installation operational profit margin, and thus for the effectiveness, a higher BESS RTE is desirable.

Taking the results of the energy efficiency and effectiveness analyses into account, as well as the fact that the 10 MW BESS in the CP hybrid installation requires more than 1.5 times the physical space of the 6 MW BESS, there are no incentives to size the BESS for the CP hybrid installation bigger than the minimum required size of 6 MW. therefore, the final size of the BESS at the CP terminal is 6 MW in terms of power and 24 MWh in terms of energy with a storage duration of 4 hours.

In order to gain insights in the effects of various hybrid installation input parameters, the following Section focuses on the sensitivity analyses which are conducted for each hybrid installation.

5.4. Sensitivity analyses

This Section elaborates on the results of the sensitivity analyses which are conducted according to the methodology as explained in Section 3.5. After completing the sensitivity analyses, Subsection 5.4.6 presents alternative scenarios with the aim to ensure economic viability of the installations. The sensitivity of the NPV to various parameters is indicated with percentages. Positive percentages refer to an increase in the NPV whereas negative percentages refer to a decreased NPV.

5.4.1. Base year

This Subsection explains the results of the sensitivity analysis of the NPV to varying the base year. With respect to the EMS analysis, the sensitivity analysis shows that the RTE only affects the operational profit and that the number of yearly cycles remains the same throughout the years. The number of yearly cycles is affected by the SoE of the BESS type, which is assumed to remain unchanged over the years.

Figure 5.21a and Figure 5.21b show the operational profit and BESS costs, respectively for four hybrid installations for two base years, 2020 and 2030. In Figure 5.21a, the values on top of the bars

represent the operational profit per unit of energy whereas in Figure 5.21b these values represent the costs per unit of energy. The sensitivity percentage values in Table 5.8 are indicating the corresponding growth or decline of the operational profitability or BESS costs over time.

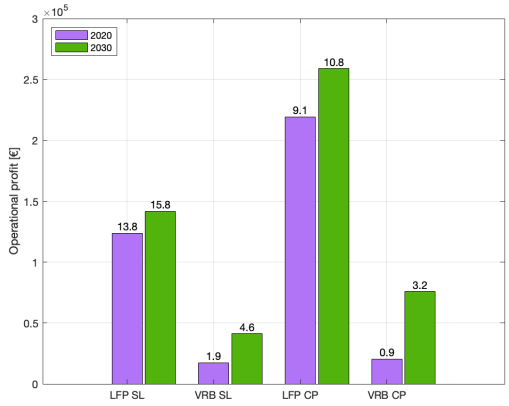

(a) Operational profit [€], operational profit [€/kWh] is shown on top of the bars

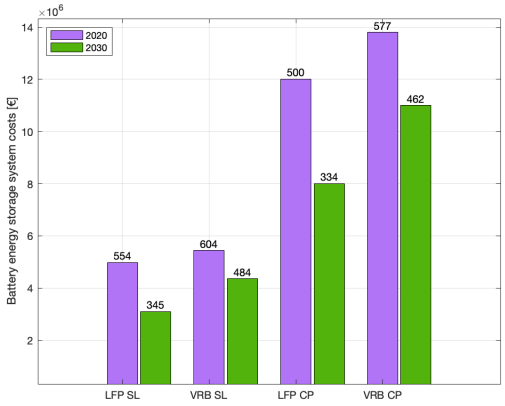

(b) Battery energy storage system (BESS) costs [€], costs [€/kWh] are shown on top of the bars

Figure 5.21: Resulting operational profit [€] and BESS costs of four hybrid installations by varying base year as sensitivity analysis, operational profit [€/kWh] is shown on top of the bars

Table 5.8: Sensitivity percentages of the operational profitability and the battery system costs of four hybrid installations to varying the base year

Parameter	Unit	LFP SL	VRB SL	LFP CP	VRB CP
Operational profit sensitivity to base year	[%]	14.5	136.2	18	269.8
Battery system costs sensitivity to base year	[%]	-37.8	-20	-33.3	-19.9

The increase in operational profit over time is solely caused by the increased RTE over time. It is observed how the smaller the original (2020) operational profit is, the more impacting the time changing RTE is to the operational profit.

The decrease in costs over time is caused by the increased cycle life as well as by the lower CAPEX due to the learning rate over time. Therefore in absolute numbers, the impact on the costs to varying the base year is more substantial compared to as the impact on the operational profit since it is affected by more factors. The sensitivity percentage values as presented in the Table are higher for the operational profit since the operational profit is smaller.

The NPV of the hybrid installations becomes higher when either the operational profit increases or the costs decrease, or both. In case of varying the base years, both the operational profit increases due to an increased RTE and the BESS costs decrease due to an increased cycle life and decreased cost components. The NPV and the accompanied increase over time in percentages are presented in Figure 5.22a and Table 5.9, respectively.

Table 5.9: Sensitivity percentages of the net present value of four hybrid installations to varying the base year

Parameter	Unit	LFP SL	VRB SL	LFP CP	VRB CP
NPV sensitivity to base year	[%]	51.4	24.2	42.5	23.5

Since the NPV is negative for both base years assessed and to determine the moment in time the hybrid installations become economically viable, the NPV is extrapolated over time, to an extended period from 2030. Assuming a linear trend and DAM 2022 data, the NPV for various base years for each hybrid installation is presented in Figure 5.22b. The crossing point between the NPV and the dashed lines indicates the moment in time when the hybrid installations become economically viable.

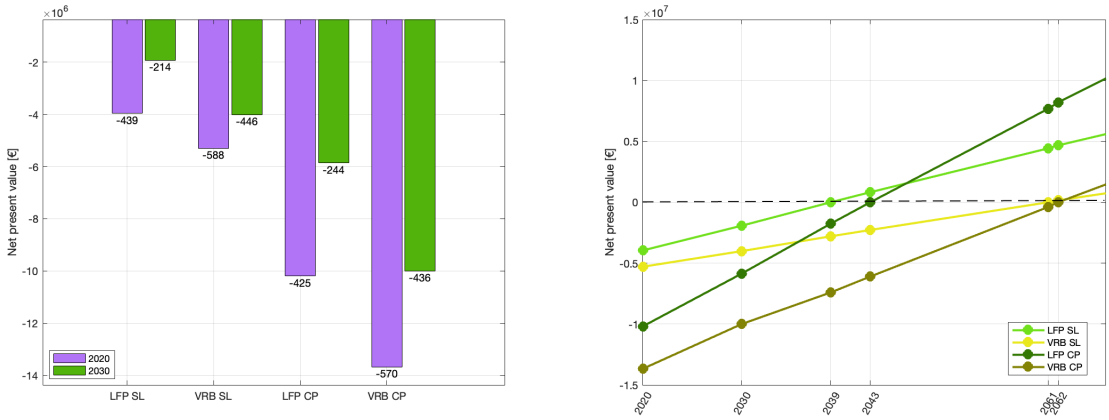

(a) Net present values (NPV) [€] by varying base year as sensitivity analysis, NPV [€/kWh] is shown on top of the bars

(b) NPV for various base years [€], the moment of economic viability is indicated by the black dashed line

Figure 5.22: NPV [€] of four hybrid installations

It must be noted that this extrapolation is only based on data from 2020 and forecasted data of 2030. Therefore, the extrapolation is more of an assumption.

It can be seen that at the SL terminal, the hybrid installations with LFP and VRB become economically viable in 2039 and 2061, respectively. At the CP terminal, the hybrid installations with LFP and VRB become economically viable in 2043 and 2062, respectively. Since the sustainability goals of the PoR are maximally projected until 2050, only the hybrid installations which become viable before 2050 are considered as interesting. However, as we rely on DAM data from 2022 for the full period of analysis, the findings of this Section tend to be conservative, as is explained in the next Subsection. Taking this into account would potentially result in shorter periods before economic viability is reached.

The upcoming Subsection focuses on the effect of the DAM data set on the resulting NPV of the four hybrid installations.

5.4.2. Day-ahead market

This Subsection elaborates on the results of the influence of the volatility and the average price of the DAM on the NPV. First, the scenarios which are tested are determined based on analysing historical DAM data sets. The results of the analysis of the historical DAM data sets is presented in Table 5.10. The historical DAM data sets are retrieved from (Entsoenergy, 2023; Pool, 2023).

Table 5.10: Volatility of the day-ahead market (DAM) of three historical years, DAM data is retrieved from (Entsoenergy, 2023; Pool, 2023)

Parameter	Unit	2020	2021	2022
Average price (μ)	[€/MWh]	32.3	103.0	241.3
Standard deviation (σ)	[€/MWh]	15.3	74.7	131.4

As mentioned in Section 2.2, eventually the grid average electricity price will decrease and the volatility will increase upon an increasing penetration of RES. However, this is not recognised in the data sets which are analysed. The average price as well as the standard deviation have increased over time. This can be clarified by the global increase of electricity demand combined with the War in Ukraine. Figure 5.23a presents the DAM electricity prices of the 25th of September in 2020, 2021 and 2022. The Figure reflects the data presented in the Table by showing the increasing average electricity price as well as the average standard deviation increase over time.

To test the sensitivity of the NPV of the four hybrid installations to the DAM data, four scenarios are compared. The first two scenarios contain the historical DAM data sets of 2021 and 2022, whereas the third and fourth scenario contain hypothetical 2023 scenarios. The first hypothetical 2023 scenario,

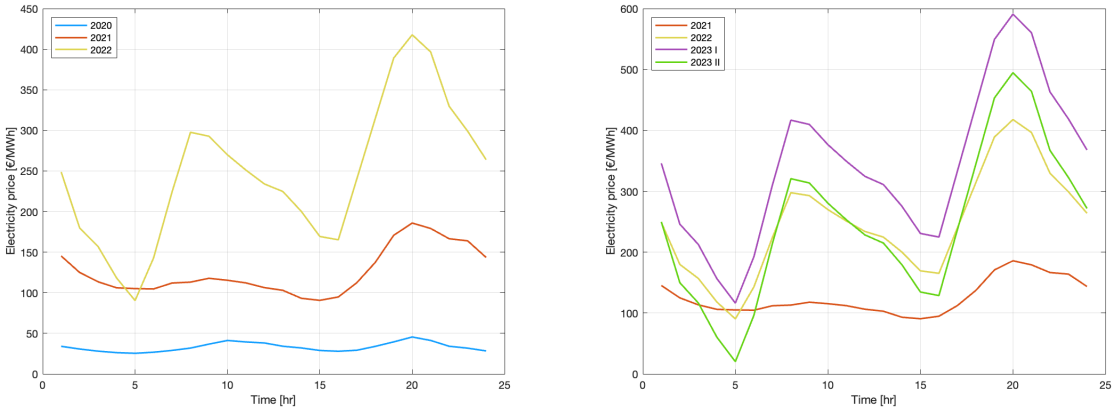

(a) In 2020, 2021 and 2022

(b) In 2021, 2022 and hypothetical 2023 I and II scenarios

Figure 5.23: Day-ahead market prices of September 25, data retrieved from (Entsoenergy, 2023; Pool, 2023)

2023 I, is based on the linear extrapolation of the historical DAM data sets, in terms of average electricity price and standard deviation. This results in a standard deviation of 190.1 €/MWh and an average electricity price of 334.5 €/MWh. The second hypothetical 2023 scenario, 2023 II, has a similar average electricity as 2022 and a linear extrapolated increased standard deviation, resulting in a standard deviation of 190.1 €/MWh and an average electricity price of 241.3 €/MWh. For clarity, Figure 5.23b presents the electricity prices of the 25th of September of each of the scenarios which are analysed.

Figures 5.24a, 5.24b, 5.25a, 5.25b show the resulting NPV upon the four different DAM data scenarios. The 2022 scenario is the initial base scenario. Table 5.11 presents the sensitivity percentages of the base scenario (2022) to the three alternative scenarios, so the percentage change of the NPV to varying the average price and/or the standard deviation of the data sets.

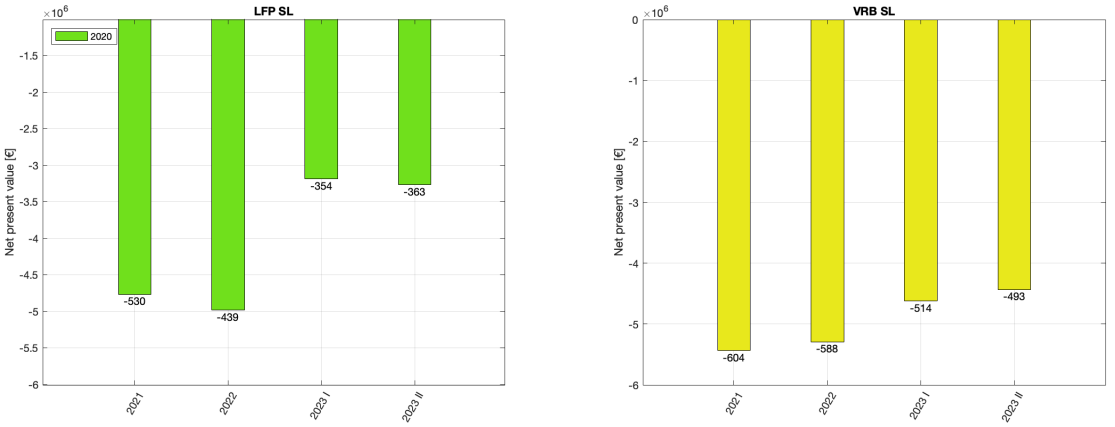

(a) Lithium iron phosphate (LFP) Stena Line (SL) hybrid installation

(b) Vanadium redox flow battery (VRB) SL hybrid installation

Figure 5.24: Net present values (NPV) [€] of the LFP and VRB SL hybrid installations for varying day-ahead market data as sensitivity analysis, NPV [€/kWh] is shown on top of the bars

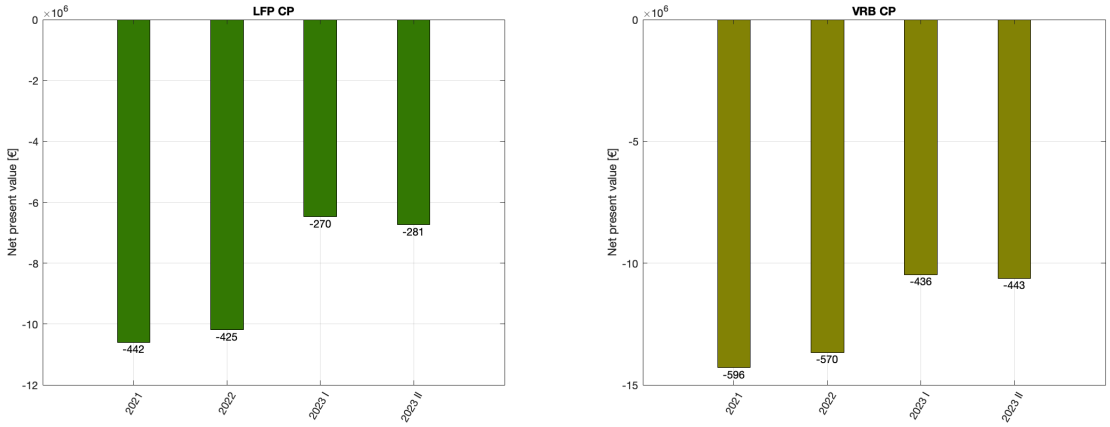

(a) Lithium iron phosphate (LFP) Cruise Port (CP) hybrid installation

(b) Vanadium redox flow battery (VRB) CP hybrid installation

Figure 5.25: Net present values (NPV) [€] of the LFP and VRB CP hybrid installations for varying day-ahead market data as sensitivity analysis, NPV [€/kWh] is shown on top of the bars

Table 5.11: Sensitivity percentages of the net present value of four hybrid installations to varying the day-ahead market data

Parameter	Unit	LFP SL	VRB SL	LFP CP	VRB CP
NPV sensitivity to 2021	[%]	-20.5	-2.7	-4.1	-4.5
NPV sensitivity to 2023 I	[%]	19.4	12.7	36.4	23.4
NPV sensitivity to 2023 II	[%]	17.4	16.3	33.9	22.3

The results show that by increasing the volatility, the NPV becomes higher. The differences between the NPV of the hypothetical 2023 I, II scenarios and the historical 2021, 2022 scenarios are the most significant. In most cases, except for the VRB SL hybrid installation, increasing the volatility and the average price results in the highest NPV. From these results it is concluded that the expected future trends of the DAM (increasing volatility and/or average price) will in any case enhance the NPV of hybrid installations.

The following Subsection shows the results of the sensitivity analysis to the third time-dependent input parameter of the hybrid installations, which is the renewable energy connection.

5.4.3. Renewable energy connection

This Subsection elaborates on the sensitivity of the NPV to the size of the connection of RES and the hybrid installations. The results of the three possible future scenarios on the NPV are presented in Figures 5.26a and 5.26b for base years 2020 and 2030, respectively. Again, the 2030 results tend to be conservative since DAM 2022 data is used.

For clarity, the resulting sensitivity percentages of each hybrid installation's NPV to varying the connection size of the installations with RES from 0 to 50 percent and 0 to 100 percent are presented in Table 5.12, for base years 2020 and 2030.

Table 5.12: Sensitivity percentages of the net present value of four hybrid installations to varying the renewable energy source connection, for base years 2020 and 2030

Parameter	Unit	LFP SL	VRB SL	LFP CP	VRB CP
2020 NPV sensitivity 0 to 50% RES	[%]	55.4	50.6	50.3	45.7
2020 NPV sensitivity 50 to 100% RES	[%]	110.7	98.6	100.5	90.0
2030 NPV sensitivity 0 to 50% RES	[%]	112.6	64.2	86.3	57.5
2030 NPV sensitivity 0 to 100% RES	[%]	225.1	128.3	172.6	115.0

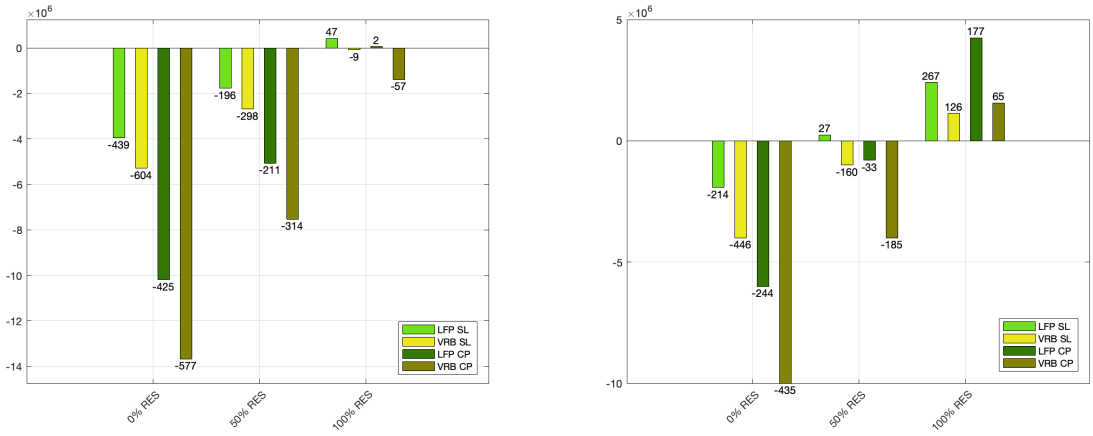

(a) In 2020 **(b)** In 2030

Figure 5.26: Net present values (NPV) [€] in 2020 and 2030 of the four hybrid installations by varying renewable energy connection as sensitivity analysis, NPV [€/kWh] is shown on top of the bars

Combining the data of the Table and the Figures, it is observed that when the sensitivity percentage is above 100 percent, the hybrid installations' NPV becomes positive, which indicates economic viability. In 2020, this is observed for the two LFP BESS containing installations at a full RES connection (100 percent). In 2030, this is observed at a half RES connection (50 percent) for the LFP SL hybrid installation and for the other three at a full RES connection.

In the results as presented, only the BESS charging costs are reduced with the same factor as the connection of RES is increased compared to the initial situation with RES (which is 50 and 100 percent). In reality, when the installation is connected to RES, the number of cycles increases as well since the BESS will be able to charge cheaply at more moments as in the initial scenario. This would affect the BESS system costs negatively, which is not incorporated in the analysis.

In addition to the effect of varying the RES connection of the installations, the influence of the various BESS functionalities on the resulting NPV of the hybrid installations is assessed, of which the results are presented in the following Subsection.

5.4.4. BESS functionalities

This Subsection shows and explains the sensitivity of the resulting NPV to varying the BESS functionalities. Figures 5.27a, 5.27b, 5.28a and 5.28b represent the resulting NPV of the four hybrid installations, for base years 2020 and 2030. The 2030 results tend to be conservative since DAM 2022 data is used. The NPV of the hybrid installations with the ability of both consumer- and wholesale energy arbitrage is similar as is presented in Figure 5.22a. The sensitivity percentages of the NPV of consumer- and wholesale energy arbitrage to varying the functionality to consumer- or wholesale energy arbitrage for both base years for the four hybrid installations are shown in Table 5.13.

Table 5.13: Sensitivity percentages of the net present value of four hybrid installations to varying the functionality of the battery system, for base years 2020 and 2030

Parameter	Unit	LFP SL	VRB SL	LFP CP	VRB CP
2020 NPV sensitivity to consumer energy arbitrage	[%]	8.5	3.6	0.9	3.2
2020 NPV sensitivity to wholesale energy arbitrage	[%]	7.6	4.6	8.4	5.2
2030 NPV sensitivity to consumer energy arbitrage	[%]	-5.0	4.0	-20.4	0
2030 NPV sensitivity to wholesale energy arbitrage	[%]	-5.0	5.7	13.4	7.3

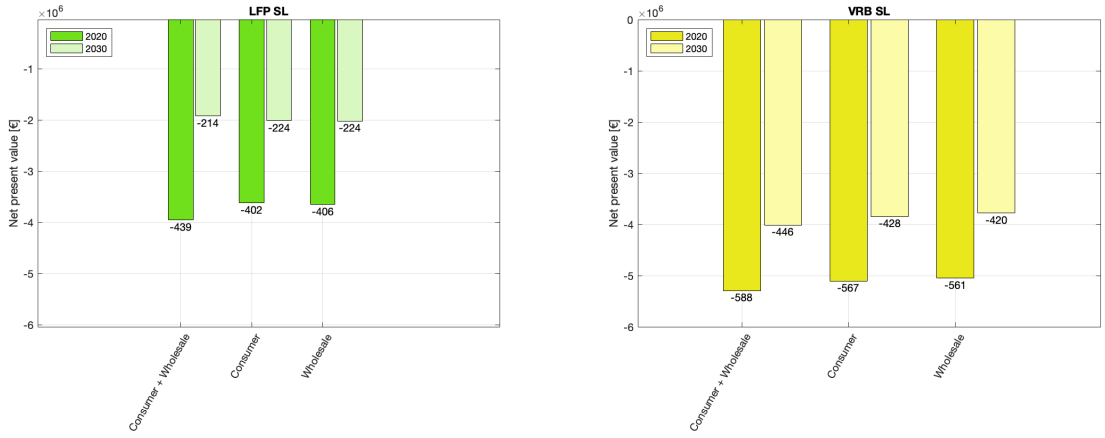

(a) Lithium iron phosphate (LFP) Stena Line (SL) hybrid installation **(b)** Vanadium redox flow batteries (VRB) SL hybrid installation

Figure 5.27: Net present values (NPV) [€] of the LFP and VRB SL hybrid installations for varying BESS functionalities as sensitivity analysis for base years 2020 and 2030, NPV [€/kWh] is shown on top of the bars

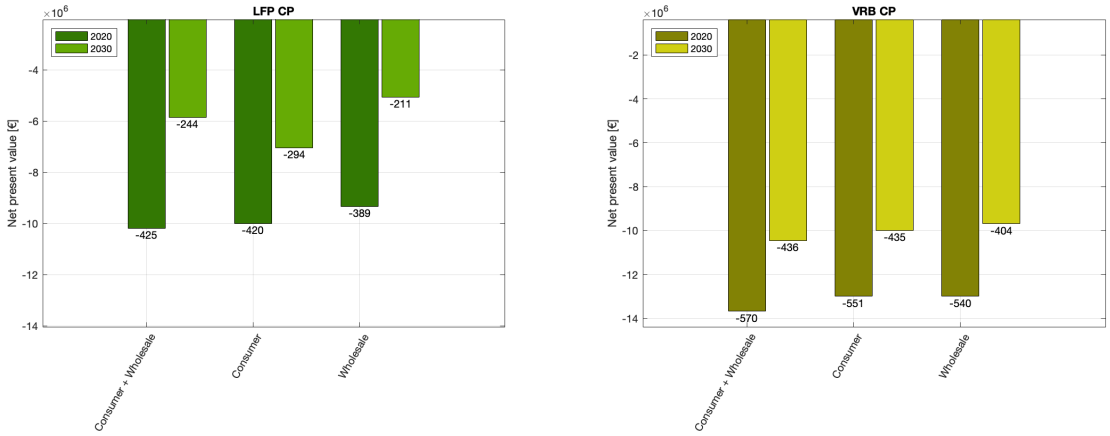

(a) Lithium iron phosphate (LFP) Cruise Port (CP) hybrid installation **(b)** Vanadium redox flow batteries (VRB) CP hybrid installation

Figure 5.28: Net present values (NPV) [€] of the LFP and VRB CP hybrid installation for varying BESS functionalities as sensitivity analysis for base year 2020 and 2030, NPV [€/kWh] is shown on top of the bars

For comparison, the scale of the installations at the SL terminal as well as of the installations at the CP terminal are aligned for both BESS types. Similar trends are observed in terms of the values of NPV among the four different hybrid installations for the two base years, namely the LFP SL installation has the highest NPV [€] whereas the VRB CP installation has the lowest NPV [€] and the NPV decreases over time.

Among the four hybrid installations, distinct results are observed for the LFP SL hybrid installation in terms of the functionality with the least negative NPV. In 2020, the LFP SL installation with the functionality of consumer energy arbitrage only, is most attractive whereas in 2030 the combined ability of consumer- and wholesale energy arbitrage is most attractive. For the remainder of the hybrid installations, the installations with the functionality of wholesale energy arbitrage only are most attractive, based on their NPV.

Furthermore, the sensitivity percentages between the three functionalities for each hybrid installation are considered as small compared to the sensitivity percentages which are observed in the previous sensitivity analyses. In addition, when taking into account the potential reduction of the size of the grid connection of the hybrid installations, which could only be achieved by either the combined functionality of consumer- and wholesale energy arbitrage or by the functionality of consumer energy arbitrage only,

there are insufficient reasons to claim that for 2020 and/or 2030 it is more interesting to opt for a hybrid installation with only the functionality of wholesale energy arbitrage.

Two other arguments to opt for a hybrid installation with the combined functionality of consumer- and wholesale arbitrage are important to take into consideration. Firstly, besides the potential possibility of reducing the size of the grid connection of the hybrid installation when consumer energy arbitrage is taken into account, another potential revenue stream could be created. The business case of a hybrid installation could be varied based on the tariff paid by the vessel owner to the terminal owner. This scenario is explained further in Subsection 5.4.6. Secondly, the risk of external scenarios which are negatively influencing the frequency of vessels visiting the hybrid installations, is mitigated when the functionality of wholesale energy arbitrage is considered as well. Therefore, based on this sensitivity analysis as well as on the arguments as mentioned, the functionalities of both consumer- and energy arbitrage are considered as most viable.

In the coming Section, the sensitivity of the resulting NPV of the four hybrid installations to the definition of threshold value T is analysed.

5.4.5. Threshold T

This Subsection elaborates on the sensitivity of the resulting NPV of the various hybrid installations for base years 2020 and 2030 to five different scenarios for threshold value T. In order to quantify the scenarios of interest, the normal distribution of the DAM in 2022, which is presented in Figure 5.29, is analysed.

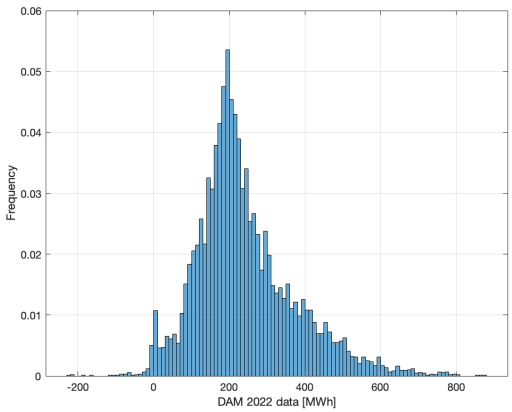

Figure 5.29: Normal distribution of 2022 day-ahead market price data, data retrieved from (Pool, 2023)

The average electricity price of the DAM 2022 data set is 241 €/MWh, the most frequently occurring electricity price of the DAM 2022 data set is 195 €/MWh and the boundary value for the 50 percent percentile is 215 €/MWh, presenting the first three scenarios. Also, the 25th and 75th percent percentiles, which are 160 €/MWh and 305 €/MWh, respectively, are used as scenarios for T in the sensitivity analysis. The results of the five scenarios for base years 2020 and 2030 on the resulting NPV of the four hybrid installations are shown in Figures 5.30a, 5.30b, 5.31a and 5.31b. The results in 2030 tend to be conservative since DAM 2022 data is used. The accompanied sensitivity percentages are presented in Table 5.14. The scenarios are sorted from low to high values for T.

By analysing the Figures and values presented in the Table, it becomes clear that the base scenario for T, where T is the average electricity price of the DAM 2022 data set, is not the most favourable scenario among the five analysed. The 25th percentile percentage scenario of T = 160 €/MWh is in most of the cases the best threshold T, based on the resulting NPV. Therefore, it can be concluded that in 2022 it is more favourable if the BESS charges less often, at lower prices. Since T depends directly on the corresponding DAM data set which is used, it is difficult to generalise the conclusion for other years.

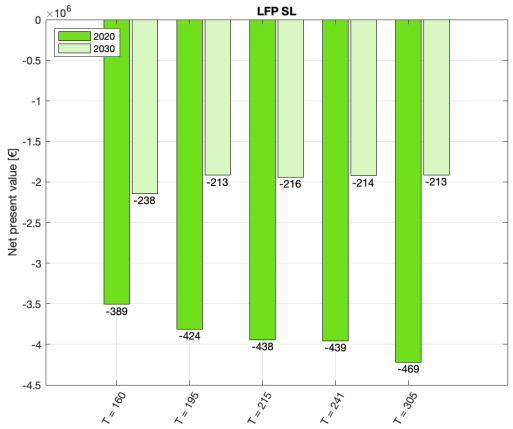

(a) Lithium iron phosphate (LFP) Stena Line (SL) hybrid installation

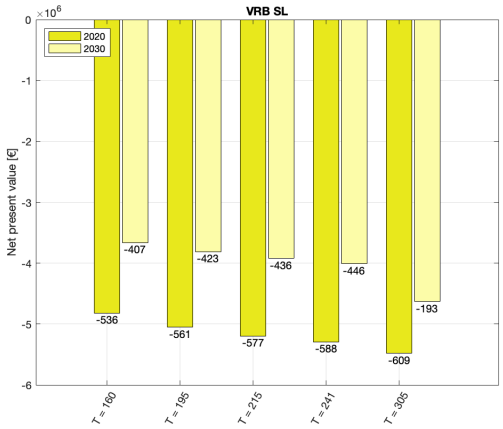

(b) Vanadium redox flow battery (VRB) SL hybrid installation

Figure 5.30: Net present values (NPV) [€] of the LFP and VRB SL hybrid installation for varying T as sensitivity analysis for base years 2020 and 2030, NPV [€/kWh] is shown on top of the bars

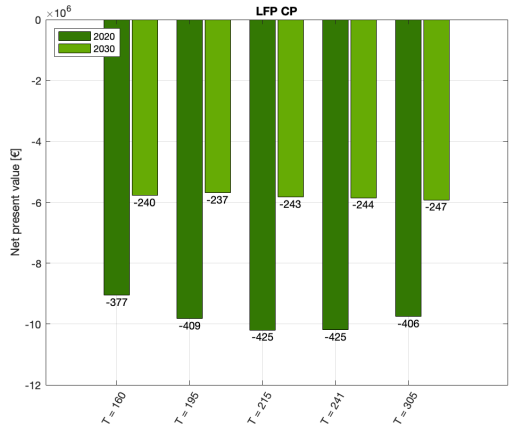

(a) Lithium iron phosphate (LFP) Cruise Port (CP) hybrid installation

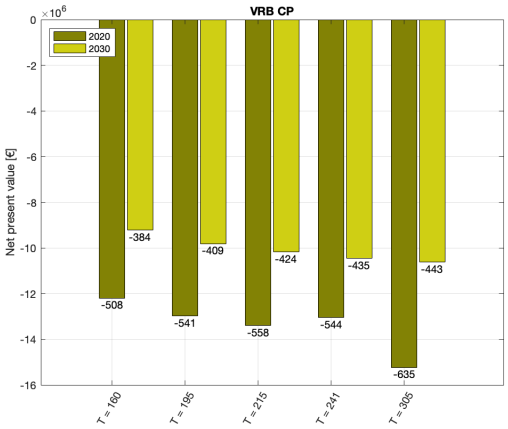

(b) Vanadium redox flow batteries (VRB) CP hybrid installation

Figure 5.31: Net present values (NPV) [€] of the LFP and VRB CP hybrid installation for varying T as sensitivity analysis for base year 2020 and 2030, NPV [€/kWh] is shown on top of the bars

To summarise all findings of the sensitivity analyses, the following Subsection provides a general conclusion of the results. This conclusion is followed by a Subsection about potential scenarios which provide economic viability of the hybrid installations.

Conclusion of results

Table C.13 provides an overview of the combined sensitivity percentages which are presented in this Section. Overall, the time-dependent parameters are more impacting the NPV compared to the choice-dependent parameters. Among all input parameters varied in the sensitivity analyses, the most impacting input parameter is the RES connection size of the hybrid installations. The impact is caused by the fact that the charging costs are decreased by 50 and 100 percent in the two scenarios, which significantly impacts the operational profit of the installations. Furthermore, when time passes by and the input parameters RTE, cycle life, cost data and the DAM data set are changed, the NPV is positively impacted automatically.

In case of the choice-dependent parameters, only the threshold value T's impact is seen. It is concluded that for the DAM 2022 data set, a lower threshold value T is more favourable, resulting in less cycles per year and charges for a lower price. The conclusion is used for the economic viability scenarios as presented in the next Subsection.

Table 5.14: Sensitivity percentages of the net present value of four hybrid installations to varying threshold value T, to varying base years 2020 and 2030

Parameter	Unit	LFP SL	VRB SL	LFP CP	VRB CP
2020 NPV sensitivity to T = 160	[%]	11.3	8.9	11.2	10.8
2020 NPV sensitivity to T = 195	[%]	3.6	4.6	3.6	5.1
2020 NPV sensitivity to T = 215	[%]	0.3	1.8	-0.07	1.98
2020 NPV sensitivity to T = 305	[%]	-6.6	-3.5	4.2	-11.4
2030 NPV sensitivity to T = 160	[%]	-11.5	8.7	1.4	11.8
2030 NPV sensitivity to T = 195	[%]	0.33	5.0	2.9	6.1
2030 NPV sensitivity to T = 215	[%]	-0.9	2.2	0.5	2.6
2030 NPV sensitivity to T = 305	[%]	0.5	-3.6	-1.1	-1.6

Furthermore, the sensitivity analyses tested the sensitivity of the NPV to five different input parameters, namely the most impacting time- and choice-dependent parameters. The input parameters are selected based on their likeliness to change. It would have been more complete if all input parameters were assessed, also the parameters which are not expected to change, such as assumptions (for example, DAM 2022 for each analysis) and uncertainties (inflation and conversion rate).

5.4.6. Scenarios

Taking the conclusions of the sensitivity analyses into consideration, this Subsection aims to establish potential scenarios where economic viability of the hybrid installations is ensured, for both base years 2020 and 2030. The scenarios are based on the most optimal but also realistic parameter conditions, as well as on an additional fee which is charged to the vessel owners upon using shore power. The input parameters which are used for the scenarios are summarised in Table 5.15.

Table 5.15: Realistic and most economically enhancing input parameters for hybrid installation scenarios, based on findings of the sensitivity analyses

Parameter	Unit	2020	2030
DAM year	[-]	2022	2023 II
RES connection	[%]	0	50
BESS functionalities	[-]	Both	Both
Threshold T	[€/MWh]	25th percentile (160)	25th percentile (124)

The 2020 scenario differs from the 2030 scenario in terms of the base year which results in (a) more favourable RTE, cycle life and BESS costs in 2030, as is explained in the sensitivity analysis. Also, the DAM data for the 2030 scenario is taken to be most similar to the hypothetical DAM data of 2023 II. Also, the RES connection is expected to be available for 50 percent of the time in 2030. Furthermore, for both scenarios the DAM 2022 most favourable threshold T, which is the 25 percent percentile of the data set, is chosen for the EMS. In the 2020 scenario (DAM 2022) this results in T is 160 €/MWh and in the 2030 scenario (DAM 2023 II) this value is 124 €/MWh. It should be noted that there is no analysis done on whether the most favourable T of the DAM 2022 data set holds for the 2023 II data set as well. The resulting NPV for both scenarios for the four hybrid installations is presented in Figure 5.32.

To reach economic viability, the NPV should be equal to or bigger than zero. As explained in Subsection 3.4.4, the LCOS represents the price of the electricity which should be paid in order for the hybrid installation to become economically viable. The LCOS of the various installations is presented in Table 5.16.

The difference between the LFP and VRB installations' LCOS in both scenarios is caused by two factors. First, the higher RTE of LFP causes less losses of electricity and the system costs of LFP BESS are lower than VRB BESS, so less system costs have to be covered with the sold electricity in

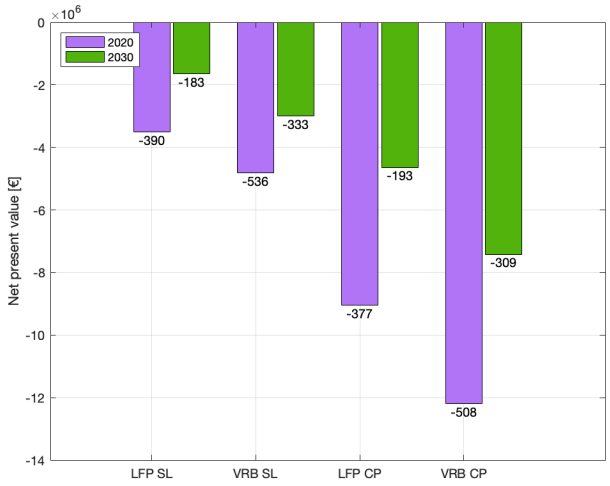

Figure 5.32: Net present values (NPV) [€] of the four hybrid installations for two scenarios, NPV [€/MWh] is shown on top of the bars

Table 5.16: Levelised costs of storage of four hybrid installations in two scenarios

Parameter	Unit	LFP SL	VRB SL	LFP CP	VRB CP
2020 LCOS	[€/MWh]	448	552	476	561
2030 LCOS	[€/MWh]	217	287	218	315

the case of LFP. Furthermore, the difference in LCOS for both years is caused by the enhanced RTE over time for both BESS types, by decreased system costs over time and by decreased charging costs due to the presence of the 50 percent RES connection in 2030.

If all the electricity which is provided to consumer- and wholesale energy arbitrage is sold for a price at the LCOS, the hybrid installation would be economically viable. Since the electricity which is sold for wholesale energy arbitrage has a fixed price, namely the DAM price, the price of the electricity sold for consumer energy arbitrage has to cover the difference between the current wholesale energy arbitrage price and the LCOS.

The NPV is used to calculate the necessary fee which should be charged by the vessel owners who are using shore power in order to ensure economic viability of the hybrid installation. In the cases where the hybrid installation is not economically attractive yet, the NPV is the minimal additional amount of money which should be charged to the vessel owners. By discounting the NPV back to a yearly value and then dividing this by the total yearly demand of vessels to the installation, the minimum fee which should be charged additionally per MWh of electricity demand to the vessel owners is determined. For each hybrid installation this additional fee is presented in Table 5.17.

Table 5.17: Minimum fixed additional fee which should be charged to vessel owners in two scenarios at four hybrid installations

Parameter	Unit	LFP SL	VRB SL	LFP CP	VRB CP
2020 additional fixed fee	[€/MWh]	82	112	102	138
2030 additional fixed fee	[€/MWh]	38	70	53	84

If the hybrid installations operate as indicated in the two scenarios, including the additional fee which is charged by using shore power, the hybrid installations are economically viable from the terminal operators' point of view. In both scenarios, the LFP SL hybrid installation requires the smallest additional fee to reach economic viability.

To discuss the potential of the scenarios from the vessel owners' point of view, the total average price which is paid by vessel owners in the case of using hybrid installations is compared to the average price which is paid for marine gasoil (MGO).

The total average price which is paid by vessel owners in the case of using hybrid installations at berth, is determined by combining the average DAM price during the moments a vessel is present at berth and the additional fixed fee. Table 5.18 represents the average DAM prices of the two terminals of the moments when vessels are present at berth, which is the average shore power price (without integration of a BESS). Then, Table 5.19 presents the total average price which is paid by vessel owners in case of using the hybrid installations in scenario 2020 and 2030.

Table 5.18: Average day-ahead market prices of a 2020 and 2030 scenario, using day-ahead data of 2022 and hypothetical data set 2023 II, respectively

Parameter	Unit	Stena Line	Cruise Port
2020 average DAM price paid by vessel owner	[€/MWh]	264	270
2030 average DAM price paid by vessel owner	[€/MWh]	275	283

Table 5.19: Total average price which is paid by vessel owners in case of using shore power in scenario 2020 and 2030

Parameter	Unit	LFP SL	VRB SL	LFP CP	VRB CP
2020 total average price paid	[€/MWh]	346	377	373	408
2030 total average price paid	[€/MWh]	313	344	335	367

According to private data obtained by the PoR Authority, the 2022 average MGO price was 1.01 €/kg. Taking the average energy efficiency of a conventional vessel engine of 35 percent into consideration, the average MGO consumption in weight per energy is 300 kg/MWh. This results in an average MGO price of 303 €/MWh in 2022.

Comparing the 2022 average MGO price with the scenarios' average DAM prices paid by vessel owners as shown in Table 5.18, the MGO price is higher. Therefore, in both scenarios, shore power is more attractive to use for fulfilment of the vessels' energy demand. However, the 2022 average MGO price is smaller than the price which must be paid when hybrid installations are used at berths, due to the additional fee.

Therefore, without regulation including a carbon tax or other incentives for using hybrid installations, the integration of a BESS in the shore power installations with the ability of consumer- and energy wholesale arbitrage is not economically viable. Fortunately, in the near future the maritime sector is added to the carbon tax system and therefore an incentive will be created to shift the utilisation of MGO to electricity (Commission, 2023a). With this shift the usage of hybrid installations will become more attractive, also from the vessel owners' point of view.

In addition to the uncertain - but with assumed high likelihood to happen - emergence of a carbon tax, the results of the study are also influenced by the uncertain - but also likely to happen - changing inflation. Throughout the research, the discount rate does not incorporate an inflation rate. In the case that the inflation changes from the in this study assumed 0 percent to a hypothetical 5 or 10 percent, the NPV of the hybrid installations are negligibly affected due to the fact that the initial CAPEX is the most significant cost component. Therefore it is accepted that there is no inflation rate taken into account in the discount rate. Appendix Subsection C.4 elaborates on the sensitivity of the NPV of the initial hybrid installations to changing the inflation factor.

Now that all the results have been outlined and discussed, including the scenarios that provide insights into how hybrid installations can become economically feasible, the research sub-questions and main question are answered in the following Chapter.

6. Conclusion and recommendations

This Chapter initiates with answering the research sub-questions as well as the research question in order to formulate the conclusion, provided in Section 6.1. Then, Section 6.2 elaborates on recommendations which are provided for future research, based on insights gained from the discussion of the results and the conclusion.

6.1. Conclusion

This study aims to provide an overview of whether different types of battery energy storage systems (BESS) can potentially improve the economic viability of shore power installations in portal areas, by consumer- and wholesale energy arbitrage. For this research, the port of Rotterdam (PoR) is used as a case study.

6.1.1. Sub-questions

This Subsection aims to provide answers to the four research sub-questions. The questions are answered in a chronological manner.

1. *Which battery energy storage systems are considered and how are they different from each other?*

   In order to be suitable for a hybrid installation as considered in this study, a BESS must be able to operate in grid-connected mode whilst also be able to provide electricity to vessels at berth, referred to as consumer energy arbitrage. A literature study has revealed that a BESS with only a single function may not be economically attractive. What also became evident is the gap in literature, indicating that there has not been a research into the integration of a BESS into a shore power installation at a berth, while shore power is prioritised and with the secondary functionality of wholesale energy arbitrage added. Both functionalities require BESS with a high energy capacity and therefore a storage duration of multiple hours.

   The BESS which were selected to be suitable for hybrid installations are lithium iron phosphate (LFP), valve regulated lead-acid, vanadium redox flow (VRB), semi-solid flow, and zinc bromine batteries. The most important characteristics shared by the selected BESS is their ability to be grid-connected and to possibly have a high energy capacity. This is proven in a literature study including practical examples (except from semi-solid flow batteries, due to their low maturity no literature was available). Also, the designs of the selected BESS have a degree of flexibility.

   Additionally, the BESS were assessed on pre-defined boundary conditions and key performance indicators (KPI's), of which the most important are the system costs, safety, the round-trip efficiency (RTE) and the cycle life. Based on the KPI's, all battery types are distinct and therefore unique. The different characteristics are caused by the nature of the BESS, conventional or flow batteries and by the distinct chemical components used in the electrolytes and/or cathode and anode materials.

   The criteria of the list of KPI's which are considered as most important for an investment in a BESS, are the system costs and safety. Since LFP has the lowest system costs[1] (549 €/MWh) and VRB has the second lowest system costs (613 €/MWh) and is the safest among the BESS considered, the selection has been narrowed down. Since each shore power installation has its own specifications and requirements, these two BESS types were selected as suitable for further

[1] The system costs for a 4-hour, 1 MW, 4 MWh 2020 system are provided, assuming 365 cycles a year

analysis.

2. *Which shore power projects are evaluated and what are their specifications?*

   Literature has shown that the implementation of shore power requires financial and/or regulatory incentives to ensure its occurrence. The integration of a BESS into a shore power installation, thereby creating a hybrid installation, potentially provides a certain financial incentive. This would therefore enhance the roll-out of shore power, which in turn contributes to the energy transition.

   The PoR, which is the largest port in Europe, is used as the location of the case study of this research. The focus was on shore power projects which have the most significant impact. A shore power project is classified as impactful when there is a substantial reduction in greenhouse gas (GHG) emissions recognised, based on both the geographical location and the power demand of the vessels during berthing. Electrifying vessel visits at berth's located near urban areas have a greater impact compared to those located far from urban areas. Additionally, the higher the power demand of the vessels, the greater the reduction in GHG emissions upon electrification.

   Vessels in ports are categorised in two groups: vessels designated for inland shipping and sea-going vessels. For the focus of this thesis, berth's for sea-going vessels were selected because sea-going vessels emit more GHG during their visits to the port. Therefore, enhancing the economic viability of shore power installations at sea-going vessel berths has a more significant impact.

   Furthermore, various berths exists for different types of sea-going vessels. For this thesis, the sea-going vessel berths located near urban areas and designated for highly-demanding vessels were of utmost importance. Therefore, the focus was on the berth of the Stena Line (SL) ferries and on the Cruise Port (CP) terminal. An important characteristic shared by both terminals is the limited physical space. As a result, it is not possible to install an infinitely large battery at the berths. This constraint was taken into account during the research.

   In addition to the fact that the berths have similarities in terms of the impact upon electrification, differences were recognised as well. The distinctions between the berths are reflected in the number of yearly visits, the maximal power demanded and the total energy demanded by vessels at berth. In 2022, the year of the case study, at the SL terminal the number of visits was 669, the maximal power demanded was 2.25 MW and the total energy demanded was 5.18 GWh. For the CP terminal the number of yearly visits was 97 with a maximal power demand of 10 MW and a total energy demand of 10.6 GWh. By comparing these numbers it becomes clear that the SL terminal experienced a more than six times higher frequency of vessel visits with a more than two times smaller total energy demand in respect to the CP terminal.

3. *How do the revenue streams generated by consumer- and wholesale energy arbitrage of battery energy storage systems contribute to the economic viability of the hybrid installations?*

   The answers to the first two sub-questions have led to the four hybrid installations that are analysed throughout this study: the LFP BESS at the SL terminal (LFP SL), the VRB BESS at the SL terminal (VRB SL), the LFP BESS at the CP terminal (LFP CP) and the VRB BESS at the CP (VRB CP) terminal. The contribution of the revenue streams generated by the two BESS functionalities consumer- and wholesale energy arbitrage to the economic viability of the four hybrid installations was primarily assessed by the net present value (NPV).

   The components which are necessary for calculating the hybrid installations' NPV are the discounted sum of the yearly operational profit and the BESS costs over the full lifetime of the installation (15 years). By modeling various battery sizes in hybrid installations using the grid search method, it was concluded that by considering the operational profit obtained by consumer- and

wholesale energy arbitrage only, for each hybrid installation the operational profit was too small to cover the total system costs within a lifetime of 15 years.

Since the NPV is negative regardless of the BESS size, it was not possible to determine an ideal system size based on the NPV. Therefore, alternatives were explored. By considering the balance between a physically smaller battery and the highest possible percentage of ships that could potentially be served, the system was sized accordingly. The resulting size for the SL terminal for both the LFP and VRB BESS was 2.25 MW, 9 MWh with a storage duration of 4 hours. For the CP terminal the LFP and VRB BESS have a size of 6 MW, 24 MWh with a storage duration of 4 hours. At the SL terminal, the BESS are able to serve 100 percent of the vessels whereas at the CP terminal only 50 percent of the vessels can be served by the BESS.

For the hybrid installations to be economically viable, the electricity which is used for consumer- and wholesale energy arbitrage must be sold at the levelised costs of storage (LCOS). The LCOS is the present value of all cost components of the storage system, including the BESS charging costs, divided by the present value of the energy output of the system.

The resulting LCOS indicated that at both terminals the installations with an LFP BESS are more economically viable compared to the hybrid installations with a VRB BESS. This is explained by the difference in RTE between the two BESS types as well as by the distinct BESS costs components. The higher RTE as well as the lower system costs of LFP batteries are beneficial for the operational profit of a hybrid installation. Secondly, the LCOS also indicated that the revenue streams were more significant at the SL terminal, due to lower energy demanding and a higher frequency of vessel visits. Therefore, the LFP SL BESS seems the most attractive for hybrid installation as considered in this study.

The sensitivity analyses have provided insights in how to enhance the economic viability of the hybrid installations to different extents. The most impactful is the future lookout. The NPV of the hybrid installations is most sensitive to parameters which are changing over time. By an increased RTE, decreased system costs, more volatile day-ahead market (DAM) prices and a part-time connection to a renewable energy source, the NPV of the hybrid installations is enhanced without actively changing the design. However, varying these parameters is insufficient for the hybrid installations to be economically viable.

The research proposed an additional fee which should be charged to the vessel owners upon using shore power from hybrid installations to cover the total BESS costs. Economic viability is thereby ensured from the terminal owner's point of view. However, analysis into the current marine gasoil (MGO) prices has shown the necessity of an incentive for vessel owners to use shore power of hybrid installations. The planned carbon taxes on MGO are an example of such an incentive.

4. *How does consumer energy arbitrage contribute to the economic viability of the hybrid installations by enhancing the energy efficiency*[2] *and effectiveness*[3]*?*

In addition to the NPV, the energy efficiency and the effectiveness of each hybrid installation were evaluated as well in order to completely assess the economic viability of the hybrid installations. If the energy efficiency of a hybrid installation is high, a potential for a smaller connection to the grid is created. When the grid connection can be reduced, a reduction of total BESS costs is created, which enhances the economic viability of the hybrid installation.

[2]The energy efficiency of a hybrid installation refers to the percentage of the total annual energy demand of the vessels that is supplied by electricity from the battery.

[3]The effectiveness of a hybrid installation refers to the percentage of the yearly total operational revenue generated by consumer energy arbitrage.

The reason why it is important for a hybrid installation to have a sufficient effectiveness is based on the difference in certainty of the revenue streams generated by consumer- and wholesale energy arbitrage. Wholesale energy arbitrage is more uncertain due to the volatility of the DAM whereas consumer energy arbitrage only relies on vessel visits, which are considered as certain.

The energy efficiencies of hybrid installations at the SL were around 30 percent whereas at the CP they were less than 10 percent. Therefore, the potential for a smaller grid connection was higher for installations at the SL. Furthermore, based on comparing the effectiveness of the installations at both terminals, it was concluded that at the CP terminal the revenue generated by consumer energy arbitrage does not contribute sufficiently to the operational profit of the hybrid installations. At the SL terminal, more than half of the revenue generated originated from the prioritised functionality of consumer energy arbitrage. Therefore, opposed to the CP, the SL hybrid installations are efficient and effective.

In line with the answer to sub-question three, when considering the profit margin of the four hybrid installations, it became clear that installations with LFP BESS were more economically attractive compared to VRB BESS. Installations with LFP BESS had a higher profit margin due to the higher RTE of LFP compared to VRB. To conclude, based on the NPV, energy efficiency, the effectiveness and the profit margin, consumer energy arbitrage at the hybrid installation LFP SL contributes most to the economical attractiveness among the various installations assessed.

6.1.2. Main question

This Subsection provides an answer to the main research question which is presented below.

Which battery energy storage systems are most suitable to enhance the economic viability of shore power projects in the portal area of Rotterdam by using consumer- and wholesale energy arbitrage?

Among the selection of BESS which were assessed on their suitability to be grid- and shore power installation connected, with the aim to be active in consumer- and wholesale energy arbitrage, LFP batteries have shown to be the most suitable in terms of economic viability whereas VRB batteries are most ideal in terms of safety. The reason why LFP batteries are enhancing the economic viability more, is based on their lowest system costs as well as their highest RTE compared to the other types of BESS assessed. A higher RTE results in lower electricity losses upon cycling the BESS.

In addition, among the two shore power installations analysed, the SL terminal was found to be the most viable to be connected to a BESS with the functionalities of consumer- and wholesale energy arbitrage. The energy efficiency and effectiveness of the hybrid installations at the SL terminal have shown that consumer energy arbitrage enhanced the hybrid installations' economic viability more than at the CP terminal. The reason is based on the higher frequency of vessel visits with a lower energy demanded, compared to at the CP terminal. Therefore, the BESS were more often available for consumer energy arbitrage with smaller cycles.

Nevertheless, the operational profit of the LFP SL hybrid installation was not sufficient to cover the total system costs over the period of the lifetime of the hybrid installation. This is due to the fact that both functionalities as well as the charging of the BESS are depending on the time dependent price differences of the DAM, which are therefore proven to be too small. Subsequently, it is concluded that under current market conditions and certain assumptions of this study, profitable energy arbitrage could not yet be achieved.

The sensitivity analyses have provided insights in two possible scenarios to ensure economic viability from the terminal owners' point of view by charging a fee to vessel owners, covering the residual uncovered costs by operating the hybrid installation. From the vessel owners' point of view, the price which is paid for using the hybrid installations is higher than the price which is paid for using MGO during berthing. Fortunately, the future carbon taxes and other regulations are likely to create incentives for using hybrid installations from the vessel owners' point of view as well.

Furthermore, it is important to realise that the conclusion of this study is grounded on results which are based on several assumptions. The discussion of the results has shown that the impact of each assumption individually did not drastically change the outcome, but it has not been explored whether a combination would result in such a change. Therefore, it is important to realise that the conclusion as provided in this Chapter applies to the specific assumptions which were made in this study.

6.2. Recommendations

Since the hybrid installations, as examined in this study, are not yet economically viable, this Section aims to provide potential research directions which could result in enhancing or ensuring economic viability of hybrid installations.

Firstly, it is recommended to look into the potential of another topology than was considered in this study. This study has examined the potential of a hybrid installation where either a BESS or the electricity grid provides electricity to a vessel for a period of 15 minutes. The potential topology would exist of simultaneously operating the electricity grid and the BESS during moments of peak demand. With this topology, the BESS is operated as a peak shaver only. Therefore, the size of the BESS can be smaller as well as the connection of the installation to the grid, both reducing the costs. In this potential topology, electricity trading could be assessed as well. It is expected that especially at the CP terminal, the potential topology could be successful. The CP terminal demands more energy less frequently compared to the SL terminal, which was more suitable for the topology as considered in this study.

Secondly, another interesting route would be to focus on creating an algorithm with the ability to use historical data and trends of the DAM to forecast future events. The algorithm of this study used real-time data to determine the resulting action of the BESS. By considering forecasts, the BESS could be operated more optimal and the operational profit could be increased.

Thirdly, it would be interesting to assess the functionality of being active on the frequency containment reserve (FCR) market. The FCR market works differently and therefore a different type of BESS would be more optimal and thus the algorithm should be designed in another fashion. The expected results are that the revenue stream created with the FCR market is higher compared to the wholesale energy arbitrage revenue stream as considered in this study. However, it should be examined whether the BESS still remains suitable for consumer energy arbitrage instead of being solely a trading device.

Finally, another interesting research area would be into the potential of a smart grid connection in the PoR where shore power- or hybrid installations are among others directly connected to renewable energy sources (RES) such as wind turbines or solar panels. By using RES, the charging costs of the BESS would be decreased. Also, grid connections could be decreased or even phased out, further decreasing costs. Simultaneously, the problem of grid congestion is potentially mitigated by using smart grids. However, investment costs would be more substantial.

References

A. Bonte, A. C. (2021). Strategy for shore power in the port of rotterdam. *Port of Rotterdam*.

ABB. (2012). *Turnkey shore-to-ship power connection at stena line b.v. ferry terminal in hoek van holland, the netherlands*.

Abu, S. M., Hannan, M., Lipu, M. H., Mannan, M., Ker, P. J., Hossain, M., & Mahlia, T. I. (2023). State of the art of lithium-ion battery material potentials: An analytical evaluations, issues and future research directions. *Journal of Cleaner Production*, 136246.

Acemoglu, D., Kakhbod, A., & Ozdaglar, A. (2017). Competition in electricity markets with renewable energy sources. *The Energy Journal*, *38*(KAPSARC Special Issue).

Action, U. N. C. (2023). *What is climate change?* Retrieved April 13, 2023, from https://www.un.org/en

Administration, B. P. (2023). *Intermittent renewable energy*. Retrieved April 17, 2023, from https://www.bpa.gov/

A.H.Gharehgozli, R. J., René B.M. De Koster. (2016). Collaborative solutions for inter terminal transport. *International Journal of Production Research*.

Albright, G., Edie, J., & Al-Hallaj, S. (2012). A comparison of lead acid to lithium-ion in stationary storage applications. *AllCell Technologies LLC*, 1–14.

Alotto, P., Guarnieri, M., & Moro, F. (2014). Redox flow batteries for the storage of renewable energy: A review. *Renewable and sustainable energy reviews*, *29*, 325–335.

AMP, C. (2012). *Cavotec amp systems officially opened at stena line ferry berths in hoek van holland*.

Arenas, L. F., Loh, A., Trudgeon, D. P., Li, X., de Leon, C. P., & Walsh, F. C. (2018). The characteristics and performance of hybrid redox flow batteries with zinc negative electrodes for energy storage. *Renewable and Sustainable Energy Reviews*, *90*, 992–1016.

Argyrou, M. C., Christodoulides, P., & Kalogirou, S. A. (2018). Energy storage for electricity generation and related processes: Technologies appraisal and grid scale applications. *Renewable and Sustainable Energy Reviews*, *94*, 804–821.

Augustine, C., & Blair, N. (2021). *Storage futures study: Storage technology modeling input data report* (tech. rep.). National Renewable Energy Lab.(NREL), Golden, CO (United States).

Bakar, N. N. A., Bazmohammadi, N., Vasquez, J. C., & Guerrero, J. M. (2023). Electrification of onshore power systems in maritime transportation towards decarbonization of ports: A review of the cold ironing technology. *Renewable and Sustainable Energy Reviews*, *178*, 113243.

Ballini, F., & Bozzo, R. (2015). Air pollution from ships in ports: The socio-economic benefit of cold-ironing technology. *Research in Transportation Business & Management*, *17*, 92–98.

Bank, A. D. (2018). Handbook on battery energy storage systems.

Beaudin, M., Zareipour, H., Schellenberglabe, A., & Rosehart, W. (2010). Energy storage for mitigating the variability of renewable electricity sources: An updated review. *Energy for sustainable development*, *14*(4), 302–314.

Benato, R., Cosciani, N., Crugnola, G., Sessa, S. D., Lodi, G., Parmeggiani, C., & Todeschini, M. (2015). Sodium nickel chloride battery technology for large-scale stationary storage in the high voltage network. *Journal of Power Sources*, *293*, 127–136.

Bender, D. A. (2000). Flywheels for renewable energy and power quality applications. *Trinity Flywheel Power. San Francisco*.

Berndt, D. (2001). Valve-regulated lead-acid batteries. *Journal of power sources*, *100*(1-2), 29–46.

Bhuvanesh, A., Christa, S. J., Kannan, S., & Pandiyan, M. K. (2018). Aiming towards pollution free future by high penetration of renewable energy sources in electricity generation expansion planning. *Futures*, *104*, 25–36.

Blanc, C., & Rufer, A. (2010). Understanding the vanadium redox flow batteries. *Paths to Sustainable Energy*, *18*(2), 334–336.

Bradbury, K. (2010). Energy storage technology review. *Duke University*, 1–34.

Braeuer, F., Rominger, J., McKenna, R., & Fichtner, W. (2019). Battery storage systems: An economic model-based analysis of parallel revenue streams and general implications for industry. *Applied Energy*, *239*, 1424–1440.

Butler, P. C. (1994). *Battery energy storage for utility applications: Phase i-opportunities analysis* (tech. rep.). Sandia National Labs., Albuquerque, NM (United States).

C. Jongsma, J. V., L. van Cappellen. (2021). Omslagpunt grootschalige batterijopslag. *CE Delft*.

Cao, J., Tian, J., Xu, J., & Wang, Y. (2020). Organic flow batteries: Recent progress and perspectives. *Energy & Fuels*, *34*(11), 13384–13411.

Caprara, G., Martirano, L., Kermani, M., e Sousa, D. d. M., Barilli, R., & Armas, V. (2022). Cold ironing and battery energy storage system in the port of civitavecchia. *2022 IEEE International Conference on Environment and Electrical Engineering and 2022 IEEE Industrial and Commercial Power Systems Europe (EEEIC/I&CPS Europe)*, 1–6.

Chakkaravarthy, C., Periasamy, P., Jegannathan, S., & Vasu, K. (1991). The nickel/iron battery. *Journal of power sources*, *35*(1), 21–35.

Change, U. N. C. (2023a). *Paris agreement - status of ratification*. Retrieved April 17, 2023, from https://unfccc.int/

Change, U. N. C. (2023b). *The paris agreement, what is the paris agreement?* Retrieved April 13, 2023, from https://unfccc.int/

Chen, H., Cong, T. N., Yang, W., Tan, C., Li, Y., & Ding, Y. (2009). Progress in electrical energy storage system: A critical review. *Progress in natural science*, *19*(3), 291–312.

Chen, P., Wang, C., & Wang, T. (2022). Review and prospects for room-temperature sodium-sulfur batteries. *Materials Research Letters*, *10*(11), 691–719.

Chen, T., Jin, Y., Lv, H., Yang, A., Liu, M., Chen, B., Xie, Y., & Chen, Q. (2020). Applications of lithium-ion batteries in grid-scale energy storage systems. *Transactions of Tianjin University*, *26*(3), 208–217.

Chen, W., Jin, Y., Zhao, J., Liu, N., & Cui, Y. (2018). Nickel-hydrogen batteries for large-scale energy storage. *Proceedings of the National Academy of Sciences*, *115*(46), 11694–11699.

Cheng, B., & Powell, W. B. (2016). Co-optimizing battery storage for the frequency regulation and energy arbitrage using multi-scale dynamic programming. *IEEE Transactions on Smart Grid*, *9*(3), 1997–2005.

Cho, K. T., Ridgway, P., Weber, A. Z., Haussener, S., Battaglia, V., & Srinivasan, V. (2012). High performance hydrogen/bromine redox flow battery for grid-scale energy storage. *Journal of The Electrochemical Society*, *159*(11), A1806.

Ciotola, A., Fuss, M., Colombo, S., & Poganietz, W.-R. (2021). The potential supply risk of vanadium for the renewable energy transition in germany. *Journal of Energy Storage*, *33*, 102094.

Colthorpe, A. (2021). *Wartsila claims 48mwh netherlands bess will be europe's first large-scale lfp battery*. Retrieved June 5, 2023, from https://www.energy-storage.news/wartsilas-48mwh-netherlands-bess-will-be-europes-first-large-scale-lfp-battery-project/

Colthorpe, A. (2022). *Freyr joins race to make lfp batteries at gigawatt-scale in europe*. Retrieved June 5, 2023, from https://www.energy-storage.news/freyr-joins-race-to-make-lfp-batteries-at-gigawatt-scale-in-europe/

Commission, E. (2023a). *Faq – maritime transport in eu emissions trading system (ets)*. Retrieved October 12, 2023, from https://climate.ec.europa.eu/eu-action/transport/reducing-emissions-shipping-sector/faq-maritime-transport-eu-emissions-trading-system-ets_en

Commission, E. (2023b). *Paris agreement*. Retrieved April 17, 2023, from https://climate.ec.europa.eu

Contractors, H. M. (2023). *Making the impossible possible offshore*. Retrieved June 8, 2023, from https://www.heerema.com/heerema-marine-contractors/fleet

Converse, A. O. (2011). Seasonal energy storage in a renewable energy system. *Proceedings of the IEEE*, *100*(2), 401–409.

Coppola, T., & Quaranta, F. (2014). Fuel saving and reduction of emissions in ports with cold ironing applications. *Proceedings of the high speed marine vehicle conference, Naples, Italy*, 15–17.

Cunha, Á., Martins, J., Rodrigues, N., & Brito, F. (2015). Vanadium redox flow batteries: A technology review. *International Journal of Energy Research*, *39*(7), 889–918.

Das, C. K., Bass, O., Kothapalli, G., Mahmoud, T. S., & Habibi, D. (2018). Overview of energy storage systems in distribution networks: Placement, sizing, operation, and power quality. *Renewable and Sustainable Energy Reviews*, *91*, 1205–1230.

Dell, R., & Rand, D. A. J. (2001). *Understanding batteries*. Royal society of chemistry.

Deng, J., Luo, W.-B., Chou, S.-L., Liu, H.-K., & Dou, S.-X. (2018). Sodium-ion batteries: From academic research to practical commercialization. *Advanced Energy Materials*, *8*(4), 1701428.

Díaz-González, F., Sumper, A., Gomis-Bellmunt, O., & Villafáfila-Robles, R. (2012). A review of energy storage technologies for wind power applications. *Renewable and sustainable energy reviews*, *16*(4), 2154–2171.

DNV. (2022).

Dunn, B., Kamath, H., & Tarascon, J.-M. (2011). Electrical energy storage for the grid: A battery of choices. *Science*, *334*(6058), 928–935.

Eftekhari, A. (2019). Lithium batteries for electric vehicles: From economy to research strategy.

Englberger, S., Hesse, H., Hanselmann, N., & Jossen, A. (2019). Simses multi-use: A simulation tool for multiple storage system applications. *2019 16th International Conference on the European Energy Market (EEM)*, 1–5.

Entsoenergy. (2023). *Day ahead prices*. Retrieved September 21, 2023, from https://transparency.entsoe.eu/

Environment, H., & Inspectorate, T. (2012). *On-shore power supply*. Retrieved April 24, 2023, from https://puc.overheid.nl/nsi/doc/PUC_1663_14/1/

Epexspot. (2023). *Monthly power trading results of june 2023*. Retrieved September 15, 2023, from https://www.eex-group.com/fileadmin/Global/News/Group/EpexSpot/2023-07-05_EPEX_SPOT_Power_Trading_Results_06-2023.pdf

epexspot.com. (2023). *Traded volume remains stable*. Retrieved July 6, 2023, from https://www.epexspot.com/en/news/traded-volume-remains-stable

Fan, X., Liu, B., Liu, J., Ding, J., Han, X., Deng, Y., Lv, X., Xie, Y., Chen, B., Hu, W., et al. (2020). B. *Transactions of Tianjin University*, *26*, 92–103.

Feng, Y., & Li, H. (2017). Study of safety and economy of utilizing shore power supply system for oceangoing ship. *2017 4th International Conference on Transportation Information and Safety (ICTIS)*, 409–413.

Fernando, J. (2023). *Net present value (npv): What it means and steps to calculate it*. Retrieved April 24, 2023, from https://www.investopedia.com/

Ferrese, A. (2015). Battery fundamentals. *GetMobile: Mobile Computing and Communications*, *19*(3), 29–32.

Fetcenko, M., Koch, J., & Zelinsky, M. (2015). Nickel–metal hydride and nickel–zinc batteries for hybrid electric vehicles and battery electric vehicles. In *Advances in battery technologies for electric vehicles* (pp. 103–126). Elsevier.

Forecast, M. D. (2023a). *Vanadium redox battery (vrb) market research report*. Retrieved June 5, 2023, from https://www.marketdataforecast.com/market-reports/vanadium-redox-battery-market

Forecast, M. D. (2023b). *Zinc-bromine battery market research report*. Retrieved June 5, 2023, from https://www.marketdataforecast.com/market-reports/zinc-bromine-battery-market

Gillis, J. (2017). Short answers to hard questions about climate change. *The New York Times*, *6*.

Hesse, H. C., Schimpe, M., Kucevic, D., & Jossen, A. (2017). Lithium-ion battery storage for the grid—a review of stationary battery storage system design tailored for applications in modern power grids. *Energies*, *10*(12), 2107.

Huang, L., Li, J., Liu, B., Li, Y., Shen, S., Deng, S., Lu, C., Zhang, W., Xia, Y., Pan, G., et al. (2020). Electrode design for lithium–sulfur batteries: Problems and solutions. *Advanced Functional Materials*, *30*(22), 1910375.

Hussain, F., Rahman, M. Z., Sivasengaran, A. N., & Hasanuzzaman, M. (2020). Energy storage technologies. In *Energy for sustainable development* (pp. 125–165). Elsevier.

IEA. (2022). *Renewable electricity*. Retrieved April 17, 2023, from https://www.iea.org/

insights, F. B. (2023). *Lead acid battery market size, share and covid-19 impact analysis, by type (flooded and vrla (agm, gel), by application (sli, stationary, e-bikes, low speed evs, and others), and regional forecast, 2023 - 2030*. Retrieved June 5, 2023, from https://www.fortunebusinesinsights.com/industry-reports/lead-acid-battery-market-100237

Institute, C. E. (2023). *Flow batteries*. Retrieved September 12, 2023, from https://www.cei.washington.edu/research/energy-storage/flow-battery/#:~:text=The%20large%20capacity%20can%20be,and%202.2MWh%20in%20capacity.

IPCC. (2021). *Climate change widespread, rapid, and intensifying - ipcc*. Retrieved April 13, 2023, from https://www.ipcc.ch

IRENA. (2017). *Electricity storage and renewables: Costs and markets to 2030*.

Isabella, O. (2022a). *Introduction to pv systems 2021-2022 (tu delft)*. Retrieved May 2, 2023, from https://brightspace.tudelft.nl/d2l/le/content/491381/viewContent/2635856/View

Isabella, O. (2022b). *Topologies of pv systems 2021-2022 (tu delft)*. Retrieved May 2, 2023, from https://brightspace.tudelft.nl/d2l/le/content/491381/viewContent/2635858/View

Kadri, A., & Raahemifar, K. (2019). Optimal sizing and scheduling of battery storage system incorporated with pv for energy arbitrage in three different electricity markets. *2019 IEEE Canadian Conference of Electrical and Computer Engineering (CCECE)*, 1–6.

Kanellos, F. D. (2017). Real-time control based on multi-agent systems for the operation of large ports as prosumer microgrids. *IEEE Access*, *5*, 9439–9452.

Kebede, A. A., Kalogiannis, T., Van Mierlo, J., & Berecibar, M. (2022). A comprehensive review of stationary energy storage devices for large scale renewable energy sources grid integration. *Renewable and Sustainable Energy Reviews*, *159*, 112213.

Kelder, E. M. (2019). Materials for electrochemical energy storage devices. In *Critical materials: Underlying causes and sustainable mitigation strategies* (pp. 53–82). World Scientific.

Kelder, E. M., Wagemaker, M., & Mulder, F. (2022). *Energy storage in batteries 2021-2022 (tu delft)*. Retrieved June 1, 2023, from https://brightspace.tudelft.nl/d2l/home/399141

Kennedy, R. (2022). *New grid-scale lfp battery from canadian solar*. Retrieved June 5, 2023, from https://www.pv-magazine.com/2022/09/16/new-grid-scale-lfp-battery-from-canadian-solar/

Ketterer, J. C. (2014). The impact of wind power generation on the electricity price in germany. *Energy economics*, *44*, 270–280.

Khor, A., Leung, P., Mohamed, M., Flox, C., Xu, Q., An, L., Wills, R., Morante, J., & Shah, A. (2018). Review of zinc-based hybrid flow batteries: From fundamentals to applications. *Materials today energy*, *8*, 80–108.

Killer, M., Farrokhseresht, M., & Paterakis, N. G. (2020). Implementation of large-scale li-ion battery energy storage systems within the emea region. *Applied energy*, *260*, 114166.

Kiriinya, L. K., Kwakernaak, M. C., Van den Akker, S. C., Verbist, G. L., Picken, S. J., & Kelder, E. M. (2023). Iron and manganese alginate for rechargeable battery electrodes. *Polymers*, *15*(3), 639.

Kooshknow, S. M. M., & Davis, C. (2018). Business models design space for electricity storage systems: Case study of the netherlands. *Journal of Energy Storage*, *20*, 590–604.

Kopera, J. J. (2004). Inside the nickel metal hydride battery. *Cobasys, MI, USA http://www. cobasys. com/pdf/tutorial/inside_nimh_battery_technology. pdf (Accessed 08/11)*.

Kumar, D., Rajouria, S. K., Kuhar, S. B., & Kanchan, D. (2017). Progress and prospects of sodium-sulfur batteries: A review. *Solid State Ionics*, *312*, 8–16.

Kumar, J., Khan, H. S., & Kauhaniemi, K. (2021). Smart control of battery energy storage system in harbour area smart grid: A case study of vaasa harbour. *IEEE EUROCON 2021-19th International Conference on Smart Technologies*, 548–553.

Kumar, J., Palizban, O., & Kauhaniemi, K. (2017). Designing and analysis of innovative solutions for harbour area smart grid. *2017 IEEE Manchester PowerTech*, 1–6.

Kumar, Y., Mooste, M., & Tammeveski, K. (2023). Recent progress of transition metal-based bifunctional electrocatalysts for rechargeable zinc-air battery application. *Current Opinion in Electrochemistry*, 101229.

Kurzweil, P. (2015). Lithium battery energy storage: State of the art including lithium–air and lithium–sulfur systems. *Electrochemical energy storage for renewable sources and grid balancing*, 269–307.

Lauer, M. (2008). Methodology guideline on techno economic assessment (tea) generated in the framework of thermanet wp3b economics. https://ec.europa.eu/energy/intelligent/projects/sites/iee-projects/files/projects/documents/thermalnet_methodology_guideline_on_techno_economic_assessment.pdf

Leung, P., Li, X., De León, C. P., Berlouis, L., Low, C. J., & Walsh, F. C. (2012). Progress in redox flow batteries, remaining challenges and their applications in energy storage. *Rsc Advances*, *2*(27), 10125–10156.

Liashchynskyi, P., & Liashchynskyi, P. (2019). Grid search, random search, genetic algorithm: A big comparison for nas. *arXiv preprint arXiv:1912.06059*.

Lim, T. M., Ulaganathan, M., & Yan, Q. (2015). Advances in membrane and stack design of redox flow batteries (rfbs) for medium-and large-scale energy storage. In *Advances in batteries for medium and large-scale energy storage* (pp. 477–507). Elsevier.

Liu, T., Wei, X., Nie, Z., Sprenkle, V., & Wang, W. (2016). A total organic aqueous redox flow battery employing a low cost and sustainable methyl viologen anolyte and 4-ho-tempo catholyte. *Advanced Energy Materials*, *6*(3), 1501449.

Luo, J., Wang, A. P., Hu, M., & Liu, T. L. (2022). Materials challenges of aqueous redox flow batteries. *MRS Energy & Sustainability*, *9*(1), 1–12.

Luo, X., Wang, J., Dooner, M., & Clarke, J. (2015). Overview of current development in electrical energy storage technologies and the application potential in power system operation. *Applied energy*, *137*, 511–536.

Mackenzie, W. (2020). Lfp to overtake nmc as dominant stationary storage chemistry by 2030. Retrieved June 13, 2023, from https://www.woodmac.com/press-releases/lfp-to-overtake-nmc-as-dominant-stationary-storage-chemistry-by-2030/

Maisch, M. (2023). *Evlo unveils lithium iron phosphate battery for utility-scale applications*. Retrieved June 5, 2023, from https://www.pv-magazine.com/2023/05/23/evlo-unveils-lithium-iron-phosphate-battery-for-utility-scale-applications/

Mancheri, N. A. (2015). World trade in rare earths, chinese export restrictions, and implications. *Resources Policy*, *46*, 262–271.

market forecast, T. (2023). *Zinc-bromine battery market insights, 2027*. Retrieved June 5, 2023, from https://www.transparencymarketresearch.com/zinc-bromine-battery-market.html

market research, A. (2023). *Global vanadium redox flow battery (vrfb) market growing at a cagr of 19.5 percent from 2023 to 2030*. Retrieved June 5, 2023, from https://www.consegicbusinessintelligence.com/press-release/vanadium-redox-flow-battery-market

McBreen, J. (1994). Nickel/zinc batteries. *Journal of power sources*, *51*(1-2), 37–44.

Meliani, M., Barkany, A. E., Abbassi, I. E., Darcherif, A. M., & Mahmoudi, M. (2021). Energy management in the smart grid: State-of-the-art and future trends. *International Journal of Engineering Business Management*, *13*, 18479790211032920.

Minke, C., & Turek, T. (2018). Materials, system designs and modelling approaches in techno-economic assessment of all-vanadium redox flow batteries–a review. *Journal of Power Sources*, *376*, 66–81.

Mirza, M. (2022). Shore power in maritime ports: Meeting the 90 percent requirement by 2025. *PTR*.

Mongird, K., Viswanathan, V., Alam, J., Vartanian, C., Sprenkle, V., & Baxter, R. (2020). 2020 grid energy storage technology cost and performance assessment. *Energy*, *2020*, 6–15.

Mongird, K., Viswanathan, V., Balducci, P., Alam, J., Fotedar, V., Koritarov, V., & Hadjerioua, B. (2020). An evaluation of energy storage cost and performance characteristics. *Energies*, *13*(13), 3307.

Mongird, K., Viswanathan, V. V., Balducci, P. J., Alam, M. J. E., Fotedar, V., Koritarov, V. S., & Hadjerioua, B. (2019). *Energy storage technology and cost characterization report* (tech. rep.). Pacific Northwest National Lab.(PNNL), Richland, WA (United States).

Murthy, G. S. (2022). Techno-economic assessment. In *Biomass, biofuels, biochemicals* (pp. 17–32). Elsevier.

Mutarraf, M. U., Terriche, Y., Nasir, M., Guan, Y., Su, C.-L., Vasquez, J. C., & Guerrero, J. M. (2021). A communication-less multimode control approach for adaptive power sharing in ship-based seaport microgrid. *IEEE Transactions on Transportation Electrification*, *7*(4), 3070–3082.

Narins, T. P. (2017). The battery business: Lithium availability and the growth of the global electric car industry. *The Extractive Industries and Society*, *4*(2), 321–328.

Nemeth, T., Schröer, P., Kuipers, M., & Sauer, D. U. (2020). Lithium titanate oxide battery cells for high-power automotive applications–electro-thermal properties, aging behavior and cost considerations. *Journal of energy storage*, *31*, 101656.

NREL. (2022). *Storage futures study - storage technology modeling input data report*.

O'sullivan, T., Bingham, C., & Clark, R. (2006). Zebra battery technologies for all electric smart car. *International Symposium on Power Electronics, Electrical Drives, Automation and Motion, 2006. SPEEDAM 2006.*, 243.

Palizban, O., & Kauhaniemi, K. (2016). Energy storage systems in modern grids—matrix of technologies and applications. *Journal of Energy Storage*, *6*, 248–259.

Petrov, M. M., Modestov, A. D., Konev, D. V., Antipov, A. E., Loktionov, P. A., Pichugov, R. D., Kartashova, N. V., Glazkov, A. T., Abunaeva, L. Z., Andreev, V. N., et al. (2021). Redox flow batteries: Role in modern electric power industry and comparative characteristics of the main types. *Russian Chemical Reviews*, *90*(6), 677.

Petrovic, S., & Petrovic, S. (2021). Nickel–cadmium batteries. *Battery Technology Crash Course: A Concise Introduction*, 73–88.

Pintér, G., Vincze, A., Baranyai, N. H., & Zsiborács, H. (2021). Boat-to-grid electrical energy storage potentials around the largest lake in central europe. *Applied Sciences*, *11*(16), 7178.

Pool, N. (2023). *Day-ahead prices*. Retrieved September 5, 2023, from https://www.nordpoolgroup.com/en/Market-data1/Dayahead/Area-Prices/ALL1/Hourly/?view=table

PoR. (2019). *Building a sustainable port*. Retrieved April 18, 2023, from https://www.portofrotterdam.com/sites/default/files/2021-06/factsheet-port-of-rotterdam-building-a-sustainable-port-en-2019.pdf

PoR. (2021). *Realizing shore power to achieve a zero emission port in 2050*. Retrieved April 18, 2023, from https://www.portofrotterdam.com/en/news-and-press-releases/realizing-shore-power-achieve-zero-emission-port-2050

PoR. (2023). *Strategy and research*. Retrieved April 21, 2023, from https://www.portofrotterdam.com/en/port-future/energy-transition/strategy-and-research

PortofRotterdam. (2023). *Fotolocaties rotterdamse haven*. Retrieved June 22, 2023, from https://portofrotterdam.maps.arcgis.com/apps/Shortlist/index.html?appid=495d8d66d582475d880684cf29683da2

Prifti, H., Parasuraman, A., Winardi, S., Lim, T. M., & Skyllas-Kazacos, M. (2012). Membranes for redox flow battery applications. *Membranes*, *2*(2), 275–306.

Prousalidis, J., Antonopoulos, G., Patsios, C., Greig, A., & Bucknall, R. (2014). Green shipping in emission controlled areas: Combining smart grids and cold ironing. *2014 International Conference on Electrical Machines (ICEM)*, 2299–2305.

Q. Hu, F. C., B. Wiegmans, & Lodewijks, G. (2019). Integration of inter-terminal transport and hinterland rail transport. *Flexible Services and Manufacturing Journal*.

Qi, J., Wang, S., & Peng, C. (2020). Shore power management for maritime transportation: Status and perspectives. *Maritime Transport Research*, *1*, 100004.

Ramasamy, V., Feldman, D., Desai, J., & Margolis, R. (2021). *Us solar photovoltaic system and energy storage cost benchmarks: Q1 2021* (tech. rep.). National Renewable Energy Lab.(NREL), Golden, CO (United States).

Redflow. (2023). *Redflow to supply transformative 20 mwh flow battery system for project in california*. Retrieved June 6, 2023, from https://redflow.com/project/redflow-to-supply-20-mwh-flow-battery-system-for-project-in-california

Renewable, I., IRENA, I. R., et al. (2017). Electricity storage and renewables: Costs and markets to 2030.

Revankar, S. T. (2019). Chemical energy storage. In *Storage and hybridization of nuclear energy* (pp. 177–227). Elsevier.

Rodby, K. E., Jaffe, R. L., Olivetti, E. A., & Brushett, F. R. (2023). Materials availability and supply chain considerations for vanadium in grid-scale redox flow batteries. *Journal of Power Sources*, *560*, 232605.

Rouholamini, M., Wang, C., Nehrir, H., Hu, X., Hu, Z., Aki, H., Zhao, B., Miao, Z., & Strunz, K. (2022). A review of modeling, management, and applications of grid connected li ion battery storage systems. *IEEE Transactions on Smart Grid*.

S. Yew Wang Chai, e. a. (2022). Future era of techno-economic analysis: Insights from review. *The Title of the Journal*, *3*, 1–22. Retrieved April 17, 2023, from https://doi.org/10.3389/frsus.2022.924047

Salkuti, S. R. (2021). Electrochemical batteries for smart grid applications. *Int. J. Electr. Comput. Eng*, *11*(3), 1849–1856.

Samadi, S., Lechtenböhmer, S., Schneider, C., Arnold, K., Fischedick, M., Schüwer, D., & Pastowski, A. (2016). *Decarbonization pathways for the industrial cluster of the port of rotterdam*. Wuppertal Institute for Climate, Environment; Energy Wuppertal, Germany.

Schmidt, O. (2018). Levelized cost of storage: Gravity storage. *Imperial College London Consultants. https://heindl-energy. com/wpcontent/uploads/2018/10/LCOS_GravityStorage-II-Okt-2018. pdf*.

Schmidt, O., Melchior, S., Hawkes, A., & Staffell, I. (2019). Projecting the future levelized cost of electricity storage technologies. *Joule*, *3*(1), 81–100.

Schmidt, O., & Staffell, I. (2023). *Monetizing energy storage*. Oxford University Press.

Sciberras, E. A., Zahawi, B., & Atkinson, D. J. (2015). Electrical characteristics of cold ironing energy supply for berthed ships. *Transportation Research Part D: Transport and Environment*, *39*, 31–43.

Services, Z. E. (2023). *Zespack*. Retrieved September 12, 2023, from https://zeroemissionservices.nl/zespack/

Shamim, N., Subburaj, A. S., & Bayne, S. B. (2019). Renewable energy based grid connected battery projects around the world—an overview. *Journal of Energy and Power Engineering*, *13*(1), 27.

Shigematsu, T., et al. (2011). Redox flow battery for energy storage. *SEI technical review*, *73*(7), 13.

Skundin, A., Kulova, T., & Yaroslavtsev, A. (2018). Sodium-ion batteries (a review). *Russian Journal of Electrochemistry*, *54*, 113–152.

Skyllas-Kazacos, M., Chakrabarti, M., Hajimolana, S., Mjalli, F., & Saleem, M. (2011). Progress in flow battery research and development. *Journal of the electrochemical society*, *158*(8), R55.

Soloveichik, G. L. (2011). Battery technologies for large-scale stationary energy storage. *Annual review of chemical and biomolecular engineering*, *2*, 503–527.

Solyali, D., Safaei, B., Zargar, O., & Aytac, G. (2022). A comprehensive state-of-the-art review of electrochemical battery storage systems for power grids. *International Journal of Energy Research*, *46*(13), 17786–17812.

Spanos, C., Turney, D. E., & Fthenakis, V. (2015). Life-cycle analysis of flow-assisted nickel zinc-, manganese dioxide-, and valve-regulated lead-acid batteries designed for demand-charge reduction. *Renewable and Sustainable Energy Reviews*, *43*, 478–494.

Stolz, B., Held, M., Georges, G., & Boulouchos, K. (2021). The co2 reduction potential of shore-side electricity in europe. *Applied Energy*, *285*, 116425.

Stram, B. N. (2016). Key challenges to expanding renewable energy. *Energy Policy*, *96*, 728–734.

Su, H., Feng, D., Zhao, Y., Zhou, Y., Zhou, Q., Fang, C., & Rahman, U. (2022). Optimization of customer-side battery storage for multiple service provision: Arbitrage, peak shaving, and regulation. *IEEE Transactions on Industry Applications*, *58*(2), 2559–2573.

Su, L., Kowalski, J. A., Carroll, K. J., & Brushett, F. R. (2015). Recent developments and trends in redox flow batteries. *Rechargeable Batteries: Materials, Technologies and New Trends*, 673–712.

Sudworth, J. (2001). The sodium/nickel chloride (zebra) battery. *Journal of power sources*, *100*(1-2), 149–163.

TAMYÜREK, B., & NICHOLS, D. K. (2004). Performance analysis of sodium sulfur battery in energy storage and power quality applications. *Eskişehir Osmangazi Üniversitesi Mühendislik ve Mimarlık Fakültesi Dergisi*, *17*(1), 99–115.

Tang, L., Leung, P., Xu, Q., Mohamed, M. R., Dai, S., Zhu, X., Flox, C., & Shah, A. A. (2022). Future perspective on redox flow batteries: Aqueous versus nonaqueous electrolytes. *Current Opinion in Chemical Engineering*, *37*, 100833.

Tanrisever, F., Derinkuyu, K., & Jongen, G. (2015). Organization and functioning of liberalized electricity markets: An overview of the dutch market. *Renewable and Sustainable Energy Reviews*, *51*, 1363–1374.

TenneT. (2022). https://tennet-drupal.s3.eu-central-1.amazonaws.com/default/2022-07/Annual_Market_Update_2021_0.pdf

Todorovic, I. (2022). *Vanadium flow megabattery comes online in china*. Retrieved June 6, 2023, from https://balkangreenenergynews.com/vanadium-flow-megabattery-comes-online-in-china/

Tran, M.-K., DaCosta, A., Mevawalla, A., Panchal, S., & Fowler, M. (2021). Comparative study of equivalent circuit models performance in four common lithium-ion batteries: Lfp, nmc, lmo, nca. *Batteries*, *7*(3), 51.

Vazquez, S., Lukic, S. M., Galvan, E., Franquelo, L. G., & Carrasco, J. M. (2010). Energy storage systems for transport and grid applications. *IEEE Transactions on industrial electronics*, *57*(12), 3881–3895.

Viswanathan, V., Mongird, K., Franks, R., & Baxter, R. (2022). 2022 grid energy storage technology cost and performance assessment. *Energy*, *2022*.

Wagner, L. (2007). Overview of energy storage methods. *Analyst*.

Wang, L., Wang, J., Wang, L., Zhang, M., Wang, R., & Zhan, C. (2022). A critical review on nickel-based cathodes in rechargeable batteries. *International Journal of Minerals, Metallurgy and Materials*, *29*(5), 925–941.

Wang, W., Peng, Y., Li, X., Qi, Q., Feng, P., & Zhang, Y. (2019). A two-stage framework for the optimal design of a hybrid renewable energy system for port application. *Ocean Engineering*, *191*, 106555.

Wang, Y.-X., Zhang, B., Lai, W., Xu, Y., Chou, S.-L., Liu, H.-K., & Dou, S.-X. (2017). Room-temperature sodium-sulfur batteries: A comprehensive review on research progress and cell chemistry. *Advanced Energy Materials*, *7*(24), 1602829.

Williamsson, J., Costa, N., Santén, V., & Rogerson, S. (2022). Barriers and drivers to the implementation of onshore power supply—a literature review. *Sustainability*, *14*(10), 6072.

Winkel, R., Weddige, U., Johnsen, D., Hoen, V., & Papaefthimiou, S. (2016). Shore side electricity in europe: Potential and environmental benefits. *Energy Policy*, *88*, 584–593.

Winter, M., & Brodd, R. J. (2004). What are batteries, fuel cells, and supercapacitors? *Chemical reviews*, *104*(10), 4245–4270.

Wu, C., Scherson, D., Calvo, E., Yeager, E., & Reid, M. (1986). A bismuth-based electrocatalyst for the chromous-chromic couple in acid electrolytes. *Journal of the Electrochemical Society*, *133*(10), 2109.

Wu, W.-F., Yan, X., & Zhan, Y. (2023). Recent progress of electrolytes and electrocatalysts in neutral aqueous zinc-air batteries. *Chemical Engineering Journal*, *451*, 138608.

Xie, Z., Liu, Q., Chang, Z., & Zhang, X. (2013). The developments and challenges of cerium half-cell in zinc–cerium redox flow battery for energy storage. *Electrochimica Acta*, *90*, 695–704.

Xu, Y., Pei, J., Cui, L., Liu, P., & Ma, T. (2022). The levelized cost of storage of electrochemical energy storage technologies in china. *Frontiers in Energy Research*, *10*, 873800.

Yan, Z., Zhao, L., Wang, Y., Zhu, Z., & Chou, S.-L. (2022). The future for room-temperature sodium–sulfur batteries: From persisting issues to promising solutions and practical applications. *Advanced Functional Materials*, *32*(36), 2205622.

Yao, Y., Lei, J., Shi, Y., Ai, F., & Lu, Y.-C. (2021). Assessment methods and performance metrics for redox flow batteries. *Nature Energy*, *6*(6), 582–588.

Zelinsky, M. A., Koch, J. M., & Young, K.-H. (2017). Performance comparison of rechargeable batteries for stationary applications (ni/mh vs. ni–cd and vrla). *Batteries*, *4*(1), 1.

Zeng, Y., Zhao, T., An, L., Zhou, X., & Wei, L. (2015). A comparative study of all-vanadium and iron-chromium redox flow batteries for large-scale energy storage. *Journal of Power Sources*, *300*, 438–443.

Zhang, S., Yao, Y., & Yu, Y. (2021). Frontiers for room-temperature sodium–sulfur batteries. *ACS Energy Letters*, *6*(2), 529–536.

Zhang, Y., Zhou, C.-g., Yang, J., Xue, S.-c., Gao, H.-l., Yan, X.-h., Huo, Q.-y., Wang, S.-w., Cao, Y., Yan, J., et al. (2022). Advances and challenges in improvement of the electrochemical performance for lead-acid batteries: A comprehensive review. *Journal of Power Sources*, *520*, 230800.

Zhao, C., Wang, Q., Yao, Z., Wang, J., Sánchez-Lengeling, B., Ding, F., Qi, X., Lu, Y., Bai, X., Li, B., et al. (2020). Rational design of layered oxide materials for sodium-ion batteries. *Science*, *370*(6517), 708–711.

Zimmermann, A. W., Wunderlich, J., Müller, L., Buchner, G. A., Marxen, A., Michailos, S., Armstrong, K., Naims, H., McCord, S., Styring, P., et al. (2020). Techno-economic assessment guidelines for co2 utilization. *Frontiers in Energy Research*, *8*, 5.

Zis, T. P. (2019). Prospects of cold ironing as an emissions reduction option. *Transportation Research Part A: Policy and Practice*, *119*, 82–95.

Zwang, J. W. (2022). *Handboek verdienmodellen batterij*.

A. Battery energy storage systems

This Appendix focuses on the background of the literature review which is conducted regarding battery energy storage systems (BESS). Topics such as the functionalities of the BESS towards the grid, BESS topologies, the electricity markets and details of the BESS types specifically can be found consequetively in Sections A.1, A.2, A.3 and A.4 with the aim to support the analysis which is provided in Chapter 2.

A.1. Battery functionalities towards the grid

The different functions BESS can have with regards to the grid which are considered as most prevalent, are presented here (Butler, 1994; Soloveichik, 2011). Generation happens at the generator side, which is in front-of-the-meter (FTM) as well as transmission and distribution. Customer services are happening at the customer site, behind-the-meter (BTM).

- Generation
  - **Spinning reserve** (power related): generation capacity which can be provided by a utility in the case of the event of failure of either a generation plant or the grid, to prevent interruption of services for customers.
  - **Frequency control** (power related): the ability to prevent the frequency from deviating too far from 50 Hz (which is the frequency of the grid in the Netherlands).
  - **Renewables** (energy related): provision of renewable energy during peak utility demand at consistent level.
  - **Peak shaving/ load leveling** (energy related): provision of inexpensive off-peak power during expensive on-peak hours.
- Transmission and distribution
  - **Transmission line stability** (power related): prevents system failure by keeping all components connected to transmission line in sync.
  - **Voltage regulation** (power related): prevents system failure by keeping the voltage of generation and loads of a transmission line within 5 percent from each other.
- Customer service
  - **Customer demand peak reduction** (energy related): peak shaving or load leveling specifically for a customer.
  - **Reliability, power quality, uninterruptible power supply** (power related): provision of spinning reserve to customers. For example, providing black-start energy to recover from a blackout.
  - **Energy trading** (energy or power related): trading on the day-ahead market (DAM), intraday market (IDM) and/or frequency containment reserve (FCR) market with the goal of generating profit.

The storage functions as mentioned above can be classified on a high power to high energy range which is related to a seconds to hours storage capacity range, which is visualised in Figure A.1.

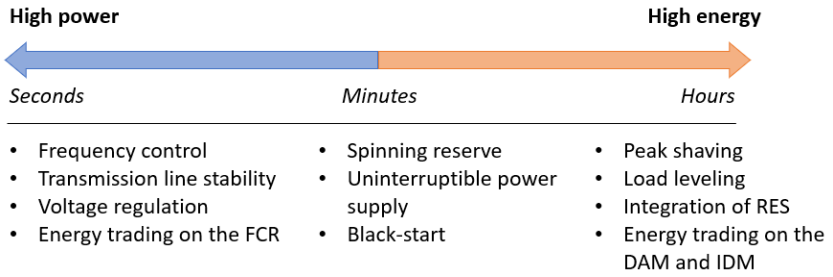

Figure A.1: Power/ energy and time range of battery functions towards the grid

A.2. Battery system topologies

The benefits of storing electricity in a battery can be utilised in various ways. The first distinction which has to be made is whether or not the battery is connected to the grid. The configuration of a battery without a grid connection is referred to as stand-alone. In a stand-alone topology, the battery is solely connected to supply and demand, to energy producers and off-takers respectively. The stand-alone topology is visualised in Figure A.2.

Furthermore, three different grid-connected topologies are known. The first topology recognised is a battery solely connected to the electricity network. The functionality of this configuration varies between all different possibilities which are mentioned in A.1. Figure A.3 shows this configuration.

The second grid-connected topology exists of a hybrid installation, including a load which is connected to the grid, with a battery placed in between. The goal of the battery is to store electricity when the price is favourable and to provide the load with electricity during times of an unfavourable price (peak shaving). Most of the times, the price of electricity in the grid is correlated with the weather conditions. When either the wind is blowing or the sun is shining or both, the share of green, cheap electricity is higher than during unfavourable conditions. Therefore, in this configuration the battery stores green, cheap electricity during times of a surplus, and provide the load with green electricity during times the load otherwise would have used grey electricity. Therefore, this configuration increases the share of green electricity used by the hybrid installation. Another functionality of this configuration is the ability to trade on the electricity markets for example, when there is no load. This topology is shown in Figure A.4.

The third topology of a grid-connected battery is composed of renewable energy producers connected to the battery as well as to the grid. The battery can leverage the green electricity production and therefore stabilises the input towards the grid, increasing reliability and also the share of green electricity (Isabella, 2022b). Figure A.5 visualises this topology, which is also referred to as a micro-grid.

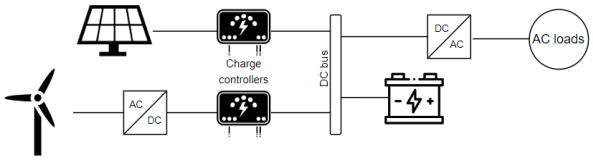

Figure A.2: Stand alone topology of a battery system

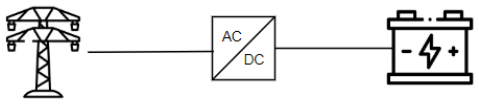

Figure A.3: Grid-connected topology of a battery system

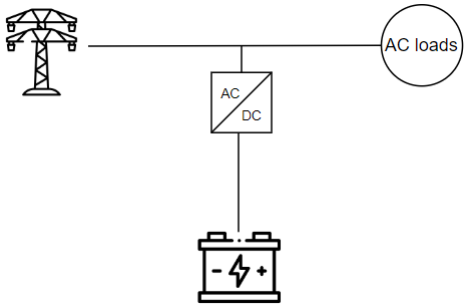

Figure A.4: Grid-connected topology of a hybrid installation

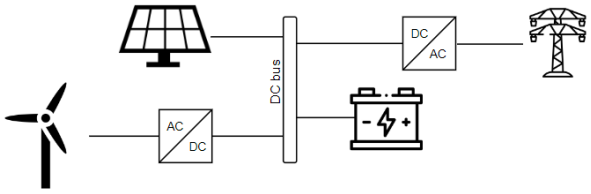

Figure A.5: Grid-connected topology of a battery and renewable energy producers

A.3. Grid-connected battery energy storage systems

As mentioned in Chapter 1, the grid-connected BESS in the hybrid installations as considered are enhancing economic viability through two functionalities, which are consumer- and wholesale energy arbitrage. This Section elaborates on the latter function and explains the system of the Dutch electricity markets, since the case study of this thesis is located in the port of Rotterdam area. The system of the Dutch electricity markets is explained first whereafter possible physical locations for grid-connected BESS are explained.

Dutch electricity markets

The electricity market in the Netherlands knows multiple actors with varying roles and interests. The electricity supply chain consists of six subsequent parts, regulated by independent responsible parties, which is visualised in Figure A.6.

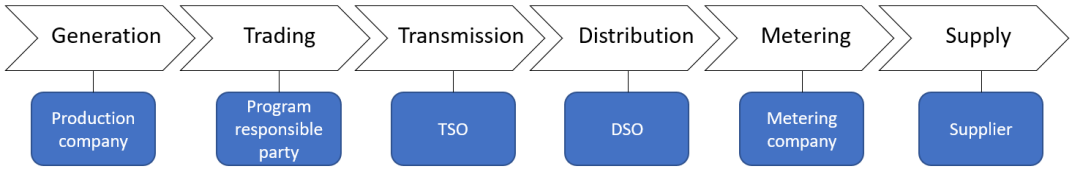

Figure A.6: Electricity supply chain in the Netherlands, based on (Tanrisever et al., 2015)

First, the competitive generation companies sell their electricity to program responsible parties (PRP) to trade. A PRP is a legal entity that manages at least one physical connection to the grid. A PRP estimates the difference between supply and demand at their connection and communicates this with the transmission system operator (TSO). When the realised net demand deviates from the forecasted value, the PRP has to pay the imbalance costs. The PRP manages the trading of the electricity by making use of regulated grid operators.

Two types of grid operators exist, TenneT is regulated as the state-owned TSO of the high-voltage (HV) grid. The 110 kV, 150 kV, 220 kV and the 280 kV grids are regulated by TenneT, thereby connecting all regional grids with each other and with the rest of Europe. In addition, eight state-owned parties are assigned to be the distribution system operators (DSO), managing the transportation and distribution low-voltage (LV) grids, connecting the HV grid and customers to each other. Operation of

the grid is an activity of natural monopoly whereas other activities (such as generation of energy) are competitive. Then, the electricity goes through the metering company to the supplier (Tanrisever et al., 2015).

BESS can play a role and earn revenue in trading, both as a supplier and as a consumer towards the grid. Therefore, the different trading channels are explained here. Within the channels, there exist various markets. First, the wholesale and balancing markets are explained whereafter the retail market is mentioned shortly. The main difference is that in the wholesale and balancing market customers are reached through market operators whereas in the retail market consumers are reached via sales force (Kooshknow & Davis, 2018).

Wholesale market and balancing market

The markets which are part of the wholesale market are classified based on their time distance to delivery time. The transactions of the wholesale market are taking place prior to the moment of power exchange whereas the transactions of the balancing market are real-time. The wholesale market contains the forward and future market, the DAM and the IDM, of which the latter two are also referred to as the spot market. In addition, a balancing market is present as well, as can be seen in Figure A.7 (TenneT, 2022).

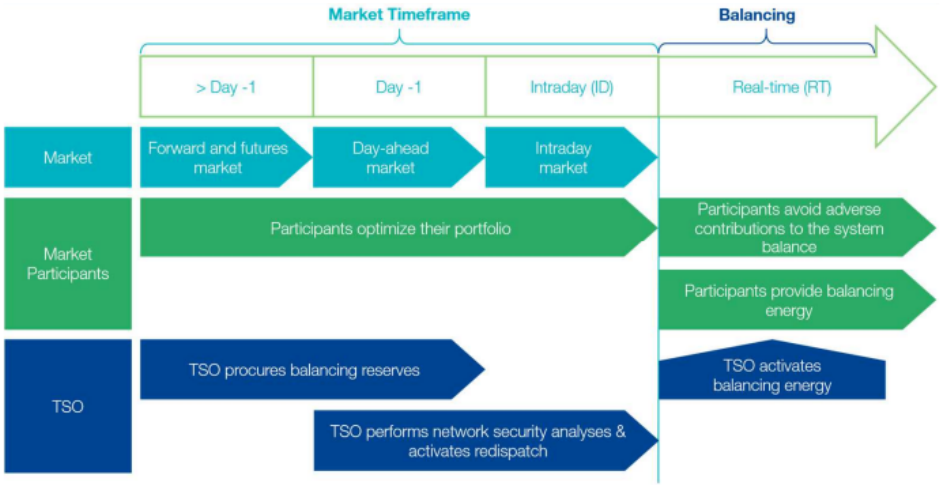

Figure A.7: Organisation of electricity markets in the Netherlands (Kooshknow & Davis, 2018; Tanrisever et al., 2015; TenneT, 2022)

Forward and futures market

The forward and futures market starts years before and ends one day before delivery of electricity. The contracts entail the amount of electricity which is supplied/taken-off at a certain moment in the future accompanied by the price. The price is thus already determined prior to the moment of power exchange. The risk of electricity price fluctuations is hereby mitigated (TenneT, 2022). Storage devices are not included within this part of the wholesale market. The volumes of energy which are traded are too big and therefore energy producers are active only.

Day-ahead market

The DAM trades electricity for one day before the moment of power exchange and the highest volumes of electricity among other spot markets (TenneT, 2022). The DAM is based on auctions where both suppliers and off-takers place anonymous hourly bids with different prices and quantities. The anonymous orders result in demand and supply curves for each hour during the 24 hours of the next day. After closing, the DAM-determined hourly prices are announced to all participants in the market (Tanrisever et al., 2015).

Intraday market

The IDM provides participants with the possibility of adjusting their positions on the spot market up

to five minutes before the moment of delivery of electricity. The IDM trades electricity per every 15 minutes. The costs associated with purchasing electricity in the IDM is historically higher compared to in the DAM (Tanrisever et al., 2015). However, in 2022 the prices were equal (Epexspot, 2023).

Balancing market
The aim of the wholesale market is to keep the balance of the network. However, when time comes by, the actual supply or demand can deviate from what was forecasted. To prevent the balance from being disturbed, TenneT employs balancing products and services on the balancing market (Kooshknow & Davis, 2018). Reserves are contracted ahead of time via auctions by TenneT to be used during imbalances. Three types of reserves are known (Kooshknow & Davis, 2018; TenneT, 2022):

- FCR, which activates within seconds for any deviation from the system frequency with the aim to stabilise the deviated frequency and prevent it from further deviation. FCR does not restore the frequency.
- Automatic activated frequency restoration reserve (aFRR) aims to automatically restore the frequency back to the initial/reference value.
- Manually activated frequency replacement reserves (mFRR) involves manual interventions by grid operators to quickly correct frequency deviations caused by unexpected events.

Imbalance market
The imbalance market sets the imbalance price. When the real-time generation or consumption deviates from the schedule, the market party causing the deviation is in imbalance. The party causing the imbalance pays the imbalance price towards the party which solves the imbalance (TenneT, 2022).

Ancillary service market
Ancillary services are supporting the TSO to guarantee security of the system. The balancing market is part of these ancillary services. The other ancillary services include control reserves, reactive power and black start capacity. All ancillary services are being traded on the imbalance market. Reactive power is meant to maintain the voltage of the grid whereas black start capacity provides back-up capacity for the case the grid needs a restart after a blackout. Tennet obtains reactive power through yearly bilateral contracts with generation units where the fees can be either fixed or variable per hour. The black start capacity is obtained via yearly contracts or longer, with a fixed fee. One condition to black-start capacity providers is the ability to start generation without any external support (Kooshknow & Davis, 2018; Tanrisever et al., 2015; TenneT, 2022).

Grid-connected BESS are most active on day-ahead, intraday and balance markets (TenneT, 2022). Within the balance market, only the FCR market is economically attractive enough for BESS (Braeuer et al., 2019; Englberger et al., 2019; Zwang, 2022). For BESS to participate in the wholesale market, some barriers must be taken into account and overcome (Kooshknow & Davis, 2018):

- The minimum capacity of a bid in FCR, aFRR and mFRR are 1 MW, 4 MW and 20 MW respectively. Therefore, if a BESS wants to participate in any of the bids, the minimum capacity must be met.
- The availability which is required to participate in some markets limits the ability to participate in other markets. For example, to participate in the FCR market, a BESS is required to keep the energy reserved for a period of 30 minutes. During this period, the BESS cannot be active on other markets and off-take is not guaranteed as well. This is a potential threat to the economic viability of the operations of the BESS.
- The profits earned by arbitrage are limited. BESS earn money through arbitrage. Arbitrage is the process of selling electricity when the price is high and buying electricity when the price is low. With the price difference, profits are made. However, when the amount of batteries is increasing, the prices will not be that high because there will be more supplying BESS and the other way around when it comes to buying electricity, the demand will increase upon an increasing amount of BESS and therefore the price will not drop so far.

Retail market
Players in the retail market are recognised as small and medium end-consumers. They do not participate in the wholesale market and therefore they receive their energy from suppliers through bilateral

contracts. The contracts can vary between fixed, variable and partially fixed in terms of price. The specific contract details and its tariffs are affecting the costs, revenues and uncertainties of the BTM BESS business models (Kooshknow & Davis, 2018).

Locations

The physical location of a BESS in the electricity network does affect the possible technical constraints. Firstly, BESS can be connected in the transmission grid, consisting of the extra HV (voltage $\geq$ 220 kV) and HV grid (35 kV $\leq$ voltage < 220 kV). Then, the BESS can also be connected to the distribution grid, consisting of the medium voltage (1 kV $\leq$ voltage < 35 kV) and LV grid (voltage $\leq$ 1 kV). The voltage differences between the different grids in the network are solved by transformers which step up or down the voltage and thereby connect the different grids.

Generating activities as well as consumption can be classified into categories. First, three generating categories are mentioned.

- Centralised generation, which is connected to the transmission grid. A transformer between the generation facilities and the grids is required to step up the voltage.
- Distributed generation, can be connected to the transmission grid or the distribution grid, depending on their size. A transformer between the generation facilities and the grids is required to step up the voltage.
- Distributed micro-generation is done BTM at consumers' private sites.

There are two distinct forms of consumption as well.

- Heavy industries can be connected to the transmission grid directly.
- Light industries, commercial consumers, and residential consumers are connected to various parts of the distribution grid.

.

There are multiple possible physical locations of BESS in the network as described above. Firstly, storage applications can be directly connected to centralised or distributed generation sites. Secondly, storage applications can also be connected to transmission or distribution substations. Also, BESS can be located near consumer sites on the distribution grid side, with the aim to provide community energy storage.

All the above mentioned possibilities for locating BESS are recognised as FTM. Storage can also be provided BTM at consumers sites (Kooshknow & Davis, 2018). BTM BESS can be considered as beneficial for the owner whereas benefits of using FTM BESS are focused on the grid (Englberger et al., 2019). Since this thesis is focusing on enhancing the economic viability from the point of view of the owner of a shore power installation, BTM BESS are considered.

A.4. Battery considerations

BESS necessarily have to meet certain requirements to be considered as suitable for the specific application for which they are used. The assessed characteristics and their minimum boundary conditions are presented in Table A.1. Additionally, besides these performance parameters with a certain boundary, other key performance indicators (KPI's) are assessed as well, presented in Table A.2 accompanied by their relevance (Kelder, 2019).

Batteries in hybrid installations as considered in this study are used for consumer- and wholesale energy arbitrage, requiring a power capacity in the range of 1 - 10 MW. The discharging time of these applications is in the range of minutes to hours and high energy density/ specific energy is desired.

For clarity, the distinction between energy in power in terms of battery performance is visualised in Figure A.8. When a battery possesses more energy, more electricity can be produced without charging. An increased power results in faster discharging of the battery. As obvious from the Figure, when batteries have low energy densities (or specific energy), the size could be increased to eventually reach

Table A.1: Performance parameters assessed

Performance parameter	Boundary	Unit	Explanation
Power	1	[MW]	Customer focused peak shaving/load leveling requires a power capacity in the range of 1-10 MW
Storage duration	4	[hr]	Similar to most standard commercially available batteries which are used for energy arbitrage and/or peak shaving
Energy capacity	4	[MWh]	The energy capacity when power of 1 MW and storage duration of 4 hours is considered
Cycle life	1826	[-]	Assuming one cycle 365,25 days for 5 years at least
Round-trip efficiency	75	[%]	Maximising cost-effectiveness (Bank, 2018)
Daily self-discharge	1	[%/day]	To maintain a significant portion of the energy capacity

Table A.2: Key performance indicators assessed accompanied by their relevance

Performance parameter	Unit	Relevance
Safety	[-]	Very critical
Thermal stability	[-]	Very critical
Cost	[€/kWh]	Very critical
Recyclability	[-]	Less critical
Specific energy	[Wh/kg]	Less critical
Specific power	[W/kg]	Less critical
Energy density	[Wh/L]	Less critical
Power density	[W/L]	Less critical

the same results (but not without costs). Since the size for stationary applications does not (always) matter, there is no restriction in terms of energy in the first place. However, higher energy densities/ specific energies is more preferred in terms of costs.

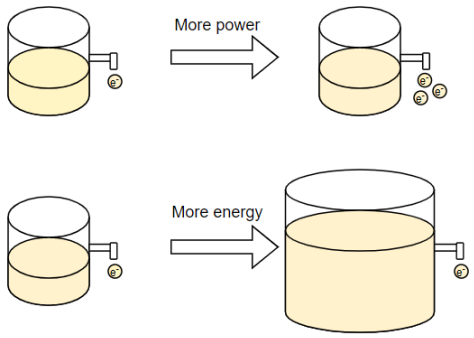

Figure A.8: The impact of energy and power in battery performance

Battery characteristic values

As mentioned in Chapter 2, the literature review has resulted in data of the batteries which are researched. The data is gathered through various reviews and sources and the values presented are an averaged value based on the data. The data is collected in various Tables and presented in this Subsection of which the sources which are used for the data are mentioned in the titles.

Battery voltages

Table A.3: Overview of battery voltages (Argyrou et al., 2018; Benato et al., 2015; Chakkaravarthy et al., 1991; McBreen, 1994; Soloveichik, 2011)

Batteries		Flow batteries			
Type	E_0 [V]	Type	E_0 [V]	Type	E_0 [V]
Li-S	2.57	V-V	1.26	H-Br_2	1.4 - 1.6
Li-air	2.91	Fe-Cr	1.18	Zn-Br_2	1.85
Li-ion	3.3 - 4.2	V-Br	1.32	Zn-Cl_2	2.02
Ni-Cd	1.29	PSB	1.36	Zn-Ce	2.48
Ni-Fe	1.37				
Ni-MH	1.35				
Ni-Zn	1.6				
Ni-H_2	1.55				
Na-S	1.78 - 2.07				
$NaNiCl_2$	2.58				
Na-ion	2.3 - 2.5				
Lead-acid	2.04				

Key performance indicators of batteries

Table A.4: Technology readiness level descriptions (Mongird et al., 2019)

Technology Readiness Level	Description
TRL 1	Basic principles observed and reported
TRL 2	Technology concept and/or application formulated
TRL 3	Analytical and experimental critical function and/or characteristic proof of concept
TRL 4	Component and/or system validation in laboratory environment
TRL 5	Laboratory scale, similar system validation in relevant environment
TRL 6	Engineering/pilot scale; similar protoytpical system validation in relevant environment
TRL 7	Full scale; similar (prototypical) system demonstrated in relevant environment
TRL 8	Actual system completed and qualified through test and demonstration
TRL 9	Actual system operated over the full range of expected mission conditions

Table A.5: Data of key performance indicators of lithium-ion batteries (Argyrou et al., 2018; Beaudin et al., 2010; Bender, 2000; Bradbury, 2010; H. Chen et al., 2009; Díaz-González et al., 2012; Fan et al., 2020; Kebede et al., 2022; Petrov et al., 2021)

KPI	Unit	LCO	LFP	LMO	NCA	NMC
Specific energy	[Wh/kg]	120 - 190	90 - 120	100 - 150	150 - 260	150 - 180
Specific power	[W/kg]			150 - 2000		
Energy density	[Wh/L]	400	350	350	550	500
Power density	[W/L]			500 - 5000		
Lifetime	[years]			5-15		
Cycle life	[-]	500 - 1000	>2000	300 - 700	500	1000 - 2000
Round-trip efficiency	[%]			85 - 97		
Self-discharge	[%/day]			0.15 - 0.25		
Depth of discharge	[%]			80		
Environmental impact	[-]	Higher	Lower	Moderate	Higher	Moderate
Safety	[-]	Lower	Higher	Moderate	Lower	Moderate
Thermal stability	[-]	Lower	Higher	Moderate	Lower	Moderate
Cost	[€/kWh]	Higher	Lower	Moderate	Higher	Moderate
Recyclability	[-]			Low		
TRL	[-]	7 - 9	7 - 9	6 - 8	6 - 8	7 - 9

Table A.6: Data of key performance indicators of nickel-based batteries (Beaudin et al., 2010; Bradbury, 2010; H. Chen et al., 2009; W. Chen et al., 2018; Das et al., 2018; Díaz-González et al., 2012; Kopera, 2004; McBreen, 1994; Solyali et al., 2022; Vazquez et al., 2010; Wagner, 2007)

KPI	Unit	Ni-Cd	Ni-Fe	Ni-MH	Ni-Zn	Ni-H_2
Specific energy	[Wh/kg]	50 - 75	50	60 - 100	55 - 75	55 - 75
Specific power	[W/kg]	140 - 180	100	200 - 300	200	220
Energy density	[Wh/L]	50 - 150	30	170 - 240	280	60
Power density	[W/L]	150-400	20 - 50	500	100 - 200	50 - 100
Lifetime	[years]	10-20	20	5 - 15	5 - 15	20
Cycle life	[-]	2000 - 2500	10000	300 - 500	300	30000
Round-trip efficiency	[%]	60 - 75	65	50 - 80	>70	85
Self-discharge	[%/day]	0.2 - 0.6	0.03 - 0.1	0.3 - 0.6	0.6 - 1.0	0.03 - 0.1
Environmental impact	[-]	Higher	Moderate	Moderate	Higher	Lower
Safety	[-]	Moderate	Higher	Higher	Lower	Higher
Thermal stability	[-]	Moderate	Higher	Moderate	Lower	Higher
Cost	[€/kWh]	Moderate	Moderate	Moderate	Higher	Higher
Recyclability	[-]	Moderate	Higher	Higher	Lower	Lower
TRL	[-]	9	6 - 7	8 - 9	4 - 6	4 - 5

Table A.7: Data of key performance indicators of sodium-based batteries (Beaudin et al., 2010; Bradbury, 2010; H. Chen et al., 2009; Converse, 2011; Díaz-González et al., 2012; Palizban & Kauhaniemi, 2016; Petrov et al., 2021; TAMYÜREK & NICHOLS, 2004; Vazquez et al., 2010)

KPI	Unit	Na-S	$NaNiCl_2$
Specific energy	[Wh/kg]	150 - 240	100 - 120
Specific power	[W/kg]	150 - 230	150 - 200
Energy density	[Wh/L]	150 - 250	150 - 180
Power density	[W/L]	150 - 250	200 - 300
Lifetime	[years]	10 - 15	15
Cycle life	[-]	2500 - 4500	4500
Round-trip efficiency	[%]	75 - 90	85 - 90
Self-discharge	[%/day]	0.05	0.03 - 0.3
Environmental impact	[-]	Lower	Lower
Safety	[-]	Moderate	Higher
Thermal stability	[-]	Moderate	Moderate
Cost	[€/kWh]	Higher	Higher
Recyclability	[-]	Moderate	Moderate
TRL	[-]	7 - 9	4 - 7

Table A.8: Data of key performance indicators of lead-acid batteries (Beaudin et al., 2010; Bradbury, 2010; Das et al., 2018; Díaz-González et al., 2012; Petrov et al., 2021; Solyali et al., 2022; Vazquez et al., 2010)

KPI	Unit	Lead-acid
Specific energy	[Wh/kg]	25 - 50
Specific power	[W/kg]	180 - 200
Energy density	[Wh/L]	50 - 80
Power density	[W/L]	10 - 400
Lifetime	[years]	3 - 12
Cycle life	[-]	500 - 2000
Round-trip efficiency	[%]	70 - 80
Self-discharge	[%/day]	0.1 - 0.3
Depth of discharge	[%]	70
Environmental impact	[-]	High
Safety	[-]	High
Thermal stability	[-]	Moderate
Cost	[€/kWh]	Moderate
Recyclability	[-]	High
TRL	[-]	9

Table A.9: Data of key performance indicators of vanadium redox flow and zinc bromine hybrid flow batteries (IRENA, 2017; Xu et al., 2022)

KPI	Unit	VRB	ZBB
Specific energy	[Wh/kg]	15 - 25	65
Specific power	[W/kg]	50 - 100	200
Lifetime	[years]	15	10
Cycle life	[-]	13000	10000
Round-trip efficiency	[%]	75 - 85	75 - 85
Self-discharge	[%/day]	Low	Low
Depth of discharge	[%]	100	100
Safety	[-]	High	Low
Cost	[€/kWh]	High	High
Recyclability	[-]	Uncertain yet	Uncertain yet
TRL	[-]	7 - 8	7 - 8

Conventional secondary batteries

Batteries are chemical devices for storage of electrical energy (Dell & Rand, 2001). A battery comprises one or multiple electrochemical cells (connected in series or parallel), consisting of two electrodes, an external circuit and an electrolyte. By converting chemical energy via reduction-oxidation (redox) reactions at the electrodes, electrical energy is generated. The electrodes are separated by an electrolyte, a substance being conductive for ions and insulative for electrons.

During the redox reactions, (i) transfer of electrons through an external circuit and (ii) transfer of ions through the electrolyte between two chemical species takes place which consequently results in a change of state of oxidation of the atoms at the electrodes involved in the reaction. One of the electrodes undergoes an oxidation, both electrons and positive ions (cations) are lost and being transported to the other electrode, which experiences a gain of electrons and cations and thus a reduction. The direction of negative ions (anions) is opposed to the direction of the cations. The oxidation electrode is either referred to as the reducing agent or the negative electrode or the anode whereas the reducing electrode is either referred to as the oxidising agent or the positive electrode or the cathode (Winter & Brodd, 2004). During discharge, the negative electrode is the anode but during charge the negative electrode becomes the cathode, since the redox reaction turns. Opposite to the label anode/cathode, the label negative/positive electrode does not change during the operation of a battery.

The reactions of discharging and charging are reversible in a battery. The discharging reaction happens naturally because of the presence of a driving force whereas the charging reaction requires extra work since this is against the natural driving force. The driving force is created by the potential difference between the half-reactions happening at the two electrodes (Dell & Rand, 2001). Figure A.9 presents an overview of the operation of a battery on cell level.

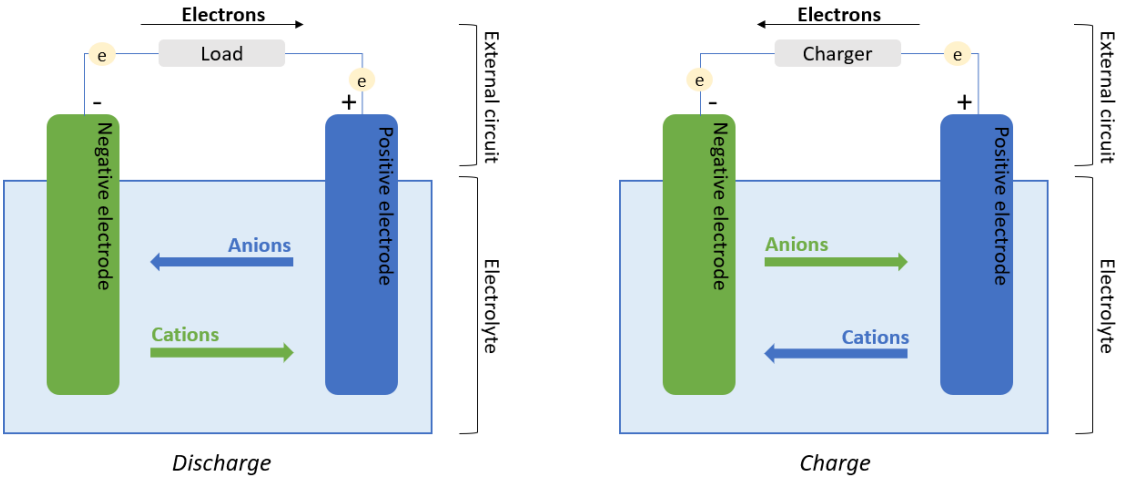

Figure A.9: Scheme of a standard battery

As mentioned, (large-scale) BESS consist of multiple electrochemical cells to increase their power capacity to be compatible with different applications. The cells are connected in series and in parallel, together composing the battery stack. The voltage is regulated by connecting multiple cells in series whereas parallel connections affect the usable capacity (Alotto et al., 2014; Hesse et al., 2017).

Characteristics

The potential of a battery (measured in Volt (V)) depends on the electrode materials and therefore on the chemical reactions taking place at the electrodes. The voltage is measured by the difference of potentials of the two electrodes. All electrode potentials are relatively measured to the standard hydrogen electrode, which is set at 0 V. When electrodes are in their standard state, the standard electrode potential (E^0) is measured. The open-circuit voltage of a battery is measured by the difference between the E^0 of the two electrodes, where the positive electrode has a positive potential and the

negative electrode has a negative potential. High cell voltages are desirable because higher voltages impose less power loss. The equation for power loss is presented in the first line of equation A.1.

$$\begin{aligned} P &= I^2 * R \\ P &= I * V \end{aligned} \tag{A.1}$$

In the first equation, P presents the power loss [W], where I presents the current [A] and R the resistance [Ω]. The current needs to be minimised to minimise power loss. The second equation expresses power and transferring the same amount of power, with a minimised current, results in a maximised voltage. Therefore, high cell voltages are desired since it is cost effective: the cell stack can be composed of a minimised amount of cells, simultaneously decreasing the electrolyte costs and optimising space while maintaining the same power output (Tang et al., 2022).

The open circuit voltage is measured when there is no current flowing through the battery, also referred to as the standard cell voltage (V^0). When the battery is operational, a current is flowing and the measured potential is lower than V^0 because of polarisation losses at the electrodes and resistive losses at the current-collectors, electrolyte and electrodes. The difference between the measured potential of a battery in operation and the standard cell voltage is the electrode overpotential (η). When η is non equal to zero, electrodes are recognised as being polarised (Ferrese, 2015).

The capacity of a battery cell is expressed in ampere-hours (Ah) and is the product of the current and the number of hours for which the battery is being (dis)charged. The amount of reactants has a linear relation with the capacity of a battery, more reactants on both sides is resulting in a higher capacity. Ambient temperature, cell aging and the rate of discharge all have an influence on the capacity. When the discharge rate increases, the stored energy which can be delivered per time decreases. Manufacturers specify a nominal capacity under standard conditions of the ambient temperature and (dis)charge rate. The C-rate is the (dis)charge rate at which the capacity is calculated. The amount of capacity withdrawn at any moment in time compared to the total capacity of a battery is the depth-of-discharge (DoD). The state-of-charge (SoC) is the fraction of the full capacity that is still available for discharging (Ferrese, 2015).

Lithium-based batteries

Lithium (Li)-based batteries are widely used in portable applications such as mobile phones, electric vehicles and others because of their high energy capacity and output voltage accompanied by their light weight (Solyali et al., 2022). In addition to their popularity in portable applications, Li-based batteries are also frequently used for stationary applications (Kurzweil, 2015). Because of the wide range of application, the use of Li-based batteries is popular and accepted. However, the biggest concern with Li-based batteries has to do with safety. Because Li violently reacts with water, this reaction can cause ignition (Kurzweil, 2015).

Li batteries can be distinguished based on their electrode materials and the electrolyte of the system. The anode can be composed of either metallic Li, making the battery primary, non-rechargeable or of intercalated Li, also referred to as Li-ion batteries. Li-ion batteries are secondary, rechargeable batteries and are therefore considered in this thesis. The electrolyte consists of either liquid or polymer material (Kurzweil, 2015). Additionally, an increasing interest was shown in different Li-based batteries than Li-ion, namely in lithium-sulfur (Li-S) and in Li-air, both improving the energy density compared to Li-ion.

A.I. Lithium-sulfur

The reaction equation of Li-S batteries is presented below (Soloveichik, 2011).

$$2Li + S \leftrightarrow Li_2S$$

The energy density of Li-S batteries is about 5 times greater compared to Li-ion (Huang et al., 2020; Solyali et al., 2022). Because of this reason, Li-S batteries are being developed for special mobile applications such as military electric vehicles, high-altitude satellite vehicles or aircrafts. However, the

drawbacks associated with Li-S are restricting their expansion on the commercial market. The main drawback is the failure mechanism of Li-S batteries. This failure happens because the degradation is not as gradual as in Li-ion batteries. For applications where a reliable battery is necessary, Li-S batteries are not selected (Solyali et al., 2022).

A.II. Lithium-air

The materials used in Li-air batteries are the metal Li or similar anodes as in Li-ion batteries. The cathode is composed of carbon mats accompanied by a transition metal oxide catalyst. Metallic Li is highly reactive in the air with water (H_2O) and carbon dioxide (CO_2) and therefore the anode should be in a non-aqueous environment (L. Su et al., 2015). The overall reaction equation is given below (Kelder, 2019).

$$2Li_{(s)} + O_{2(g)} \leftrightarrow Li_2O_{2(s)}$$

The reaction product $Li_2O_{2(s)}$ is insoluble in organic electrolytes and therefore accumulation on the surface of the cathode is likely to happen, decreasing the theoretical capacity by blocking the oxygen (O_2) inlet. Additionally, more challenges are faced and explained here (L. Su et al., 2015). Li-air batteries are attractive due to their highest theoretical capacity of metallic Li, namely 11248 Wh/kg as well as the use of free O_2 (L. Su et al., 2015). However, the challenges are blocking the commercial development of Li-air batteries.

A.III. Lithium-ion

The performance of a Li-ion battery is determined by the electrode materials which are used. The positive electrode consists of Li-containing transition metal oxides whereas the negative electrode often is composed of carbonaceous material, such as graphite or hard carbons (Mongird et al., 2019). The electrodes are made of active material particles and held together with a binder and a conductive filler such as graphite or carbon black. The smaller the size of the particles, the larger the surface area and the better the performance of the battery. The electrolyte of a Li-ion battery is often based on a Li salt dissolved in organic solution (Kurzweil, 2015). Due to the thermodynamic instability of the interface of the organic electrolyte and the electrodes, a solid electrolyte interphase (SEI) is formed at the anode during the first charge-discharge cycles. This SEI protects the anode against contact with the electrolyte. However, the formation is rather slow so Li can be lost, resulting in a decrease of capacity and in an increase of resistance (Hesse et al., 2017).

Li-ion batteries are promising for stationary storage systems because of their high specific energy and power as well as because of the low capital costs (Abu et al., 2023; Mongird et al., 2019). They exhibit a high energy efficiency of approximately 85-95 percent, they are capable of providing a large number of (dis)charge cycles, their lifetime is around 10 years and their response time between modes of operation is fast (Kebede et al., 2022; Petrov et al., 2021).

As mentioned, the positive electrode consists of Li-containing metal oxides. These Li-metal oxides can be formed into different structures, determined by the specific materials. These structures all exhibit different specific performance parameters and is explained next (Kurzweil, 2015).

A.III.a. Lithium cobalt oxide

Li-ion batteries with a positive electrode composed of lithium cobalt oxide ($LiCoO_2$) are referred to as LCO. The reaction equation is given below.

$$LiCoO_2 + C_6 \leftrightarrow LiC_6 + CoO_2$$

The LCO electrode has a high specific energy (Abu et al., 2023). Drawbacks of this structure are the security problems and the high costs, mainly associated with the usage of cobalt. Prices of cobalt are fluctuating and the material potentially causes environmental and toxic hazards (Kurzweil, 2015).

A.III.b. Lithium iron phosphate

Li-ion batteries with a positive electrode based on lithium iron phosphate ($LiFePO_4$) are referred to as LFP batteries. The reaction equation is given below.

$$LiFePO_4 + C_6 \leftrightarrow LiC_6 + FePO_4$$

The LFP electrode provides high security and cycle life for moderate costs. Since LFP also generates a high power and packing density, this type of Li-ion is considered likely to be encountered for a wide use of application (Abu et al., 2023). Besides this, a cycle life analysis has shown the superior stability of the LFP cathode compared to other Li-ion cathode materials (Hesse et al., 2017). Furthermore, LFP batteries show a plateau in their voltage curve during discharge. 80 percent of the energy stored in the batteries falls within this voltage plateau, causing the voltage to be very constant during discharge, simplifying application design (Rouholamini et al., 2022). However, the specific capacity and voltage are considered to be low (Kurzweil, 2015). The combination of characteristics cause LFP batteries to be most interesting among other Li-ion batteries for stationary applications (Hesse et al., 2017).

A.III.c. Lithium manganese oxide

Li-ion batteries with a positive electrode composed of lithium manganese oxide ($LiMn_2O_4$) are referred to as LMO batteries. The reaction equation is given blow.

$$LiMnO_2 + C_6 \leftrightarrow LiC_6 + LiMn_2$$

LMO electrodes have a high specific power only at moderate costs. However, stability in the electrolyte solution is lacking in this type of lattice (Kurzweil, 2015).

A.III.d. Lithium nickel cobalt manganese oxide

Li-ion batteries with a positive electrode composed of lithium nickel manganese cobalt oxide ($LiNiMnCoO_2$) are referred to as NMC batteries. The reaction equation is given below.

$$LiNiMnCoO_2 + C_6 \leftrightarrow LiC_6 + NiMnCoO_2$$

NMC batteries are ternary Li-batteries, where the cathode material is composed of three or more substances. The ratio between the materials can be adjusted to reach desired levels of costs, safety and cell voltage (Rouholamini et al., 2022). Among all Li-ion batteries, NMC batteries are characterised by their safety, lifetime and high energy density. Also, their costs are considered as competitive. However, the costs and use of Co are not ideal (Hesse et al., 2017).

A.III.e. Lithium nickel cobalt aluminum oxide

Li-ion batteries with a positive electrode composed of lithium nickel cobalt aluminum oxide ($LiNiCoAlO_2$) are referred to as NCA batteries. The reaction equation is given below.

$$LiNiCoAlO_2 + C_6 \leftrightarrow LiC_6 + NicoAlO_2$$

NCA batteries are also classified as ternary Li-ion batteries. NCA batteries possess a high specific energy of around 250 Wh/kg, making them suitable for implementation in portable devices and electric vehicles. However, the use of cobalt causes the capital costs to be high. Also, the cycle life of NCA is considered as lower compared to other batteries (Hesse et al., 2017). Lastly, NCA batteries are not as safe as other batteries which is disadvantageous (Tran et al., 2021).

NCA and NMC cells both exhibit suitable characteristics for the same category of applications and therefore both are used in similar types of BESS. However, NCA batteries are targeted most for electric vehicle applications whereas NMC batteries are more widely used for grid applications.

A.III.f Lithium titanate oxide

Li-ion batteries with a negative electrode composed of lithium titanate oxide (Li_2TiO_3) are referred to as LTO. Most Li-ion batteries are composed of a graphite anode and LTO has not yet been developed very widely. However, LTO seems to be a promising type of anode for Li-ion batteries since they possess a high cycle life as well as a high power capacity. Additionally, LTO batteries have the capability of fast-charging (Nemeth et al., 2020). Li-ion batteries based on an LTO anode are most suitable for high-power applications (Nemeth et al., 2020). Besides this, the costs of titanate are high (Hesse et al., 2017).

Conclusion on lithium-based batteries

First, two sorts of Li-based batteries were assessed, Li-S and Li-air. Both types of batteries are promising candidates in terms of enhancing the energy density compared to Li-ion batteries, however they are still facing too many challenges before being developed on the commercial scale. Since there is no knowledge on whether these challenges are going to be solved and when, these two Li-based batteries are not taken into account for the remainder of this study.

Among the Li-ion batteries, five different cathode materials combined with a graphite anode are contemplated. The KPI's of the five cathode materials assessed for Li-ion batteries, as mentioned in Table A.2, are compared against each other in Figure A.10. The performance increases with scale (0-5). To be clear, LFP batteries have the best performance in terms of costs and are therefore the cheapest among the Li-ion batteries assessed in the chart.

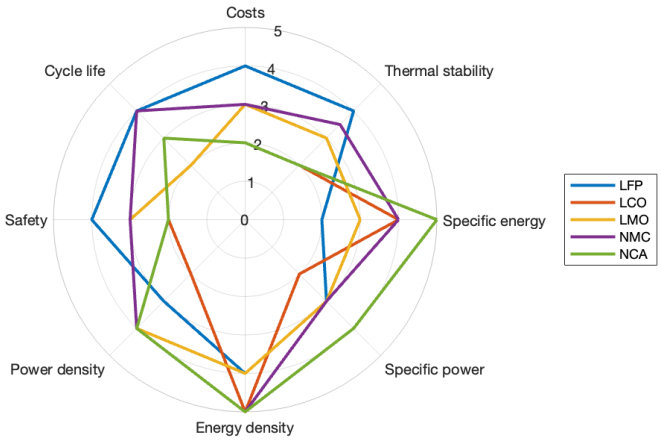

Figure A.10: Radar chart of key performance indicators of lithium-ion batteries

Based on the data inserted in the radar plot, which is presented in Table A.5, LFP and NMC batteries are considered as most suitable Li-based BESS for this study. The trade-off between the two cathode materials are the lower costs and higher safety of LFP to a higher energy density of NMC. Since costs and safety are more important for this thesis, NMC is not taken into consideration for the remainder of the research. Also, the anode material LTO was assessed. Since the hybrid installation does not necessarily require such high power characteristics as LTO has, graphite anodes are considered only. This decision is based on costs since titanate is expensive.

B. Nickel-based batteries

Nickel (Ni)-based batteries are unique in their high energy density and great storage capacity, at low costs. Ni is the fifth most common element on Earth and occurs extensively in the Earth's crust and core. This causes the Ni supply chain to be very reliable and replenished (L. Wang et al., 2022). Typical Ni-based batteries use a $Ni(OH)_2$ cathode whereas the anode varies between different metals. The electrolyte consists of a concentrated potassium hydroxide (KOH) solution or a combination of KOH and sodium hydroxide (NaOH) solution (L. Wang et al., 2022).

B.I. Nickel-cadmium

Nickel-cadmium (Ni-Cd) batteries were the first Ni-based batteries discovered (L. Wang et al., 2022). Ni-Cd batteries employ metallic Cd and nickel oxide hydroxide (NiOOH) as electrodes (anode, cathode respectively) where the metallic Cd electrode has a greater capacity. The electrolyte consists of an alkaline KOH solution and a separator is present (Fan et al., 2020; Petrovic & Petrovic, 2021). The reaction equation of Ni-Cd batteries is presented below (Soloveichik, 2011).

$$Cd + 2NiOOH + 2H_2O \leftrightarrow Cd(OH)_2 + 2Ni(OH)_2$$

The low maintenance (costs), long cycle life (2000-2500) and an efficiency of around 75 percent are beneficial performance parameters of the Ni-Cd battery (Kebede et al., 2022). The cycle life is around 1000 cycles when the DoD is above 80 percent and around 5000 when the DoD is only 60 percent (Salkuti, 2021). However, the low energy density as well as the high capital costs and the toxicity of Cd are major disadvantages (Fan et al., 2020). Another disadvantage of Ni-Cd batteries is the memory effect. The lifetime and capacity of the battery drastically decrease over time when the battery is multiple times recharged after being partially discharged (Argyrou et al., 2018). The development of Ni-Cd batteries was limited to specific applications only, for example for health care machines (Solyali et al., 2022). The process of recycling of Ni-Cd was explored during the past few years and successfully improved (Salkuti, 2021).

B.II. Nickel-iron

Nickel-iron (Ni-Fe) batteries were the first commercialised Ni-based batteries (L. Wang et al., 2022). Ni-Fe batteries use metallic Fe and NiOOH electrodes (anode, cathode respectively). The reaction equation of a (dis)charge cycle is presented below (Chakkaravarthy et al., 1991).

$$Fe + 2NiOOH + 2H_2O \leftrightarrow Fe(OH)_2 + 2Ni(OH)_2$$

The typical characteristics of Ni-Fe batteries are their low energy and power density as well as their low energy efficiency (around 60 percent) (Chakkaravarthy et al., 1991). Despite the unfavourable performance mentioned, Ni-Fe batteries are specially deployed for applications where vibration exists because they can withstand shocks very well (Chakkaravarthy et al., 1991; Solyali et al., 2022). Also, the manufacturing of the electrodes is considered simple, as well as that the costs are considered low, the performance good and there are no environmental hazards. However, the costs are four times as high compared to lead-acid and Li-ion (Hussain et al., 2020).

B.III. Nickel metal hydride

Nickel-metal hydride (Ni-MH) batteries were developed with the aim to replace the toxic Ni-Cd batteries. Ni-MH batteries consist of a MH negative electrode and a NiOOH positive electrode. The electrodes are separated by a porous membrane, all in an alkaline electrolyte solution of KOH (Zelinsky et al., 2017). The MH is an intermetallic compound, consisting of various metals with regular order and distinct composition. Different from an alloy, a MH does not allow all compositions of metal mixtures. The MH can have the composition AB_5, where A is a mixture of various rare-earth materials and B a transition metal or aluminum. Additionally, AB_2 is another possible composition for the MH, where A is either vanadium or titanium and B is nickel or zirconium (Kelder, 2019). The reaction equation is presented below (Soloveichik, 2011).

$$MH + NiOOH \leftrightarrow M + Ni(OH)_2$$

Ni-MH batteries provide a 40 percent higher energy density compared to Ni-Cd batteries (Hussain et al., 2020; L. Wang et al., 2022). Ni-MH batteries are widely used in the transportation sector because of their high specific power of 200-300 W/kg (Kebede et al., 2022). Additionally, their long cycle life and compact size makes them suitable for stationary applications as well (Salkuti, 2021; Zelinsky et al., 2017). Also, no toxic materials are used and Ni-MH batteries are commercially recyclable. The ability of the battery to tolerate high heat conditions is important for stationary grid-connected applications (Zelinsky et al., 2017). Additionally, Ni-MH batteries do net get so much affected by the memory effect. The only drawbacks recognis ed is a decreased performance in the lower part of the temperature range [-30 $^\circ$ C - 70 $^\circ$ C] and the moderate efficiency (50-80 percent) (Fan et al., 2020).

B.IV. Nickel-zinc

Nickel-zinc (Ni-Zn) batteries consist of a NiOOH positive electrode and a zinc oxide (ZnO) negative electrode. The reaction equation is presented below (McBreen, 1994).

$$Zn + 2NiOOH + H_2 \leftrightarrow 2Ni(OH)_2 + ZnO$$

Advantages of Ni-Zn batteries are their environmentally friendliness and their non-toxicity. The problems however, which were encountered with Ni-Zn batteries have to do with penetration through the separator (Chakkaravarthy et al., 1991) as well as with the electrode shape changes (Spanos et al., 2015). These non-solved constraints resulted in a low degree of commercialisation of Ni-Zn batteries (Fetcenko et al., 2015). Also, the cycle life of Ni-Zn batteries is low (around 300 cycles only) (Hussain et al., 2020).

B.V. Nickel-hydrogen

Nickel-hydrogen (Ni-H_2) batteries use gaseous H_2, stored in a pressurised cell. Similar to other Ni-based batteries, the positive electrode consists of NiOOH. During discharge, the gaseous H_2 is oxidised into water while the positive electrode is reduced to NiOOH. The water is created at the negative H_2 electrode and consumed at the positive electrode. The chemical reaction is presented below (W. Chen et al., 2018).

$$NiOOH + \frac{1}{2}H_2 \leftrightarrow Ni(OH)_2$$

The greatest advantage of Ni-H_2 batteries is their extended lifetime of around 15 years or more at 80 percent DoD. Also, their cycle life is extremely long, around 30.000 cycles. The specific energy is considered low, their self-discharge is rather high and also their costs are very high. The reason for the high costs is the need for a pressurised vessel as well as the use of platinum catalysts in this type of battery. Therefore, Ni-H_2 batteries are mostly used for aerospace applications such as in satellites (W. Chen et al., 2018).

Conclusion on nickel-based batteries

Among the five Ni-based batteries evaluated, Ni-MH is chosen to be most suitable for the remainder of this research. The KPI's of the five Ni-based batteries as mentioned in Table A.2 are compared against each other in radar chart A.11. The performance increases with scale (0-5).

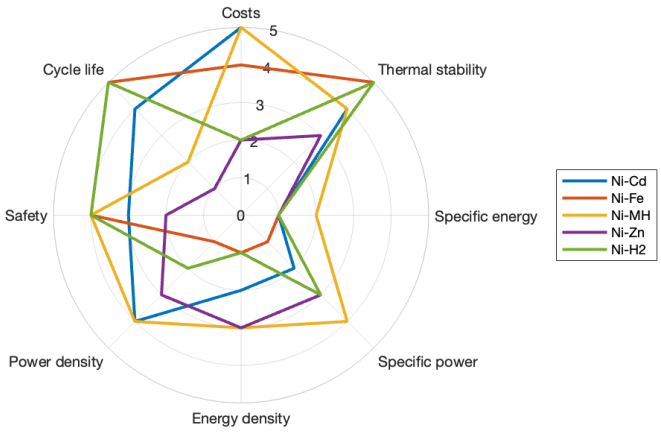

Figure A.11: Radar chart of key performance indicators of nickel-based batteries

The unsafety of Cd used in Ni-Cd batteries is decisive for not selecting this battery. Then, the efficiency of Ni-Fe batteries falls below the boundary condition of a minimum efficiency of 75 percent. Ni-Zn batteries are not selected because of the fact that there are too many uncertainties which are unsolved. Last, Ni-H_2 batteries are not considered as suitable for this research as they are mainly used for very specific applications. Also, their high costs are decisive. Table A.6 presents the data inserted in the radar plot.

C. Sodium-based batteries

One of the reasons why sodium (Na)-based batteries are being developed, among others, for large-scale BESS, is the abundance of Na on Earth. However, the temperature range wherein Na batteries are operating is considered as a drawback. The cells are placed within a thermal enclosure to maintain the internal battery temperature to prevent damage (Butler, 1994). Because of this enclosure, services on cell level are impossible. The operational temperature range requires installation of a regulation system as well which increases overall costs (Solyali et al., 2022). However, the necessary energy for this regulation is minimal when the system is used routinely (e.g. once per day). Also, Na-based batteries possess several advantages such as their low material costs and their high energy density and efficiency (Butler, 1994).

C.I. Sodium-sulfur

Sodium sulfur (Na-S) batteries are characterised by their high operational temperature (300-350 ° C), causing the active Na and S to be molten, separated by a solid oxide electrolyte. The electrolyte is able to conduct the Na^+ ions (Fan et al., 2020). At this temperature, the cell functions at an inverse structure compared to other conventional secondary electrochemical batteries, since the electrodes containing the active materials are liquid and the rest of the components are solid-state. The system requires heat regulation since damage occurs if the system reaches the high operational temperature (Solyali et al., 2022). The reaction equation is presented below (D. Kumar et al., 2017).

$$2Na + 4S \leftrightarrow Na_2S_4$$

Compared to other electrochemical storage devices, Na-S batteries possess a high specific energy and power in the range of 150 - 240 Wh/kg and 150 - 230 W/kg, respectively (Fan et al., 2020; Kebede et al., 2022). The cycle life and lifetime are up to 4500 cycles and 15 years, respectively. The self-discharge on an annual basis is negligible and the efficiency is around 85 percent. Na-S batteries are considered especially suitable for high specific energy demanding applications (Kebede et al., 2022). Na-S batteries are typically used for load leveling and peak shaving as well as for spinning reserves because of their ability of pulsing power for over six times their continuous rating (30 s) (Fan et al., 2020; Soloveichik, 2011). The capital costs are considered higher compared to lead-acid batteries because of the necessary components which can withstand such high temperatures, however the costs are still much lower than of Ni-Cd batteries for example (Mongird et al., 2019; Petrov et al., 2021). Because of the need for the high temperature the chance of the emergence of fire is high, therefore safety concerns are taken serious. However, since Na and S are both abundantly available, their raw material costs are low and the battery is considered environmentally friendly (Yan et al., 2022).

Additionally, research into room temperature (RT) Na-S batteries was conducted during the past few years. RT Na-S batteries are considered as very suitable for large-scale stationary energy storage systems because of their high theoretical energy density, low costs and environmental benignity (Y.-X. Wang et al., 2017; Yan et al., 2022). However, RT Na-S batteries face serious problems such as low electroactivity, limited cycle life and high self-discharge rates (Y.-X. Wang et al., 2017). Research into solutions of those problems has been done extensively in terms of cathode material improvement, electrolyte optimisation, separator modification and anode protection (D. Kumar et al., 2017; S. Zhang et al., 2021). However, research is still ongoing and the problems are not fully solved yet (P. Chen et al., 2022).

C.II. Sodium-nickel chloride

Sodium-nickel chloride batteries ($NaNiCl_2$ or ZEBRA) are made up of the active species Ni, NaCl and Na (Mongird et al., 2019). The negative electrode consists of liquid Na, which is separated from the positive electrode by a Na^+ ion conduction solid electrolyte, beta alumina (Sudworth, 2001). The positive electrode consists of solid NiCl. An additional liquid electrolyte is present namely sodium chloroaluminate ($NaAlCl_4$). The second electrolyte provides fast transport of Na-ions from the positive electrode to and from the beta ceramic electrolyte. The melting point of $NaAlCl_4$ (157 ° C) determines the minimum operational temperature of the battery (Sudworth, 2001). However, optimal performance is observed in the high temperature range between 270 and 350 ° C (Solyali et al., 2022). The reaction equation is presented (Benato et al., 2015).

$$NiCl_2 + 2Na \leftrightarrow 2NaCl + Ni$$

The presence of the second electrolyte makes $NaNiCl_2$ batteries fault tolerant since a single cell failure does affect neighbouring cells (Benato et al., 2015). The sufficient energy density, better degree of safety, and the high efficiency makes $NaNiCl_2$ batteries very suitable for a.o. load leveling applications (Benato et al., 2015).

C.III. Sodium-ion

Sodium-ion (Na-ion) batteries are promising for large-scale energy storage systems since their working principle is similar to Li-ion and Na is abundantly available (Zhao et al., 2020). However, materials that allow Li to be reversibly incorporated were found to be unsuitable for Na incorporation because of the difference in size (Skundin et al., 2018). Research has been done into suitable electrode materials for Na-ion batteries and the results show that anodes which are developed are based on carbon, metal alloys and transition metal oxides. The cathode materials are searched among Na containing oxides and salt systems (Skundin et al., 2018). Additionally, research should be extended even more in the future since there are challenges still preventing Na-ion batteries from being developed on the commercial market (Deng et al., 2018).

Conclusion on sodium-based batteries

The disadvantages of the high operational temperature range of Na-based batteries are minimal when used for application which are used routinely (e.g. once per day), which is the case for the hybrid installation as considered in this study. Also, RT Na-S batteries were analysed. However, despite the high potential but due to the uncertainty, RT Na-S batteries are not considered as suitable for hybrid installation in this study. Also, Na-ion batteries are not selected for deeper analysis since there are not enough insights in whether these challenges will be overcome and when. Compared to Na-S batteries, ZEBRA batteries are considered as extra safe, due to the additional electrolyte which is present in the battery cell. This extra safety supports the decision for only considering ZEBRA batteries for the remainder of this study. The KPI's of the two Na-based batteries which are considered for analysis, as mentioned in Table A.2, are compared against each other in Figure A.12. The performance increases with scale (0-5). The data inserted in the radar plot is presented in Table A.7.

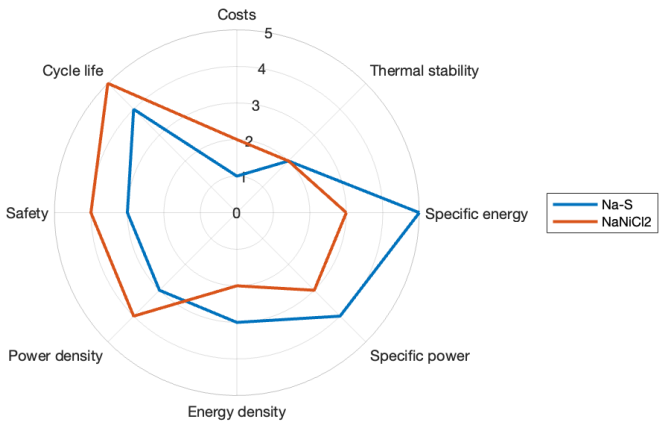

Figure A.12: Radar chart of key performance indicators of sodium-based batteries

D. Lead-acid batteries

The positive electrode of lead-acid batteries consists of PbO_2 whereas the negative electrode is made of Pb (Mongird et al., 2019). The electrolyte solution present in lead-acid batteries is H_2SO_4 (Solyali et al., 2022). The reaction chemistry is presented below (Soloveichik, 2011).

$$Pb + PbO_2 + 2H_2SO_4 \leftrightarrow 2PbSO_4 + 2H_2O$$

Lead-acid batteries are dealing with three drawbacks: their short cycle life of 500-1000 cycles, their low specific energy compared to conventional secondary electrochemical cells, namely around 35-40 Wh/kg, which is due to the high density of Pb and their poor low temperature performance, causing the battery to need thermal regulation (Fan et al., 2020; Kebede et al., 2022; Y. Zhang et al., 2022). Despite these drawbacks, lead-acid batteries are a mature technology and widely used in stationary and portable applications already. Lead-acid batteries also exhibit low capital and operational costs, good safety and also recyclability (Petrov et al., 2021). Lead-acid batteries have the lowest cradle-to-gate environmental footprint among other secondary batteries (Spanos et al., 2015). Their performance is stable however, when overcharging occurs, evolution of H_2 and O_2 cause water losses. Their specific power reaches 180 W/kg (Kebede et al., 2022), making lead-acid batteries suitable for transportation applications such as in electric vehicles. For stationary applications, the valve-regulated lead-acid (VRLA) battery is used most often, however flooded batteries are used as well (Soloveichik, 2011). VRLA batteries are more costly compared to flooded lead-acid batteries because of their increased complexity (Albright et al., 2012).

D.I. Flooded lead-acid

Flooded lead-acid batteries contain an electrolyte solution which is free to move through the battery. Therefore, an upright standing configuration is necessary to prevent leakage. When charged, toxic H_2 and O_2 is released which needs to be ventilated to prevent it from immediately getting free towards the environment in an uncontrolled manner. Distilled water needs to be added to the battery to compensate for electrolyte losses (Albright et al., 2012).

D.II. Valve regulated lead-acid

In VRLA batteries, the electrolyte is immobilised by either soak it into an adsorbent glass mat (AGM) or by gelling it by adding silicon dioxoide (Berndt, 2001). This report focuses on VRLA AGM batteries since this dominates the market of lead-acid batteries. Also, the gel type VRLA is most suitable for long-term standby power because of their long lifetimes when held at a fully charged state (Spanos et al., 2015). VRLA batteries are completely sealed off so that the H_2 which is produced at the negative electrode of the battery is forced to react with the O_2, which is produced at the positive electrode. The immobilised electrolyte allows gas migration. The H_2 and O_2 are combined to produce H_2O (Butler, 1994). This eliminates the need for adding H_2O, as is in flooded lead-acid batteries and therefore makes the system maintenance free as well as the lifetime longer (Soloveichik, 2011). Also, VRLA batteries have a pressure relief vent valve that permits an increase of internal pressure but prevents excessive pressure build up during overcharging that could cause leakages (Butler, 1994).

Conclusion on lead-acid batteries

Compared to flooded lead acid batteries, VRLA batteries are considered as more suitable for large scale energy storage due to their high recyclability, low costs, and the maintenance-free design. The short cycle life is an important drawback which should be kept in mind by selecting VRLA batteries. However, due to the maturity, recyclability, safety and low costs VRLA batteries are selected for the remainder of this thesis. The data associated with lead-acid batteries is presented in Table A.8.

Flow batteries

Flow batteries (FB) exhibit a high potential for being deployed as stationary, large-scale grid connected storage systems (Shigematsu et al., 2011). Their capability of independent sizing of energy and power, operating room temperature, rapid responses (necessary for activities on the electricity markets) and their long cycle life because of chemical stability makes them suitable for hybrid installations as considered in this study, since they can fulfil peak shaving and load leveling tasks (Alotto et al., 2014; Kelder, 2019). Additionally, FB possess no self-discharge (Argyrou et al., 2018). Also, FB are economically attractive since the electrolyte can be reused after the lifetime of the FB, therefore making maintenance costs lower (Petrov et al., 2021). FB distinguish themselves by their principle of operation compared to standard batteries, as explained in Subsection A.4. Figure A.13 visualises the (dis)charging cycle of a generic FB. Table A.9 shows characteristic data of two FB.

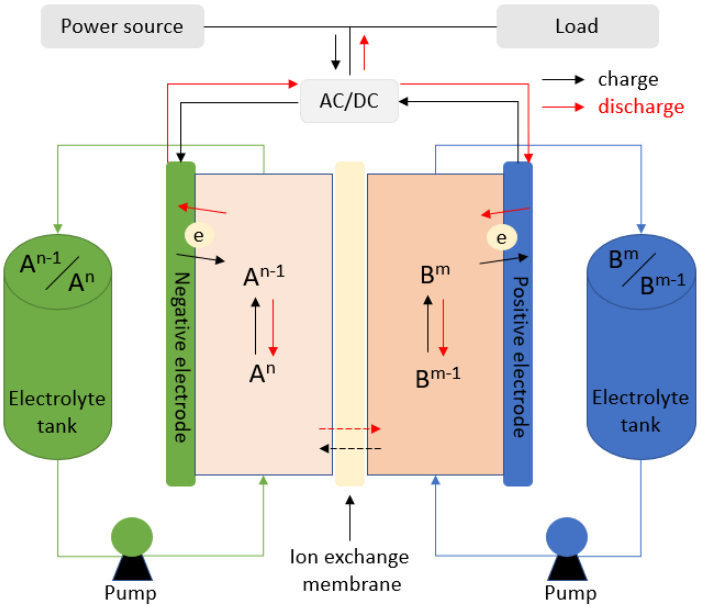

Figure A.13: Scheme of a redox flow battery

In a FB, energy is converted through a redox reaction between two electrolyte solutions which are saved in two separate, external reservoirs. The electrolytes contain active species in the form of dissolved metal ions (Kelder, 2019). Henceforth, conversion and storage is separated, ensuring no self-discharge. The electrolytes are being pumped out of the external storage reservoirs towards the electrochemical cell, where the redox reaction takes place. Inside the cell, the electrolytes are being separated by an ion exchange membrane, preventing the electrolytes from mixing but allowing ions to transfer (Prifti et al., 2012). Opposed to generic batteries, electrodes in FB cells are inert. The chemical reaction takes place between the two electrolytes, instead of between the electrode and the electrolyte (Lim et al., 2015). This phenomenon is beneficial for a long cycle life by keeping the electrode materials unaffected during cycling, which is desired since electron transfer goes through the electrodes (Blanc & Rufer, 2010). During discharge, an oxidation reaction occurs in the anolyte, the negative half-cell. After the oxidation, the free electron transfers through the external circuit and the load to produce power, towards the catholyte to be accepted for reduction. During charging, the reaction is opposed.

In FB, power and energy are independent since they are determined by the number of cells used in the stack and the volume of electrolyte utilised, respectively. Their independency allows them to potentially be optimised over a greater range because of the possibility of individual scaling. Adding energy storage by increasing the volume of the electrolyte tanks can be easily implemented without adding costs to the cell stack (Skyllas-Kazacos et al., 2011). Therefore, the investment costs decrease by an increasing energy-to-power ratio.

Besides advantages, FB exhibit disadvantages as well. The active materials are metal ions, solved in the electrolyte. Since solubility is limited here, the volume of the external tanks is large. Therefore, the energy density of FB is lower compared to other types of batteries. However, when size is not a limiting condition, this disadvantage can be ignored. Second, the electrolyte needs an external force to reach the inside of the cell, this requires extra power. Also, shunt-current losses may occur in FB through the electrolyte because of the series composition of multiple bipolar cells in the same stack with the electrolyte flowing through (Alotto et al., 2014).

A and B. Redox flow batteries

Redox flow batteries (RFB) can be distinguished from hybrid flow batteries (HFB) based on the electrochemical reactions which are taking place during operation. As explained above, in RFB, the energy is stored in the external tanks, which are containing the electrolyte solutions. Within RFB, a distinction is made between aqueous and non-aqueous RFB. The first category uses water-based electrolytes. Us-

ing water is cheap, makes the system non-flammable, safe and highly conductive. This results in fast ion transport kinetics and good compatibility with the ion selective membrane. The challenge of aqueous RFB is to obtain high cell voltages since these are limited by the voltage of water electrolysis, which is 2 V (Tang et al., 2022). Non-aqueous RFB dissolve their electrolyte in organic solvents. Thereby suffering from poor ionic conductivity, low ion transfer coefficients and high security risks. However, non-aqueous RFB have a higher operating voltage which is desirable for reducing costs and optimising space (Cao et al., 2020).

Within the category of aqueous RFB, both inorganic and organic electrolyte solutions are present. Inorganic aqueous RFB utilise water-based electrolytes, containing inorganic redox-active species. The redox-active species typically are metal ions, providing high energy efficiencies and power densities (J. Luo et al., 2022). The drawbacks of using inorganic species are corrosion, toxicity, high costs and slow redox reaction kinetics. The inorganic aqueous RFB which are selected for further analysis are based on the active species duo's vanadium-vanadium, iron-chromium and vanadium-bromine. To overcome the drawbacks of inorganic aqueous RFB, organic aqueous RFB were designed, using water-based electrolytes as well and containing organic redox-active species. The advantage of using organic species is the abundant availability of the species and therefore the potential of scaling the production from a bio-based feedstock. Additionally, organic species have a great diversity in structure, therefore they can be much more flexible in design for RFB by molecular engineering (Cao et al., 2020; Liu et al., 2016). However, the drawback of organic aqueous RFB comes from the molecule size, which influences the electrolyte viscosity and thus resistance, therefore lowering the current performance and power density (J. Luo et al., 2022). The organic aqueous RFB which are assessed are zinc-air and semi-solid FB.

Non-aqueous RFB also consist of multiple different categories based on the solvents. However, this type of RFB is not assessed here because their further development is currently prevented because of the low ionic conductivity of the non-aqueous systems (Tang et al., 2022).

A.I. Vanadium-vanadium

Among all, vanadium-based (also known as all-vanadium) RFB (VRB) are most widely commercialised and have a high chance to be widely adopted for (large-scale) storage applications. VRB benefit from their simplicity (Blanc & Rufer, 2010). Vanadium is the only reactive specie present in a VRB, in four different oxidation states. Both half-cells contain vanadium ions in an acidic solution with the redox couple V^{2+}/V^{3+} operating in the negative half-cell and $VO^{2+}/VO_2{}^{+}$ in the positive half-cell. The advantage of using vanadium as the only metal ion both in the positive and negative half cell, results in the fact that the capacity of the cell does not decrease over time when the electrolytes experience mixing (Alotto et al., 2014). When the battery is charged, ion migration could cause self-discharge of around 3 percent per day. Since vanadium is the only reactive species present, this is not fatal (Soloveichik, 2011). However, less self-discharge was experienced when the proton exchange membranes were modified, thereby increasing proton selectivity. The reaction equation of VRB is given below (Lim et al., 2015).

$$VO_2{}^{+} + V^{2+} + 2H^{+} \leftrightarrow VO^{2+} + V^{3+} + H_2O$$

VRB possess high energy efficiencies (75-85 percent), long lifetime (12000-14000 cycles), high safety, low operating costs and easy maintenance (Fan et al., 2020). However, VRB also have drawbacks, namely the prevailing scarcity of vanadium production as well as the supply chain risks resulting in higher capital costs of vanadium (Petrov et al., 2021). The global availability and production of vanadium is comparable to those of materials such as lithium, cobalt and nickel (Rodby et al., 2023). Although vanadium is considered to be relatively abundantly available, the production is highly geographical concentrated causing strong price volatility. 62 percent of all vanadium production is located in China and the remaining 38 percent is spread over three production countries (Ciotola et al., 2021). Also, vanadium supply chain disruptions can be caused by competing sectors. Vanadium is an important feedstock for the steel and chemical industries for example and vanadium used for batteries is non-recyclable yet. Additionally, the highly toxic material vanadium pentoxide used in VRB electrolytes is another downside (Ciotola et al., 2021). On top of this, the low energy density of VRB (10-50 Wh/kg) results in the need for bigger installations. Since the PoR is lacking physical space, this is an important

aspect to take into account (Fan et al., 2020). VRB installations are suitable to be used for load leveling applications (Argyrou et al., 2018).

A.II. Iron-chromium

Iron chromium based RFB (ICB) were the first RFB being analysed (Zeng et al., 2015). ICB are based on the low-cost and abundantly available redox couples Fe^{3+}/Fe^{2+} and Cr^{3+}/Cr^{2+} in an hydrochloric acid electrolyte solution. The Fe solution is referred to as the catholyte and the Cr is solved in the anolyte. The reaction equation is given below (Revankar, 2019).

$$Fe^{3+} + Cr^{2+} \leftrightarrow Fe^{2+} + Cr^{3+}$$

Compared to VRB, ICB benefits from the low costs and low toxicity of the electrolytes used. The electrode materials typically are either carbon fiber, carbon felt or graphite, affecting both redox couples differently. The Fe^{3+}/Fe^{2+} redox couple exhibits high reversibility and fast kinetics on all of these electrode materials. Opposite to this, the Cr^{3+}/Cr^{2+} redox couple has slow kinetics when combined with these carbon-based electrodes (Revankar, 2019). Therefore, the use of a catalyst on the negative side of the cell is necessary to enhance the kinetics of the half-reaction. One condition the catalyst must meet is a high overpotential towards the H_2 evolution reaction that occurs. H_2 is thermodynamically reduced more easily than Cr is and thus H_2 evolution causes capacity decay (Zeng et al., 2015). Potential catalysts counteracting this phenomenon are gold, lead, thallium and bismuth (Leung et al., 2012; C. Wu et al., 1986). Besides the drawback of the necessity of using a noble catalyst in ICB, the low energy density is a disadvantage as well (Leung et al., 2012). Furthermore, the electrolytes are unstable at room temperature. Henceforth, during operation either the temperature has to be kept at about 65° C or the accessible capacity of the battery is decreased (Petrov et al., 2021).

A.III. Vanadium-bromine

High costs of VRB triggered research into the potential of vanadium-bromine (V-Br) RFB (VBB), where vanadium is solely used in the negative half-cell. The vanadium in the positive half-cell of VRB is replaced by the redox couple Br_2/Br^-. The reaction equation of VBB is presented below (Soloveichik, 2011).

$$2V^{2+} + Br_2 \leftrightarrow 2V^{3+} + 2Br^-$$

VBB benefits from the same advantages as the VRB. For example, cross contamination is eliminated here as well since the same electrolyte is used for both the catholyte and the anolyte. Also, the energy density is increased because bromine is more soluble resulting in eventually a reduction of 25 percent of the electrolyte volume which is necessary in VRB (Cunha et al., 2015). Therefore, the costs of VRB is reduced by 40 percent for VBB by replacing vanadium with bromine (Soloveichik, 2011). However, the disadvantage experienced with VBB is the potential of formation of bromine vapour. This risk is mitigated by addition of bromine complexing agents, whereby costs are increased. Therefore, VBB are not commercialised as much as VRB is.

A.IV. Polysulfide-bromine

Polysulfide bromine RFB (PSB) consist of a redox reaction between two salt-based electrolytes. The catholyte consists of NaBr whereas the anolyte consists of sodium polysulfide (Na_2S_2), separated by a cation-selective, polymer membrane such as nafion (Argyrou et al., 2018). The reaction equation of PSB is presented here (Fan et al., 2020).

$$2Na_2S_2 + NaBr_3 \leftrightarrow Na_2S_4 + 3NaBr$$

Due to their fast response times, PSB are suitable for power related BESS applications. However, drawbacks experienced by this type of RFB are the complexity of preparation of Na_2S_2 and the potential environmental hazards. When a failure occurs, bromine gas is rejected towards the environment, which is harmful. These negative aspects are slowing down commercialisation of PSB (Argyrou et al., 2018).

B.I. Zinc-air

The advantages of organic aqueous zinc-air (Zn-air) batteries are the abundance of the materials, the low costs and the high safety. Also, the theoretical energy density of Zn-air batteries is four times as high as from Li-ion batteries, namely around 1000 Wh/kg (W.-F. Wu et al., 2023). Zn-air batteries

consist of a Zn anode and an air cathode with a catalyst focused on the oxygen reduction and evolution reactions. The electrolyte is an alkaline solution and because of the ease towards the oxygen reduction and evolution reactions, low-cost non-precious catalyst are sufficient. However, alkaline electrolytes suffer from side reactions. Therefore, efficiency loss happens after certain (dis)charge cycles. Also, dendrite formation in the zinc electrode is a disadvantage since this could cause short circuits (Leung et al., 2012). Research has been done into different types of electrolytes (W.-F. Wu et al., 2023). Currently, this problem limits commercial development of Zn-air batteries (Y. Kumar et al., 2023).

B. II. Semi-solid

A promising but immature organic aqueous RFB is based on the principle of semi-solid FB, of which the scheme is presented in Figure A.14.

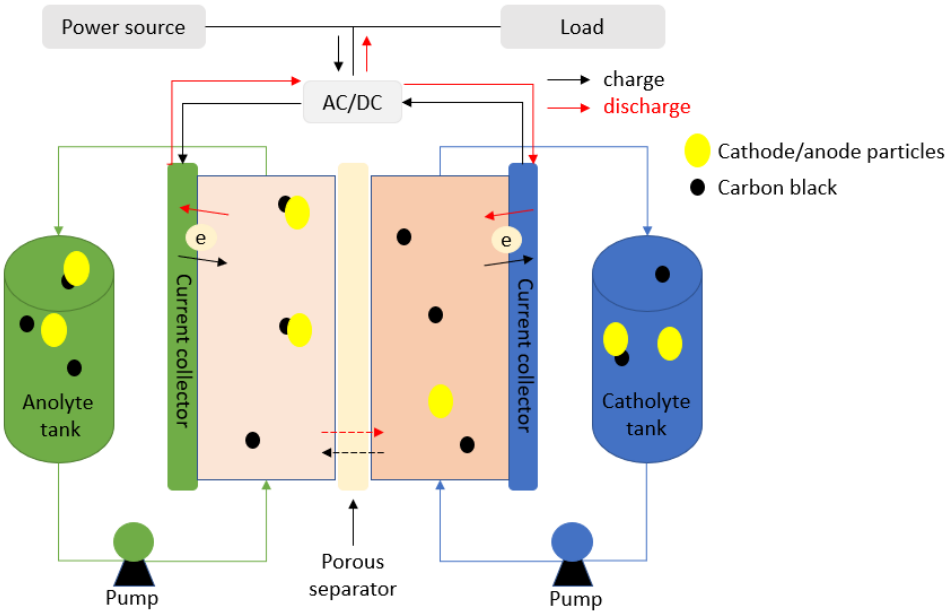

Figure A.14: Scheme of a semi-solid flow battery

The electrolyte is aqueous, so based on water and organic active materials are present inside the solution. The active material particles (presented as yellow dots) are mixed with carbon black particles (presented as black dots). The carbon black particles are high in viscosity. The viscosity has an effect on the work done by the pumps of the battery, which is increased compared to conventional RFB. The active particles are low in electronic conductivity, opposed to the carbon black particles. Therefore, the role of the carbon black particles is to support the active materials to move through the battery, in the watery solution.

The specific material of the active particles can be chosen. An example is a semi-solid RFB with active material particles based on alginates. Alginates are composed of long chains of repeating units of sugar molecules. Transition metal cations can be captured by the alginate chains when the chains are positioned parallel to each other, which is referred to as an egg-box structure, visualised in Figure A.15.

One of the two transition metal oxide ions is iron (Fe), where the oxidation state from the Fe ions can change from Fe^{3+} to Fe^{2+} by accepting an electron. The Fe(III)-Alg is at the negative electrode. Simultaneously, the other transition metal oxide ions are manganese (Mn), where the oxidation state from the Mn ions change upon electron depletion from Mn^{2+} to Mn^{3+}. The Mn(II)-Alg is at the positive electrode. These reactions are reversed during (dis)charging of the system. The advantages of the two active materials are their abundance, low costs and low toxicity (Kelder et al., 2022; Kiriinya et al., 2023).

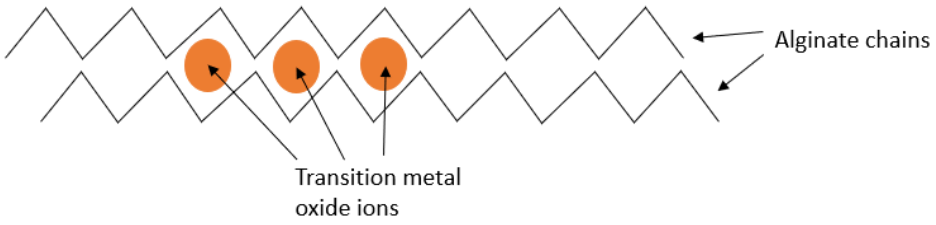

Figure A.15: Simplification of the egg-box structure

Another example of a semi-solid RFB is based on magnesium (Mg) ions. To improve the energy density of the system, Mg ions are used instead of Fe or Mn ions. An implication of this system is the reactivity of Mg with water. A solution has been found by researchers from the Technical University of Delft and Shell, namely by coating the Mg particles and therefore stabilising the system. The coating of the Mg ions is a layer which is transparent for ions and electrons but protective towards water (Kelder et al., 2022).

The remarkable aspect of this type of semi-solid RFB is that it possesses both the advantages of conventional RFB and the additional benefit of being cost-effective and highly safe, thanks to its organic aqueous nature. The drawback however is the maturity of the system. The technology is proven on lab scale and is currently being developed to scale-up. So far, there is no reason not to include these promising systems in the research. The only limitation is the scarcity or lack of available data.

C. Hybrid flow batteries

In HFB, at least one active species of the electrolyte solution is reacting with one of the electrodes during (dis)charging (Soloveichik, 2011). This phenomenon is referred to as electrodeposition (Argyrou et al., 2018). Some advantages of HFB over RFB are the higher energy and power densities as well as the improved efficiency. However, a drawback associated with these improvements is the higher degree of complexity in system design. On the other hand, some advantages of RFB over HFB are their scalability, their long cycle life and their simpler maintenance and replacement. However, RFB suffer from lower energy and power densities and lower energy efficiencies compared to HFB. The HFB which are selected for further analysis are H_2/Br_2 and three Zn negative electrode couples. Advantages of using Zn negative electrodes is their negative standard electrode, high solubility of Zn(II)-ions, fast kinetics as well as the low costs, abundance and recyclability of Zn-compounds (Arenas et al., 2018). However, some drawbacks experienced are their relatively low charging efficiency, difficult uniform Zn electrodeposition and some degree of self-discharge.

C.I. Hydrogen-bromine

The electrochemical performance of hydrogen-bromine HFB (HBB) is promising for grid-scale energy storage due to their high efficiencies at relatively high power densities (Cho et al., 2012). HBB are based on the redox couples Br_2/Br^- and H_2/H^+. HBB is categorised as hybrid because of the two half-reactions, at the negative electrode the standard fuel cell half-reaction takes place whereas at the positive electrode a typical RFB reaction takes place (Petrov et al., 2021). During discharge, the catholyte, existing of a bromine solution (HBr), reacts with H^+ ions provided by the negative side of the cell to become bromide (Br^-). At the negative side of the half-cell, $H_{2(g)}$ is fed and oxidised to H^+ ions. When the battery is being charged by a power source, the reaction reverses and H_2 and Br_2 are formed. The reaction equation is given below (Cho et al., 2012).

$$H_{2(g)} + Br_{2(aq)} \leftrightarrow 2HBr$$

The toxicity of the HBB is however a major drawback. $H_{2(g)}$ as well as $Br_{2(g)}$ are formed which could potentially leak towards the environment, which is toxic. Therefore, the system is rather complex.

C.II. Zinc-bromine

A zinc-bromine HFB (ZBB) consists of a Zn anode and a Br_2 cathode, with a microporous separator. The electrolyte consists of an aqueous solution of $ZnBr_2$. During charge, Zn from the electrolyte solution is

deposited on the Zn electrode surface. At the cathode, Br_2 is converted into Br^- which is consecutively stored in the electrolyte solution. During discharge, the reverse process occurs and Zn is dissolved back into the electrolyte. The reaction chemistry of a ZBB is presented in the reaction equation below (Fan et al., 2020).

$$Zn + Br^-_3 \leftrightarrow ZnBr_2 + Br^-$$

As with ICB, the redox couples exhibit dissimilar electrode kinetics. The Zn/Zn^{2+} couple has much faster electrode kinetics compared to the kinetics of the Br_2/Br^- couple. To compensate for this, the cathode is made of high surface area carbon. Some advantages of ZBB are the high energy density (30-85 Wh/kg), deniable electrode polarisation and low costs. On the other hand, the expensive electrodes, potential Zn dendrite formation during charge, low energy efficiency and low cycle life are considered as disadvantageous (Cunha et al., 2015). Additionally, ZBB are not safe and considered as hazardous for the environment. However, ZBB are being used for load-leveling applications (Soloveichik, 2011).

C.III Zinc-chlorine

The electrolyte of a zinc-clorine (Zn-Cl_2) HFB is composed of a solution of NaCl. The reaction equation is provided below (Soloveichik, 2011). During charging, $Cl_{2(g)}$ is evolved at the positive electrode whereafter it is stored in another chamber by mixing with water to form solid chlorine hydrate. When discharging, Cl_2 is reduced back to the solution state (Khor et al., 2018).

$$Zn + Cl_2 \leftrightarrow ZnCl_2$$

The Zn-Cl_2 HFB has an increased energy density compared to other FB, namely 154 Wh/kg. However, the system requires additional chambers, increasing the costs. Also, $Cl_{2(g)}$ evolution cause energy loss therefore reducing the energy efficiency as well as highly increasing the potential environmental risks (Khor et al., 2018).

C. IV Zinc-cerium

In zinc-cerium HFB (ZCB), the redox couple consists of Zn/Zn^{2+} and Ce^{3+}/Ce^{4+}. In ZCB, the anolyte and catholyte are methane sulfonic acid so both the active species, Ce and Zn are present in this solution as salts, Zn on the negative side of the cell and Ce in the positive half-cell (Xie et al., 2013). Zn deposition and dissolution takes place in acid media at the negative electrode. Conversion of Ce(III) and Ce(IV) takes place at the positive electrode (Arenas et al., 2018). To prevent $H_{2(g)}$ evolution, small amounts of indium or tin are added. With addition of these species, the H_2 overpotential increases (Xie et al., 2013). The chemical reaction of ZCB is presented below (Soloveichik, 2011).

$$Zn^{2+} + 2Ce^{3+} \leftrightarrow Zn + 2Ce^{4+}$$

The potential of ZCB is high because it has the highest theoretical cell voltage among all RFB (ca. 2.50V vs. 1.29V). Under certain electrolyte concentrations, a high voltage could result in a higher cell energy and power (Xie et al., 2013). The main limitation of ZCB are the high costs of the Pt/Ti electrodes which are used and cross-mixing of the electrolyte (Arenas et al., 2018).

Conclusion on flow batteries

FB are being considered as suitable for the hybrid installations as considered in this thesis because of their high cycle life, safety and reliability as well as their flexible design. Compared to conventional secondary batteries, their energy and power densities are lower but their operational window in terms of installed capacity is higher. Because of the scalability and required system space, different types of locations are most suitable. Therefore, both types of batteries are most suitable for different types of hybrid installations.

The selection consists of aqueous inorganic and organic RFB and a HFB. The trade-off between RFB and HFB is based on different energy and power densities and energy efficiencies. With increasing these performance parameters, the complexity of the system increases accordingly. Therefore, both RFB and HFB are suitable for different applications. Regarding the RFB, the inorganic system VRB has reached commercialisation already and the ability for being used for load leveling applications has been proven. Therefore, this system is considered as potential. On the other hand, the less developed organic solid-state RFB have the potential to mitigate some challenges (costs for example)

of the already-known VRB. Since there are no substantial challenges known yet, this type of RFB is assessed as well. Additionally, the HFB which is selected is the ZBB. The safety and physical space concerns are taken into account as well as the ability to be used for load leveling. Therefore, ZBB are included.

B. Shore power

This Appendix focuses on shore power. The Chapter is chronologically organised, first the shore power strategy of the port of Rotterdam (PoR) is explained in Section B.1. Then, important aspects of the development of shore power in the portal area are discussed in Section B.2. Section B.3 elaborates on the current situation regarding the shore power projects in the PoR.

B.1. Shore power strategy

As already mentioned in Chapter 1, the development of shore power is part of the overarching sustainability strategy of the PoR. The roll-out of shore power has made a start already for the inland shipping in the city centre of Rotterdam. The Rotterdam climate agreement has stated that the carbon emissions in Rotterdam must be decreased by 50 percent in 2030 compared to in 2017. The development of shore power in the PoR is therefore supported on a regional level by the municipality of Rotterdam and on an international level as well, as stated in the Fit for 55 package. The shore power strategy from the City of Rotterdam and the PoR takes the deployment to the next step, namely by focusing on providing shore power at berths for sea going vessels (A. Bonte, 2021). The details of the strategy, which is based on three pillars is provided in the following Subsection.

Pillars of the strategy

The shore power strategy is a joint strategy of the Port and City Authorities of Rotterdam and is based on three pillars (A. Bonte, 2021):

Pillar 1
Quality of the living environment is central
When berths are near urban or Natura 2000 areas, shore power makes most impact in terms of improving health circumstances compared to when auxiliary engines are used. The aim is to fit the public berths in those areas with shore power by 2030 and that shore power is used 90 percent of the visits.

Pillar 2
Large steps forward where possible
Within all sea-going vessels, some categories are more easily retrofitted and used for shore power. Also, bigger vessels using shore power makes more impact. Examples are RoRo, ferry, cruise and container vessels. The aim is to use shore power for more than 90 percent of the visits of roll-on/roll-off (RoRo), offshore, ferry and cruise vessels and for at least 50 percent of the visits of ultra large container vessels (i.e. > 10000 twenty-foot-equivalent unit) by 2030.

Pillar 3
Encouraging innovation and standardisation where necessary
For the categories of sea-going vessels for which retrofitting or using shore power is less easy, the PoR strives to actively support innovation and standardisation. The more complex segments are liquid bulk and dry vessel. Most results are achieved here when international collaboration takes place.

To translate the strategy into action, a development program has been set up with the aim of breaking through the economic challenges of shore power as explained in Chapter 2. The goal of the development program is to achieve a viable business case both from the perspective of vessel owner as well as from the port operator. To achieve the goal, subsidies are still be required to create the incentive for investing in shore power.

Within the development program, Rotterdam Shore Power B.V. (RSP) is established and collaboration between the port and RSP is indispensable. RSP is a joint venture between the PoR and Eneco, both owning 50 percent of the shares. RSP provides shore power as a service whereby RSP devel-

ops, invests and operates shore power installations for terminals in ports. With the arrival of RSP, the development of shore power is expected to be accelerated in an efficient manner.

B.2. Shore power development

It is of importance to take into account both the ship-side and the shore-side aspects by designing and developing shore power projects. Regarding the ship-side aspects, there are two variables (not taking the technology into account yet). First, the type of vessels which are berthing at the specific location and second the occupancy per vessel type per period of time. Since the PoR is the biggest port in Europe, all different categories of sea-going vessels are present at berths. All the different types of vessels have different requirements in terms of onboard electricity usage when berthing. For example, cruise ships have a high electricity demand to provide hotelling services whereas ferries require less electricity when berthing. In addition, the occupancy of the berths depends on the vessel types which are berthing as well. Both the frequency and berthing time must be considered here. Some vessel types are frequently visiting the berths in the port and their schedule is exactly known for over a long period of time whereas other vessel types are visiting the port less frequent.

From the shore-side perspective, the specifications of the terminal have to be taken into account. Physically, the space which is available is important as well as the availability of a connection to the electricity grid. The challenges imposed by grid congestion are explained next. Contractually, terminals can be owned either by the PoR or by clients of the PoR. In the latter case, development of shore power is generally more complicated since there are more stakeholders involved.

Grid congestion

The electricity grid in and around the portal area of Rotterdam is experiencing an increasing demand of customers wanting to connect to the grid. The capacity limit of the grid is within reach and even already reached at some locations. Therefore, at these locations it is already impossible for customers to acquire a connection to the congested grid. As a result, some customers submit their request to connect to the grid prior to the moment they actually need the connection. This diminishes the chances for new customers to obtain a connection. At some locations in the PoR, grid congestion is limiting the development of for example shore power.

The grid congestion problem can be mitigated in two ways. First, the capacity of the grid can be expanded, which is executed by the grid operator Stedin. Expansion does not happen on a short-term basis since this requires a very detailed planning as well as imposes high costs. Since there is need for a short term solution in order to electrify the portal area as soon as possible, the existing capacity needs to be managed strategically in order to optimise its utilisation.

The capacity of a connection to the grid is calculated based on the peak demand of the application. However, an application does not reach its peak demand very often during a year. A solution would therefore be to either provide the connection with a smaller capacity than the peak capacity or to provide the connection with the peak capacity but not for the full year. In both cases the connection can be used most of the times except for the moments the capacity is reaching the limit or when the connection is not active. When the limit or inactivity is known beforehand and the demand could be pre-scheduled, the application can anticipate on the moment of no electricity supply by either being turned off or using a BESS or conventional power supply for example.

It should be noted that the latter solution provided above is not possible for all applications in the portal area. Industrial processes running on electricity can not be curtailed for some period, whereas shore power installations ofcourse can, especially when a BESS is present.

B.3. Shore power projects

In the portal area of Rotterdam, shore power projects in various phases are recognised. Currently, there are already several locations in the port area that are using shore power. In addition, there are some locations where shore power is not yet installed but already contracted and there are also projects which are in the research phase. This Section covers the existing projects in the different

phases based on different types of vessels. To generate realistic and helpful results for the PoR, this thesis solely focuses on shore power projects that are in one of the three phases and excludes berthing locations where shore power has not yet been considered.

Cruises

The PoR has one cruise terminal which is located at the Wilhelminakade. Cruise vessels are large passenger ships created for recreation and leisure, travelling between destinations around the world. Cruise vessels typically operate on planned itineraries, visiting multiple ports of call during a single voyage. The vessels provide hotelling services to passengers during their stay onboard. The size of the vessels can vary.

Cruise Port Rotterdam

The Wilhelminakade connects the PoR to the city centre of Rotterdam since the cruise visitors play a significant role in the city's tourism and because of the location of the terminal which is near the urban area. Because of the location as well as because of the fact that cruises use a lot of electricity while berthing, the impact of using shore power is significant and therefore the shore power strategy has a focus here. A visualisation of the terminal is shown in Figure B.1 and the location on a map is shown in Figure B.8.

Figure B.1: The cruise terminal with the AIDA cruise at berth (PortofRotterdam, 2023)

The cruise terminal is owned by a subsidiary company of the PoR, a client of which the PoR is 100 percent shareholder, Cruise Port Rotterdam. The decision to implement shore power has already been made and the design and subsequently the implementation is planned to start in the near future. The shore power installation is expected to be operational in the third quarter of 2024. The client has shown interest in the addition of a BESS to the shore power installation to enhance economic viability.

Ferries

Multiple ferry companies are located in the portal area. Ferries are used to transport trucks and people with their cars through Europe. According to Bonte, ferries are a promising vessel category for shore power since they have line services (A. Bonte, 2021). Simultaneously, the line services are a reason why implementation of a battery at a ferry shore power installation is expected to enhance the economic viability by optimised (dis)charging and energy arbitrage. The two ferry companies which are already using shore power and in the research phase are Stena Line and P&O Ferries, respectively.

Stena Line

Stena Line is one of the world's largest ferry companies, operating RoRo and RoRo passenger (RoPax) vessels. RoRo vessels are used to im- or export cars or trucks between destinations whereas RoPax vessels are also transporting passengers (A. Bonte, 2021). Stena Line owns a terminal in the Hook of Holland in the PoR, which is visualised on the map in Figure B.8. Another terminal is owned by Stena Line solely designated for freight transport. Since there is no clear vision on the development of shore power here, this terminal is not considered as a shore power project and therefore not mentioned in

the remainder of this thesis.

Stena Line is committed to be actively involved in the energy transition and therefore Stena Line already uses shore power at the berth of the ferry in Hook of Holland since 2012 (ABB, 2012). Since the berth is near an urban area, the impact is significant. The fact that Stena Line both owns the vessels as well as the terminal caused the rapid implementation of shore power. The economic risks of both perspectives were mitigated by subsidies and because of the fact that the vessels and the terminals simultaneously were retrofitted. Also, the economic viability of both perspectives is shared by Stena Line, simplifying the business case. The connection from shore-to-ship is visualised in Figure B.2.

Figure B.2: The cable connection between shore and ship at the Stena Line ferry terminal in the Port of Rotterdam (AMP, 2012)

P&O Ferries

P&O Ferries is also a ferry operating company which is based in the PoR. P&O Ferries connects several destinations in Europe with each other by their ferry routes. In terms of fleet, P&O Ferries and Stena Line are similar. Also, P&O Ferries is owner of both the terminal as well as of the ferries. The dissimilarities are not considered as important for this study since this is in their market position and company structure. The location of P&O Ferries' terminal is presented in Figure B.8.

P&O Ferries has shown its interest towards deployment of a shore power installation on their terminal, however the problem of grid congestion is the bottle neck in this shore power project. The grid does not have enough capacity at that specific location to provide the connection of the terminal with the peak load during 365 days a year. Currently solutions are being analysed whether the connection could be provided with either less capacity or with the peak load for less days than a full year.

Container vessels

Since the PoR is an international hub for importing and exporting goods, container vessels comprise a significant portion of the total number of vessels entering and leaving the PoR. Many companies located in the PoR are part of the network of transporting goods and therefore are operating container terminals. At the terminals, container vessels are able to berth. Subsequently, their containers are off- and on-loaded before they continue their route at sea. Most container terminals are located at the Maasvlakte but they are located at the Eemhaven and the Waalhaven as well. The terminals and container vessels are owned by two distinct parties, complicating the roll-out of shore power. The three locations are shown on the map in Figure B.3.

This thesis focuses on the container terminals at the Maasvlakte only. The reason is based on the increased exploration of shore power utilisation in this area compared to the in the Waalhaven and Eemhaven. The increased exploration of shore power is attributed to the impact of shore power installations which is more significant at the Maasvlakte compared to at the Waalhaven and the Eemhaven. The impact is correlated with the amount and the size of vessels at the berths in the terminals. As can be seen from the map, the Maasvlakte is easier accessible for (large) container vessels. As a result, the berths in the Maasvlakte area experience the presence of many more and larger ships. Despite

Figure B.3: Location on the map of the container terminals in the port of Rotterdam

the fact that this thesis focuses on the Maasvlakte regarding container terminals and shore power, it does not mean that there are no shore power ambitions and plans in the other container terminals in the Waalhaven and Eemhaven.

Maasvlakte

The Maasvlakte consists of two parts, Maasvlakte 1 and Maasvlakte 2. They differentiate from each other in their moment of construction since Maasvlakte 1 is constructed in 1960 whereas the construction of Maasvlakte 2 was finished in 2013. Both areas were designed and subsequently constructed to accommodate for the increasing demand of containers to reach the port. During design and construction of Maasvlakte 2 there was awareness for the ongoing energy transition and therefore this area is strongly focused on sustainability. According to this, various shore power projects are in the research phase in the Maasvlakte area. Figure B.4 provides an overview of the existing terminals in the Maasvlakte area and Table B.5 presents the legend of the names of the terminals associated with the numbers on the map. The colours associated with the terminals on the map are based on the operating company. The blue, black, green and red terminals are operated by ECT, Rotterdam World Gateway, APM and Kramer respectively. The map is reconstructed based on maps provided by (A.H.Gharehgozli, 2016; Q. Hu & Lodewijks, 2019).

Figure B.4: Container terminals in the Maasvlakte area

Number	Terminals
1	ECT Euromax Terminal
2	APM Terminals Maasvlakte 2
3	Rotterdam World Gateway
4	APM Terminals Maasvlakte 1
5	ECT Delta Terminal
6	ECT Delta Barge Terminal
7	Kramer Barge Center Hartelhaven
8	Kramer Delta Depot
9	Van Doorn Container Depot

Figure B.5: Legend of the terminals associated with the numbers on the map

DNV has written a report for PoR, examining the readiness of container vessels towards receiving shore power, their power and energy demand at Maasvlakte terminals and the possible impact of new fuels on the power and energy demand (DNV, 2022). The energy demand of container vessels berthing at the Maasvlakte was found to be 170 GWh/year in 2021, which is expected to increase to 220 GWh/year by 2030. The impact of shifting the provision of the demanded energy from auxiliary engines to shore power is therefore significant. Besides the fact that the container vessels represent a large amount of the total demanded electricity in the PoR, the newest ultra large container vessels have the potential to be most shore power ready among all vessels. This can be explained by the size of the vessel, the capital costs of retrofitting the ship per volume or weight decreases with an increasing vessel size. Therefore, the shore power strategy focuses on the segment of container vessels, which is recognised in the second pillar of the shore power strategy, as explained in Appendix B.1.

By considering shore power implementation at the Maasvlakte, two important aspects have to be kept in mind. First, the capacity of the grid is reaching limit in the Maasvlakte area so possible grid congestion should be taken into consideration when designing shore power installations here. However, this is the responsibility of the terminal operators and is therefore not considered for the remainder of this thesis. Second, the fact that the vessel owners are different parties than the terminal owners and the fact that the terminal owners are clients of the PoR, complicates the development of shore power at the Maasvlakte. The complexity results in the problem whether the PoR or terminal owners should invest in shore power installations. Since this is beyond the scope of this research, this is not considered for the remainder of this thesis.

Offshore vessels

In the PoR there are also berths designated for off-shore vessels. After being operational offshore for a period of time, the vessel returns to the port and stays at berth. During berthing, the crew and equipment which is unnecessary for the upcoming stay offshore are unloaded and the vessel is prepared for the next journey. When required, this is the opportune time for vessel maintenance. Among the offshore vessel terminals, the most known shore power project is for Heerema Marine Contracters (HMC). Other offshore terminals are not considered here as their shore power ambitions are not far enough yet.

Heerema Marine Contracters

HMC owns multiple offshore vessels of which the Sleipnir and the Thialf have their berthing stations at the Landtong Rozenburg (Contractors, 2023). The terminal has a similar construction as Stena Line has, namely ownership of both the terminal and the vessel. Therefore, shore power has already been installed here as well. The project was realised by RSP. The shore power installation can be seen in Figures B.6 and B.7.

Figure B.6: Front view of the shore power installation of Heerema's offshore vessels Thialf and Sleipnir in Landtong Rozenburg

Figure B.7: Side view of the shore power installation of Heerema's offshore vessels Thialf and Sleipnir in Landtong Rozenburg

Figure B.8: Location on the map of the Stena Line, P&O Ferries, Heerema's offshore and Cruise Terminals in the port of Rotterdam

Remaining berths

In addition to the berths mentioned above, all of which serve as berths for a specific type of vessel, there are also remaining berths intended for various types of vessels. To be specific, all types of vessels are allowed at those remaining berths for different purposes such as for waiting to enter the portal area or for vessel maintenance. Remaining berths are operated and owned by the PoR, simplifying the business case for developing shore power. This Subsection focuses on remaining berths near urban areas, for example the Lloydkade and the Parkkade.

Lloydkade and Parkkade

The location of the Lloydkade and Parkkade are shown on the map visualised in Figure B.9.

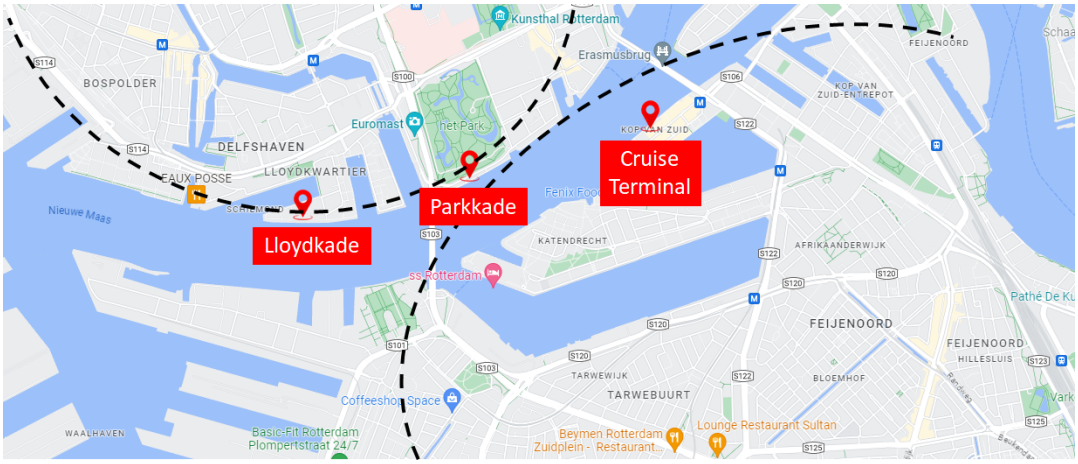

Figure B.9: Location on the map of the Lloydkade, Parkkade and the Cruise Terminal, urban areas fall within the area marked with a dashed line

Since the berths are really close to urban areas, there are clear ambitions of deploying shore power at these berths to facilitate the vessels which are either waiting or in maintenance with electricity. The occupancy of these berths varies and therefore the impact in terms of emission reduction is expected to be smaller compared to berths intended for specific vessels.

C. Additional results

This Appendix contains results which are additional to the findings which are discussed in Chapter 5. The results are of importance for the full explanation of the research, but less important to correctly formulate the conclusion. Therefore, these additional findings are presented here. First, the additional results of the EMS algorithm are presented in Section C.1. Then, the additional results accompanied by the total battery systems costs are explained in Section C.2. Section C.3 includes additional results of the analysis of the net present values (NPV) of the various hybrid installations. Lastly, Section C.4 provides additional results of the sensitivity analysis.

C.1. Energy management strategy algorithm

This Section presents the additional results of section 5.1. First, the yearly number of cycles and the total annual profit for each type of BESS at the Stena Line Terminal is shown. Then, the same results but for the Cruise Port Terminal are shown.

Stena Line Terminal

First, the yearly number of cycles are explained, then the annual profit is elaborated on. Both for the four types of BESS considered, LA refers to lead-acid.

Yearly number of cycles

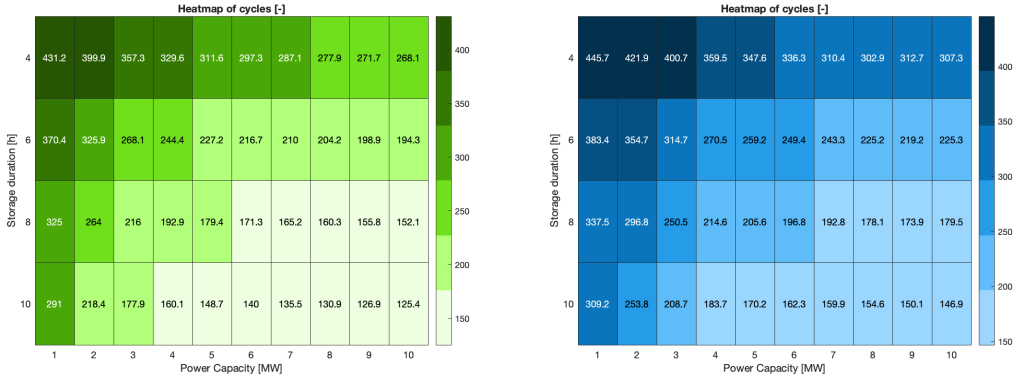

(a) Lithium iron phosphate (LFP) batteries

(b) Lead-acid (LA) batteries

Figure C.1: Heat maps depicting the number of yearly cycles of LFP and LA for various energy capacities with colors for the Stena Line Terminal in 2022

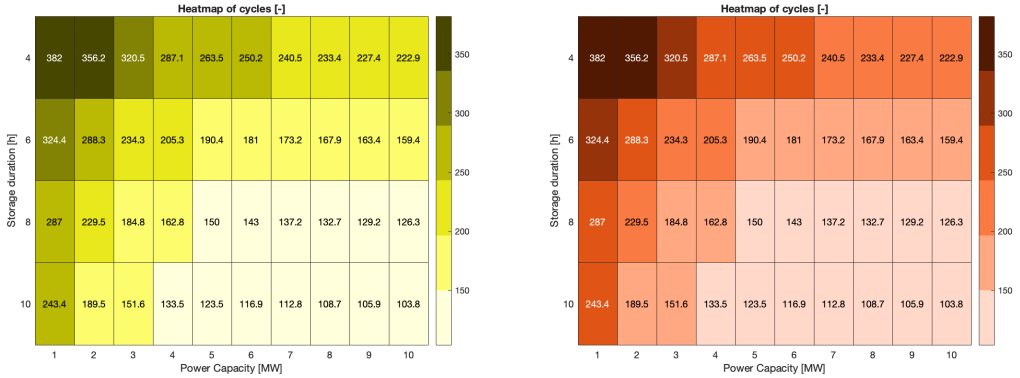

(a) Vanadium redox flow batteries (VRB) **(b)** Zinc bromine hybrid flow batteries (ZBB)

Figure C.2: Heat maps depicting the number of yearly cycles of VRB and ZBB for various energy capacities with colors for the Stena Line Terminal in 2022

Total annual profit

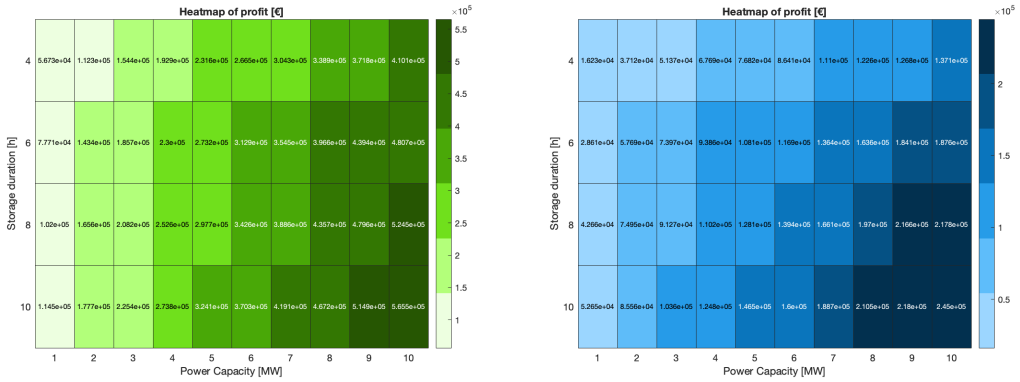

(a) Lithium iron phosphate (LFP) batteries **(b)** Lead-acid (LA) batteries

Figure C.3: Heat maps depicting the total annual profit of LFP and LA batteries for various energy capacities with colors for the Stena Line Terminal in 2022

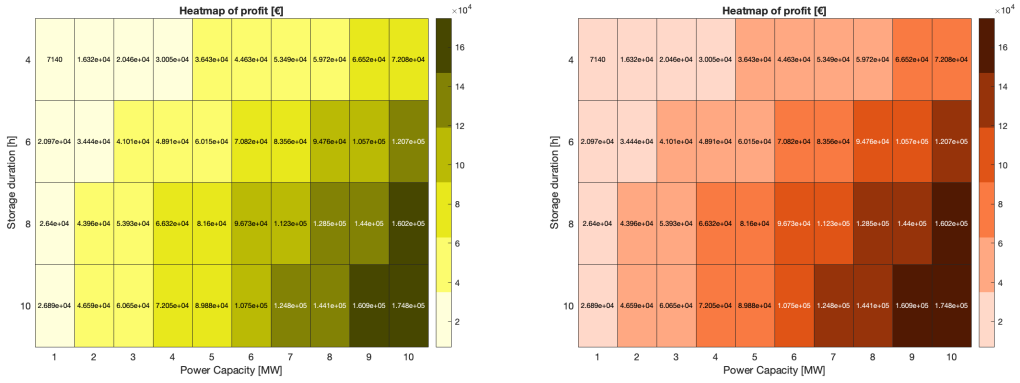

(a) Vanadium redox flow batteries (VRB) **(b)** Zinc bromine hybrid flow batteries (ZBB)

Figure C.4: Heat maps depicting the total annual profit of VRB and ZBB for various energy capacities with colors for the Stena Line Terminal in 2022

Cruise Port Terminal

First, the yearly number of cycles are explained, then the annual profit is elaborated on. Both for the four types of BESS considered. LA refers to lead-acid.

Yearly number of cycles

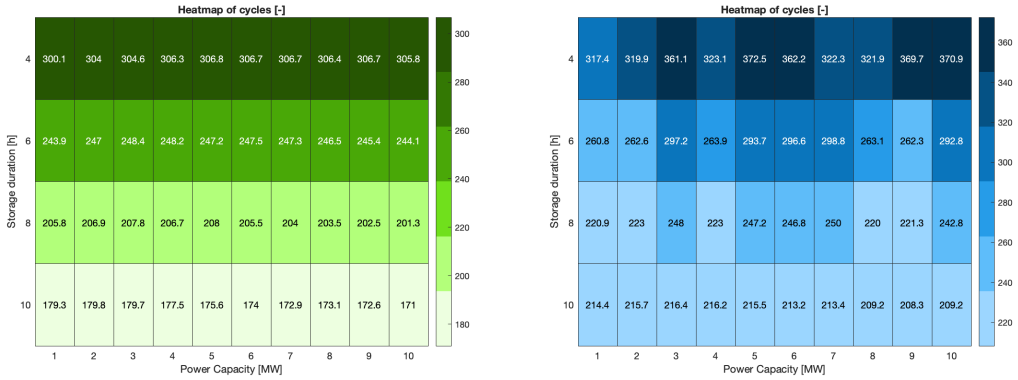

(a) Lithium iron phosphate (LFP) batteries

(b) Lead-acid (LA) batteries

Figure C.5: Heat maps depicting the number of yearly cycles of LFP and LA batteries for various energy capacities with colors for the Cruise Port Terminal in 2022

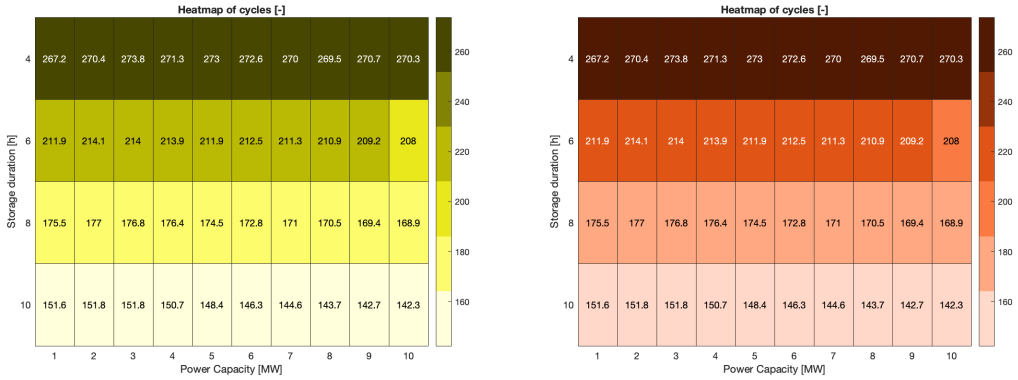

(a) Vanadium redox flow batteries (VRB)

(b) Zinc bromine hybrid flow batteries (ZBB)

Figure C.6: Heat maps depicting the number of yearly cycles of VRB and ZBB for various energy capacities with colors for the Cruise Port Terminal in 2022

Total annual profit

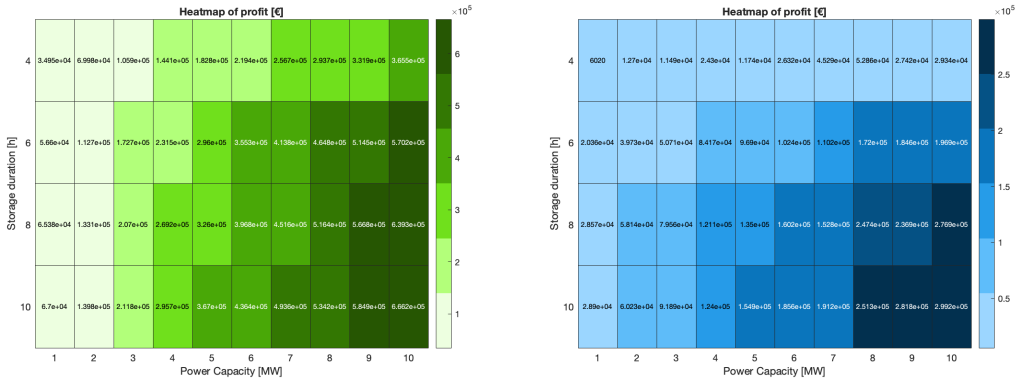

(a) Lithium iron phosphate (LFP) batteries **(b)** Lead-acid (LA) batteries

Figure C.7: Heat maps depicting the total annual profit of LFP and LA batteries for various energy capacities with colors for the Crusie Port Terminal in 2022

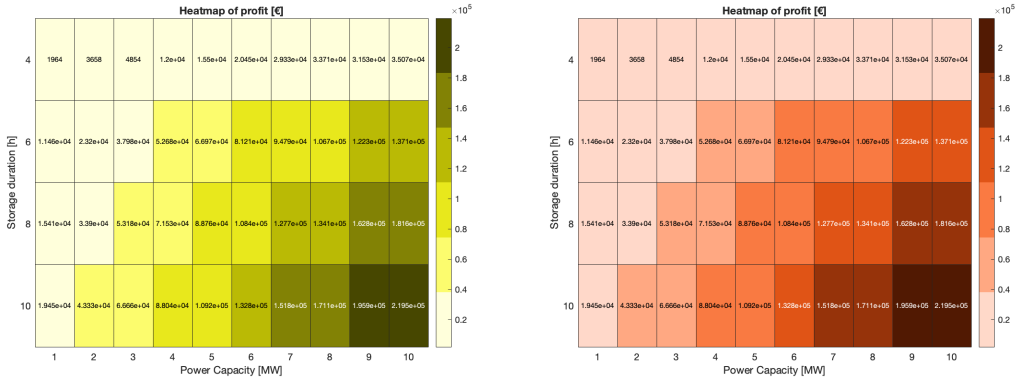

(a) Vanadium redox flow batteries (VRB) **(b)** Zinc bromine hybrid flow batteries (ZBB)

Figure C.8: Heat maps depicting the total annual profit of VRB and ZBB for various energy capacities with colors for the Cruise Port Terminal in 2022

C.2. Battery energy storage system costs

This Section offers additional material of the results of the cost analysis of the various sorts of BESS.

Initial capital expenditure

The *CAPEX initial* cost component data which is extracted from the Excel model and which is used to create the Figures in Section 5.2, is presented in Tables C.1, C.2, C.3 and C.4.

Table C.1: Initial capital expenditure in terms of energy [€/kWh] for LFP 4 and 6 hour batteries of power capacities 1 and 10 MW in 2020 and 2030, data retrieved from (Mongird, Viswanathan, Alam, et al., 2020; Viswanathan et al., 2022)

Power	**1 MW**	**1 MW**	**10 MW**	**10 MW**	**1 MW**	**1 MW**	**10 MW**	**10 MW**
Duration	**4 hr**	**6 hr**	**4 hr**	**6 hr**	**4 hr**	**6 hr**	**4 hr**	**6 hr**
Parameter	**2020**	**2020**	**2020**	**2020**	**2030**	**2030**	**2030**	**2030**
Storage block	182	181	174	172	109	108	104	103
Storage balance of system	42	41	40	39	30	29	28	27
Power equipment and c&c	31	21	20	13.5	25	17	17	11
EPC	111	106	103	99	86	81	79	75
Project development	73	70	67	65	60	57	55	53
Grid integration	8	5	6	4	6	4	5	3
CAPEX	**447**	**424**	**411**	**393**	**317**	**296**	**288**	**273**

Table C.2: Initial capital expenditure in terms of energy [€/kWh] for LA 4 and 6 hour batteries of power capacities 1 and 10 MW in 2020 and 2030, data retrieved from (Mongird, Viswanathan, Alam, et al., 2020; Viswanathan et al., 2022)

Power	**1 MW**	**1 MW**	**10 MW**	**10 MW**	**1 MW**	**1 MW**	**10 MW**	**10 MW**
Duration	**4 hr**	**6 hr**	**4 hr**	**6 hr**	**4 hr**	**6 hr**	**4 hr**	**6 hr**
Parameter	**2020**	**2020**	**2020**	**2020**	**2030**	**2030**	**2030**	**2030**
Storage block	180	180	171	171	167	167	159	159
Storage balance of system	41	41	39	39	38	38	37	37
Power equipment and c&c	49	33	35	24	40	27	30	20
EPC	99	95	93	89	82	78	76	73
Project development	67	64	62	59	55	52	51	49
Grid integration	8	5	6	4	6	4	5	3
CAPEX	**444**	**418**	**407**	**386**	**389**	**366**	**357**	**341**

Table C.3: Initial capital expenditure in terms of energy [€/kWh] for VRB 4 and 6 hour batteries of power capacities 1 and 10 MW in 2020 and 2030, data retrieved from (Mongird, Viswanathan, Alam, et al., 2020; Viswanathan et al., 2022)

Power	**1 MW**	**1 MW**	**10 MW**	**10 MW**	**1 MW**	**1 MW**	**10 MW**	**10 MW**
Duration	**4 hr**	**6 hr**	**4 hr**	**6 hr**	**4 hr**	**6 hr**	**4 hr**	**6 hr**
Parameter	**2020**	**2020**	**2020**	**2020**	**2030**	**2030**	**2030**	**2030**
Storage block	289	257	275	245	231	205	220	196
Storage balance of system	58	51	55	49	40	36	38	34
Power equipment and c&c	49	33	35	24	40	27	30	20
EPC	118	104	109	96	97	86	90	79
Project development	80	71	73	65	66	58	60	53
Grid integration	8	5	6	4	6	4	5	3
CAPEX	**602**	**521**	**554**	**483**	**481**	**416**	**443**	**385**

Table C.4: Initial capital expenditure in terms of energy [€/kWh] for ZBB 4 and 6 hour batteries of power capacities 1 and 10 MW in 2020 and 2030, data retrieved from (Mongird, Viswanathan, Alam, et al., 2020; Viswanathan et al., 2022)

Power	**1 MW**	**1 MW**	**10 MW**	**10 MW**	**1 MW**	**1 MW**	**10 MW**	**10 MW**
Duration	**4 hr**	**6 hr**	**4 hr**	**6 hr**	**4 hr**	**6 hr**	**4 hr**	**6 hr**
Parameter	**2020**	**2020**	**2020**	**2020**	**2030**	**2030**	**2030**	**2030**
Storage block	364	308	329	293	311	277	296	263
Storage balance of system	95	85	90	80	76	68	72	64
Power equipment and c&c	31	21	20	14	25	17	17	11
EPC	100	95	93	89	77	73	71	68
Project development	66	63	60	59	54	51	50	48
Grid integration	8	5	6	4	6	4	5	3
CAPEX	**620**	**554**	**574**	**516**	**537**	**478**	**498**	**446**

Replacement capital expenditure

Table C.5: Replacement capital expenditure in terms of energy [€/kWh] for LFP, lead-acid, VRB and ZBB 4 and 6 hour batteries of power capacities 1 and 10 MW in 2020 and 2030

Power	**1 MW**	**1 MW**	**10 MW**	**10 MW**	**1 MW**	**1 MW**	**10 MW**	**10 MW**
Duration	**4 hr**	**6 hr**	**4 hr**	**6 hr**	**4 hr**	**6 hr**	**4 hr**	**6 hr**
Parameter	**2020**	**2020**	**2020**	**2020**	**2030**	**2030**	**2030**	**2030**
LFP	61	61	58	58	18	18	17	17
Lead-acid	271	271	258	258	80	80	76	76
VRB	0	0	0	0	0	0	0	0
ZBB	0	0	0	0	0	0	0	0

Total capital expenditure

Table C.6: Total capital expenditure in terms of energy [€/kWh] for LFP, lead-acid, VRB and ZBB 4 and 6 hour batteries of power capacities 1 and 10 MW in 2020 and 2030

Power	**1 MW**	**1 MW**	**10 MW**	**10 MW**	**1 MW**	**1 MW**	**10 MW**	**10 MW**
Duration	**4 hr**	**6 hr**	**4 hr**	**6 hr**	**4 hr**	**6 hr**	**4 hr**	**6 hr**
Parameter	**2020**	**2020**	**2020**	**2020**	**2030**	**2030**	**2030**	**2030**
LFP	508	485	469	450	334	314	305	289
Lead-acid	715	689	665	644	469	447	434	417
VRB	602	521	554	483	481	416	443	385
ZBB	620	554	574	516	537	478	498	446

Operational capital expenditure

Table C.7: Operational expenditure learning rates between 2020 and 2030 for LFP, lead-acid, VRB and ZBB

Battery type	**Learning rate**	**Unit**
LFP	3.4	percent
Lead-acid	1.3	percent
VRB	2.22	percent
ZBB	1.43	percent

Table C.8: Operational expenditure in terms of energy [€/kWh-yr] for LFP, lead-acid, VRB and ZBB 4 and 6 hour batteries of power capacities 1 and 10 MW in 2020 and 2030

Power Duration Parameter	1 MW 4 hr 2020	1 MW 6 hr 2020	10 MW 4 hr 2020	10 MW 6 hr 2020	1 MW 4 hr 2030	1 MW 6 hr 2030	10 MW 4 hr 2030	10 MW 6 hr 2030
LFP	1.9	1.8	1.8	1.7	1.4	1.3	1.2	1.2
Lead-acid	1.9	1.8	1.7	1.7	1.7	1.6	1.5	1.5
VRB	2.6	2.2	2.4	2.1	2.1	1.8	1.9	1.7
ZBB	12.4	11.1	11.5	10.3	10.7	9.6	10.0	8.9

Decommissioning costs

Table C.9: Decommissioning costs in terms of energy [€/kWh-yr] for LFP, lead-acid, VRB and ZBB 4 and 6 hour batteries of power capacities 1 and 10 MW in 2020 and 2030 for industrial and urban locations

Power Duration Parameter	1 MW 4 hr 2020	1 MW 6 hr 2020	10 MW 4 hr 2020	10 MW 6 hr 2020	1 MW 4 hr 2030	1 MW 6 hr 2030	10 MW 4 hr 2030	10 MW 6 hr 2030
LFP industrial	113	108	105	101	86	81	79	75
LFP urban	125	119	116	111	95	89	87	83
Lead acid industrial	99	95	93	89	82	78	76	73
Lead acid urban	109	105	102	98	90	86	84	80
VRB industrial	118	104	109	96	97	86	90	79
VRB urban	130	114	120	106	107	95	99	87
ZBB industrial	100	95	93	89	77	73	71	68
ZBB urban	110	105	102	98	85	80	78	74

End of life value

Table C.10: End of life value in terms of energy [€/kWh-yr] for LFP, lead-acid, VRB and ZBB 4 and 6 hour batteries of power capacities 1 and 10 MW in 2020 and 2030

Power Duration Parameter	1 MW 4 hr 2020	1 MW 6 hr 2020	10 MW 4 hr 2020	10 MW 6 hr 2020	1 MW 4 hr 2030	1 MW 6 hr 2030	10 MW 4 hr 2030	10 MW 6 hr 2030
LFP	32	32	30	30	99	98	94	93
Lead-acid	63	63	60	60	29	29	28	28
VRB	167	149	159	142	134	119	127	113
ZBB	157	139	149	132	141	125	134	119

Total system costs

Table C.11: Total system costs in terms of energy [€/kWh-yr] for LFP, lead-acid, VRB and ZBB 4 and 6 hour batteries of power capacities 1 and 10 MW in 2020 and 2030 for industrial and urban locations

Power Duration Parameter	1 MW 4 hr 2020	1 MW 6 hr 2020	10 MW 4 hr 2020	10 MW 6 hr 2020	1 MW 4 hr 2030	1 MW 6 hr 2030	10 MW 4 hr 2030	10 MW 6 hr 2030
LFP industrial	546	521	504	484	342	320	311	294
LFP urban	549	524	507	486	344	322	313	296
Lead acid industrial	741	713	688	666	497	473	460	442
Lead acid urban	744	716	691	668	500	475	462	444
VRB industrial	610	499	560	487	488	422	448	390
VRB urban	613	530	563	490	490	424	451	392
ZBB industrial	707	634	654	590	608	543	563	506
ZBB urban	710	637	657	593	611	545	565	508

C.3. Net present value

This Section offers additional material of the results of the NPV analysis of the four hybrid installations which are considered, namely the shore power installations at the Stena Line Terminal and the Cruise Port Terminal, both with an LFP and VRB BESS.

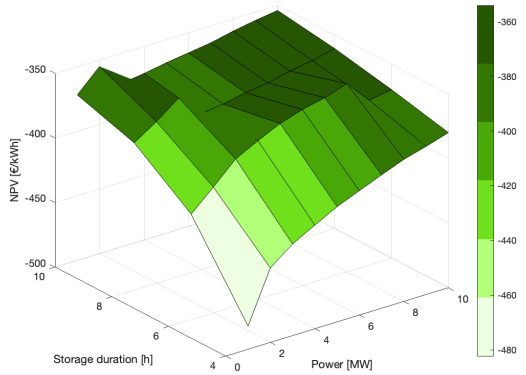

Figure C.9: Net present value per unit of energy [€/kWh] for various sizes of LFP batteries at the Stena Line Terminal

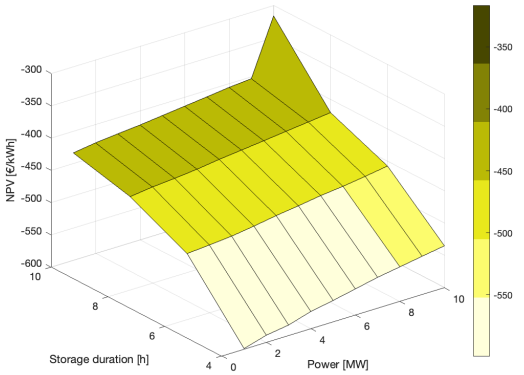

Figure C.10: Net present value per unit of energy [€/kWh] for various sizes of VRB batteries at the Stena Line Terminal

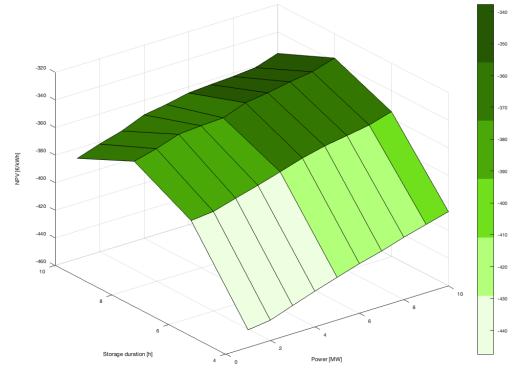

Figure C.11: Net present value per unit of energy [€/kWh] for various sizes of LFP batteries at the Cruise Port Terminal

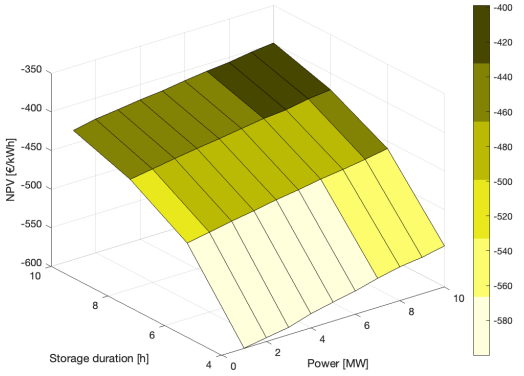

Figure C.12: Net present value per unit of energy [€/kWh] for various sizes of VRB batteries at the Cruise Port Terminal

C.4. Sensitivity analyses

This Section consists of two parts. First in Subsection C.4, the input parameters of the EMS algorithm and the costs model are presented in order to select the most impacting parameters for the sensitivity analyses, which is provided in Section 5.4. Then, Subsection C.4 provides an overview of the sensitivity percentages which are provided throughout Section 5.4.

Input parameters

This Section contains a categorised list of the input parameters of hybrid installations, presented in Table C.12.

Table C.12: Categorised list of input parameters of hybrid installations for sensitivity analyses

Dependence	EMS parameters	Unit	Excel parameters	Unit
Time	RTE	[%]	Cost data, RTE, cycle life	[€/kWh, %, -]
	DAM	[€/MWh]		
	Renewable energy connection	[%]		
	Conversion rate	[$/€]		
Choice	BESS functionalities	[-]	Discount rate r	[%]
	T	[€/MWh]		
	$SoE_{initial}$	[MWh]		
	$P_{bat,t0}$	[€/MWh]		
Fixed	DoD	[%]	DoD	[%]
	Shore power demand	[MWh]	Location factor	[-]
			N	[years]
			Deg	[%]
			OPEX	[€/kWh]

The various parameters are analysed and a decision is being made on which parameters are going to be focused on in the sensitivity analyses and which parameters are not, based on their expected effect on the resulting NPV. The category of fixed parameters does not change over time or by choice and is obtained through literature or facts. Therefore, these parameters will not be the focus of the sensitivity analyses.

Secondly, the time-dependent EMS parameter RTE is going to be focused on in the sensitivity analyses, simultaneously with the cost data, RTE and cycle life input of Excel. Additionally, the DAM and percentage of renewable energy connection EMS input parameters are analysed in the sensitivity analyses as well. The EMS input parameter conversion rate and the Excel input parameter dutch electricity price are not examined in the sensitivity analyses since these parameters are inherently unpredictable and their outcomes wouldn't carry much significance.

Then, the choice-dependent EMS input parameters $SoE_{initial}$ and $P_{bat,t0}$ are not affecting the output significantly. The choice-dependent Excel input parameter r is not taken into consideration either, since this is the required ROI of the PoR. On the other hand, the remaining choice-dependent EMS input parameters BESS functionalities and T are going to be the focused on in the sensitivity analyses.

In addition to the input parameters listed in the table, certain parameters have already been evaluated during the course of this research. These parameters include the size of the BESS (energy and power capacities and storage duration), the BESS type, and the shore power installation location. Each combination of these parameters leads to a different hybrid installation. Therefore, every iteration of the sensitivity analyses will be performed for all four unique hybrid installations.

Summary of results

This section provides an overview of the resulting sensitivity percentages to the various analyses of which the results are explained in Section 5.4. The overview is presented in Table C.13.

Table C.13: Overview of sensitivity percentages of the net present value of four hybrid installations

Parameter	Unit	LFP SL	VRB SL	LFP CP	VRB CP
2020 NPV sensitivity to base year 2030	[%]	51.4	24.2	42.5	23.5
2020 NPV sensitivity 2022 DAM to 2021 DAM	[%]	-20.5	-2.7	-4.1	-4.5
2020 NPV sensitivity 2022 DAM to 2023 I DAM	[%]	19.4	12.7	36.4	23.4
2020 NPV sensitivity 2022 DAM to 2023 II DAM	[%]	17.4	16.3	33.9	22.3
2020 NPV sensitivity 0 to 50% RES	[%]	55.4	50.6	50.3	45.7
2020 NPV sensitivity 0 to 100% RES	[%]	110.7	98.6	100.5	90.0
2030 NPV sensitivity 0 to 50% RES	[%]	112.6	64.2	86.3	57.5
2030 NPV sensitivity 0 to 50% RES	[%]	225.1	128.3	172.6	115.0
2020 NPV sensitivity to consumer energy arbitrage	[%]	8.5	3.6	0.9	3.2
2020 NPV sensitivity to wholesale energy arbitrage	[%]	7.6	4.6	8.4	5.2
2020 NPV sensitivity to consumer energy arbitrage	[%]	-5.0	4.0	-20.4	0
2020 NPV sensitivity to wholesale energy arbitrage	[%]	-5.0	5.7	13.4	7.3
2020 NPV sensitivity to T = 160	[%]	11.3	8.9	11.2	10.8
2020 NPV sensitivity to T = 195	[%]	3.6	4.6	3.6	5.1
2020 NPV sensitivity to T = 215	[%]	0.3	1.8	-0.07	1.98
2020 NPV sensitivity to T = 305	[%]	-6.6	-3.5	4.2	-11.4
2030 NPV sensitivity to T = 160	[%]	-11.5	8.7	1.4	11.8
2030 NPV sensitivity to T = 195	[%]	0.33	5.0	2.9	6.1
2030 NPV sensitivity to T = 215	[%]	-0.9	2.2	0.5	2.6
2030 NPV sensitivity to T = 305	[%]	0.5	-3.6	-1.1	-1.6

Inflation

The discount factor which is used throughout the study is the required ROI which is used by the PoR, which is 8.5 percent. This factor does not include possible inflation. Since the inflation is uncertain and varying over time, it is chosen to exclude the possible inflation factor to this research. However, since the chance of inflation is hard to predict but possibly affects the outcome of this research, the sensitivity of the four hybrid installations in 2022 (cost data of 2020) to varying the inflation is shown in this Section.

Three scenarios are assessed, the first scenario is the initial scenario in 2020 where no inflation is incorporated into the discount factor. The second scenario includes an inflation percentage of 5 percent, thereby increasing the discount factor to 13.5 percent. Thirdly, the last scenario uses a discount factor of 18.5 percent, assuming an inflation percentage of 10 percent.

The discount rate influences the discounted operational profit as well as the discounted total system costs. An increased discount rate means that the value change of money over time is increased. Therefore, an increased discount rate decreases the discounted operational profit as well as the discounted total system costs. This is combined by evaluating the NPV of the hybrid installations. Figures C.13a, C.13b, C.14a and C.14b show the resulting NPV upon the three different inflation rate scenarios in 2022 (cost data of 2020) for the four hybrid installations.

The results show that the effect of the inflation on the NPV is negligible. Therefore, an increasing inflation does not significantly change the NPV of the hybrid installations. The reason why the effect is negligible is because the CAPEX costs which are independent of the inflation factor are most substantial among the components assessed with the NPV.

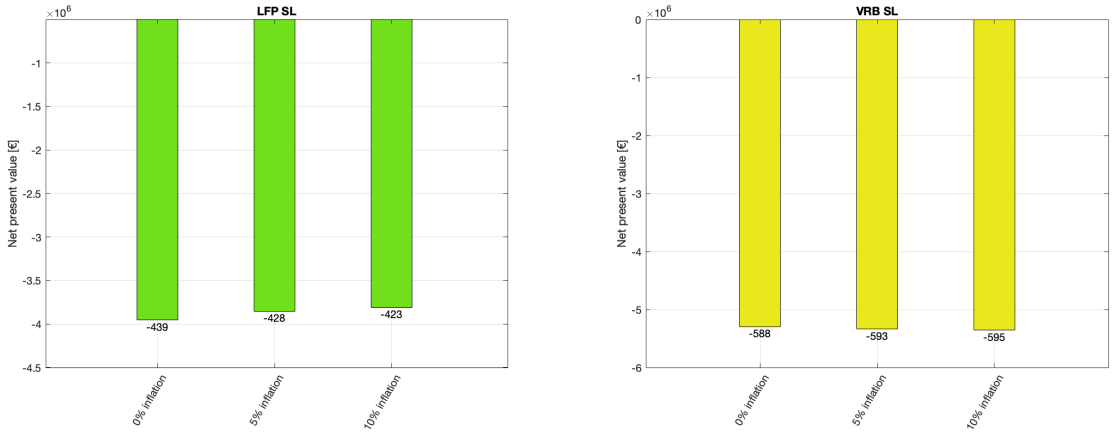

(a) Lithium iron phosphate (LFP) batteries **(b)** Vanadium redox flow batteries (VRB)

Figure C.13: Net present values (NPV) [€] of the LFP and VRB Stena Line hybrid installations for varying inflation factor as sensitivity analysis, NPV [€/kWh] is shown on top of the bars

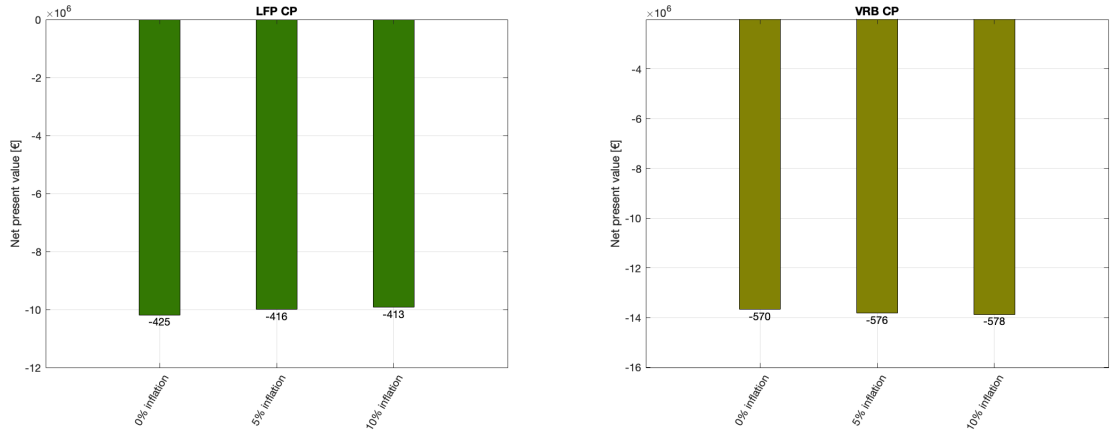

(a) Lithium iron phosphate (LFP) batteries **(b)** Vanadium redox flow batteries (VRB)

Figure C.14: Net present values (NPV) [€] of the LFP and VRB Cruise Port hybrid installations for varying inflation factor as sensitivity analysis, NPV [€/kWh] is shown on top of the bars